Impact of UV Light on the Plant Cell Wall, Methane Emissions and ROS Production

David James Messenger

A thesis prepared in fulfilment of the requirements for the degree of Doctor of Philosophy (Ph.D.), The University of Edinburgh
2009

Declaration

This thesis has been composed by my self and the work, of which it is a record, has been carried out by myself. All sources of information have been specifically acknowledged by means of a reference.

David James Messenger

Acknowledgments

First of all, I want to thank Steve Fry and Andy McLeod as my two main supervisors who have given me much needed guidance in all aspects of this work. Sirwan Yamulki, as my supervisor in Forest Research, gave me a lot of help with my fieldwork. While advice from all three was always appreciated and welcome, the last three years have also been a lesson in people management!

In the laboratory, I would like to especially thank Sandra for help throughout and excellent advice on the whole PhD-experience, as well as Ben for running the many HPLC samples I sent his way, teaching me to run and repair the HPLC, and (maybe) always remaining positive about work and life. Janice, Harriet, Amjad, Kyle, Lenka, Airianah, Sally, Robert and John have also all helped make this an enjoyable experience.

I would like to thank my family for continuous support throughout my studies and for many hours of tedious proof-reading.

Other people who have helped me in ways too varied to detail include in no particular order Robert Howard, Graham Walker, Jamie Awdry, Tony Bright, Mark Oram, Andy Pearson, Dave Reay, Keith Smith, Kevin Newsham, Brenda Howard, Jason Wargent, Graeme Allan, Ann Mennim and Colin Chilcott.

To Sandra

Abstract

This study presents the first attempt to combine the fields of ultraviolet (UV) photobiology, plant cell wall biochemistry, aerobic methane production and reactive oxygen species (ROS) mechanisms to investigate the effect of UV radiation on vegetation foliage. Following reports of a 17% increase in decomposition rates in oak (*Quercus robur*) due to increased UV, which were later ascribed to changes in cell wall carbohydrate extractability, this study investigated the effects of decreased UV levels on ash (*Fraxinus excelsior*), a fast-growing deciduous tree species. A field experiment was set up in Surrey, UK, with ash seedlings growing under polytunnels made of plastics chosen for the selective transmission of either all UV wavelengths, UV-A only, or no UV. In a subsequent field decomposition experiment on end-of-season leaves, a significant increase of 10% in decomposition rate was found after one year due to removal of UV-B. However, no significant changes in cell wall composition were found, and a sequential extraction of carbohydrate with different extractants suggested no effects of the UV treatments on cell wall structure.

Meanwhile, the first observations of aerobic production of methane from vegetation were reported. Pectin, a key cell wall polysaccharide, was identified as a putative source of methane, but no mechanism was suggested for this production. This study therefore tested the effect of UV irradiation on methane emissions from pectin. A linear response of methane emissions against UV irradiation was found. UV-irradiation of de-esterified pectin produced no methane, demonstrating esters (probably methyl esters) to be the source of the observed methane. Addition of ROS-scavengers significantly decreased emissions from pectin, while addition of ROS without UV produced large quantities of methane. Therefore, this study proposes that UV light is generating ROS which are then attacking methyl esters to create methane. The study also demonstrates that this mechanism has the potential to generate several types of methyl halides. These findings may have implications for the global methane budget.

In an attempt to demonstrate ROS generation *in vivo* by UV irradiation, radio-labelling techniques were developed to detect the presence of oxo groups, a product of carbohydrate attack by ROS. Using NaB^3H_4, the polysaccharides of ash leaflets from the field experiment were radio-labelled, but did not show any significant decrease in oxo groups due to UV treatments. However, UV-irradiation of lettuce leaves showed a significant increase in radio-labelling, suggesting increased UV irradiation caused an increase in the production of ROS. The study shows that the use of this radio-labelling technique has the potential to detect changes in ROS production due to changes in UV levels and could be used to demonstrate a link between ROS levels and methane emissions.

Table of contents

List of Figures

List of Tables

Abbreviations

AIR	Alcohol-insoluble residue
Ara	Arabinose
BAW	Butanol:acetic acid:water
cpm	Counts per minute
DCC	Dicyclohexylcarbodiimide
EPW	Ethylacetate:pyridine:water
EtOH	Ethanol
Gal	Galactose
GalA	Galacturonic acid
GalAMe	Galacturonic acid methyl ester
Glc	Glucose
GlcA	Glucuronic acid
HG	Homogalacturonan
HGMe	Homogalacturonan methyl ester
HPLC	High performance liquid chromatography
Man	Mannose
ManA	Mannuronic acid
MeOH	Methanol
PAR	Photosynthetically Active Radiation
PyAW	Pyridine:acetic acid:water
Rha	Rhamnose
ROS	Reactive oxygen species
SE	Standard error
TFA	Trifluoroacetic acid
TLC	Thin layer chromatography
UV	Ultraviolet
Xyl	Xylose

1. INTRODUCTION

Research into the effects of ultraviolet (UV) light on plants, on cell wall biochemistry, on methane emissions and on reactive oxygen species (ROS) production in the environment have each been individually reviewed extensively and are quite well understood, but they have rarely been studied together and little literature exists to link them. These topics are thus discussed separately to serve as a general introduction and are followed by a brief summary of the aims of this project.

1.1 Ultraviolet light and its ecological effects

1.1.1 UV and the ozone layer

The sun emits light with wavelengths well into and below the UV-C region of the electromagnetic spectrum (200 – 280 nm) as would be expected of an almost perfect 6000°K black body. Wavelengths below 280 nm are absorbed by atmospheric O_2 and O_3, so do not reach the earth's surface and are therefore of no biological relevance (Newsham *et al*., 1996). The ozone layer also absorbs a large part of the longer wavelength UV-B light (280 – 320 nm), and only a small part of UV-A (320 – 400 nm). O_3 depletion due to anthropogenic pollution (Solomon, 1990) is now a well understood process, and results in an increase in the amounts of UV-B light reaching the surface (Kerr *et al*., 1993). Even though a large reduction in O_3 concentration only results in a small increase in total UV at the Earth's surface (Figure 1.1.1), the relative UV enhancement increases exponentially as wavelength decreases (Caldwell & Flint, 1994). This is of great biological importance because the shorter wavelengths of the UV-B have a greater biological effect. This

relationship between biological effect and wavelength can be modelled using an action spectrum.

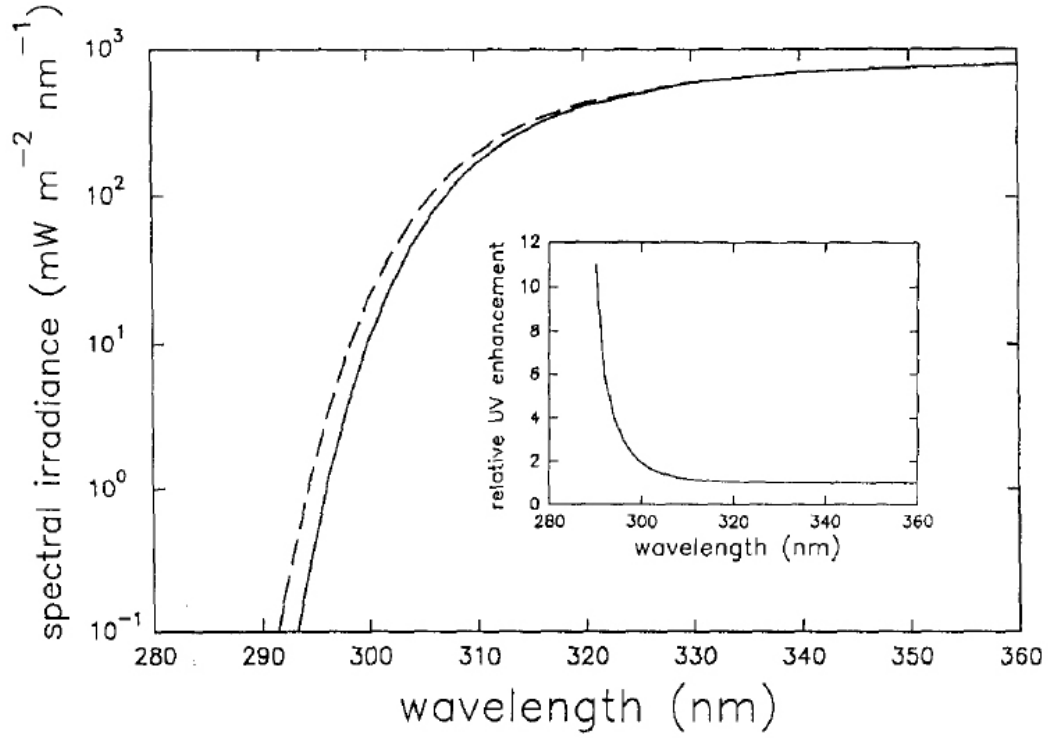

Figure 1.1.1 Computed solar spectral irradiance for normal ozone column thickness and a 20% ozone column reduction.
Solar angle was appropriate for midday in the summer at temperate latitudes. Dashed line represents the irradiance for the same conditions, but with a 20% ozone column reduction. The relative factor by which irradiance is increased due to ozone reduction at different wavelengths is shown in the inset (Caldwell & Flint, 1994).

1.1.2 Action spectra and weighting functions

Living organisms react differently to electromagnetic radiation depending on its wavelength. A spectral weighting function can be applied to each wavelength of light which will take this into account by giving more importance to the wavelengths that are more biologically active. The biological response studied can range from a molecular change to a whole organism effect.

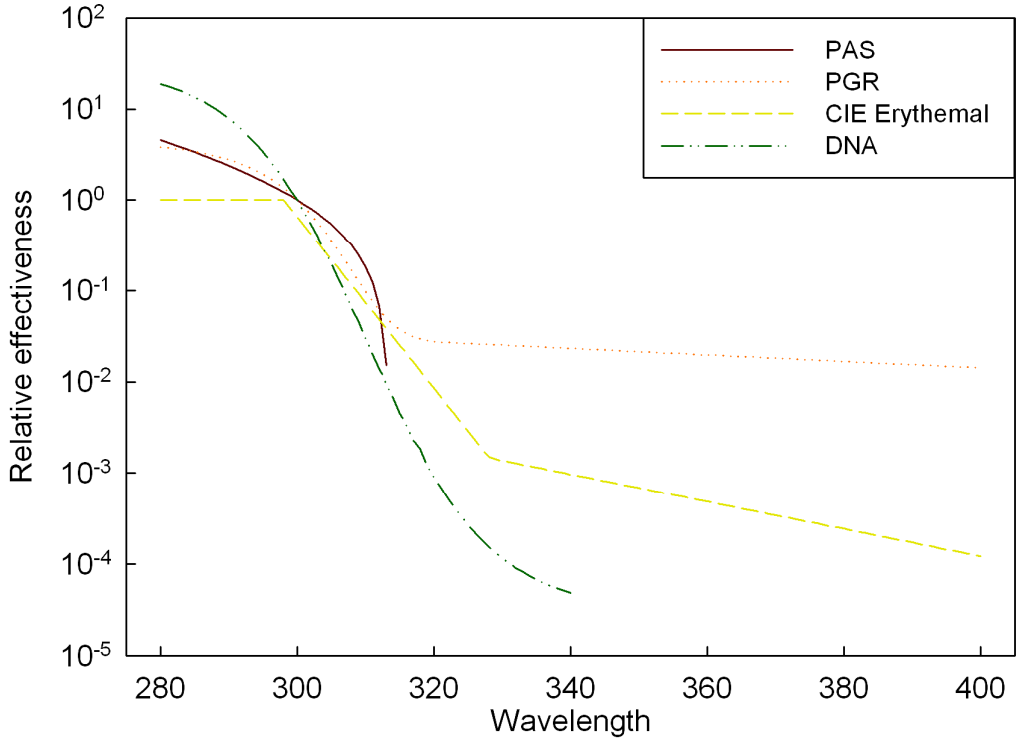

Figure 1.1.2 Plot of four commonly used action spectra.
PAS: Plant damage action spectrum (Caldwell, 1971), PGR: Plant Growth Response (Flint & Caldwell, 2003), CIE (International Commission on Illumination) Erythemal action spectrum (McKinlay & Diffey, 1987) and DNA damage action spectrum (Setlow, 1974).

General functions can be made such as the generalised plant damage action spectrum (Caldwell, 1971 as formulated by Green *et al*., 1974) which can be used to describe the relative effect of different wavelengths on plant damage (Figure 1.1.2). There are many other generalised effects which have been modelled in action spectra, such as effects on plant growth (Flint & Caldwell, 2003), effects of UV on human skin (McKinlay & Diffey, 1987) or damage to DNA (Setlow, 1974; Quaite *et al*, 1992). The widely used Plant damage spectral weighting function (Caldwell, 1971) however assigns no biological effectiveness to wavelengths above 313 nm, while recent research suggests that UV-A can have important effects on plants (Newsham *et al*., 1996; Krizek *et al*., 1997; Fiscus & Booker, 2002). This observation, supported by data such as the Plant growth response action spectrum

(Flint & Caldwell, 2003) which includes UV-A effects, means that general functions only have limited use and that to get best results specific spectral weighting functions for each mechanism or process need to be developed.

1.1.3 UV research in the field

While UV research in medicine and biology has often focused on the effect of UV on DNA and the repair mechanisms of enzymes (Sinha & Häder, 2002), this is beyond the scope of this project so will not be discussed. Instead, the results from ecological studies, which have focused mainly on plant growth, interaction with the environment and chemical composition have been investigated.

The effect that UV has on plants has been assessed in two ways, either by increasing ambient UV levels with lamps (usually fluorescent lamps), or by reducing ambient UV levels with filters. While reduction of UV levels is relatively simple with either the use of plastics of known transmission levels that can be used for long periods of time (some commercially available examples include Mylar®, cellulose acetate, courtgard™ or Teflon®) or filtration of ambient UV levels with a layer of O_3 between sheets of plexiglass (Tevini *et al.*, 1990), the use of lamps is more complicated. Early lamp supplementation studies simply used lamps inside growth chambers or glasshouses to increase the amount of UV-B that plants received, which typically created conditions with unnaturally high ratios of UV-B:UV-A and UV-B:PAR (Caldwell & Flint, 1997). Instead, studies conducted outside which used lamps to supplement ambient levels of UV are considered to be more realistic. So called 'square-wave' supplementation systems simply turn lamps on centred around noon each day to provide a large amount of UV-B in one go, whereas 'modulated' systems have a feed-back mechanism which measures ambient UV levels and

regulates the lamps output to provide a proportional addition above ambient throughout the day. 'Modulated' systems therefore keep the UV-B:UV-A ratio constant and can provide more realistic representations of ozone depletion scenarios (McLeod, 1997). Most UV-B fluorescent lamp types also emit small amounts of UV-A, and therefore the use of a UV-A control treatment is important (Newsham *et al*., 1996; Fiscus & Brooker, 2002).

While early UV-B supplementation studies in greenhouses under unrealistic lighting conditions found that increased UV-B can cause reduction of leaf and/or stem growth (Tevini *et al*., 1990), supplementation studies in the field with more realistic conditions have not seen this growth effect (Day, 2001; Searles *et al*., 2001). Ballaré *et al*. (2001) showed that removal of ambient UV-B with plastic filters caused increased growth of certain plants in southern Argentina. When compared with plants exposed to ambient UV-B, differences of around 10% in size of local ferns (*Gunnera magellanica*, *Blechnum penna marina*) and mosses (*Sphagnum magellanicum*) were observed, while no effect was noted in several deciduous trees (*Nothofagus antarctica*, *Nothofagus pumilio*). These results suggest ambient UV-B can have an inhibitory effect on plant growth, but that this effect cannot be generalised to all species.

Chemical changes in leaves under different levels of UV are varied. While it has often been observed that increases in UV levels lead to increased production of UV-absorbing compounds (Searles *et al*., 2001), this can by no means be generalised to all species as UV-B sensitivity is not always proportional to UV-absorbing compound concentration or epidermal transmittance (Sullivan *et al*., 1996).

Newsham *et al*. (2005) have shown in *Cephaloziella varians* a positive correlation between levels of anthocyanin pigments and UV-B levels, which act as a protecting agent for the leaf. They also showed a negative correlation between UV-B levels and concentration of chlorophyll, and a positive correlation between other UV-B screening pigments and UV-B levels. However, in a study of *Quercus robur*, Newsham *et al*. (2001b) found that a 30% supplement in ambient levels of UV-B did not change concentrations of UV-B screening compounds such as phenylpropanoids (vanillin, vanillic acid) and polyphenolics (tannins, lignin). Recently, Kotilainen *et al*. (2008) found that in UV exclusion experiments on alder and birch leaves the change in concentration of phenolic metabolites depended on the type of UV excluded. For some metabolites, UV-A and UV-B affected concentrations in the same direction, while for a few compounds there was evidence suggesting opposite effects of UV-A and UV-B radiation. Also, the concentration of some phenolics did not significantly respond to changes in UV. Most importantly, they only observed minor effects on the total phenolic concentration, therefore suggesting that measuring only total phenolic concentration may not be an accurate way of determining UV effects. Indeed, the construction of an action spectrum for the effect of UV on total plant phenolics would therefore not be possible and would need to be determined individually for each compound.

Leaf litter quality can also be affected by UV, which will affect decomposition rates and potentially the surrounding ecosystem. Higher levels of UV-B often reduce insect herbivory which has been associated with chemical changes in the leaves such as increased nitrogen content (Hatcher & Paul, 1994), or even lower sucrose content (Yazawa *et al*., 1992). Many studies have reported

increased as well as decreased decomposition rates, with sometimes chemical changes in the leaves, in many different species but the cause of these effects are not well understood. 'Indirect' changes such as in the carbohydrate composition, nitrogen content or carbon-to-nitrogen ratio can occur, and these have great effects on the leaf litter quality, which in turn affects the decomposition rate (Melillo *et al*., 1982; Taylor *et al*., 1989; Aber *et al*., 1990). Meanwhile, 'direct' effects of UV on leaf litter during decomposition can affect two processes. First, the composition or activity of the decomposer community, with many complex responses to UV, would generally be assumed to be inhibited by UV (Moody *et al*., 1999), which would reduce the decomposition rate (Gehrke *et al*., 1995). Plant fungal and viral diseases have been shown to react in different ways to UV-B radiation, sometimes being promoted and sometimes being inhibited; however, it is unclear whether it was direct irradiation of the pathogens which might have damaged them, or if it was a chemical change in the leaves which made them more or less resistant (Manning & Tiedemann, 1995). Secondly, elevated UV may increase photodegradation, the direct physico-chemical breakdown of litter (Moorhead & Callaghan, 1994; Austin & Vivanco, 2006), and so increase the rate of decomposition. All these effects have been investigated, independently or sometimes at the same time, on leaves during growth as well as during the decomposition phase.

Rozema *et al*. (1997) exposed the dried dune grassland grass *C. epigeios* to elevated UV (simulating a 15% stratospheric ozone depletion, 2.5 kJ m^{-2} day^{-1} erythemally-weighted UV-B) and ambient UV levels during growth, as well as during decomposition, and found a 56% increase in lignin production and a decrease of up to 10% in decomposition rate with increased UV. However, the aerial

decomposition method used in this study is unrealistic and renders the results questionable. Experiments on spring wheat (*Triticum aestivum*) by Yue *et al*. (1998) showed a decrease in N, P, K, Mg, Fe and Zn concentrations with several levels of increased UV-B irradiation (0 – 5.31 kJ m^{-2} day^{-1} erythemally-weighted UV-B) as well as an increase of 7 – 25% in decomposition rate depending on the dose of UV-B. Cybulski *et al*. (2000) found no effect of two levels of elevated UV-B (corresponding to a 16% and a 25% ozone depletion scenario) on chemical composition of loblolly pine (*Pinus taeda* L.) needles from one source, but elevated lignin/N ratios and lower holocellulose content in the same species from a different seed source. Additionally, no changes in decomposition rates were noted in the first case but a decrease of 36% was seen in the latter case under low elevated UV-B. Interestingly, the higher increased UV-B level did not increase this effect. These data suggest that results may not only be species specific, but also seed-source specific, and not necessarily dose dependent. Moody *et al*. (2001) tested the effect of enhanced UV-B (simulating a 15% ozone depletion) on the decomposition of *Betula pubescens* leaves at four sites in Europe with different ecosystems. The only significant changes observed associated with UV-B were a reduction in N concentration at one site and an increase in C:N at another site. Significant effects on decomposition were only observed at those two sites, suggesting that effects of enhanced UV-B on decomposition can be site specific. Newsham *et al*. (2001a; 2001b) found no significant change in litter composition of *Quercus robur* with increased UV-B, but nevertheless saw a significant increase of 17% in decomposition rate.

There have been several reviews on the effects of UV radiation on gene expression and the signalling pathways used as a response in plants (A.-H.-Mackerness, 2000; Brosché & Strid, 2003). Several UV photoreceptors which trigger these genetic responses have been identified (Batschauer *et al*., 1996; Kagawa *et al*., 2001; Wade *et al*., 2001; Nagy & Schäfer, 2002) and it is thought that phytochromes (a common plant pigment sensitive to light in the red and far-red region of the visible spectrum), while not acting as primary UV-B photoreceptors, may modulate various UV-B responses. There are also a range of second messenger systems such as calcium signalling and/or ROS production which are thought to be involved in the response of plants to UV (A.-H.-Mackerness, 2000). While these responses are interesting from a molecular biology point of view, this project did not focus on this aspect of UV research.

1.2 The plant cell wall

The plant cell wall governs many aspects of a cell such as shape, growth rate and strength of the tissue. There are two main types of cell walls, primary and secondary: the primary cell wall is that present while the cell is growing, and once growth is finished a secondary cell wall is laid down and growth is terminated.

While the cell wall composition of different plant families can be generalised, there are many taxonomic variations (Popper & Fry, 2005). Dry cell wall matter is typically around 90% polysaccharides and 10% proteins. The polysaccharides, which this project has focused on, fall into two categories, the microfibrillar phase and the matrix phase.

1.2.1 The microfibrillar phase

Microfibrils are bundles of cellulose chains held together through hydrogen bonds and van der Waals forces to form a highly crystalline rigid structure. Cellulose makes up about 20 – 40% of the dry weight of the primary cell wall, increasing to 40 – 60% in the secondary cell wall (Leschine, 1995; Sticklen, 2008). Each year, photosynthesis fixes more than 10^{11} tons of plant material, over 50% of which is in the form of cellulose (Eriksson *et al*., 1990). Cellulose is a linear chain of (1→4) β-linked glucose residues and the size of the molecule can vary from 7000 to 14000 sugar moieties in the secondary cell wall, but can be as low as 500 glucose units in the primary cell wall (Richmond, 1991).

1.2.2 The matrix phase

Around 30% of the dry weight of the primary cell wall of dicots (flowering plants, angiosperms, with two cotyledons) is composed of pectins, while monocots (angiosperms with only one cotyledon) are generally thought to have very small amounts of pectin (McNeil *et al*., 1984), although Jarvis *et al*. (1988) found large variability of pectin levels between different monocot species, some containing similar amounts as the dicots. The main constituents of pectin are galacturonic acid (GalA), rhamnose, arabinose and galactose (Brett & Waldron, 1996) and there are four main categories of pectin: homogalacturonan (HG), xylogalacturonans, rhamnogalacturonan-I and rhamnogalacturonan-II (Willats *et al*., 2001) (Figure 1.2.1b). These are covalently bonded together, though several models exist as to the exact nature of this bonding (Ishii & Matsunaga, 2001; Vinken *et al*., 2003). Homogalacturonans are the most common type of pectin and are made up of a linear (1→4)-GalA backbone, while xylogalacturonans are very similar but contain many

xylose residues. Rhamnogalacturonans are more complex polymers with many side-chains but still contain many GalA residues (Seymour & Knox, 2002; O'Neill & York, 2003). Many of the GalA residues found in HG and rhamnogalacturonan-I regions are methyl-esterified (Figure 1.2.1a) in a block-wise fashion (Limberg *et al*., 2000), while some *O*-acetylated ester groups are also present (Ishii, 1997; Perrone *et al*., 2002) and, in certain plants, phenolic groups such as ferulic acid (Fry, 1983).

(a)

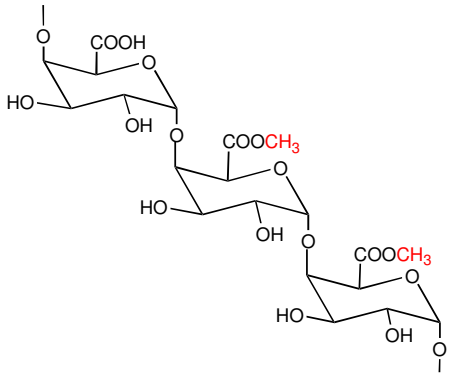

(b)

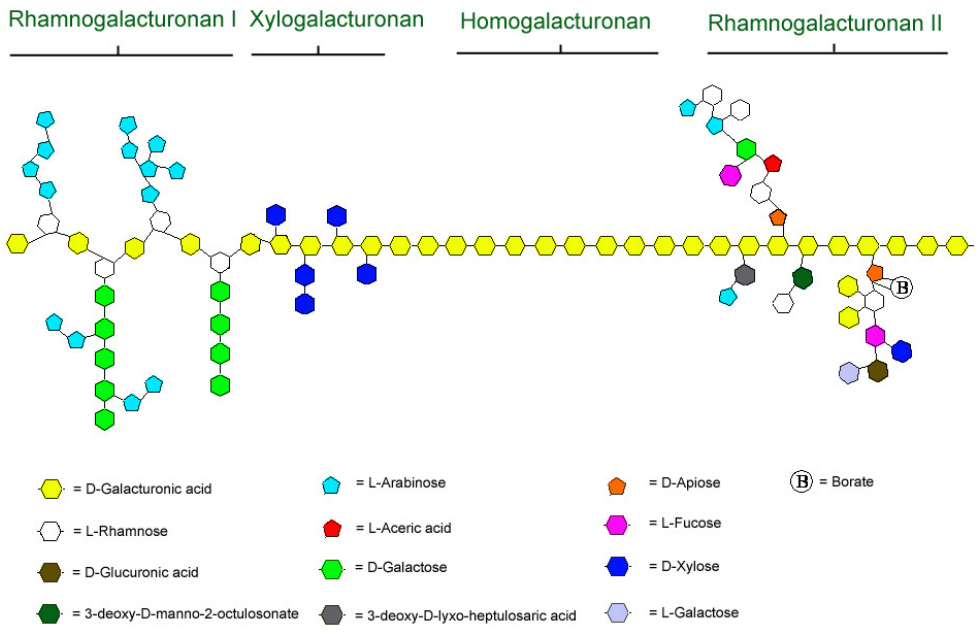

Figure 1.2.1 Schematic representation of the structure of pectin.
(a) Three galacturonic acid residues with methyl ester groups in red. (b) Schematic representation of the structure of the four main domains of pectin, with different sugars identified by colour (adapted from Schellera *et al*., 2007).

The non-esterified GalA residues will have a negative charge which enables them to bind with Ca^{2+} and create cross-links, or "Calcium bridges", between several pectin molecules (Jarvis, 1982; Baydoun & Brett, 1984). This bridging is severally impeded by the presence of rhamnogalacturonans or if the GalA backbone is heavily methyl-esterified (Fry, 1986). For extensive reviews into the genetics and biochemistry behind pectin biosynthesis, which is beyond the scope of this study, see Schellera *et al*. (2007) and Willats *et al*. (2001).

Xyloglucans, xylans, mannans and mixed-linkage glucans are the main types of hemicelluloses found in plant cell wall and make up almost 30% of their dry weight. Xyloglucans are composed of a backbone of β-(1→4)-D-glucopyranose residues, about 75% of which have a single α-D-xylopyranose residue attached, some of which also have a β-D-galactopyranose residue attached to a α-L-fucopyranose residue (Fry, 1989). They are thought to cross-link cellulose microfibrils via hydrogen bonding (Hayashi *et al*., 1987; McCann *et al*., 1990) and therefore have an important role in wall-loosening and cell expansion (Fry *et al*., 1992). Meanwhile, other hemicelluloses are thought to play an important role in the strength of wood, in particular mannans which are found in large quantities in soft woods but not in hard woods (Sweet & Winandy, 1999). Figure 1.2.2 shows a diagram of a primary cell wall and the interactions between different components.

(a)

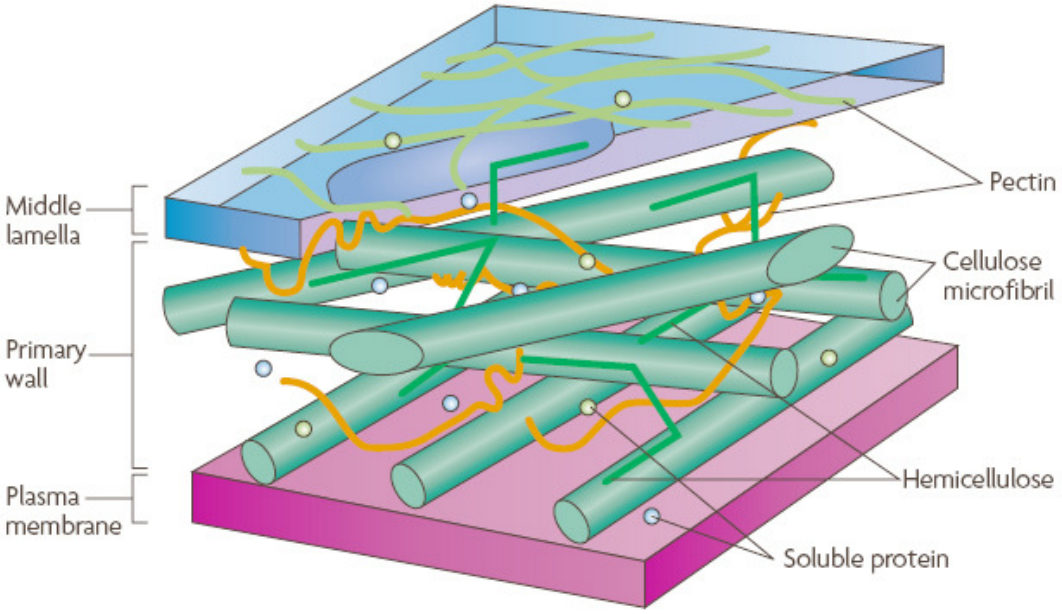

(b)

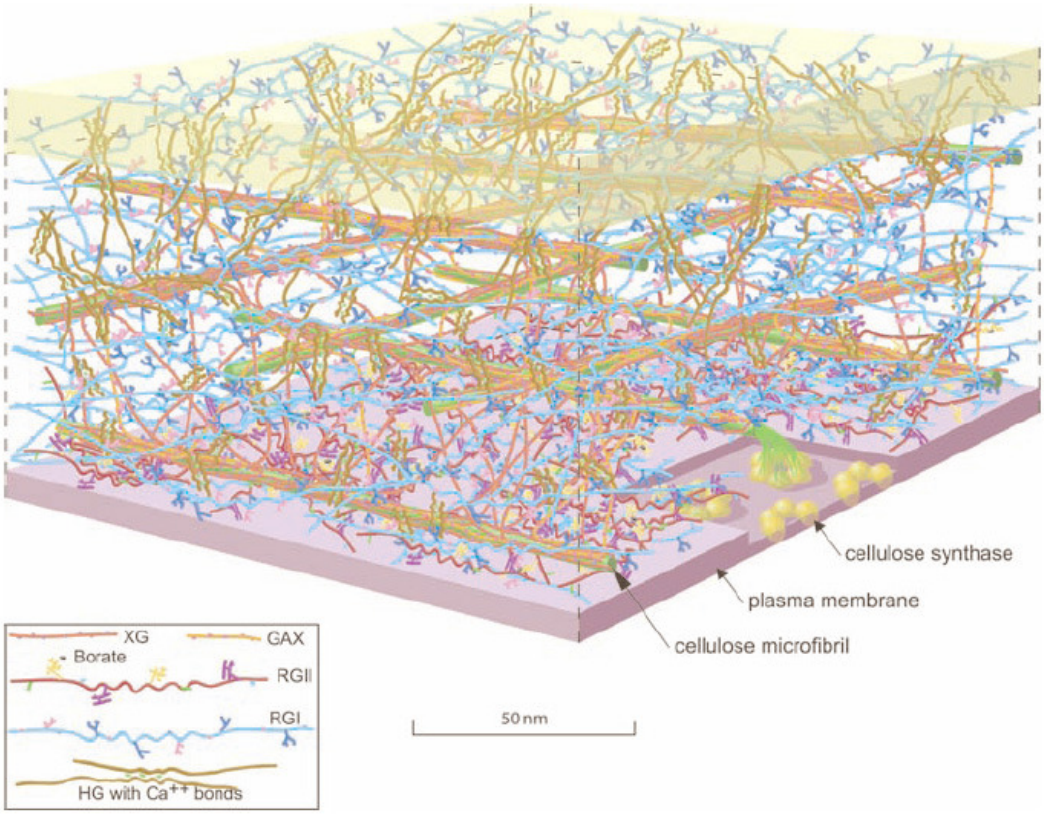

Figure 1.2.2 Schematic representation of the structure of the plant cell wall. (a) A simple model of the primary cell wall (Sticklen, 2008) (b) A more detailed representation. The amount of microfibrils has been reduced for clarity, and distance between microfibrils has been exaggerated making hemicellulose cross-links abnormally extended (Somerville *et al*., 2004).

1.2.3 Effects of UV on the plant cell wall

The majority of previous studies into the effects of UV on the plant cell wall have focused on the changes in content of cell wall-bound UV-absorbing compounds (phenolic compounds) in environments subjected to enhanced UV, in particular UV-B, due to ozone depletion or the presence of fluorescent lamps. Ruhland & Day (2000) studied phenylpropanoids in cell walls of *Deschampsia antarctica* and *Colobanthus quitensis*, the only vascular plants native to continental Antarctica, and found an increase in ferulic acid production with increasing UV-B. Ruhland *et al*. (2005) later found in *Deschampsia antarctica* that reducing UV levels by 83% with filters caused a significant reduction in production of insoluble *p*-coumaric acid, caffeic acid and ferulic acid, all compounds found in the cell wall. Semerdjieva *et al*. (2003) meanwhile found that increasing UV levels (to a 15% ozone depletion scenario level) increased the concentration of UV-absorbing compounds in the cell walls of *Vaccinium vitis-idaea*, a dwarf shrub grown in the north Sweden influenced by ozone depletion over the Arctic. Clarke & Robinson (2008) looked at soluble and insoluble UV-absorbing compound concentration in *Bryum pseudotriquetrum*, *Ceratodon purpureus* and *Schistidium antarctici*, three moss species found in Antarctica, to try to explain the greater UV tolerance of *Ceratodon purpureus*. Despite containing less soluble UV-absorbing compounds than *Bryum pseudotriquetrum*, *Ceratodon purpureus* was found to have six times more cell wall-bound phenolic compounds than soluble phenolics. Clarke & Robinson therefore postulated that it was this concentration of phenolic compounds in the cell wall which confers *Ceratodon purpureus* increased UV tolerance by acting as a more efficient barrier to UV than soluble phenolics (Figure 1.2.3).

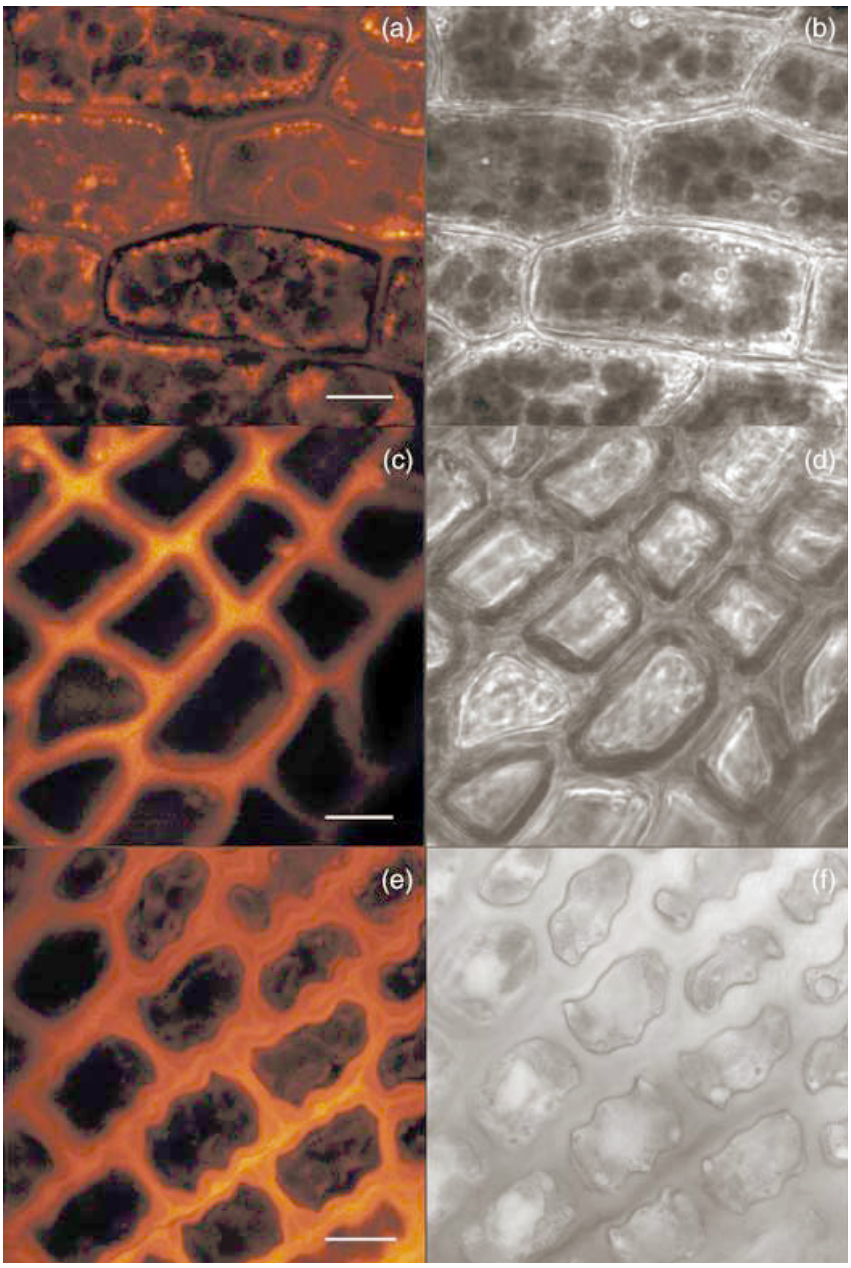

Figure 1.2.3 Confocal and light transmission images showing location of UV absorbing compounds.
(a, b) *Bryum pseudotriquetrum*, (c, d) *Ceratodon purpureus* and (e, f) *Schistidium antarctici*, stained with Naturstoffreagenz A to show the localization of UV-screening compounds in each species (orange fluorescence) (Clarke & Robinson, 2008).

Newsham *et al*. (2001b) found little changes in chemical composition due to UV irradiation of *Quercus robur*, but McLeod *et al*. (2007) found on the same samples that the extractability of carbohydrates from the leaf litter was affected. A sequential solvent extraction showed that exposure to elevated UV-B reduced the

amount of carbohydrates released, which may explain a previous observation that UV-B supplementation increased the decomposition rate of *Quercus robur* by 17% (Newsham *et al*., 2001a). This change in extractability was suggested to result from a modification of the plant cell wall structure.

1.3 Methane in the environment

1.3.1 The global methane budget

The global carbon cycle is a complex mixture of natural and anthropogenic processes, some very fast and some very slow, which contribute to the cycling of carbon based compounds through the atmosphere, biosphere, hydrosphere and lithosphere (Figure 1.3.1).

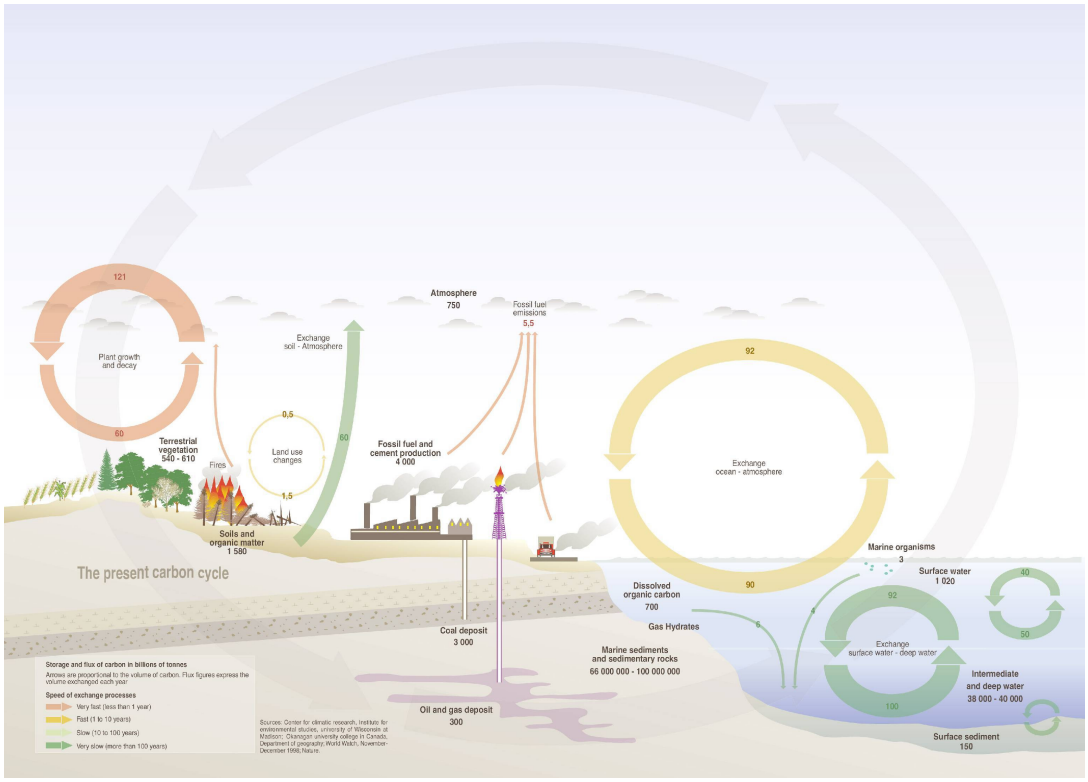

Figure 1.3.1 The global carbon cycle.
Data are expressed in gigatonnes of carbon (UNEP/GRID-Arendal).

Methane has a short half-life in the atmosphere of 8.4 years during which it can be converted to CO_2, a much more stable compound which also forms the

majority of the carbon-based compounds emitted into the atmosphere in the global carbon cycle. However, methane is a significant contribution to the carbon cycle and is formed from a range of natural and anthropogenic sources (Table 1.3.1).

Source or sink	Methane flux (Tg CH_4 yr^{-1}) estimated by									
	Hein *et al.*, 1997	Houweling *et al.*, 2000	Olivier *et al.*, 2005	Wuebbles & Hayhoe, 2002	Scheehle *et al.*, 2002	Wang *et al.*, 2004	Mikaloff Fletchet *et al.*, 2004	Chen & Prinn, 2006	IPCC TAR	IPCC AR4
	for the base year									
	1983 - 1999	not stated	2000	not stated	1990	1994	1999	1996 - 2001	1998	2000 - 2004
Natural sources		**222**		**145**		**200**	**260**	**168**		
Wetlands	231	163		100		176	231	145		
Termites		20		20		20	29	23		
Ocean		15		4						
Hydrates				5		4				
Geological sources		4		14						
Wild animals		15								
Wildfires		5		2						
Anthropogenic sources	**361**		**320**	**358**	**264**	**307**	**350**	**428**		
Energy					74	77				
Coal mining	32		34	46			30	48		
Gas, oil, industry	68		64	60			52	36		
Landfills & waste	43		66	61	69	49	35			
Ruminants	92		80	81	76	83	91	189		
Rice agriculture	83		39	60	31	57	54	112		
Biomass burning	43			50	14	41	88	43		
C3 vegetation			27							
C4 vegetation			9							
Total sources	**592**			**503**		**507**	**610**	**596**	**598**	**582**
Sinks										
Soils	26			30			30		30	30
Tropospheric $^{\bullet}OH$	488			445			507		506	511
Stratospheric loss	45			40			40		40	40
Total sink	**559**			**515**			**577**		**576**	**581**
Imbalance	+33			-12			+33		+22	+1

Table 1.3.1 Published methane flux from natural and anthropogenic methane sources and sinks.

Total global pre-industrial methane emissions are estimated at 200 – 250 Tg yr^{-1} (Chappelaz *et al.*, 1993; Etheridge *et al.*, 1998; Houweling *et al.*, 2000; Ferretti *et al.*, 2005; Valdes *et al.*, 2005), of which 190 – 220 Tg yr^{-1} originates from natural sources and the rest from anthropogenic sources (rice agriculture, livestock, biomass burning and waste). However, current methane emissions are estimated at 500 – 610 Tg yr^{-1}, with 300 – 430 Tg yr^{-1} from anthropogenic sources (Hein *et al.*, 1997;

Wuebbles & Hayhoe, 2002; Mikaloff Fletchet *et al*., 2004; Chen & Prinn, 2006). There are many natural methane sinks, the main sink being reaction with tropospheric $^{\bullet}OH$ to form methyl radicals, but the net imbalance between production and destruction is estimated at −12 – 33 Tg yr^{-1} (Table 1.3.1).

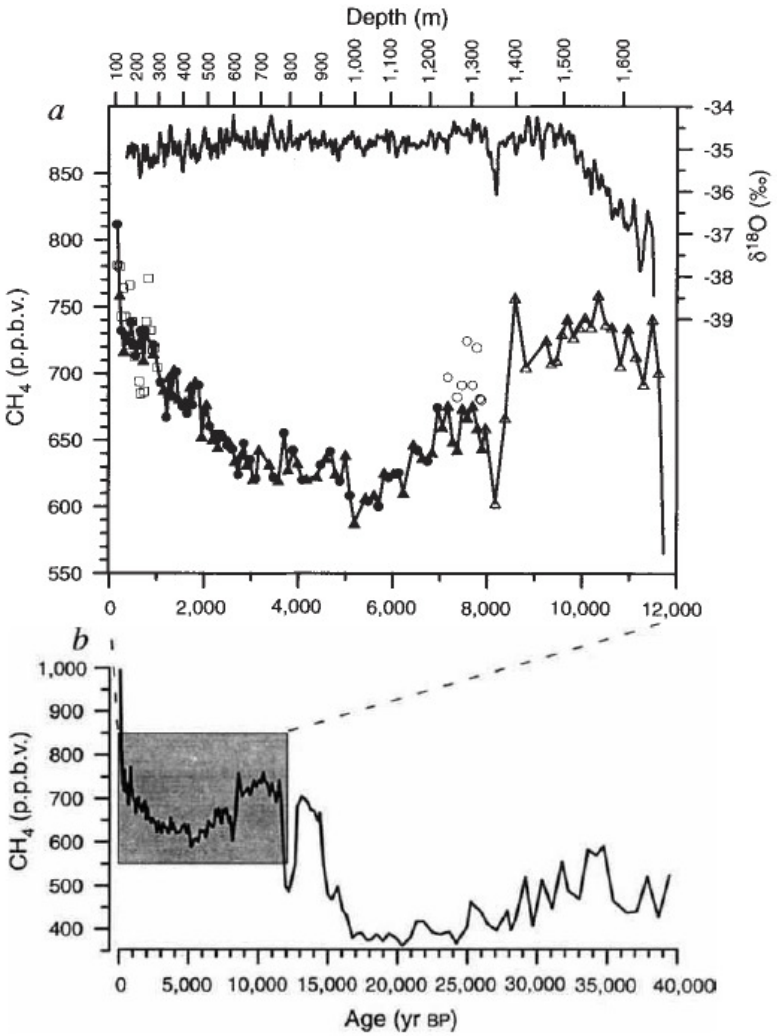

Figure 1.3.2 Record of global methane concentration.
(a) Mean atmospheric methane concentration from Greenland ice-cores and Eurocores. (b) Expanded scale to the last 40000 years (Blunier *et al*., 1995).

Global methane concentrations in the atmosphere have been increasing throughout the 19th and 20th century, from around 700 ppb to over 1700 ppb nowadays (Figure 1.3.2). Although these emissions seemed to be stabilising in the

late 1990's and levelling off around 1750 ppb (Dlugokencky *et al*., 2003), recent observations suggest that emissions may be growing again (Bousquet *et al*., 2006).

Human activities result in emissions of four long-lived greenhouse gases: carbon dioxide (CO_2), methane (CH_4), nitrous oxide (N_2O) and halocarbons (a group of gases containing fluorine, chlorine or bromine). In 2004, methane constituted 14.3% of total anthropogenic emissions in terms of CO_2 equivalents (IPCC AR4, 2007). While emissions of CO_2 are the largest in absolute quantity, CH_4 is twenty-five times more effective as a greenhouse gas than CO_2 over a 100-year period (Wahlen, 1993). Methane absorbs radiation emitted from the Earth's surface in the 4 – 100 μm range and therefore affects atmospheric temperature directly (Lacis *et al*., 1981; Ramanathan, 1988). It also influences the abundance of ozone in the troposphere and in the stratosphere (Johnston, 1984) and it is a major source of stratospheric water (Pollock *et al*., 1980). Methane thus also affects temperature indirectly through its chemical interactions. Radiative forcing is the change in net irradiance at the tropopause (i.e. the difference between the incoming radiation energy and the outgoing radiation energy in a given climate system) and is based on measured difference relative to the year 1750, the defined starting point of the industrial era. A positive forcing (more incoming energy) will tend to warm the system, while a negative forcing (more outgoing energy) will tend to cool it. Figure 1.3.3 shows the current radiative forcing of natural and anthropogenic components in the atmosphere. At 0.48 W m^{-2}, methane is the second largest contributor to the overall positive radiative forcing due to anthropogenic factors.

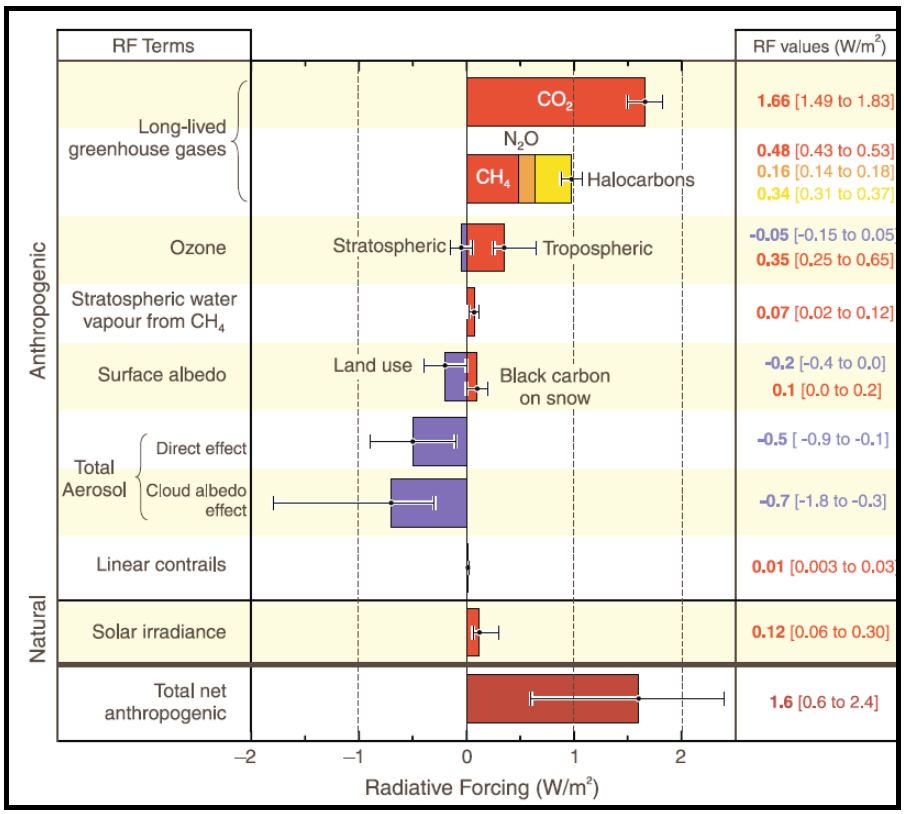

Figure 1.3.3 Radiative forcing components in the atmosphere.
IPCC AR4 (2007) report.

Even though the observed quantities of methane emissions and their allocation to the different sources are still debated (Table 1.3.1), the nature of these sources was thought to be well known. However, recent studies have controversially suggested the possibility of a novel source of aerobically-produced methane, originating from vegetation, which could form a large contribution to the global methane budget and require its re-evaluation.

1.3.2 Methane emissions from vegetation in an aerobic environment

The process of microbial anaerobic methane formation is now well understood (Zengler *et al*., 1999) and was until recently thought to be the only natural generator of methane. However, Keppler *et al*. (2006) detected for the first time net emissions of methane from vegetation in an aerobic environment. The emission rates varied with species (12 – 370 ng g^{-1} (dry weight) h^{-1}), increased both with heat and sunlight,

and were shown to be non-microbial in origin. From their data, they estimated that aerobic methane emissions from living plants could be responsible for 62 – 236 Tg yr^{-1}, and that plant litter may produce 1 – 7 Tg yr^{-1}, which meant that this process could be responsible for up to ~30% of total global methane emissions. While these estimates were quickly regarded as overestimates (Houweling *et al*., 2006; Kirschbaum *et al*., 2006; Miller *et al*., 2007) since the initial estimates were made using data from net primary production (therefore assuming that all plant matter contributes equally to methane emissions, despite roots and woody material receiving less light and being metabolically less active than leaves), the findings remained controversial and caused much debate (Schiermeier, 2006). Efforts to replicate the experiments by Dueck *et al*. (2007), using ^{13}C-labelling techniques on six plant species, were unsuccessful, while Beerling *et al*. (2008) also saw no significant methane emissions from *Zea mays* and *Nicotiana tabacum*. However, Wang *et al*. (2008), using measurements in the dark, reported methane emissions from several woody species, but not from grasses, whereas Cao *et al*. (2008), using chambers covered with white mesh, reported methane emissions from grasses but not from a shrub community.

The source of the aerobically-produced methane was suggested by Keppler *et al*. (2006), based on δ^{13}C measurements, to originate from the plant's C_1 metabolite pool. Such an example would be the methyl ester groups of pectic polysaccharides, major components of the primary cell walls of dicots and most other non-poalean plants (Popper & Fry, 2003; 2004) and of the middle lamella. Keppler *et al*. (2008) carried out experiments with ^{13}C-labelled pectin which confirmed this was a potential source and that UV light may be involved in the process. Sharpatyi (2007) suggested

that reactive oxygen species (ROS) may be involved. Interestingly, it has also been recently reported that methane emissions from the oceans may be formed aerobically from methylphosphonate decomposition (Karl *et al*., 2008). This lack of understanding about the mechanism for methane production could explain the conflicting findings of other papers (e.g. Dueck *et al*., 2007).

1.4 Reactive oxygen species

Reactive Oxygen Species (ROS) are a group of compounds, including oxygen ions, free radicals and peroxides, which are highly reactive due to the presence of unpaired electrons in the valence shell. While their existence was suggested almost one hundred years ago, their importance in biological systems was not recognised until the mid 1950's. Early studies focused mainly on their toxicity and role in damaging DNA and other proteins, but it was later realised that ROS also have important roles in cell processes, such as growth, cell cycle, programmed cell death, hormone signalling, biotic and abiotic stress responses and development (Laloi *et al*., 2004).

The origin and uses of ROS in the environment will firstly be discussed briefly, following a description of studies of ROS in plant cell walls and on their generation through UV and other types of radiation *in planta* that were conducted as part of this project.

1.4.1 Reactive oxygen species in the environment

Typical examples of ROS found in the natural environment are the hydroxyl radical ($^{\bullet}OH$), superoxide ($O_2^{\bullet-}$), its non-ionised equivalent the hydroperoxyl radical ($HO_2^{\bullet}$), singlet oxygen ($^1O_2$), hydrogen peroxide (H_2O_2), ozone (O_3) and nitrogen monoxide (NO). The generation of ROS *in vivo* can generally be linked to two processes: a

response to an external stimulus which may be a threat (e.g. heat stress, drought, UV, nutrient deficiency, pathogen infection, herbicides, heavy metals or ozone); or a signalling process in the cell which typically happens during growth, hormone production or even programmed cell death (Apel & Hirt, 2004). These two types of ROS production will be discussed separately.

A common response of plants to an external stress is the rapid formation of a high concentration of many types of ROS, a process which is termed an "oxidative burst". ROS in this case are considered to be secondary messengers as their production follows the perception of potential damage using a vast array of receptors, each specific to individual types of stress. This oxidative burst can be due to either biotic stress or abiotic stress, depending on whether the threat is a pathogen or a physical process.

Doke (1985) was the first to report the oxidative burst in potato tuber tissue due to a biotic stress, where inoculation of an avirulent race of *Phytophthora infestans* caused the generation of superoxide which was rapidly transformed into hydrogen peroxide. These findings have since been observed with a wide variety of bacteria, fungi and viruses (Low & Merida, 1996). We can therefore generalise that a biotic stress caused by infection from a pathogen characteristically leads to rapid generation of superoxide and accumulation of H_2O_2 (Lamb & Dixon, 1997; Wojtaszek, 1997; Grant *et al*., 2000).

Exposure to abiotic stress such as high concentrations of ozone can also lead to an oxidative burst and the production of ROS in the presence of water (Grimes *et al*., 1983), particularly in the apoplast and symplast (Lyons *et al*., 1999). Drought,

cold and salt stress are also capable of producing ROS such as superoxide, hydrogen peroxide and hydroxyl radicals in vegetation (Hasegawa *et al*., 2000; Xiong *et al*., 2002). Deficiency in soil content of K^+, a vital nutrient for plants, has been shown to cause H_2O_2 production in root cells (Shin & Schachtman, 2004). Meanwhile, Conklin *et al*. (1996) showed that an ascorbic acid deficient mutant of *Arabidopsis thaliana* (*soz1*) had a lower tolerance of UV-B irradiation than the wild type. Ascorbic acid is a well known scavenger of ROS and they therefore showed an indirect link between abiotic stress (UV-B radiation) and ROS production (see Section 1.4.3). It is now known that a background concentration of ROS exist throughout the life of a plant. The regulation of this concentration is very complicated (Figure 1.4.1) and involves 152 genes in the case of *Arabidopsis thaliana* (Mittler *et al*., 2004).

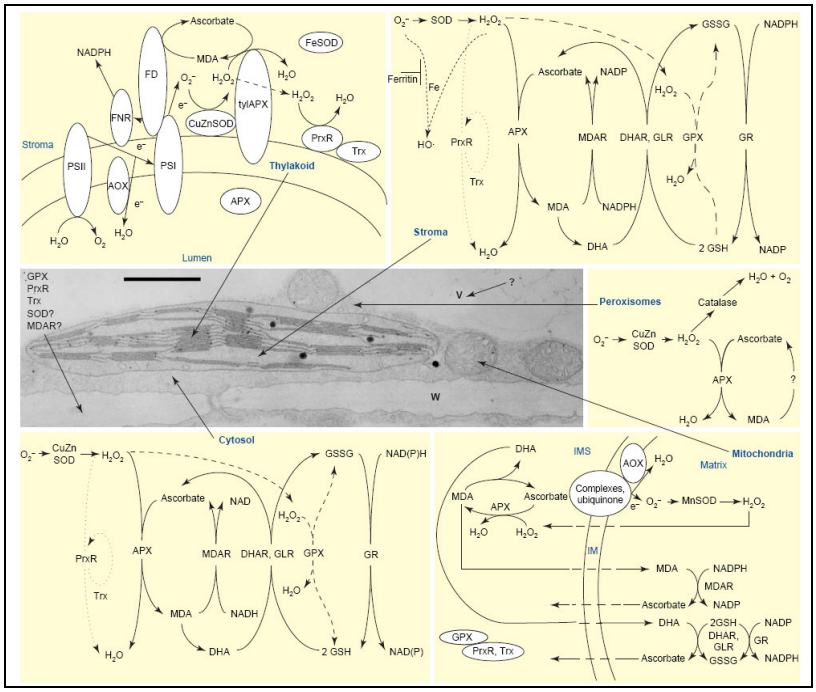

Figure 1.4.1 Localization of reactive oxygen species scavenging pathways in plant cells.

A transmission electron micrograph of a portion of a plant cell is used to demonstrate the relative volumes of the different cellular compartments and their physical

separation (middle left). The enzymatic pathways responsible for ROS detoxification are shown. The water–water cycle detoxifies O_2^- and H_2O_2, and alternative oxidase (AOX; *Immutans*) reduces the production rate of O_2^- in thylakoids [top left; in some plants iron superoxide dismutase (FeSOD) might replace CuZnSOD in the chloroplast]. ROS that escape this cycle and/or are produced in the stroma undergo detoxification by SOD and the stromal ascorbate–glutathione cycle. Peroxiredoxin (PrxR) and glutathione peroxidase (GPX) are also involved in H_2O_2 removal in the stroma (top right). ROS produced in peroxisomes during photorespiration, fatty acid oxidation or other reactions are decomposed by SOD, catalase (CAT) and ascorbate peroxidase (APX) (middle right). SOD and other components of the ascorbate–glutathione cycle are also present in mitochondria. In addition, AOX prevents oxidative damage in mitochondria (bottom right). In principle, the cytosol contains the same set of enzymes found in the stroma (bottom left). However, these are encoded by a different set of genes and the major iron-chelating activity in the cytosol responsible for preventing the formation of $^{\bullet}OH$ radicals is unknown. The enzymatic components responsible for ROS detoxification in the apoplast and cell wall (W) are only partially known, and the ROS-scavenging pathways at the vacuole (V) are unknown. Membrane-bound enzymes are depicted in white, GPX pathways are indicated by dashed lines and PrxR pathways are indicated by dotted lines in the stroma and cytosol. Although the pathways in the different compartments are mostly separated from each other, H_2O_2 can easily diffuse through membranes and antioxidants such as glutathione and ascorbic acid (reduced or oxidized) can be transported between the different compartments. Abbreviations: DHA, dehydroascrobate; DHAR, DHA reductase; FD, ferredoxin; FNR, ferredoxin NADPH reductase; GLR, glutaredoxin; GR, glutathione reductase; GSH, reduced glutathione; GSSG, oxidized glutathione; IM, inner membrane; IMS, IM space; MDA, monodehydroascorbate; MDAR, MDA reductase; PSI, photosystem I; PSII, photosystem II; Trx, thioredoxin; tyl, thylakoid. (Mittler *et al*., 2004).

It was only recently discovered that ROS also took part in many important signalling and developmental processes in cells. McAinsh *et al*. (1996) showed that H_2O_2 induced stomatal closure while Joo *et al*. (2001) demonstrated that H_2O_2 may have an important role in auxin signalling and gravitropism in maize roots. Concentrations of ROS have also been shown to increase during certain phases of a plant's life such as programmed plant cell death (e.g. senescence (Pennell & Lamb, 1997)). Foreman *et al*. (2003) showed that Ca^{2+} uptake was defective in an *rhd2* mutant of *Arabidopsis thaliana* and therefore cell expansion was compromised, but most importantly that RHD2 is an NADPH oxidase, a protein that transfers electrons from NADPH to an electron acceptor leading to the formation of ROS. This was the

first time ROS were linked to regulation of plant cell expansion through the activation of Ca^{2+} channels. Mori & Schroeder (2004) then demonstrated that this involvement of ROS in Ca^{2+} uptake had implications for polar growth, hormone transduction, stress signalling, and possibly mechanotransduction. Meanwhile, Uhrig & Hülskamp (2006) have linked ROS production from NADPH oxidases and plant growth via a Rho-like small GTPase, a well known group of intracellular signalling molecules. This research led Knight (2007) to speculate as to the function of this ROS signalling in root hair growth and in to their involvement in cell wall processes such as rigidification.

1.4.2 Studies of reactive oxygen species in plant cell walls

Reactive oxygen species have only recently been discovered to have important roles in the plant cell wall, particularly during fruit ripening, cell growth and cell wall degradation.

While production of superoxide and hydrogen peroxide have been observed after biotic stress (Doke, 1985), their biological reactivity and that of other ROS differ widely. Superoxide is only moderately reactive and has a negative charge which hinders it from crossing biological membranes, unlike H_2O_2 which is uncharged. In acidic environments such as cell walls, its protonation to form the hydroperoxyl radical ($HO_2^{\bullet}$; pK_a=4.8) occurs readily. $HO_2^{\bullet}$ is much more reactive than superoxide: it can attack fatty acids directly, has been shown to convert linolenic, linoleic, and arachidonic acids to lipid peroxides (Halliwell & Gutteridge, 1990), and is able to cross biological membranes because it is less polar than $O_2^{\bullet-}$. H_2O_2 has been demonstrated to be present in plant cell walls, although its metabolic

origin has been debated (Fahry & Schopfer, 1998; Lin & Kao, 2002; Zarra *et al*., 1999).

Because of the extremely short half-life of the hydroxyl radical, detecting its presence and action directly within a cell is very difficult. An indirect way of identifying $^{\bullet}OH$ action in the cell wall involves detecting the presence of particular 'fingerprints', compounds created only after $^{\bullet}OH$ attack of cell wall polysaccharides (Fry *et al*., 2001; Miller & Fry, 2001). This includes membrane-impermeant probes, such as [^{3}H]benzoylated hydrophilic polymers, which react with $^{\bullet}OH$ to give a quantifiable product, $^{3}H_2O$ (Fry *et al*., 2002; Miller & Fry, 2004). These data were then used to hypothesise that apoplastic H_2O_2 and polysaccharide-bound Cu^{+} (formed by reduction of Cu^{2+}, an ion widely present in plant cell walls, by non-enzymic electron donors (Fry, 1998)) could undergo a Fenton reaction ($H_2O_2 + Cu^{+} \rightarrow {}^{\bullet}OH + OH^{-} + Cu^{2+}$; Fenton, 1894) as a potential mechanism for $^{\bullet}OH$ formation *in vivo* (Fry *et al*., 2002). This Fenton reaction would also use naturally present ascorbic acid as a catalyst (Vreeburg & Fry, 2005; Lindsay & Fry, 2007).

Meanwhile, $^{\bullet}OH$ generated *in vivo* and *in vitro* with several species of plants (Schopfer, 2001) showed that $^{\bullet}OH$ attack could be linked to cell wall loosening and may have implications for the control of cell elongation growth. Liszkay *et al*. (2004) then demonstrated $O_2^{\bullet-}$ and H_2O_2 production, as well as peroxidase activity, in the growing zone of maize roots using specific histochemical assays and electron paramagnetic resonance spectroscopy. They also observed that experimental generation of ROS led to cell wall loosening, while scavenging of ROS suppressed

elongation, thereby demonstrating the necessity of ROS for normal plant growth through cell wall loosening.

1.4.3 Reactive oxygen species generation by radiation *in planta*

While ROS are regularly produced *in planta* because of natural environmental conditions, one way of increasing this production is through the use of external electromagnetic radiation. UV radiation, particularly UV-B and UV-C, have been used to study the effects of increased ROS production on plant material (Björn, 2002). There are two possible routes for UV-B-induced formation of ROS in the cell: a non-specific production of ROS during high UV-B levels after absorption of the energy content of the radiation by photosensitizers, such as aromatic amino acids or phenolic compounds; or a specific UV-B-dependent catalytic production of ROS at much lower levels of radiation, for instance by oxidases or peroxidases.

As previously discussed, there has been much interest in the genetic response of plants to UV-B. Only recently however has it been discovered that ROS may be intermediaries in these responses (A.-H.-Mackerness, 2000; Jordan, 2002). The effects of UV-B, as well as air pollutants such as ozone which often cause a similar reaction in plants, have been well reviewed by Langebartels *et al*. (2002), particularly with respect to the production of ROS. The use of mutants with over– or under–expression of genes coding for the production of known antioxidants is an effective way of investigating these effects. Indeed, the *soz1* (now renamed *vtc1*) mutant of *Arabidopsis thaliana*, deficient in ascorbic acid (an important ROS–scavenger), of Conklin *et al*. (1996) showed lower tolerance to UV-B irradiation than the wild type, thereby showing a link between UV-B irradiation and the production of ROS in plants, as well as the importance of UV-screening pigments and ROS scavengers for

plant survival. Subsequently, A.-H.-Mackerness *et al*. (2001) made the first attempt at identifying the nature of the ROS produced as a response to UV-B irradiation. They found that the increased expression in two pathogenesis-related genes were due to two different pathways. In the case of the up-regulation of *PR-1* transcript, it was through pathways involving hydrogen peroxide derived from superoxide, whereas the up-regulation of *PDF1.2* transcript was mediated through a pathway involving superoxide directly.

Another effective way of producing high levels of ROS *in vivo* is to use γ radiation. γ-rays have a much higher energy than UV radiation and are known to produce $^{\bullet}OH$ from water, approximately 40% of which lead to the production of hydrogen peroxide (LaVerne, 2000). Many studies have reported the effect of γ radiation on vegetation (Kovacs & Keresztes, 2002; Wi *et al*., 2007) and the importance of dose and rate on the level of ROS production (Kim *et al*., 2005). While the main focus of γ-irradiation experiments has been the study of its effects on DNA damage (Jiang *et al*., 1997; Britt, 1999), this was not the purpose of this study and so will not be discussed in depth. There is much interest in this field of research as high levels of radioactive pollution containing γ-emitters (e.g. ^{137}Cs, ^{60}Co) have been emitted in the last century, such as from the Chernobyl accident. Interestingly, Maxie *et al*. (1965) found that γ-irradiation of unripe lemons caused them to degreen faster and start emitting ethylene and carbon dioxide, though the mechanism for this effect is unknown. Experimental γ-irradiation of leaf material with a sealed source and at an unrealistic irradiation rate is the most common type of experimental study. Whilst some useful understanding can be obtained from such experiments, more realistic experiments using plant material collected from contaminated areas around

Chernobyl or areas of naturally high γ radiation have been carried out (Sawidis, 1988). It is possible that many of the effects of γ radiation on vegetation are due to the generation of ROS *in vivo*, and the fact that γ radiation can penetrate much deeper into plant material than UV make it a potentially useful tool for studies into the effects of ROS on plants.

1.5 Project aims

1.5.1 Effects of UV filtration on *Fraxinus excelsior* seedlings

- Identify candidate species and field sites for a study into the effects of selective UV-filtration on leaf litter decomposition and changes in cell wall content.

- Set up a field experiment using a set of selective UV-absorbing plastic and grow seedlings under polytunnels.

- Collect leaf litter after senescence and monitor subsequent changes in decomposition rate.

- Analyse leaf litter for chemical changes, particularly within the cell wall.

1.5.2 Aerobic methane production from pectin

- Investigate the reports made by Keppler *et al*. (2006) to identify potential mechanisms for methane emissions.

- UV-irradiate pectin with a range of lamp types and UV levels, as well as ambient UV, and monitor for methane emissions.

- Investigate the origin of the methane using a range of commercially available products and compounds synthesised in the laboratory.

- Identify possible mechanisms for methane emissions from pectin using ROS scavengers and generators.

- Monitor production of other gases such as methyl halides from pectin.

1.5.3 Reactive oxygen species in UV research

- Design a set of experiments to investigate changes in ROS levels experienced by polysaccharides using NaB^3H_4.

- Radio-label leaf litter from the UV-filtration field experiment to investigate possible changes in ROS levels due to removal of UV.

- Expose plant foliage to UV or γ radiation and monitor changes in radio-labelling.

2. MATERIALS AND METHODS

2.1 Routine laboratory techniques

All chemicals, unless stated otherwise, were obtained from the Sigma-Aldrich Chemical Company, Poole, UK. Any centrifugation was carried out with a Centaur 2 (MSE Ltd, London, UK) or a Micro Centaur for samples in 2-ml vials or less.

2.1.1 Alcohol-insoluble residue (AIR)

A sample of plant material was cooled with liquid nitrogen in a mortar and ground to a fine powder with a pestle, re-ground in 75% EtOH (v/v, 5 min) and centrifuged (3000 rpm, 5 min). The supernatant was rejected and the process was repeated until the supernatant was colourless. The sample was washed twice with acetone and dried overnight.

2.1.2 Sequential extraction of sugars

AIR (0.2 g) was loaded into an empty chromatography column (10 ml bed volume, 'Polyprep'; Bio-Rad Laboratories, Hercules, CA, USA) and an aliquot of phosphate buffer (6 ml) (Table 2.1.1) was added. The column was capped and gently shaken (24 h). The extractant was drained and stored at –25°C. The process was repeated, sequentially, with each solvent listed in Table 2.1.1.

The solid material that remained after the final extraction was dried (70°C, 48 h) and weighed.

A portion of extractant was diluted 80-fold with H_2O and analysed for total carbohydrate content.

Step	Solvent	Concentrations and conditions
1	Phosphate buffer	200 mM NaH_2PO_4, 0.5% w/v chlorobutanol, 10 mM $Na_2S_2O_3$, final pH adjusted to 7.0 with NaOH
2	Ammonium oxalate	0.2 M, 0.5% w/v chlorobutanol, 10 mM $Na_2S_2O_3$, final pH adjusted to 7.5 with NaOH
3	Urea	8 M H_2NCONH_2, 50 mM HEPES at pH 7.5
4	Sodium hydroxide	6 M NaOH, 1% w/v $NaBH_4$ at 37°C
5	Formic acid	5% v/v HCO_2H

Table 2.1.1 Solvents utilised for the sequential extraction of sugars.

2.1.3 Total sugar composition analysis

2.1.3.1 TFA hydrolysis

TFA (2 M, 1 ml) was added to the AIR sample (2 – 20 mg), heated (120°C, 1 h) and centrifuged (3000 rpm, 5 min). The supernatant was dispensed into a screw-cap Sarstedt tube, dried and redissolved in 0.5% (w/v) chlorobutanol. The sample was analysed by HPLC or paper chromatography.

2.1.3.2 Driselase digestion

Driselase (purified, as described in Fry (1982); 0.5% w/v, 500 µl, in PyAW 1:1:98 that contained 0.5% w/v chlorobutanol) was added to a sample of polysaccharide material (10 mg). The sample was incubated and gently shaken (37°C, 96 h). The sample was analysed by HPLC or eluted on a paper chromatogram.

If a sample had been previously subjected to TFA hydrolysis, the pellet was washed three times with water and dried before addition of the Driselase solution.

In the case of a time-course experiment, crude Driselase (0.1% w/v, 5 ml, in PyAW 1:1:98 that contained 0.5% w/v chlorobutanol) was added to a sample of leaf AIR (10 mg) and incubated at room temperature on a rotating wheel. After centrifugation (3000 rpm, 5 min), an aliquot (100 µl) of supernatant was removed after 1 h, 2 h, 3 h, 7 h, 24 h, 96 h, 168 h, 336 h, 504 h, 672 h, stored at –20°C and

analysed for total carbohydrate content. Samples with no Driselase added as well as samples with no AIR added were used as controls.

2.1.3.3 Total carbohydrate content

To 0.4 ml of an aqueous sample containing 2 – 15 µg carbohydrate, phenol (80% w/w, 10 µl) was added, followed by concentrated H_2SO_4 (1 ml). The solution was vortexed and allowed to stand at room temperature for 10 min. The sample was cooled in a water bath for 10 min and the absorbance was read (485 nm) with a spectrophotometer (CECIL, series 8000). Standards that contained known amounts of dextran (1 – 20 µg) were used for a calibration curve.

2.1.4 Assays

2.1.4.1 *m*-Hydroxybiphenyl assay for uronic acid content

A solution of borax ($Na_2B_4O_7.10H_2O$, 0.5% w/v, 10 ml) in concentrated H_2SO_4 was added to a 2-ml solution/suspension of the sample that contained 1 – 20 µg of uronic acid. The solution was incubated in a boiling water bath (5 min), cooled and the absorbance (520 nm) was read on a spectrophotometer (CECIL, series 8000). *m*-Hydroxybiphenyl (0.15% w/v, 20 µl) in NaOH (1 M) was added to the solution, incubated at room temperature (5 min) and the absorbance (520 nm) was read. The difference between the two readings indicated the uronic acid content. A calibration curve produced with galacturonic acid standards was used.

2.1.4.2 Determination of methyl ester content

Two replicate 0.75-ml samples of polysaccharide were set up and KOH (200 mM, 200 µl) was added to one of them and incubated at room temperature for 1 h, then KH_2PO_4 (1 M, 66 µl) was added. To the other replicate, 266 µl of 200 mM KOH/1

M KH_2PO_4 (3:1 v/v) was added. To 500 µl of each sample 50 µl of a solution containing 20 mM 4-aminoantipyrine and 120 mM phenol was added, followed by a horse-radish peroxidase solution (200 U/ml, 50 µl). Alcohol oxidase (400 U/ml, 40 µl) was then added to the solutions and, after mixing, left to incubate at room temperature for 10 minutes. The absorbance at 546 nm of the first solution was taken and the absorbance of the second solution was deducted from it.

Total methyl ester content was determined with a calibration curve made from standard solutions containing 50 – 500 nmol of methanol.

2.1.4.3 Assay for lignin

A solution of acetyl bromide/acetic acid (1:3 v/v, 1 ml) was added to a sample of leaf AIR (1 mg) and incubated (70°C, 30 min). After cooling to room temperature, NaOH (2 M, 0.9 ml) was added followed by glacial acetic acid (5 ml). Hydroxylamine-HCl (7.5 M, 0.1 ml) was added, and the solution was diluted to exactly 10 ml with acetic acid. Absorbance (280 nm) was read with a spectrophotometer (CECIL, series 8000).

2.1.5 Chromatography and electrophoresis

2.1.5.1 Paper electrophoresis

Samples were loaded onto Whatman 3MM paper. The paper was wetted with a PyAW buffer (1:10:189, pH 3.5), placed into a glass tank and hung from a trough situated at the top of the tank which contained the PyAW buffer. The bottom of the tank contained the same buffer to immerse the opposite end of the paper. The tank was filled with white spirit to act as an immiscible coolant. A voltage (2.9 kV) was applied through the buffer for 1.5 h.

2.1.5.2 Descending paper chromatography

Samples were dispensed onto Schleicher and Schuell 2045 B paper or Whatman 3MM paper. The paper was placed into a glass chromatography tank and hung from a trough situated at the top of the tank that contained the solvent (butanol/acetic acid/water (BAW) 12:3:5, ethyl acetate/pyridine/water (EPW) 8:2:1 or phenol (80% w/w). The tank was then sealed with a glass lid and the chromatogram removed after the appropriate time.

2.1.5.3 Thin-layer chromatography

The samples were loaded onto a TLC plate (MERK, non-fluorescent, silica gel 60, 20 × 20 cm) and placed into a glass tank containing 100 ml BAW (3:1:1). The tank was sealed with a glass lid and the plate was removed when the solvent front was approximately 2 cm from the top of the plate.

2.1.5.4 High-pressure liquid chromatography

2.1.5.4.1 Monosaccharide separation

A 20-µl sample of the monosaccharide solution was injected onto a CarboPac PA1 column fitted with a guard (Dionex, Leeds, UK) and detected with an ED40 amperometer (Dionex, Leeds, UK). The eluent system used was H_2O (1 ml min^{-1}) for 35 min, followed by an increasing NaOH gradient (from 0 mM to 800 mM) for 25 min.

2.1.5.4.2 Analysis of phenolics

A 50-µl sample of the phenolic solution was injected onto a Luna C18 column fitted with a guard (Phenomenex, Cheshire, UK) and analysed with a PDA100 detector (Dionex, Leeds, UK). The eluent system used was an increasing methanol gradient

(from 50% (v/v) to 96% (v/v) over 40 min; 1 ml min^{-1}) with a decreasing acetic acid gradient (from 0.015% (v/v) to 0.001% (v/v) over 40 min).

2.1.5.5 Staining

2.1.5.5.1 Silver nitrate stain

The paper chromatogram was dipped through three solutions (a – c). The paper was dried for 15 min each time before it was dipped through the next solution.

(a) $AgNO_3$ (5 mM in acetone; H_2O was used to redissolve any precipitate).

(b) NaOH (0.125 mM in 96% ethanol).

(c) $Na_2S_2O_3$ (10% w/v in water).

The paper was immediately transferred to a basin of water, washed for 1 h and then air-dried.

2.1.5.5.2 Thymol stain

A 0.53% (w/v) thymol solution was prepared in ethanol. Concentrated H_2SO_4 (to 5.3% v/v) was slowly added to the solution. The TLC plate was quickly dipped through this solution, dried and then placed in an oven (120°C, 10 min).

2.1.6 ^{1}H-Nuclear magnetic resonance (NMR) spectroscopy

Samples were dried and redissolved in D_2O (0.75 ml) or deuterated DMSO. ^{1}H-NMR spectra were measured at 25°C at 250 MHz in a Bruker ARX250 spectrometer. Chemical shifts are referenced to methyl signals in trimethylsilyltetradeuteriopropionate Na^+ salt (TSP) as zero ppm.

2.1.7 Quantitative assay of radio-labelled compounds by scintillation counting

Radioactivity was assayed in a Beckman LS 6500 multi-purpose scintillation counter. Aqueous samples were assayed with a 10:1 (v/v) ratio of 'OptiPhase HiSafe' scintillation fluid (Wallac, Milton Keynes, Bucks, UK) to aqueous sample. When the sample was needed for further experimental work, the sample was centrifuged (3000 rpm, 5 min), the scintillation fluid was removed and the pellet was washed four times with acetone.

2 ml of 'OptiScint HiSafe 3' (Wallac, Milton Keynes, Bucks, UK) scintillation fluid was added to the dry paper before assaying for radioactivity. When the sample was needed for further experimental work, the sample was washed four times with toluene.

2.1.8 Detection of compounds by fluorography

The paper was dipped through a solution of 2,5-diphenyloxazole (PPO, 7 % w/v) in diethyl ether. Kodak BioMax MR-1 film was positioned with the matt side down and fogged by a single flash from an orange hand-held flash gun (Amersham, UK) at a distance of 2 m from the film. Papers were then exposed to the fogged film for 4 weeks.

2.1.9 Elution of samples from paper

The section of paper containing the sample was rolled up and placed in the barrel of a 5-ml syringe. The barrel was placed into a 15-ml centrifuge tube and the paper was wetted with water. The tube was then centrifuged (3000 rpm, 10 min). The elution process was repeated five times (Eshdat & Mirelman, 1972).

2.1.10 Statistical analysis of data

Data are expressed as means ± SE, with number of replicates N and type of statistical analysis indicated in figure legends. All statistical tests were performed with the MiniTab statistical package (version 14.1, Minitab Ltd, Coventry, UK).

2.2 Effects of UV filtration on *Fraxinus excelsior* seedlings

2.2.1 Preparing the seed beds and planting the seeds

Four strips of soil (20 × 1.2 m) were prepared at the nursery site of Forest Research in Headley, Surrey (UK National Grid Reference SU 812381). Each strip was divided into four plots three metres long, separated by two metres, giving sixteen plots which were allocated to four replicates of the three types of UV treatments and the controls. The location of the 16 treatments was divided into four blocks and randomised (Figure 2.2.1).

Five trenches ~2 cm deep and 15 cm apart were dug along each strip with a tractor, and another two trenches were dug by hand on either side, for the whole length of the strip. Ash seeds (*Fraxinus excelsior*, 1.5 kg) were then closely sown by hand on 10th April 2007 in the sixteen plots and covered with soil. A layer of grit was placed over each seed bed.

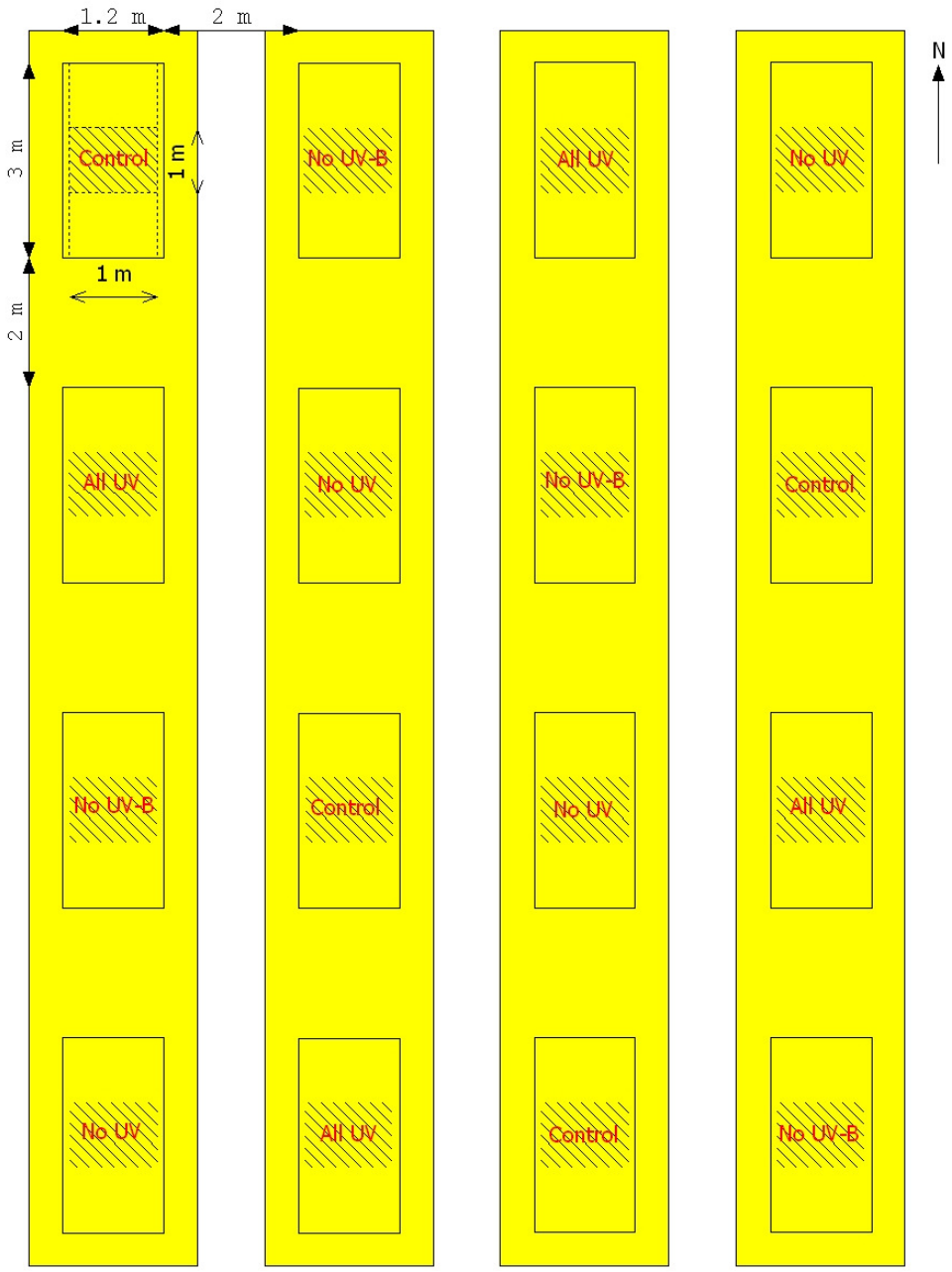

Figure 2.2.1 Layout of the UV exclusion field plots.
Black rectangles show individual plots, labelled in red with respective treatment applied. Shaded area represents area of data collection and the four yellow rectangles represent the four blocks used for statistical analysis.

2.2.2 Construction of polytunnels

Stainless steel hoops (semi circular, 1.2 m wide and 50 cm high) were placed at the ends of each of the sixteen plots and in the middle of each plot. A bird net was placed over each strip and held down with tent pegs. UV-absorbing and UV-

transmitting plastics (BPI agri, Leominster, Herefordshire, UK) and UV-B-absorbing plastic Mylar (Hifi Industrial Film, Stevenage Hertfordshire, UK) were cut to dimension (1.75 × 3.2 m) and attached to the hoops with metal springs. A layer of UV-transmitting plastic was placed over each Mylar treatment to create the same amount of shading in each treatment. A wooden stake was then placed at each corner of the plots and the hoops were tied to them with rope. An electrified rabbit-proof fence was placed around the whole site and remained on for the duration of the experiment, apart from short intervals when access to the site was necessary.

An irrigation system was installed on each end of the plots and was set to sprinkle water (15 min, every twelve hours) until the seeds germinated, after which it was reduced (20 minutes, daily). Weeding was carried out by hand about once a month to prevent shading of the seedlings. Herbicides were used to control weed growth outside the experimental plots, but a screen was placed around the plots to avoid chemical contamination. A layer of fertiliser (Sinclair 1:1:2 NPK) was applied in June 2007 because of the soil's low levels of phosphates and potassium, as commonly carried out at this site.

Photos taken at the field site (Figure 2.2.2) show several important intermediary steps in the process of the construction of the polytunnels and the planting of seeds for the field experiment.

Figure 2.2.2 Photos of several stages in the construction of the fieldsite.
(a) The plot before the construction of the polytunnels. (b) Planting the Ash seed. (c) The finished fieldsite with polytunnels.

2.2.3 Monitoring of field site environmental conditions

2.2.3.1 UV levels

2.2.3.1.1 UV dosimeters

UV dosimeters (Biosense Company, Bornheim, Germany) were placed horizontally on metal poles at the same height as the average seedling (~4 cm) of one plot of each

treatment for 7 days. The sensors were collected and sent to the company for analysis.

2.2.3.1.2 UV transmission measurement of plastics

A sample of each type of plastic filter was collected at regular intervals during the field experiment and its transmission over the 280 – 800 nm range was recorded with a 75-W Xenon arc lamp (LOT Oriel, Leatherhead, UK), a 10-cm integrating sphere and a scanning spectroradiometer with a double monochromator (Macam Photometrics, Livingston, UK) (data collected by Dr. J. Wargent, Lancaster University).

2.2.3.1.3 Spectral distribution of UV irradiance

A grid consisting of thirty rectangles (30 × 50 cm) was marked with string under each type of polytunnel. The UV levels were recorded at the corners of each rectangle with an erythemally-weighted broad-band UV sensor (Model PMA1102 analogue detector, Solar Light Co., Philadelphia, PA, USA; weighted with the McKinlay-Diffey erythema action spectrum) on an evenly overcast day around solar noon in September 2008. Ambient erythemally-weighted UV levels were recorded simultaneously. Sensors were calibrated for a clear sky, 30° solar zenith angle, 2.7-mm ozone column thickness, zero albedo and sea level. Data were averaged over one minute.

2.2.3.2 Temperature and humidity logging

Temperature and humidity sensors (USB-502, Adept Scientific, Letchworth, Hertfordshire, UK) were placed in the centre of one replicate plot of each treatment

at a height of 25 cm. The sensors were covered with white plastic lids to shield them from direct sunlight. Data was collected every 30 min.

2.2.4 Measurement of seedling height and leaflet number

The height above ground surface of 40 seedlings per plot was determined with a 30-cm ruler in August 2007. Leaflet number of each seedling was recorded at the same time.

2.2.5 Monitoring of mass loss during decomposition

On 9 – 10 October 2007, three layers of bird netting (mesh size ~2 cm) were placed over an area of 1 m^2 in the centre of each plot and held down with tent pegs (Figure 2.2.1). On 5 – 6 December 2007, the netting was removed and the fallen leaves were collected in individual plastic containers, in which they were air-dried for the next 10 days. The air-dried leaves (1 g) were placed in nylon mesh bags (Plastok® Associates Ltd., Merseyside, UK; mesh size 1000 µm, wrapped over twice), which were sealed with a heat gun and labelled. A plot (2 × 4 m) at the Dawyck Botanic Gardens (Ordnance Survey grid reference NT(36)173 352), selected for its proximity to 6 Ash trees (*Fraxinus excelsior*), was cleared of leaf litter, wooden stakes were placed at the corners and a rabbit-proof fence was erected. This plot was divided into 12 blocks, the decomposition bags were placed in them in a randomized way on 14 March 2008 and the plot was covered with ambient leaf litter (Figure 2.2.3). Three bags of each treatment were collected after 0.08 y, 0.16 y, 0.34 y, 0.52 y and 1.05 y, and the leaves were removed from the nylon mesh bag, dried in an oven (70°C, 24 h) and weighed. The temperature and humidity under the leaf litter was

monitored throughout with two sensors (USB-502, Adept Scientific, Letchworth, Hertfordshire, UK) at 30-min intervals.

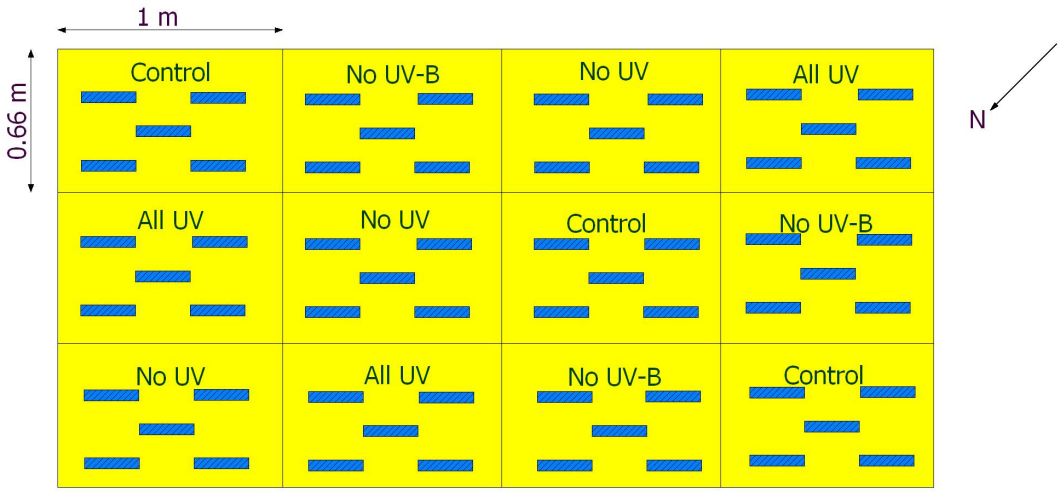

Figure 2.2.3 Layout of fenced enclosure at Dawyck Botanic Gardens used for litter bag decomposition studies.
Blue hashed boxes represent exact location of the bags.

2.2.6 Carbon, nitrogen and $\delta^{13}C$ content analysis

Carbon and nitrogen content were analysed with a NA 2500 Elemental Analyser (CE Instruments, Wigan, UK). Isotopic data were obtained with a PRISMIII dual inlet mass spectrometer (VG Analytical, Manchester, UK).

2.3 Methane production from pectin

2.3.1 UV irradiation experiments and measurement of CH_4 emissions

2.3.1.1 UV source type, location and measurement

UV radiation was provided by three types of lamp (UV313, UV340, UV351, The Q-Panel Company, Cleveland, USA) filtered with closely-wrapped 125-µm cellulose diacetate (CA lamp filter), which removed ultraviolet-C wavelengths (<280 nm). A filter of 36-µm UV-opaque polyester ('Courtgard', CPFilms Inc., Martinsville, USA) was used to remove UV-B and most UV-A wavelengths (< 380 nm). Lamp

irradiation was adjusted using a phase-angle dimming system. Experiments performed in natural sunlight took place in the horticultural gardens of the University of Edinburgh at UK National Grid Reference NT 270705 (55^{o} 55' N, 3^{o} 10' W), between 6 and 21 September 2006. Ultraviolet spectral irradiance was measured with a double monochromator spectroradiometer (SR991-PC, Macam Photometrics, Livingstone, UK) which was calibrated against tungsten and deuterium lamps traceable to National Physical Laboratory Standards (SR903, Macam Photometrics, Livingstone, UK). During outdoor experiments the solar spectrum was scanned at approximately 15-min intervals and monitored continuously with a broad-band UV sensor (Model PMA2102, Solar Light Inc., Glenside, USA) that was used to calculate changes in spectral irradiance between scans.

2.3.1.2 Preparation of impregnated glass fibre sheets

Glass fibre sheets (20.3 × 25.4 cm) were prepared from glass microfibre filters (Whatman GF/A, Maidstone, Kent, UK) and baked overnight in a furnace at 300°C. Commercial pectin (0.250 g) derived from citrus fruits (Sigma P9135, galacturonic acid content 84%, methoxy content 9.4%, loss on drying 4.1%) was dissolved in deionised water (25 ml) and let to dry on the GF sheet overnight. The ROS scavengers (DABCO (2 mmol), KI (2 mmol), mannitol (2 mmol and 20 mmol)) and generators (tryptophan, 2 mmol) were respectively added to the solution before the addition of pectin. Controls were made using water only with respective ROS scavenger or generator.

2.3.1.3 UV irradiation of glass fibre sheets

Glass fibre sheets with impregnated substrate were placed in new 5-l gas sampling bags of 25-µm UV-transparent polyvinylfluoride film (SKC Inc., Eighty Four, PA, USA) previously cut open on one side and then re-sealed using 40-µm aluminium adhesive tape. Bags were flushed five times before filling with 250 ml of stock external ambient air. Each pair of sample bags was used for three replicate experiments (which were determined not to have modified UV transmission of the bag material). One sample bag containing one pectin-impregnated glass fibre sheet and another sample bag containing a control glass fibre sheet were UV-irradiated simultaneously. Bags were supported on a black butyl rubber sheet (pond liner) on the surface of a thermostatically controlled water bath at 30°C. After 2 h, the CH_4 production was determined and then the pectin-impregnated and control sheets were reversed between bags for a further 2-h exposure. Outdoor experiments were performed with bags clipped to a temperature-controlled brass plate also covered with a black butyl rubber sheet. Temperature was measured inside a sample bag with thermocouples connected to a PC-based control system that adjusted the temperature of water from a re-circulating water bath. As outdoor UV levels were variable, experiments were conducted for one period of 2 h without reversing the treatment and control bags. However, the bags were reversed before the next experiment.

2.3.1.4 Gas concentration measurement

Methane and methyl halide concentrations were determined with a gas chromatograph (Hewlett Packard Series II 5890, Altrincham, UK) equipped with a flame ionisation detector and compounds were separated on a column packed with Haysep 80-100 mesh "Porapak Q" at 70°C (120°C in the case of methyl halides)

using a N_2 carrier gas. All experiments used an automatic sampler to which gas sample bags were directly attached, apart from the ROS attack of polysaccharide solution experiments for which 2 ml of the air space in the vial was injected directly into the carrier gas. The vials were fitted with syringes filled with 6 ml of ambient air to compensate for volume reduction and keep air pressure constant. Peak integration and autosampling was controlled using a chromatography data system (PeakSimple Model 203, SRI Instruments, Torrance, CA, USA).

2.3.2 Washing of pectins

A pectin solution (1% w/v) was precipitated in ethanol (75%, final conc.), filtered and the residue lyophilised. This was solubilised (1% w/v) and the process was repeated with EtOH:formic acid (15:1 v/v).

2.3.3 Synthesis of pectate

Pectate (de-methylesterified pectin) was prepared by addition of NaOH (1 M, 25 ml) to a pectin solution (1% w/v, 250 ml) previously cooled to 0°C, and incubated at 20°C for 2 h. Then, with vigorous shaking, sufficient H_3PO_4 (1 M) was added to bring the pH to 7.4 – 7.6 and the solution was lyophilised.

2.3.4 Synthesis of galacturonic acid methyl ester (GalAMe)

2.3.4.1 Acidified methanol method

Dowex 50 (1.25 g) was added to 25 ml of a solution of MeOH containing 2.5 ml of a 10% (w/v) GalA solution and stirred for 24 h. The Dowex 50 was removed by filtration and the sample was dried, redissolved in H_2O and lyophilised. The compounds were separated by TLC (BAW 3:1:1).

2.3.4.2 1,2;3,4-Di-*O*-Isopropylidene galacturonic acid method

Dowex 50 (50 mg) was added to 9 ml of a solution of MeOH containing 10 mg of 1,2;3,4-di-*O*-isopropylidene galacturonic acid (prepared by Prof. S. Fry) and of H_2O (1 ml). The reaction completion was assayed by TLC (BAW 3:1:1) at 24 h, 48 h and 72 h.

2.3.4.3 Dicyclohexylcarbodiimide (DCC) method

GalA (0.424 g) was dissolved in MeOH (10 ml) with 4-dimethylaminopyridine (DMAP) (0.02 g) at 0°C in an ice bath. DCC (0.456 g) was slowly added over 5 minutes, after which the ice bath was removed and the solution was stirred (room temperature, 3 h). The reaction completion was assayed by TLC (BAW 3:1:1) over 5 h, and the compounds were separated on a silica gel column in BAW (3:1:1).

2.3.5 Synthesis of homogalacturonan methyl ester (HGMe)

A homogalacturonan (HG) solution ("polygalacturonic acid" (Sigma), 5% w/v, pH 7 adjusted with $(C_4H_9)_4NOH$) was lyophilised and redissolved in a minimum volume of DMSO (dried with molecular sieves, type 4A) in a sealed flask. CH_3I was added (1.1 mol per mol GalA residues) and stirred in darkness (24 h). The solution was dialysed once against NaCl (0.2 M), twice with deionised water, and lyophilised.

2.3.6 ROS attack of polysaccharide solutions

A solution of each substance in d-H_2O (1% w/v, 15 ml) was placed in a 20-ml glass vial with a seal and crimp cap. Effects of superoxide ($O_2^{\bullet -}$), and/or its non-ionised equivalent the hydroperoxyl radical ($HO_2^{\bullet}$), were determined by addition of KO_2 crystals to a final concentration of 5 mM. Effects of H_2O_2 were determined by addition of a suitable volume of a 33% (v/v) solution to obtain a final concentration

of 5 mM H_2O_2. Effects of $^{\bullet}OH$ were determined by addition of Fenton reagent to achieve a final concentration of 5 mM ascorbic acid, 5 μM $CuSO_4$ and 5 mM H_2O_2. Effects of $^{\bullet}OH$-scavenging were determined by addition of mannitol to a final concentration of 0.5 M. For exclusion of sunlight, all vials were wrapped in Al foil.

2.4 Generation of reactive oxygen species by UV and γ-irradiation

2.4.1 Collection of plant material for radio-labelling

Ten leaves from trees within a 1 × 1 m area around the centre of each polytunnel at Headley were collected on 25th August 2007 and immediately placed in a screw-cap Sarstedt tube and stored on dry ice for transport to Edinburgh the next day. The samples were stored at –80°C before further analyses.

For γ-irradiation experiments, branches with 6 – 8 attached leaves of ash (*Fraxinus excelsior*) and birch (*Betula pendula*) were collected from the King's Buildings campus (National Grid Reference NT 270705).

2.4.2 γ-Irradiation of leaves

Within 30 minutes of collection, the branch was placed in a gamma irradiator (^{137}Cs source, activity of 55 TBq, ionising energy of 0.66 MeV). The samples were irradiated (12 Gy h^{-1}) for 0.1 h, 1 h or 20 h and were then stored at –80°C before further analyses. Un-irradiated leaves were used as controls.

2.4.3 UV-irradiation of plant material

The abaxial and adaxial sides of *Kalanchoe blossfeldiana* leaves were exposed to UV irradiation (8.71 W m^{-2}; UV313, The Q-Panel Company, Cleveland, USA) for 18 h at room temperature, as were lettuce leaves (*Lactuca sativa*). Irradiated leaves under a

filter of 36-µm UV-opaque polyester ('Courtgard', CPFilms Inc., Martinsville, USA) were used as controls. The UV-irradiated epidermis of the Kalanchoe leaves, the epidermis of the white tissue of the lettuce and the green tissue of the lettuce were then isolated and submitted to NaB^3H_4-labelling.

2.4.4 ^{3}H-labelling of ROS-attacked polysaccharides

The leaf was frozen with liquid nitrogen and ground to a fine powder with a pestle and mortar. A solution of $Na_2S_2O_3$ (10 mM, 10 ml) in EtOH/pyridine/acetic acid/H_2O (75:2:2:21, cooled to –20°C) was added and the leaves were ground further (5 min). An aliquot (1 ml) of the solution was collected and stored at –20°C. The supernatant was removed and the solid was washed with ethanol (75% v/v) and centrifuged (3000 rpm, 5 min). The washing was repeated three times. The supernatant was removed and NaOH (200 mM, 200 µl) was added to each leaf pellet and mixed well to saponify the methyl esters. After 5 minutes, a 500-µl aliquot of a $NaBH_4$ solution (1 mM, with 50 MBq of NaB^3H_4 in NH_3 (1 M)) was added to each sample and incubated at room temperature for 2 days. A xylose solution (100 mM, 10 µl) was added to each sample and incubated for 24 hours to react with any NaB^3H_4 remaining in solution. The lids of the tubes were then removed and the NH_3 was evaporated overnight. Acetic acid (50 µl) was added, followed by ethanol (3.5 ml). After centrifugation (3000 rpm, 5 min), the pellet was washed with ethanol (75% v/v) (this process was repeated three times), suspended in deionised water (100 µl) and assayed for ^{3}H. The ethanol washings were assayed for [^{3}H]xylitol by paper chromatography.

3. RESULTS

3.1 Effects of UV filtration on *Fraxinus excelsior* seedlings

3.1.1 Environmental conditions

3.1.1.1 UV levels

3.1.1.1.1 Comparison of polytunnel UV transmission

The transmission spectra of the three types of light filtration plastics used are shown in Figure 3.1.1.

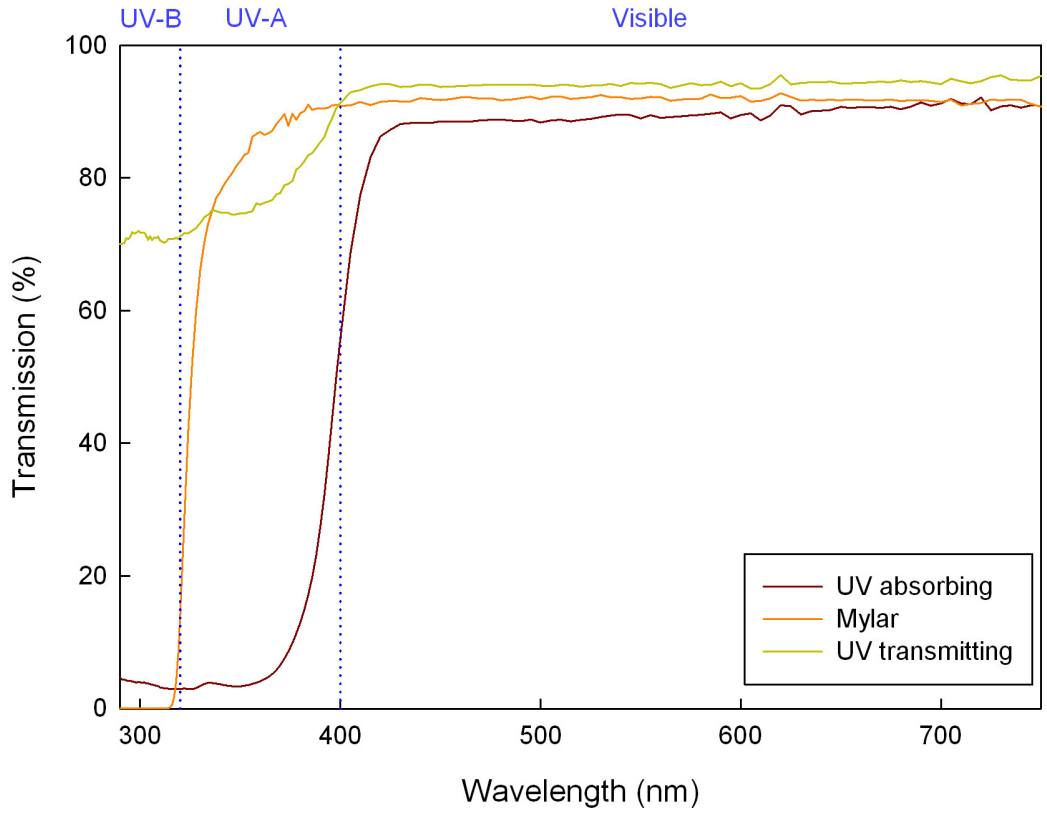

Figure 3.1.1 Transmission spectra of the three types of plastics.
Data was recorded with a 75-W Xenon arc lamp (LOT Oriel, Leatherhead, UK), a 10-cm integrating sphere and a scanning spectroradiometer with a double monochromator (Macam Photometrics, Livingston, UK) (data collected by Dr. J.Wargent).

The high absorbance of wavelengths below 320 nm (<1% transmission) of Mylar and the high transmission level above that make it an effective plastic for the

removal of UV-B only. One of the plastics supplied by BPI agri has a high absorbance below 400 nm (average of 11% transmission of UV-A and <5% transmission of UV-B) which makes it an effective plastic to use for the UV-absorbing treatment, while the high transmission levels (~75% transmission) down to 280 nm make the other plastic good for a UV-transmitting treatment. All plastics transmitted 85–95% of wavelengths above 400 nm. The treatments using these plastics will be named "No UV-B", "No UV" and "All UV" respectively. The treatment using no plastic will be named "Control".

The erythemally-weighted total UV levels under the polytunnels were recorded with broad-band UV sensors and compared to ambient levels. From these data, a contour plot of erythemally-weighted total UV transmission as a percentage of ambient erythemally-weighted total UV for each point under the three types of polytunnels was constructed (Figure 3.1.2).

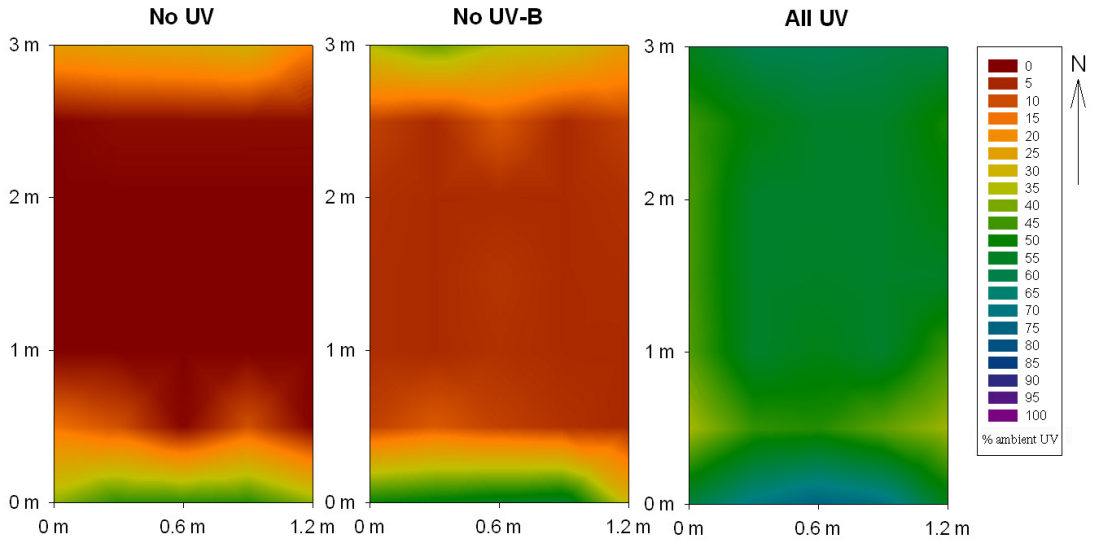

Figure 3.1.2 Contour plot of erythemally-weighted total UV levels for each type of polytunnel.
Data is shown as percentage transmission of ambient erythemally-weighted total UV level at each point. UV levels were recorded with broad-band UV sensors (Model PMA1102).

From these contour plots, it is possible to see how the UV levels vary under the polytunnels. In particular, they reveal that the plants within the outermost 50 cm of the north and south sides of each polytunnel experience higher UV levels than those in the centre. To account for such edge-effects, only trees within a 1 × 1 m area in the centre of the plots, where the UV distribution was uniform, were used for experimental analyses.

The erythemally-weighted total UV levels over a one week period were recorded with UV dosimeters (Biosense, Germany) (Table 3.1.1).

	Total UV level		
	$J.m^{-2}$	MED	% of ambient UV
Control	13316	53.3	100
No UV	<160	0.6	<1
No UV-B	2241	9.0	17
All UV	7565	30.3	57

Table 3.1.1 Summary of UV levels for the four treatments.
Data shows total erythemally-weighted UV dose received over seven days, expressed in $J.m^{-2}$, Mean Erythemal Dose (MED) and as a percentage of ambient levels.

The "All UV" treatment reduced erythemally-weighted UV levels to 57% of ambient, possibly due to the diffusing properties of the plastic and its slightly opaque nature. Also, as will be discussed in section 3.1.1.1.2, the weathering of the plastic may have reduced the ability of the plastic to transmit UV light. This effect can also be seen in Figure 3.1.2 where the UV levels were reduced to about 55% of ambient levels, evenly throughout the 1 × 1 m area in the centre of the polytunnel. The UV-B filter reduced UV levels to about 17% of ambient, while the UV-A and UV-B filter removed over 99% of ambient UV. These data suggest that at the start of the experiment the polytunnel design was adequate and that the plastics were effective for the selective removal of UV wavelengths.

3.1.1.1.2 Plastic spectral transmission changes in time

Due to weathering effects, the transmission levels of the plastics were expected to change with time. Small samples were therefore collected at regular intervals throughout the field experiment and their transmission levels against time were recorded (Figure 3.1.3).

Although the transmission levels in the UV range of the plastics before being placed outdoors fit the criteria for the UV exclusion experiment, Figure 3.1.3c shows that the transmission of UV-A and UV-B of the UV transmitting plastic gradually decrease with time until after 6 months only ~30% of all UV is being transmitted. The UV absorbing plastic (Figure 3.1.3a) showed very little change in spectral transmission throughout the experiment, while the UV-B absorbing plastic (Figure 3.1.3b) showed a gradual decrease in UV-A transmission with time (ranging from a 10% to 50% decrease depending on the wavelength). These data suggest that the seedlings grown under UV absorbing plastics received less than 5% of ambient UV, while the seedlings under UV-B absorbing plastics may have progressively received less UV-A and those under UV transmitting plastic will have been exposed to progressively much less total UV light than desired.

3.1.1.1.3 Radiation levels during field experiment

The daily UV levels from a near-by site in Chilton, Surrey, recorded by the Health Protection Agency for 2006 and 2007, were obtained for comparison with measurements at Headley (Figure 3.1.4).

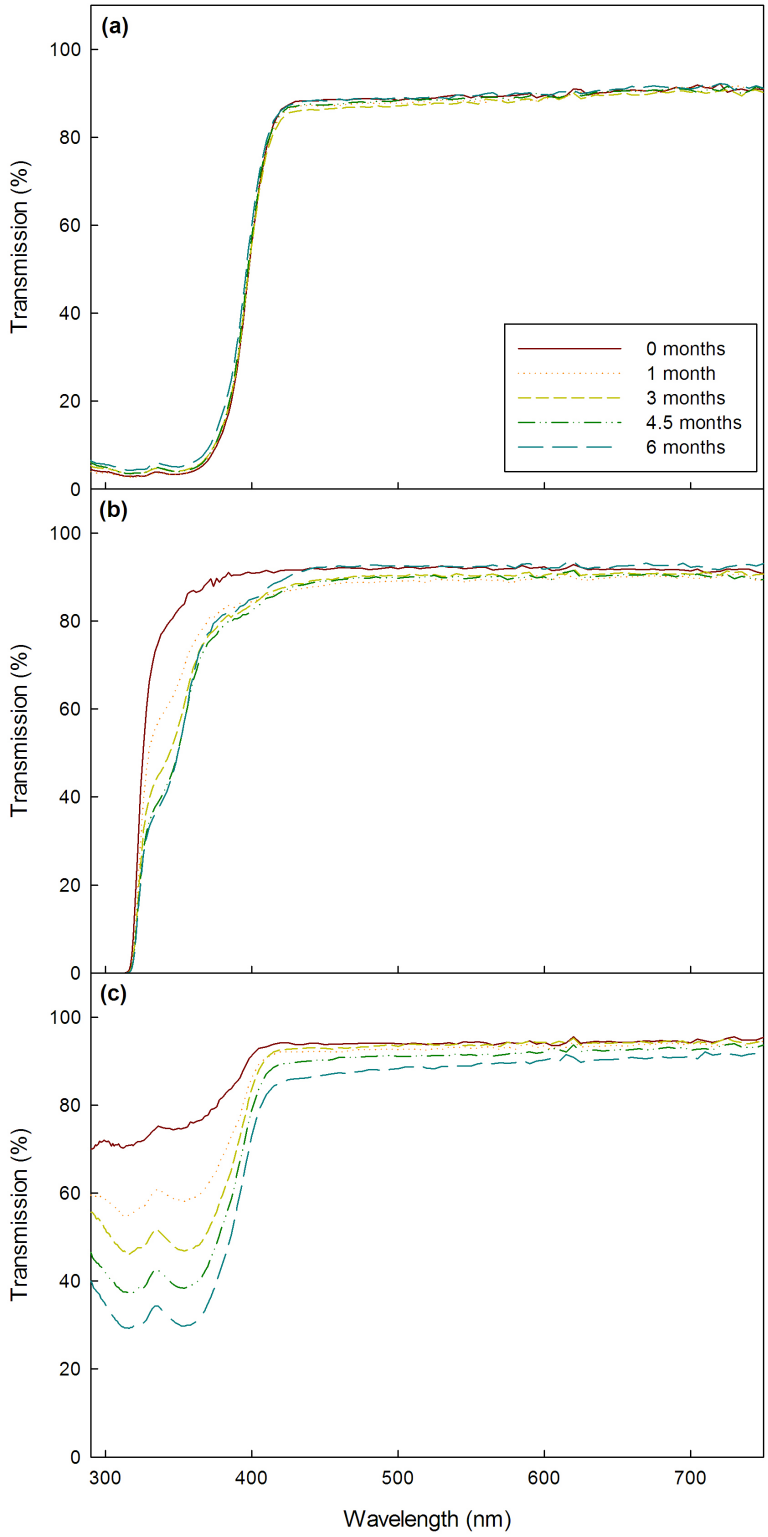

Figure 3.1.3 Change in spectral transmission of plastics with time.

(a) UV absorbing plastic, (b) UV-B absorbing plastic and (c) UV transmitting plastic sampled after 0, 1, 3, 4.5 and 6 months. Data were recorded as per Figure 3.1.1 by Dr. J.Wargent.

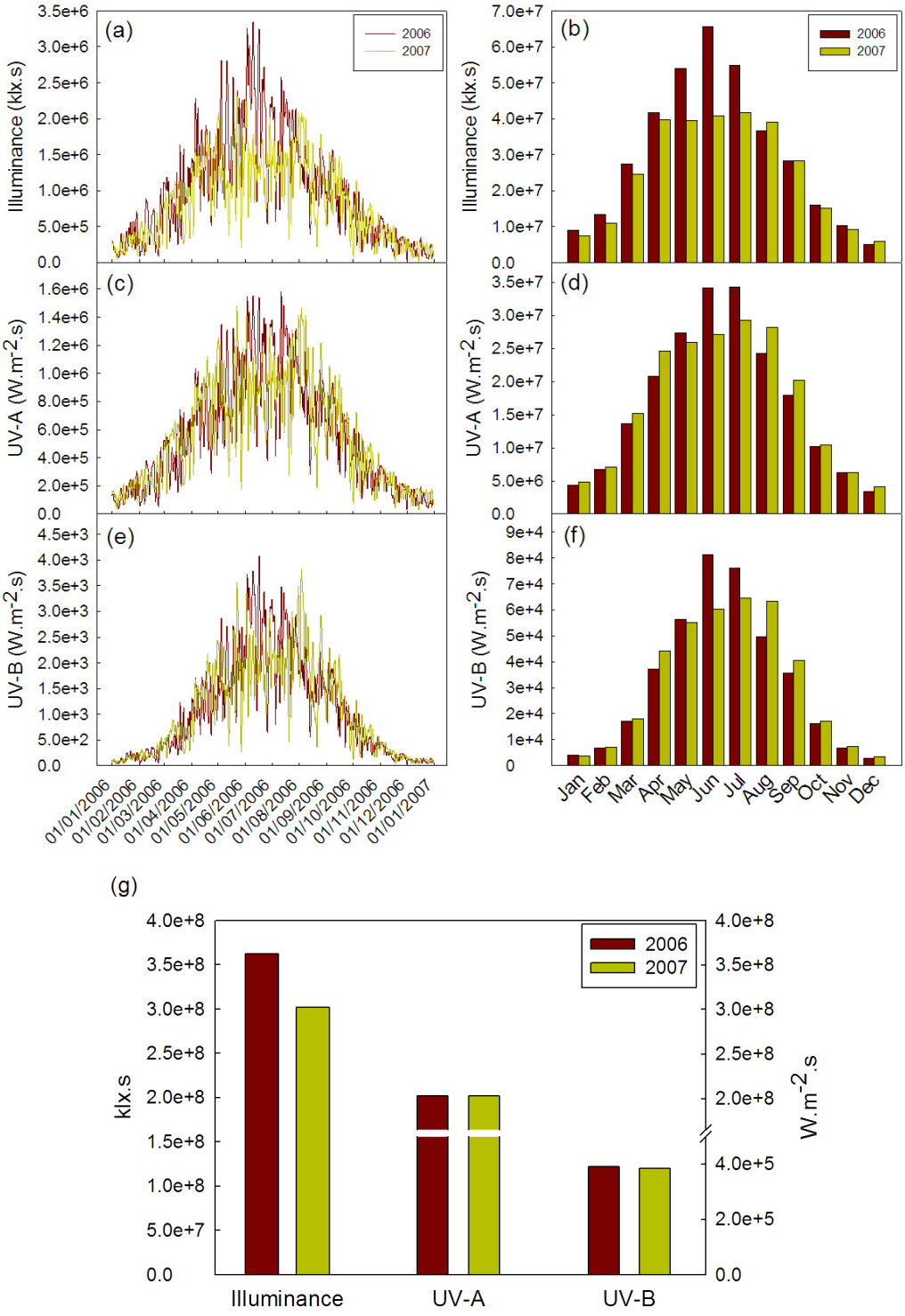

Figure 3.1.4 Radiation averages for 2006 and 2007.

(a, b) Illuminance, (c, d) UV-A levels, (e, f) erythemally-weighted UV-B levels and (g) yearly averages. Data were recorded with a SD14L-cos sensor (Macam Photometrics, Livingston, UK), a SD14A-cos sensor (Macam Photometrics, Livingston, UK) and a RB 501A sensor (Solar Light Company, Glenside, PA, USA) respectively and were collected by the Health Protection Agency (HPA) at their station in Chilton, Surrey, UK.

While the illuminance levels of 2007 were lower than in 2006 (3.02×10^8 klx s and 3.62×10^8 klx s respectively), the UV-A levels (2.03×10^8 W m^{-2} s and 2.03×10^8 W m^{-2} s) and the erythemally-weighted UV-B levels (3.84×10^5 W m^{-2} s and 3.89×10^5 W m^{-2} s) were almost identical.

From these data and the spectral scans of the plastics throughout time (see Section 3.1.1.1.2), it is possible to calculate an estimate of the UV-A and erythemally-weighted UV-B levels the plants under different treatments experienced. From the start of the experiment in March 2007 until the final point of leaf collection in early December 2007, the plants grown under "ambient" conditions received 1.8×10^8 W m^{-2} s of UV-A and 3.7×10^5 W m^{-2} s of erythemally-weighted UV-B, based on the data recording by the HPA in Chilton. Multiplying these values by the transmission levels of the plastics in the UV-A and UV-B region, and taking their change in transmission levels with time into account, one can calculate the amount of UV-A and UV-B the plants received and the percentage of ambient levels. In the "No UV" treatment, the seedlings received 2.3×10^7 W m^{-2} s of UV-A and 1.5×10^4 W m^{-2} s of UV-B (12% and 4% of ambient respectively). The "No UV-B" treatment consisted of a layer of Mylar and a layer of UV transmitting plastic (because the former was not a diffusing plastic like the other two) and therefore both changes in transmission levels need to be taken into account. The seedlings under this treatment therefore received 6.6×10^7 W m^{-2} s of UV-A and 375 W m^{-2} s of UV-B (35% and <1% of ambient respectively). The "All UV" treatment only transmitted 1.0×10^8 W m^{-2} s of UV-A and 1.7×10^5 W m^{-2} s of UV-B (54% and 47% of ambient respectively). These data are summarised in Table 3.1.2.

Levels	Control	No UV	No UV-B	All UV
UV-A (W m^{-2} s)	1.8×10^8 (100%)	2.3×10^7 (12%)	6.6×10^7 (35%)	1.0×10^8 (54%)
UV-B (W m^{-2} s)	3.7×10^5 (100%)	1.5×10^4 (4%)	375 (<1%)	1.7×10^5 (46%)

Table 3.1.2 Summary of UV-A and UV-B levels for each treatment.

3.1.1.2 Temperature and humidity

While an open-ended polytunnel was used to minimise any "greenhouse effects" (Debevec & MacLean, 1993), the temperature and the humidity under the polytunnels were still expected to differ from that experienced by the trees grown under no plastics. Sensors (USB-502) placed in the centre of the polytunnels recorded temperature and humidity every 30 min for the duration of the experiment (Figure 3.1.5). Averages of temperature and humidity data are found in Table 3.1.3.

While the average humidity under the plastics diminished slightly when compared to the Control treatment, the average temperature under the polytunnels increased by 1.0 – 1.5°C. These environmental changes are expected to affect some attributes of plant development (Grantz, 1990; Berry & Björkman, 1980; Iba, 2002) and will make comparisons with the control trees grown under ambient UV difficult. Since only four sensors were available, no replication of these measurements was carried out.

Average	Control	No UV	No UV-B	All UV
Temperature (°C)	13.9	14.9	15.4	15.3
Humidity (%rh)	80.7	79.1	77.1	76.1

Table 3.1.3 Temperature and humidity averages under UV treatments in 2007.
Data were recorded with USB-502 sensors (Adept Scientific) and averaged over the duration of the field experiment.

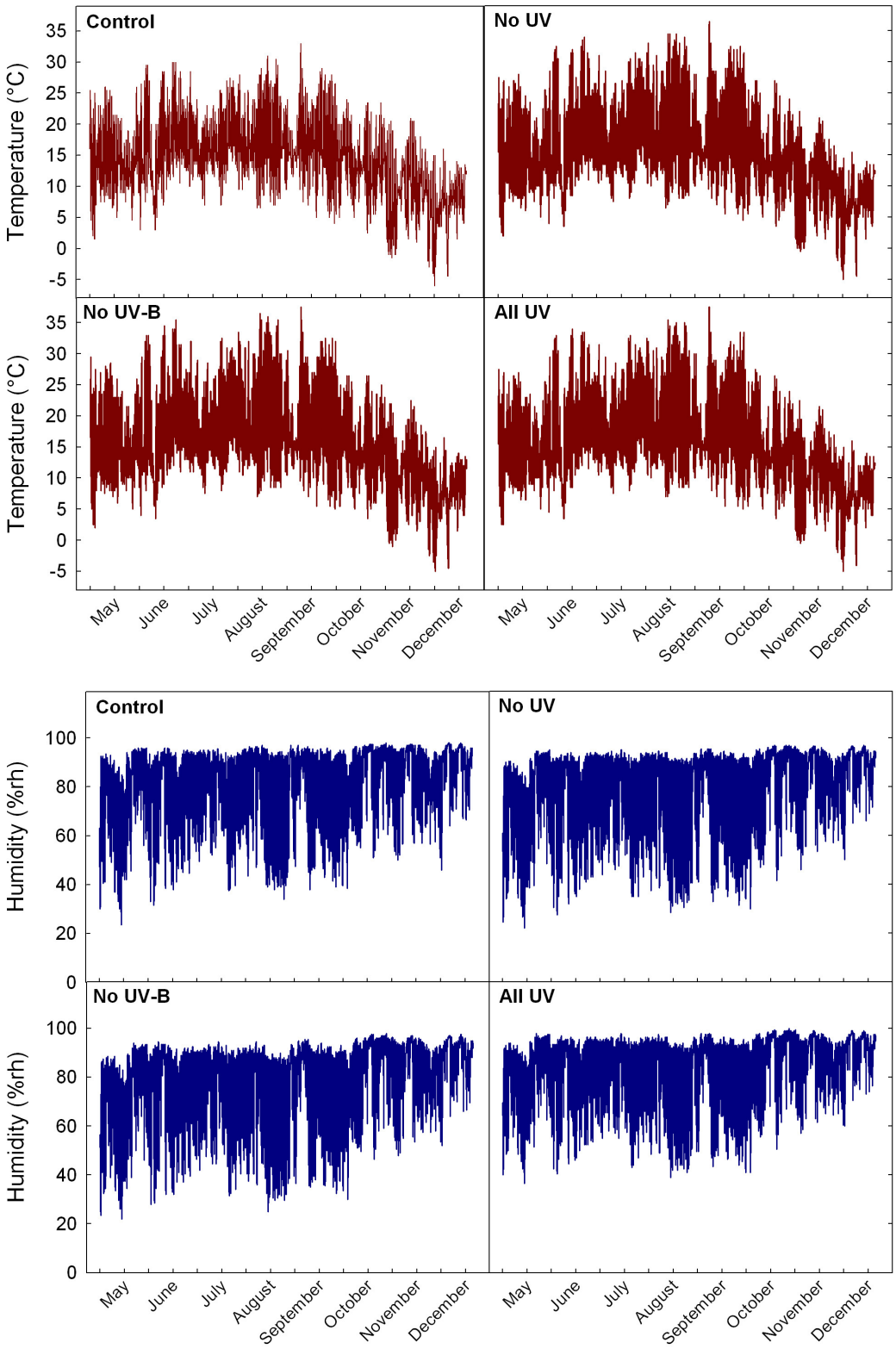

Figure 3.1.5 Profile of (a) Temperature and (b) Humidity for the four treatments.

Data were recorded every 30 min throughout the experiment with USB-502 sensors (Adept Scientific).

3.1.2 Effects of UV removal on tree growth and leaflet number

The tree height and leaflet number of 40 trees within a 1 × 1 m area in the centre of the plots was recorded in August 2007. Averages of the data can be seen in Table 3.1.4.

	Treatment				ANOVA	
	Control	No UV	No UV-B	All UV	*F* ratio	*P* value
Tree height (cm)	3.4 ± 0.1[a]	5.1 ± 0.2[b]	5.2 ± 0.5[b]	4.5 ± 0.4[a,b]	5.96	0.01
Leaflet number	16.1 ± 0.6	19.2 ± 2.1	21.4 ± 3.3	17.9 ± 2.3	0.95	0.45

Table 3.1.4 Average tree height and leaf number for each treatment.
Data were analysed with a one-way ANOVA (±SE, N=3). Subscript letters denote distinct groups after Tukey's multiple comparisons test.

A statistically significant ($P<0.05$) difference in tree height was observed between treatments. Using Tukey's multiple comparisons test, it was found that the height of the control trees was significantly different from the height of those grown under two of the plastic polytunnels. This is possibly due to the increase in temperature average under the tunnels leading to an increase in growth rate (Berry & Björkman, 1980). However, there was no significant difference in tree height between each of the three UV treatments with a plastic filter. Average leaflet number was not found to be statistically significant between treatments ($P=0.45$).

3.1.3 Effects on decomposition rate

Due to a lower germination rate than expected, insufficient leaf mass was recovered from individual plots to carry out decomposition studies with sufficient replicates from each individual plot as originally planned. Therefore, the leaves from each replicate treatment were pooled and fifteen 1-g samples of each treatment were placed in nylon mesh bags under leaf litter at the Dawyck Botanic Gardens (Figure 3.1.6).

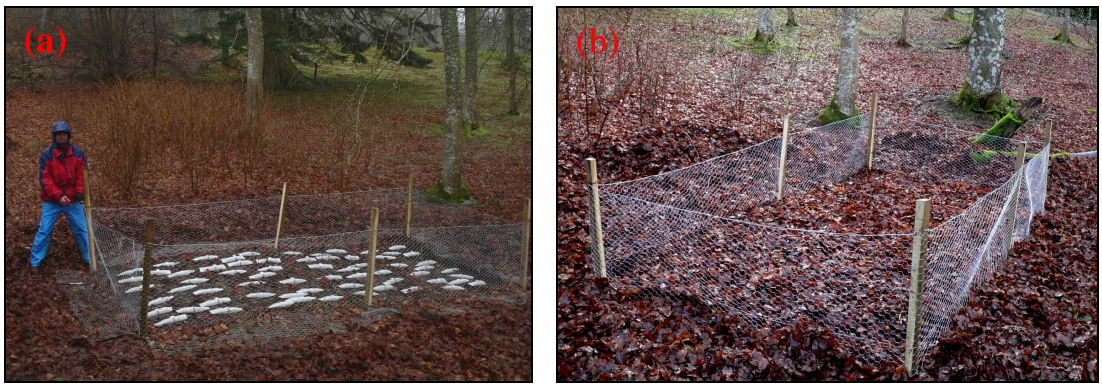

Figure 3.1.6 Photos of experimental plot for decomposition of leaf litter at Dawyck Botanic Gardens.
(a) Photo of layout of nylon mesh bags. (b) Photo of finished plot after covering with ambient leaf litter, with Ash trees in the background.

While some statistical data will be lost by pooling replicates, the decomposition study remained statistically valid and did not represent pseudo-replication. The location of the plot was chosen for its proximity to 12 *Fraxinus excelsior* trees, thereby ensuring that the appropriate fungi, bacteria and species of invertebrates for decomposition were present. Mass loss of the leaves was monitored against time (Figure 3.1.7).

The leaf litter followed the expected pattern of an exponential decomposition rate of mass loss against time (Figure 3.1.7a). After 1.05 y, the dry mass remaining, as a percentage of the starting mass, for the Control, No UV, No UV-B and All UV treatments were 41.9%, 32.3%, 31.7% and 42.2% respectively. Figure 3.1.7b shows a plot of $\ln(W_i/W_o)$ against time, where W_i is the mass remaining at time i and W_o is the mass before decomposition, and a linear regression of these data (of equation $\ln(W_i/W_o) = a - kt$, where t is time in years and a is the intercept). This allowed determination of the annual fractional weight loss values (k) for each treatment to be 0.70, 0.98, 0.99 and 0.69 respectively (r^2=0.83, 0.94, 0.96 and 0.84 respectively).

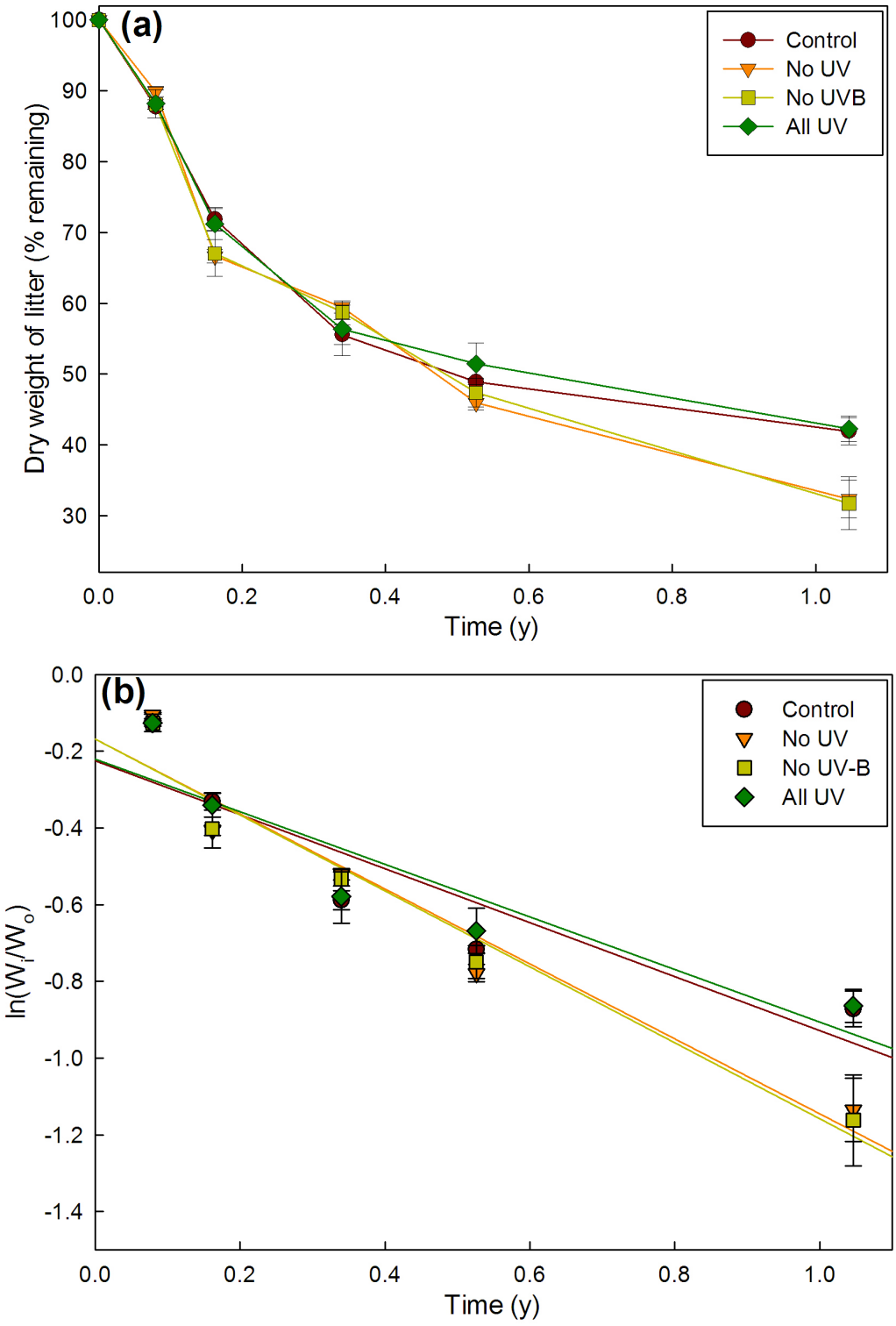

Figure 3.1.7 Effects of decomposition on mass of leaves from each UV treatment.

(a) Mass loss of leaves as percentage of starting mass against time; (b) Plot with fitted linear regression of $\ln(W_i/W_o)$ against time. Values are means of three replicates with standard error.

No significant difference in decomposition rate was found during the first six months, but after 1.04 y, a significant difference of 10% in mass remaining after decomposition between the No UV and No UV-B treatments and the All UV and Control treatments was found (P=0.03, after one-way ANOVA). The time in years for 95% loss of material to occur was estimated by 3/k, assuming an exponential rate of decomposition (Olson, 1963), and was calculated to be 4.3 y, 3.1 y, 3.0 y and 4.3 y for the Control, No UV, No UV-B and All UV treatments respectively. A photo (Figure 3.1.8) of a representative sample of leaf material from each treatment at different stages of decomposition shows no visible difference between treatments.

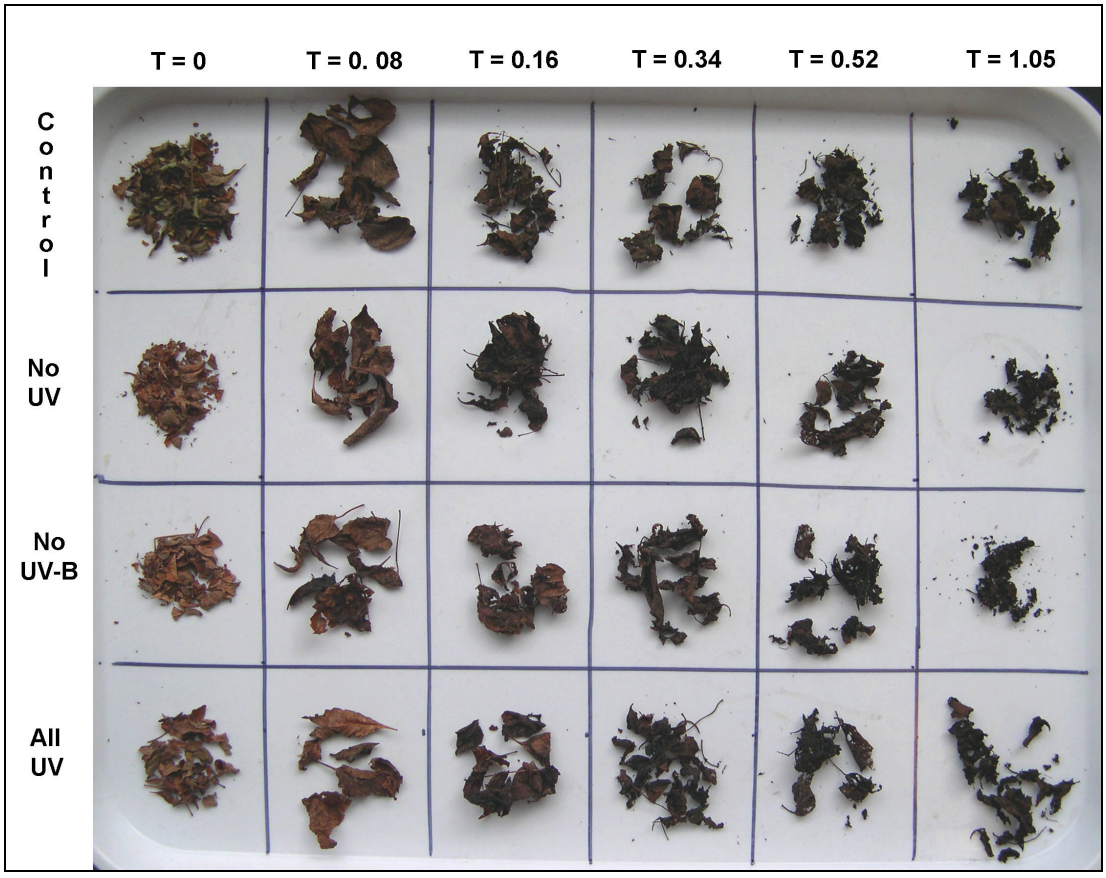

Figure 3.1.8 Photo of leaf material from each UV treatment at different stages of decomposition.
Amount of leaf material shown is not representative of the total amount remaining at each timepoint.

Two sensors (USB-502, Adept Scientific) were placed under the leaf litter for the duration of the experiment and recorded temperature and humidity at 30-min intervals (Figure 3.1.9). Data is only shown until September 2008 as failure of the sensors resulted in the loss of subsequent data.

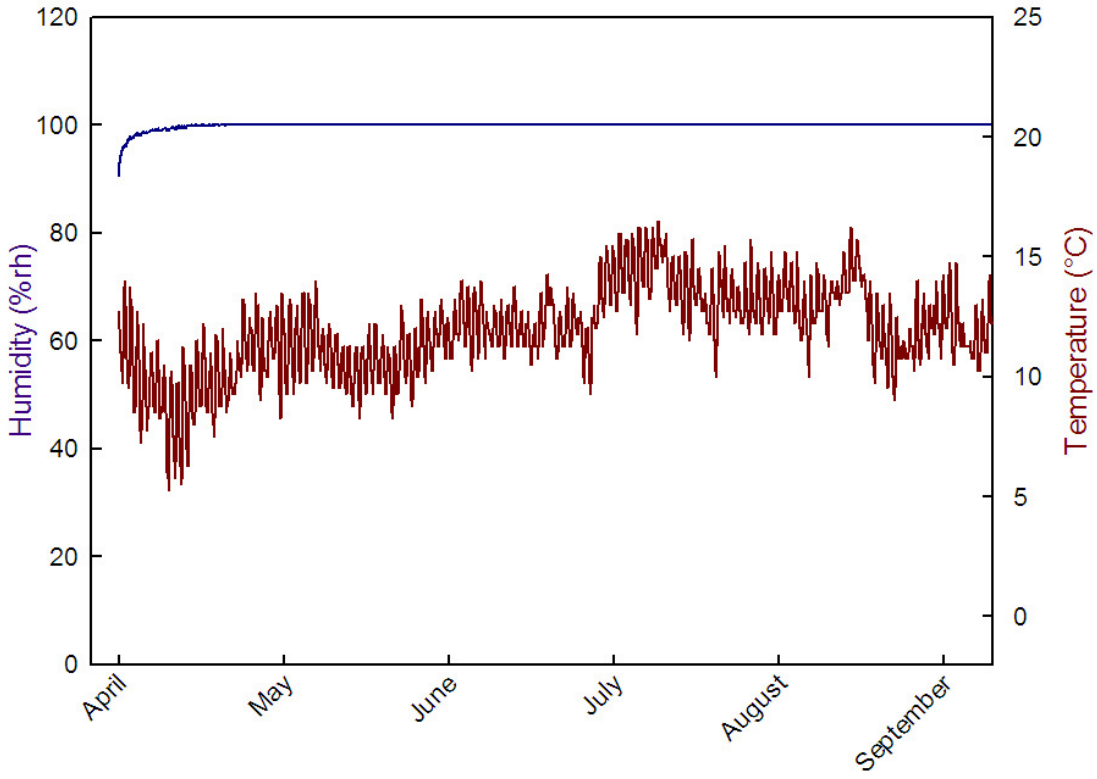

Figure 3.1.9 Temperature and humidity under leaf litter during decomposition. Data shows average of data from two sensors (USB-502, Adept Scientific) recorded at 30-min intervals.

3.1.4 Cell wall analysis

3.1.4.1 Sequential extraction of sugars

The leaves of each replicate treatment were extracted with 75% ethanol. The alcohol insoluble residue (AIR) was then submitted to a sequential extraction of sugars, following a similar protocol to McLeod *et al*. (2007). The phosphate buffer extracts the most weakly bound polysaccharides (Koimann, 1969), while the sodium

hydroxide will solubilise hemicelluloses. The residual carbohydrate after the final extraction is considered to be cellulose (Fry, 2000).

Solvent step	Carbohydrate (mg g^{-1})				ANOVA	
	Control	No UV	No UV-B	All UV	*F* ratio	*P* value
1. Phosphate	73 ± 3	93 ± 5	94 ± 8	103 ± 11	2.64	0.09
2. Am. Oxalate	79 ± 3^{a}	67 ± 4^{a,b}	63 ± 1^{b}	56 ± 3^{b}	8.08	<0.01
3. Urea	23 ± 3	25 ± 1	23 ± 3	23 ± 1	0.27	0.84
4. Sodium hydroxide	245 ± 21	279 ± 18	259 ± 8	241 ± 15	1.04	0.41
5. Formic acid	9 ± 1	10 ± 3	12 ± 2	10 ± 1	0.18	0.91
Cumulative 1-2	151 ± 2	160 ± 8	157 ± 8	158 ± 14	0.16	0.92
Cumulative 1-3	174 ± 2	185 ± 7	180 ± 7	181 ± 15	0.25	0.86
Cumulative 1-4	420 ± 20	465 ± 24	439 ± 8	422 ± 20	1.15	0.37
Total (steps 1-5)	429 ± 20	475 ± 25	452 ± 34	432 ± 22	1.07	0.40
Cellulose content	267 ± 20	277 ± 9	289 ± 5	265 ± 6	0.84	0.50

Table 3.1.5 Mass of carbohydrate extracted by each solvent from the four UV treatments.

Values are means (n=4) ± standard error. Data were analysed by one-way ANOVA, differently superscripted means were significantly different (P<0.05) after Tukey's multiple comparisons test.

While the ammonium oxalate extraction did show a significant difference, it did not follow the UV trend. No significant effect was observed in any other extraction. The cumulative step and total carbohydrate extracted were not significantly different between treatments, and the cellulose content left after extraction was not either.

3.1.4.2 Monosaccharide composition by TFA hydrolysis

The pooled AIR of each replicate treatment was submitted to TFA hydrolysis before decomposition, as well as after one year of decomposition. The sugar content was analysed by HPLC and the monosaccharide concentration was quantified (Table 3.1.6).

Before decomposition						
	Monosaccharide concentration (mg g^{-1})				ANOVA	
	Control	No UV	No UV-B	All UV	*F* ratio	*P* value
Fucose	1.1 ± 0.1	0.8 ± 0.1	1.1 ± 0.2	0.8 ± 0.1	2.20	0.14
Rhamnose	17.0 ± 0.6^{a}	18.8 ± 0.6^{a,b}	22.8 ± 1.0^{c}	21.4 ± 1.0^{b,c}	9.55	<0.01
Arabinose	19.4 ± 1.6	17.8 ± 0.3	20.9 ± 1.6	17.9 ± 0.9	1.37	0.30
Galactose	16.2 ± 0.6^{a}	17.2 ± 0.7^{a,b}	20.6 ± 1.5^{b}	18.7 ± 0.7^{a,b}	4.08	0.03
Glucose	25.2 ± 0.4^{a}	35.2 ± 1.3^{b}	38.8 ± 1.2^{b}	37.2 ± 1.9^{b}	21.91	<0.01
Xylose	12.9 ± 1.6	14.5 ± 0.9	15.5 ± 1.6	13.6 ± 1.0	0.71	0.56
Mannose	2.1 ± 0.3	2.3 ± 0.2	2.4 ± 0.1	2.6 ± 0.3	1.15	0.37
GalA	15.8 ± 2.5	22.5 ± 1.9	18.5 ± 2.3	21.3 ± 0.2	2.45	0.11
Total	109.7 ± 3.8^{a}	129.3 ± 3.3^{a,b}	140.6 ± 7.5^{b}	133.7 ± 5.1^{b}	6.50	<0.01
	Monosaccharide concentration (% total)				ANOVA	
	Control	No UV	No UV-B	All UV	*F* ratio	*P* value
Fucose	1.0 ± 0.1^{a}	0.7 ± 0.1^{b}	0.8 ± 0.1^{a,b}	0.6 ± 0.1^{b}	9.00	<0.01
Rhamnose	15.6 ± 1.0	14.6 ± 0.2	16.2 ± 0.4	16.0 ± 0.4	1.57	0.25
Arabinose	17.7 ± 1.1^{a}	13.8 ± 0.1^{b}	14.8 ± 0.4^{b}	13.4 ± 0.2^{b}	10.44	<0.01
Galactose	14.8 ± 0.6	13.3 ± 0.4	14.6 ± 0.5	14.0 ± 0.2	2.47	0.11
Glucose	23.1 ± 1.0^{a}	27.3 ± 1.2^{b}	27.7 ± 0.9^{b}	27.8 ± 0.4^{b}	6.02	0.01
Xylose	11.7 ± 1.3	11.2 ± 0.4	10.9 ± 0.6	10.2 ± 0.4	0.70	0.57
Mannose	1.9 ± 0.3	1.8 ± 0.1	1.7 ± 0.1	2.0 ± 0.3	0.41	0.75
GalA	14.2 ± 2.0	17.4 ± 1.3	13.2 ± 1.6	16.0 ± 0.6	1.69	0.22
After one year of decomposition						
	Monosaccharide concentration (mg g^{-1})				ANOVA	
	Control	No UV	No UV-B	All UV	*F* ratio	*P* value
Fucose	1.3 ± 0.1	1.8 ± 0.3	1.4 ± 0.1	1.1 ± 0.1	2.72	0.09
Rhamnose	27.4 ± 0.8^{a}	36.9 ± 3.9^{b}	35.2 ± 0.6^{a,b}	33.7 ± 0.4^{a,b}	4.14	0.03
Arabinose	8.0 ± 0.7^{a}	7.2 ± 1.0^{a,b}	5.8 ± 0.4^{a,b}	4.7 ± 0.7^{b}	4.30	0.03
Galactose	11.7 ± 0.8	11.9 ± 0.9	9.9 ± 0.3	9.2 ± 0.7	3.39	0.05
Glucose	48.2 ± 2.4^{a}	68.2 ± 7.1^{b}	61.4 ± 1.9^{a,b}	58.5 ± 2.3^{a,b}	4.25	0.03
Xylose	7.2 ± 1.2	7.6 ± 0.5	6.7 ± 0.6	6.0 ± 0.3	0.84	0.49
Mannose	5.1 ± 0.6	5.7 ± 0.4	4.8 ± 0.4	4.5 ± 0.3	1.46	0.27
GalA	6.3 ± 0.3^{a,b}	7.0 ± 0.2^{a}	6.0 ± 0.3^{a,b}	4.3 ± 1.2^{b}	3.27	0.06
Total	115.2 ± 6.4^{a}	146.3 ± 11.6^{b}	131.2 ± 2.7^{a,b}	122.2 ± 4.2^{a,b}	3.56	0.04
	Monosaccharide concentration (% total)				ANOVA	
	Control	No UV	No UV-B	All UV	*F* ratio	*P* value
Fucose	1.2 ± 0.1	1.2 ± 0.1	1.0 ± 0.1	0.9 ± 0.1	3.07	0.07
Rhamnose	23.8 ± 0.6^{a}	25.1 ± 0.6^{a,b}	26.9 ± 0.9^{a,b}	27.7 ± 0.8^{b}	4.58	0.02
Arabinose	7.0 ± 0.2^{a}	5.1 ± 1.0^{a,b}	4.4 ± 0.3^{b}	3.9 ± 0.5^{b}	5.08	0.02
Galactose	10.1 ± 0.3^{a}	8.2 ± 0.4^{b}	7.6 ± 0.1^{b}	7.5 ± 0.5^{b}	13.17	<0.01
Glucose	41.9 ± 0.7^{a}	46.4 ± 1.8^{a,b}	46.8 ± 0.6^{a,b}	47.9 ± 1.2^{b}	5.27	0.01
Xylose	6.1 ± 0.7	5.3 ± 0.6	5.1 ± 0.4	4.9 ± 0.2	1.00	0.42
Mannose	4.4 ± 0.2	4.0 ± 0.4	3.7 ± 0.2	3.7 ± 0.2	1.56	0.25
GalA	5.5 ± 0.2^{a}	4.8 ± 0.2^{a,b}	4.6 ± 0.2^{a,b}	3.5 ± 0.8^{b}	3.5	0.05

Table 3.1.6 Concentration of monosaccharides after TFA hydrolysis of ash leaf AIR before and after one year decomposition.

Values are means (n=4) ± standard error and were obtained by HPLC (Dionex, Leeds, UK). Data were analysed by one-way ANOVA, differently superscripted means were significantly different (P<0.05) after Tukey's multiple comparisons test.

The concentrations of rhamnose and galactose before decomposition were found to have significant differences between treatments, but only the Control and the No UV-B treatment were always different. The data did not show a trend when compared to UV levels. The amount of glucose extracted from the Control samples was significantly different from the other three treatments (P<0.01), which were not significantly different from each other, suggesting that the effect was not due to a difference in UV levels but from the presence of plastics, possibly due to a temperature effect. Significant differences in content of rhamnose, arabinose and glucose were found after one year of decomposition, but no trend with UV was observed.

3.1.4.3 Driselase digestion time-course

Samples of leaf AIR from each UV treatment were submitted to Driselase digestion and aliquots of the solutions were removed at selected time-points and assayed for total carbohydrate content (Figure 3.1.10).

Although significantly lower levels of carbohydrate were solubilised by the Driselase from the Control samples within the first 7 h (P<0.05), after 24 h they were no longer significantly different from the samples grown under plastic (Table 3.1.7). There was no significant trend of digestibility with respect to UV levels. The control experiments show that similar small levels of carbohydrate are solubilised in the PAW buffer only from the leaf AIR irrespective of UV treatment (~100 mg g^{-1} by the end of the time-course) and that the Driselase only samples contributed ~30 mg g^{-1} of total carbohydrate assayed. Table 3.1.8 shows the monosaccharide content in solution at several timepoints, but no trend with UV was found.

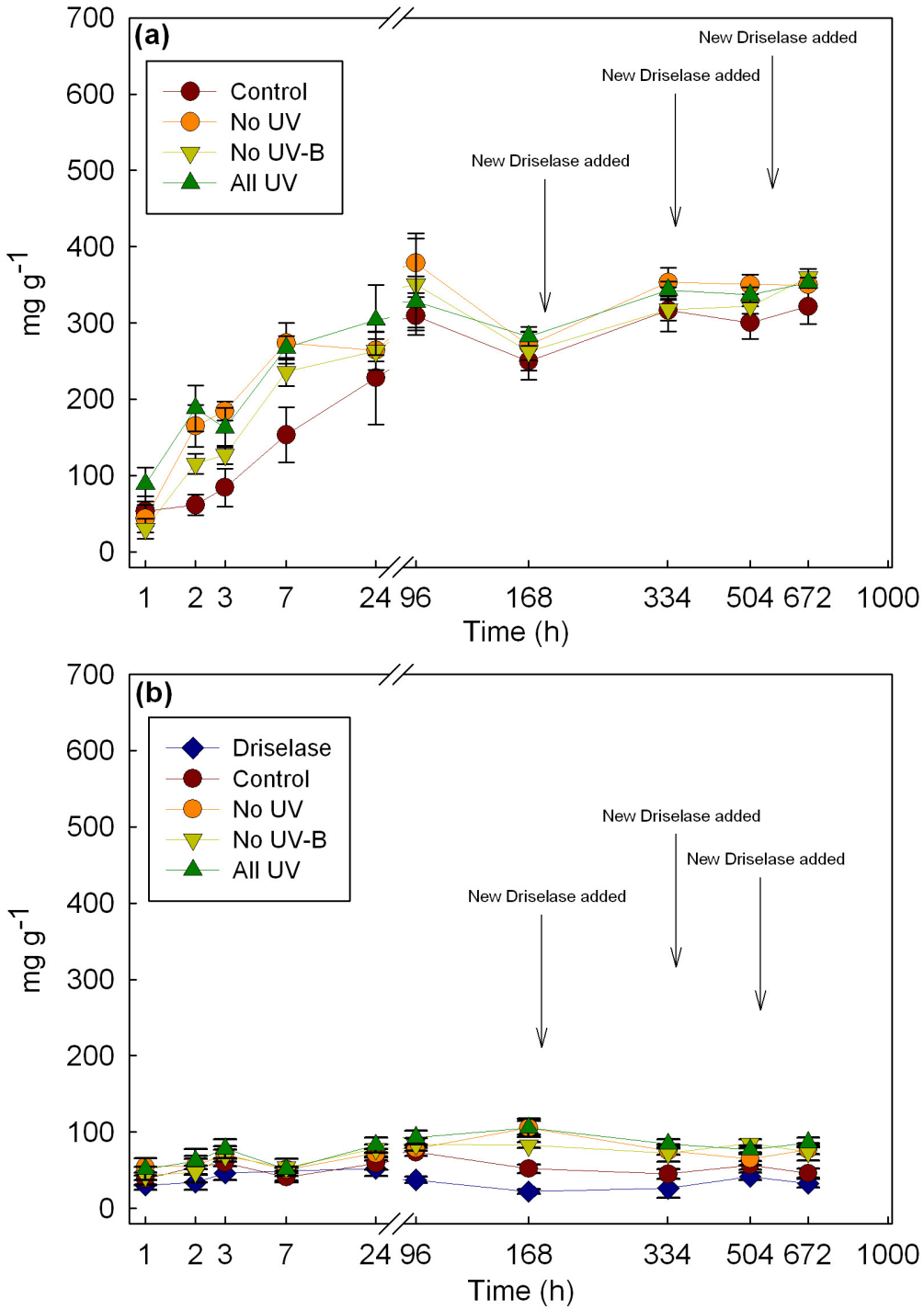

Figure 3.1.10 Total carbohydrate extracted by Driselase digestion of leaf AIR against time.

(a) Values of total carbohydrate extracted by Driselase from AIR with control sample values subtracted. (b) Total carbohydrate present in Driselase only control, and in AIR in buffer only control. Samples (10 mg) were suspended in PAW (1:1:98, 5 ml, with 0.5% chlorobutanol) buffer and where required a Driselase solution was added (0.1% w/v final concentration). Values of total carbohydrate present in solution were obtained with the phenol/sulphuric acid assay.

Time (h)	Monosaccharide concentration (mg g^{-1})				ANOVA	
	Control	No UV	No UV-B	All UV	*F* ratio	*P* value
1	53 ± 19	44 ± 18	30 ± 13	89 ± 22	1.81	0.199
2	61 ± 13 ^{a}	165 ± 27 ^{b}	116 ± 13 ^{a,b}	188 ± 30 ^{b}	6.35	0.008
3	84 ± 24 ^{a}	185 ± 12 ^{b}	127 ± 12 ^{a,b}	163 ± 26 ^{a,b}	4.83	0.020
7	153 ± 36 ^{a}	274 ± 26 ^{b}	236 ± 18 ^{a,b}	268 ± 15 ^{b}	4.78	0.021
24	228 ± 60	264 ± 15	263 ± 25	304 ± 46	0.58	0.639
96	309 ± 25	379 ± 39	351 ± 60	328 ± 33	0.51	0.680
168	250 ± 24	270 ± 19	263 ± 25	282 ± 12	0.43	0.734
334	317 ± 13	353 ± 19	318 ± 29	343 ± 11	0.91	0.466
504	300 ± 22	350 ± 13	322 ± 10	337 ± 10	2.21	0.140
672	322 ± 23	350 ± 3	360 ± 12	353 ± 7	1.52	0.260

Table 3.1.7 Total carbohydrate solubilised from leaf AIR by Driselase against time.

Values were obtained with the phenol/sulphuric acid assay. Values are means (n=4) ± standard error. Data were analysed by one-way ANOVA, differently superscripted means were significantly different (P<0.05) after Tukey's multiple comparisons test.

Time (h)	Compound	Monosaccharide concentration (mg g^{-1})				ANOVA	
		Control	No UV	No UV-B	All UV	*F* ratio	*P* value
2	Rhamnose	0.7 ± 0.1	0.8 ± 0.2	0.7 ± 0.2	0.3 ± 0.1	1.91	0.18
	Arabinose	0.8 ± 0.2	1.2 ± 0.1	1.2 ± 0.3	0.9 ± 0.1	1.53	0.26
	Galactose	1.4 ± 0.3^{a}	2.6 ± 0.2^{b}	2.3 ± 0.3^{a,b}	2.1 ± 0.1^{a,b}	4.77	0.02
	Glucose	8.3 ± 1.2	11.7 ± 0.5	10.7 ± 1.2	8.9 ± 0.4	3.03	0.07
	Xylose	0	0	0	0	-	-
	Mannose	0	0	0	0	-	-
24	Rhamnose	0.5 ± 0.1	0.5 ± 0.1	0.5 ± 0.1	0.4 ± 0.1	2.16	0.14
	Arabinose	3.6 ± 0.4	4.6 ± 0.3	4.2 ± 0.4	3.7 ± 0.2	1.53	0.26
	Galactose	4.9 ± 0.4^{a}	7.9 ± 0.6^{b}	6.9 ± 0.5^{b}	6.7 ± 0.3^{a,b}	7.10	<0.01
	Glucose	29.1 ± 1.7^{a}	37.2 ± 1.8^{b}	34.7 ± 2.5^{a,b}	31.6 ± 1.1^{a,b}	3.65	0.04
	Xylose	0.7 ± 0.1	0.7 ± 0.1	0.6 ± 0.1	0.6 ± 0.1	3.33	0.05
	Mannose	0.3 ± 0.1	0.3 ± 0.1	0.4 ± 0.1	0.4 ± 0.1	2.43	0.11
672	Rhamnose	3.6 ± 0.1^{a}	3.9 ± 0.2^{a,b}	6.3 ± 0.3^{c}	4.7 ± 0.2^{b}	31.7	<0.01
	Arabinose	15.9 ± 1.7^{a}	18.6 ± 1.1^{a}	27.8 ± 3.5^{b}	22.2 ± 0.6^{a,b}	6.32	<0.01
	Galactose	15.0 ± 1.1^{a}	22.0 ± 1.1^{a,b}	29.3 ± 3.9^{b}	24.9 ± 0.6^{b}	8.16	<0.01
	Glucose	77.1 ± 4.0^{a}	111.2 ± 5.5^{a,b}	170.6 ± 22.0^{b}	135.5 ± 3.1^{b}	11.5	<0.01
	Xylose	4.9 ± 0.2^{a}	7.3 ± 0.6^{a,b}	9.2 ± 0.2^{b}	9.4 ± 0.5^{b}	11.5	<0.01
	Mannose	11.2 ± 0.5^{a}	15.2 ± 0.6^{a}	30.5 ± 3.7^{b}	24.3 ± 0.3^{b}	20.72	<0.01

Table 3.1.8 Concentration of monosaccharides in solution during Driselase digestion at selected time points.

Values are means (n=4) ± standard error and were obtained by HPLC (Dionex, Leeds, UK). Data from controls and Driselase only samples have been subtracted. Data were analysed by one-way ANOVA, differently superscripted means were significantly different (P<0.05) after Tukey's multiple comparisons test.

3.1.4.4 Other chemical analyses

The uronic acid concentration, methyl ester content and lignin concentration of leaf AIR were determined (Table 3.1.9). A significant difference in methyl ester content (P<0.01) between the Control samples and the samples under polytunnels was observed, but no trend when compared to UV levels. No significant differences in lignin or uronic acid concentration were observed between treatments.

	Concentration (mg g^{-1})				ANOVA	
	Control	No UV	No UV-B	All UV	*F* ratio	*P* value
Uronic acid	7.3 ± 0.7	5.6 ± 0.4	5.6 ± 0.7	5.3 ± 0.3	2.48	0.111
Methyl esters	$9.72 \times 10^{-3} \pm 2.4 \times 10^{-3}$ [a]	$1.89 \times 10^{-2} \pm 8.1 \times 10^{-4}$ [b]	$1.83 \times 10^{-2} \pm 1.0 \times 10^{-3}$ [b]	$1.87 \times 10^{-2} \pm 1.1 \times 10^{-3}$ [b]	9.76	<0.01
Lignin	202.8 ± 14.1	255.9 ± 33.8	241.6 ± 6.9	246.6 ± 8.9	1.49	0.27

Table 3.1.9 Uronic acid, methyl ester and lignin concentration in leaf AIR of each UV treatment.
Values are means (n=4) ± standard error. Data were analysed by one-way ANOVA, differently superscripted means were significantly different (P<0.05) after Tukey's multiple comparisons test.

Sample		Treatment				ANOVA	
		Control	No UV	No UV-B	All UV	*F* ratio	*P* value
AIR	%N	1.7 ± 0.1[a]	1.2 ± 0.1[b]	1.2 ± 0.1[b]	1.2 ± 0.1[b]	7.22	<0.01
	%C	38.4 ± 0.2	38.2 ± 0.2	37.1 ± 0.7	36.6 ± 0.7	2.86	0.08
	C:N	23.2 ± 1.5	32.3 ± 2.6	32.4 ± 1.5	32.2 ± 3.8	3.32	0.05
	$\delta^{13}C$	-29.7 ± 0.2[a]	-28.5 ± 0.1[b]	-28.9 ± 0.3[b]	-29.0 ± 0.1[a,b]	7.09	<0.01
AIR after 1 year decomposition	%N	2.4 ± 0.1[a]	2.3 ± 0.1[a,b]	2.1 ± 0.1[b]	2.1 ± 0.1[b]	5.41	0.01
	%C	39.8 ± 0.3	41.0 ± 0.2	40.4 ± 0.8	40.4 ± 0.4	1.10	0.39
	C:N	16.3 ± 0.2[a]	18.0 ± 0.4[a,b]	19.5 ± 0.6[b]	19.5 ± 0.8[b]	7.26	<0.01
	$\delta^{13}C$	-30.8 ± 0.1[a]	-29.9 ± 0.1[b]	-29.9 ± 0.1[b]	-30.1 ± 0.1[b]	14.51	<0.01

Table 3.1.10 Carbon and Nitrogen content of samples under each UV treatment.
Samples were analysed with a NA 2500 Elemental Analyser (CE instruments, Wigan, UK). Isotopic data were obtained with a PRISMIII dual inlet mass spectrometer (VG Analytical, Manchester, UK). Values are means (n=4) ± standard error. Data were analysed by one-way ANOVA, differently superscripted means were significantly different (P<0.05) after Tukey's multiple comparisons test.

The carbon and nitrogen content as well as the $\delta^{13}C$ of the AIR of leaves before and after 1 year of decomposition were determined and the C:N ratio was calculated for each treatment (Table 3.1.10). A significant difference in %N was

found in the AIR samples between the Control leaves and the UV treatments in both cases, but no trend with respect to UV. %C values were not significantly different between treatments. C:N ratios of decomposed leaves and $\delta^{13}C$ values of decomposed and non-decomposed leaves showed significant differences, but no trend when compared to UV levels.

3.1.5 Effect of UV filtration on leaf phenolic content

The phenolic compounds present in the ethanolic extract from two leaves from four replicates of the four treatments were separated by HPLC. Absorbance at 298 nm per gram fresh weight of leaf was recorded and then averaged (N=4) for each treatment (Figure 3.1.11).

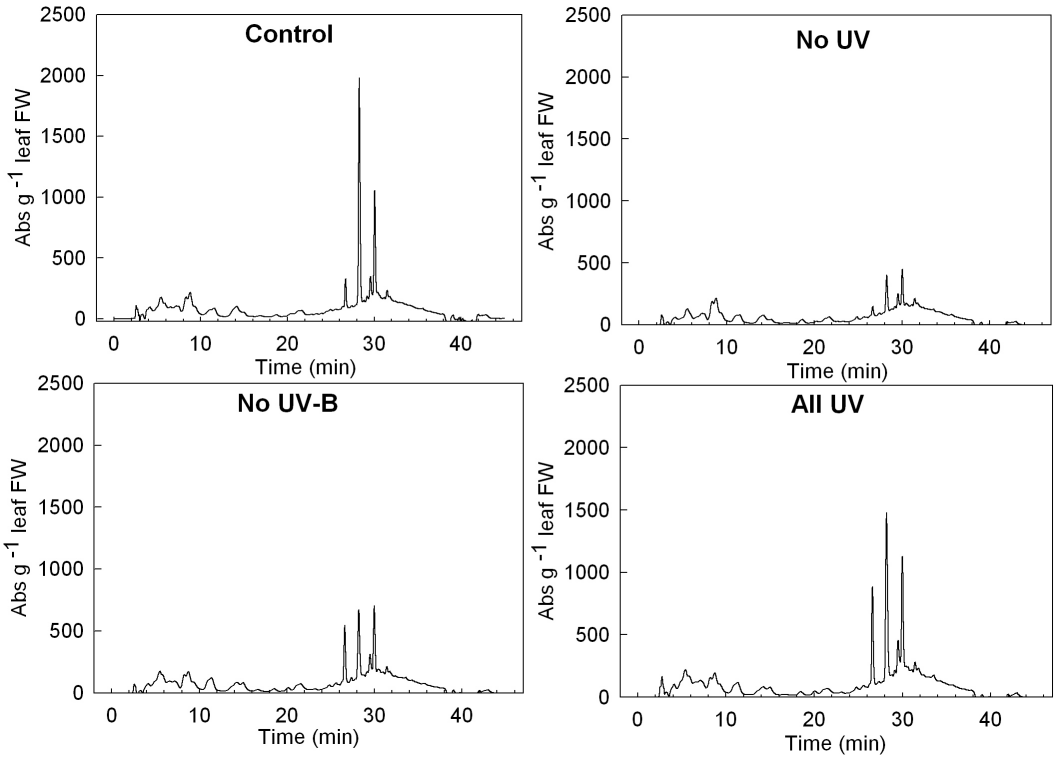

Figure 3.1.11 Average HPLC graphs of ethanolic extracts of each treatment. Samples were separated with a Phenomenex Luna C18 column fitted with a guard and analysed with a PDA-100 detector (1 ml min^{-1}, 50% (v/v) methanol with an acetic acid gradient). Data was expressed as absorbance at 298 nm per gram fresh weight against time.

The four large peaks in the 26 – 32 min range did not co-elute with any of the standards, but are in the range of coumaric acid (28.8 min) and cinnamic acid (32.5 min). Superimposing the averaged graphs of the four treatments (Figure 3.1.12) allows a better comparison. This shows that the area of these peaks, and hence of the amount of compound present, increases with increasing UV.

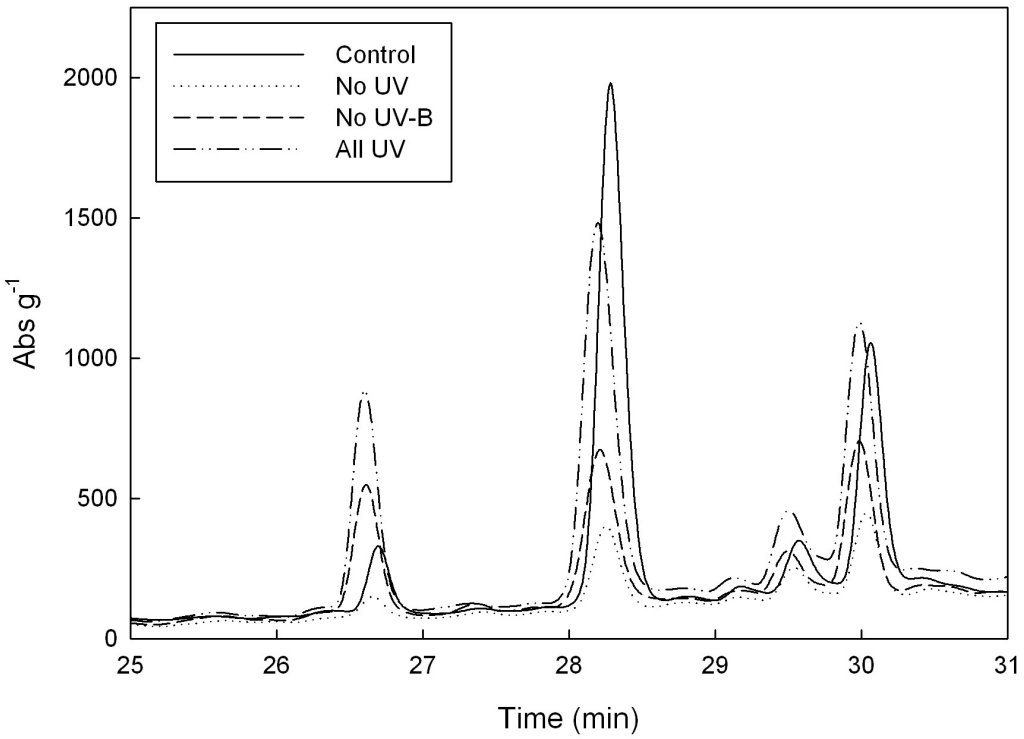

Figure 3.1.12 Superimposition of averaged HPLC phenolic data.
Data was recorded as per Figure 3.1.11.

These four peaks (retention times of 26.8 min, 28.1 min, 29.7 min and 30 min respectively) were isolated with a fraction collector. Their absorption spectra were recorded (Figure 3.1.13) and showed strong absorbance peaks between 331 nm and 351 nm, apart from the 30-min peak which only had an absorbance peak at 239.1 nm. They were submitted to mass spectrometry and ^{1}H-NMR, but too little compound

was present to allow identification. Further identification at this stage is not possible and the exact identity of these compounds remains unknown.

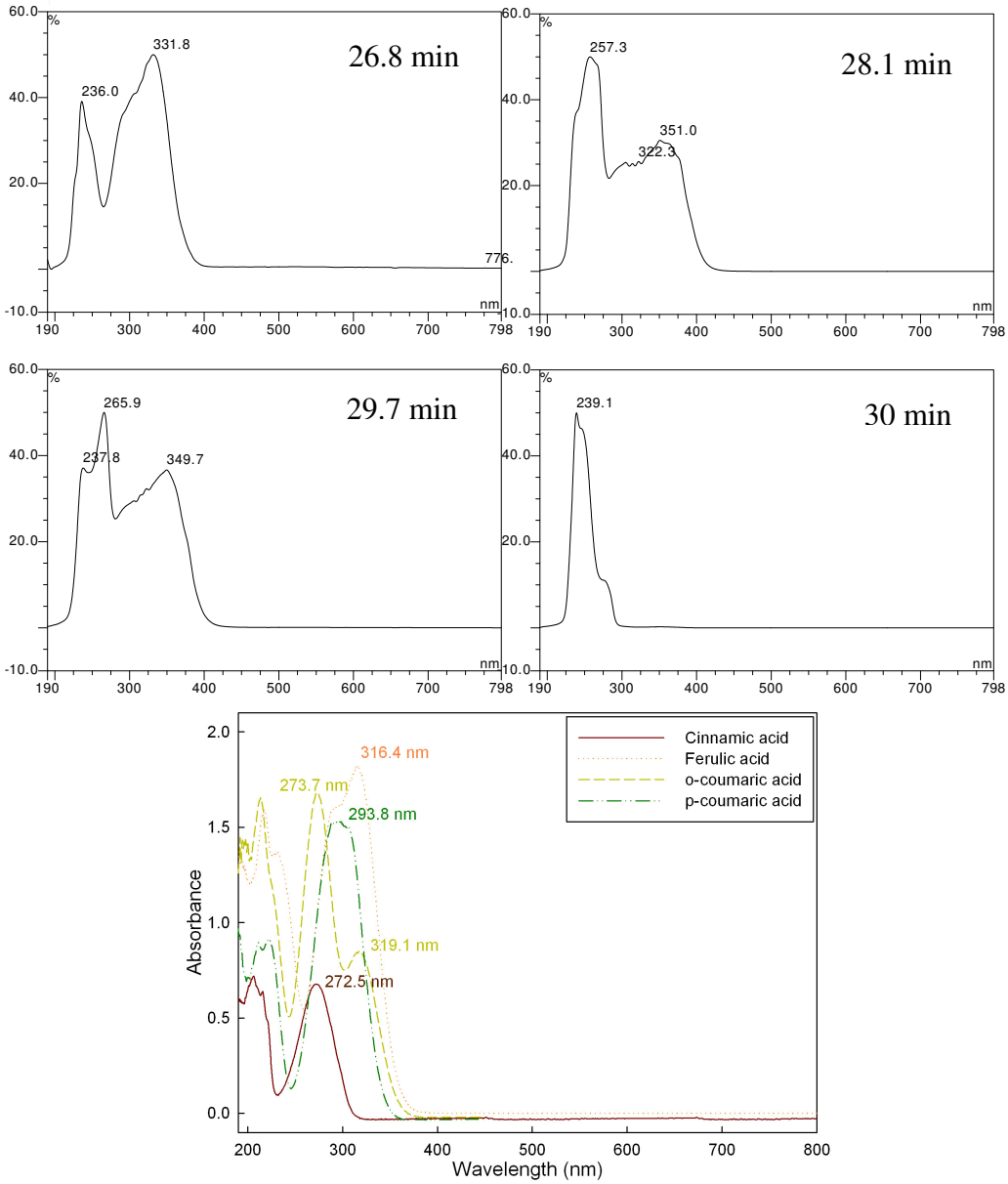

Figure 3.1.13 Absorption spectra of isolated phenolic peaks and of some standards.

Absorption spectra of standards were recorded on a spectrophotometer (CECIL, series 8000) while the absorption spectra of the HPLC peaks were recorded on a PDA-100 photodiode array detector (Dionex).

3.2 Methane production from pectin

3.2.1 Effects of UV irradiation on pectin and other compounds

3.2.1.1 Methane production from pectin sheets

Pectin sheets were placed in gas bags and irradiated with various levels of UV light from CA-filtered fluorescent lamps as well as several levels of ambient sunlight and methane emissions were recorded after two hours (Figure 3.2.1).

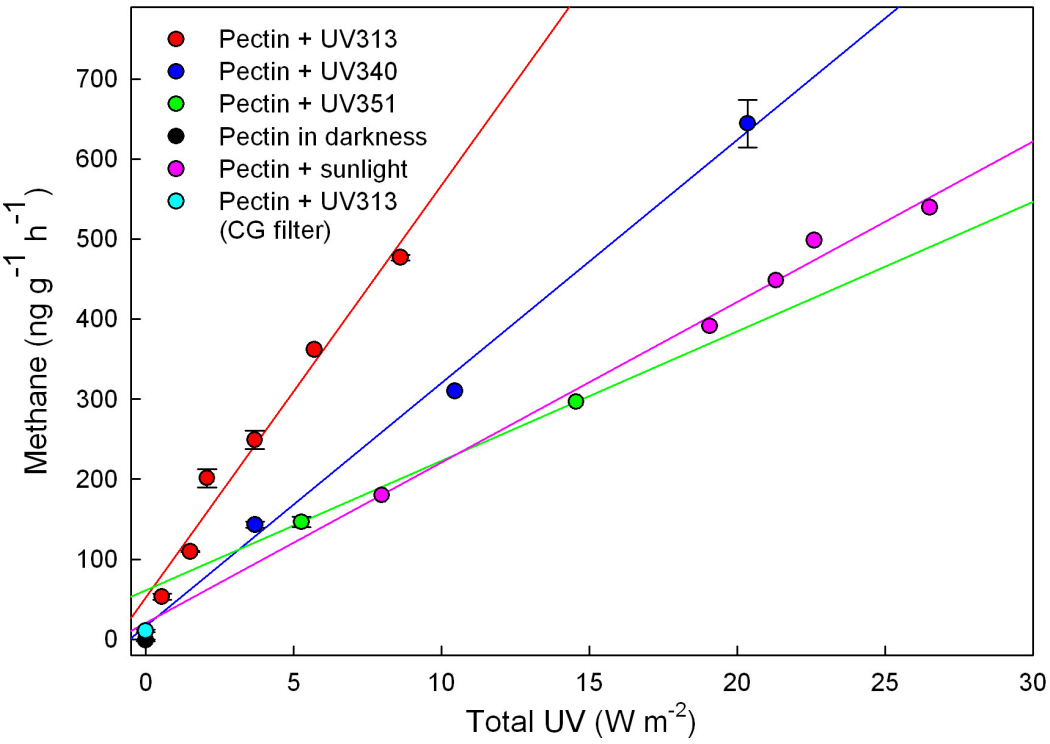

Figure 3.2.1 Methane production from pectin sheets against total UV level. Data were recorded on a gas chromatograph (Hewlett Packard Series II 5890) equipped with a flame ionisation detector and separated on a column packed with Haysep 80-100 mesh "Porapak Q" at 70°C using a N_2 carrier gas. Total UV levels were measured with Ultraviolet spectral irradiance was measured with a double monochromator spectroradiometer (SR991-PC, Macam Photometrics). Temperature was 30°C. Glass fibre sheets contained 250 mg of pectin. Values are means of three replicates with standard error bars, apart from the case of sunlight where data represent a one-time measurement.

To ensure that all the pectin present received a similar amount of UV radiation, the pectin was dissolved in deionised water and dried onto a glass fibre

sheet, a neutral compound which was shown to not produce methane under UV-irradiation (data not shown). A control in the dark was carried out, as well as a control with a UV filter ('Courtgard' (CG), removal of wavelengths below 380 nm). The temperature in all cases was controlled with a water bath and set at 30°C. Approximately half the data points were collected by Dr. A.McLeod using pectin sheets prepared by Prof. S.Fry.

A linear regression between total UV dose and methane emissions was fitted for each type of lamp (UV313, UV340 and UV351) and for sunlight (spectral irradiances of lamps and sunlight shown in Figure 3.2.2). No significant emissions were observed from pectin sheets in the dark or from the experiments using a total UV filter.

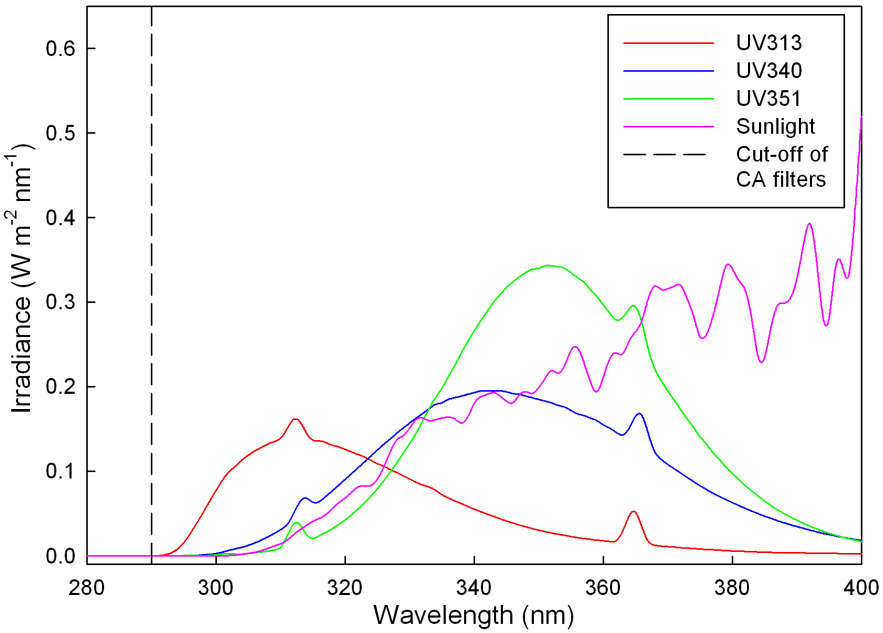

Figure 3.2.2 Spectral irradiance of each lamp type and of sunlight.
Spectral irradiance was recorded with a double monochromator spectroradiometer (SR991-PC, Macam Photometrics). Two lamps fitted with cellulose acetate (CA) filters were used in each measurement.

A range of published spectral and theoretical weighting functions were applied to the data (analysis performed by Dr. A.McLeod), and the best fit was obtained with an idealized weighting function that decayed one decade for every 80 nm (Figure 3.2.3).

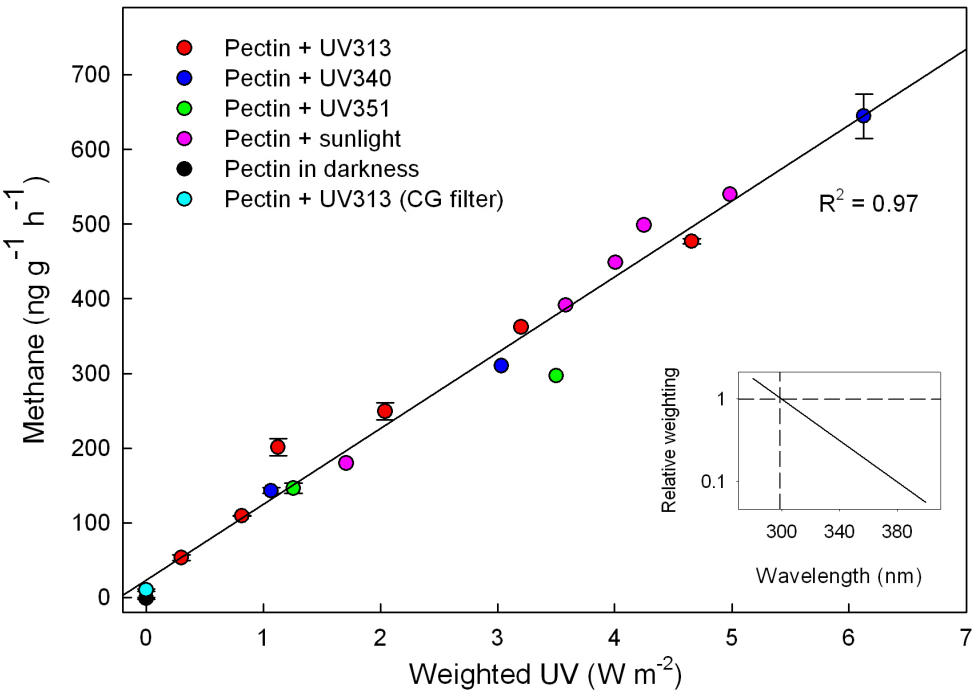

Figure 3.2.3 Methane production from pectin sheets against weighted-UV.
Data were recorded as per Figure 3.2.1. Spectral weighting function inset bottom right (constructed by Dr. A.McLeod). Values are means of three replicates with standard error, apart from in the case of sunlight where data represents a one-time measurement.

3.2.1.2 Methane production from washed pectin and pectate

While pure sugar residues do not absorb much in the UV-A or UV-B region (Bednarczyk & Marchlewski, 1938; Slein & Schnell, 1953; Hershenson, 1956), pectin solutions do absorb in the UV range, possibly due to the presence of phenolic compounds (Figure 3.2.4).

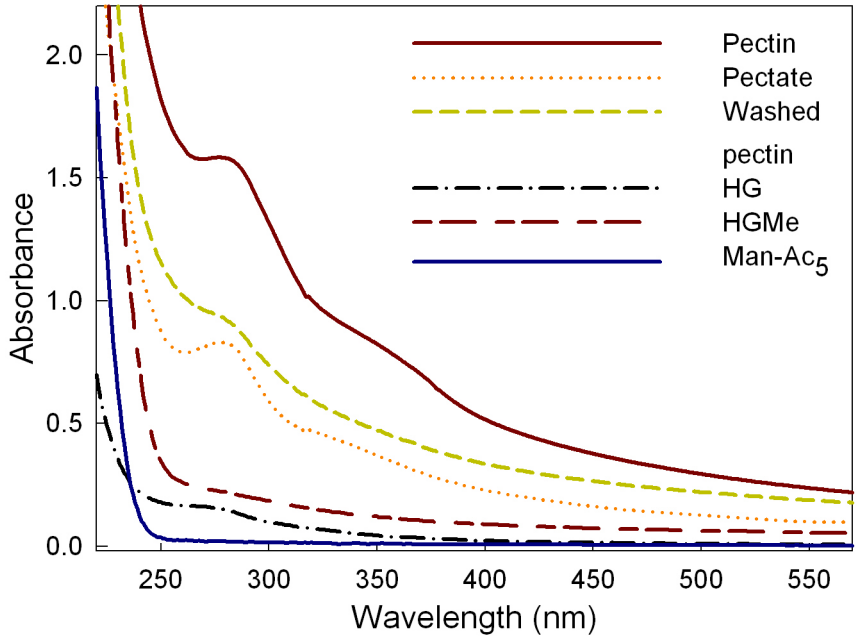

Figure 3.2.4 Absorption spectra of solutions of pectin and other putative methane sources.
All solutions were made at 0.5% w/v. Spectra were recorded on a spectrophotometer (CECIL, series 8000).

To ascertain whether this UV absorption was due to non-covalently bound impurities from the manufacturing process, the pectin solution was washed several times with ethanol (75% final concentration). This process solubilises small molecular weight compounds and precipitates large polysaccharides such as pectin. About 40% of UV-absorbing material was removed by this process, suggesting that at least 60% was covalently bound to the pectin (Figure 3.2.4). UV irradiation of washed pectin sheets showed a reduction of methane emissions of about 36% (Figure 3.2.5).

Demethylated pectin (pectate) was synthesised by saponification of commercial pectin. Upon UV irradiation of glass fibre sheets of pectate, only trace amounts of methane were evolved (Figure 3.2.5).

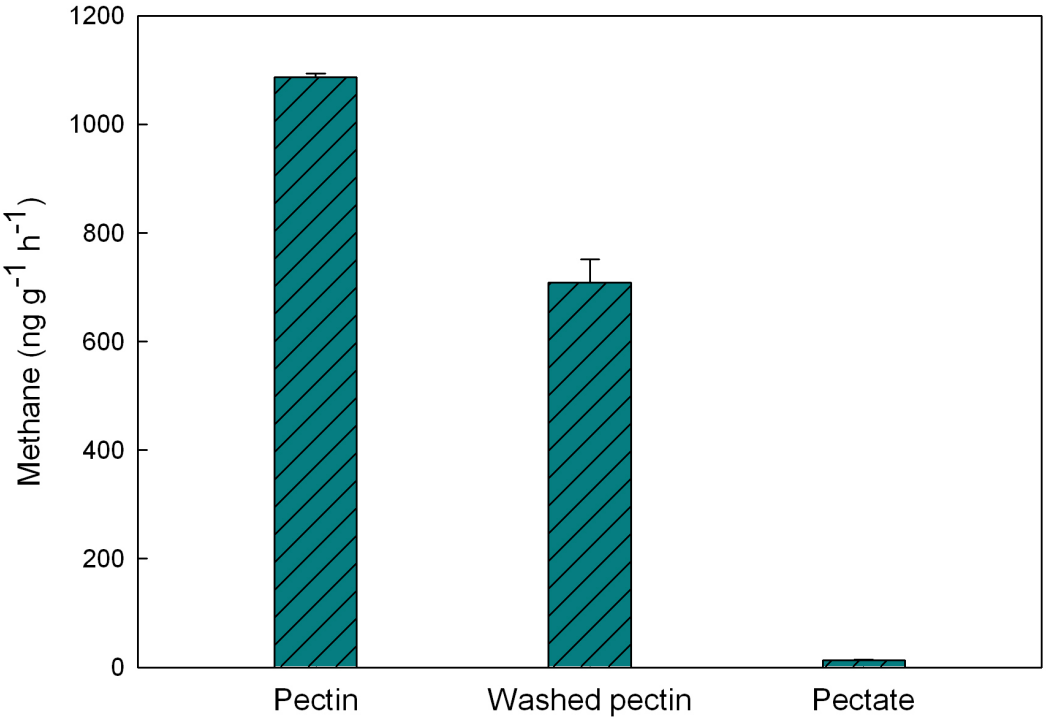

Figure 3.2.5 Methane emissions upon UV irradiation of washed pectin and pectate.
Data were recorded as per Figure 3.2.1. The unweighted UV-irradiation treatment was 8.71 W m^{-2} (equivalent to 5.14 W m^{-2} weighted for CH_4 production). Values are means of three replicates with standard error.

3.2.1.3 Methane production from HGMe and other methyl sources

Pectin contains methyl groups of three kinds: methyl esters, '*C*-methyl-pentose' residues (e.g. rhamnose), and the —CH_3 group of *O*-acetyl esters. Saponification of pectin removed methyl esters and *O*-acetyl esters. As each type of methyl group could be contributing to the observed methane emissions, they needed to be analysed separately.

The commercial pectin sample was 84% w/w galacturonic acid (GalA; as stated by manufacturer), most of which makes up a backbone with partially methylated GalA residues. A simpler model for pectin would therefore be homogalacturonan (HG) with partially methylated GalA residues (HGMe). This was

synthesised from commercial homogalacturonan and a methyl ester assay showed that 43% of GalA residues were methylated. Irradiation of HGMe sheets with UV produced very small amounts of methane, similar to that from HG sheets (Figure 3.2.6).

UV irradiation of rhamnose, mannose (as a control with a similar structure to rhamnose but with no methyl group) and mannose pentaacetate (Man-Ac_5) produced very small amounts of methane in all cases. The absorption spectra of all compounds were recorded (Figure 3.2.4) and show very little absorbance in the UV range.

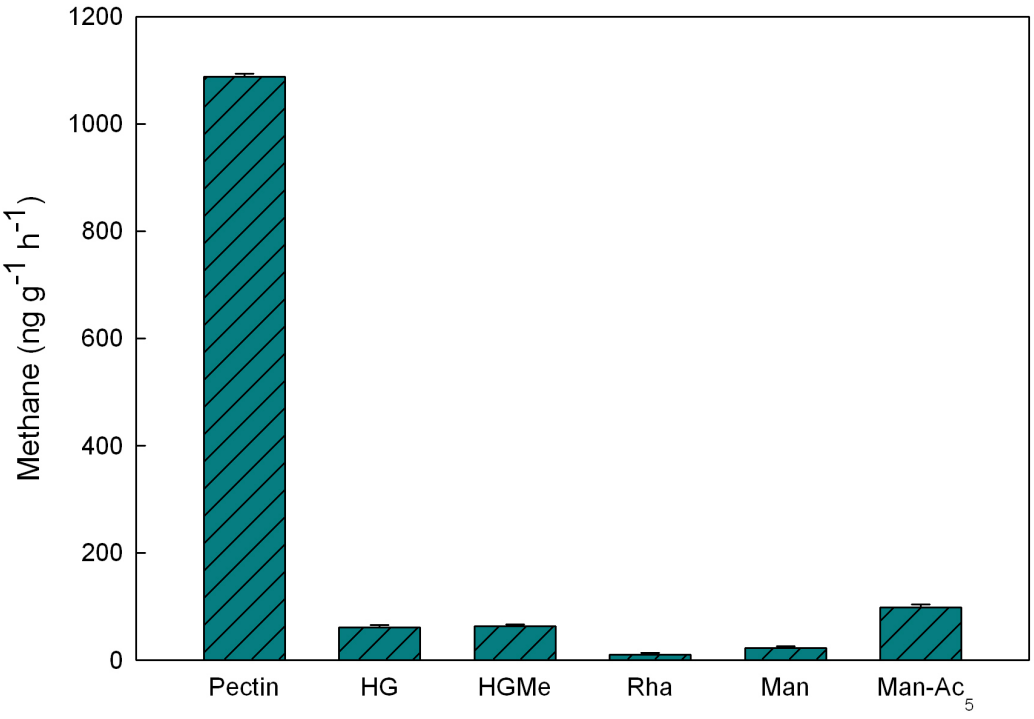

Figure 3.2.6 Methane emissions upon UV irradiation from HG, HGMe, Rhamnose, Mannose and Mannose pentaacetate.
Data were recorded as per Figure 3.2.5. Values are means of three replicates with standard error.

3.2.1.4 Synthesis of galacturonic acid methyl ester

Methylation of the uronic acid position can easily be achieved by using methanol and an acid catalyst; however there is another competing reaction where methylation of the anomeric position occurs, albeit at a slower rate. A preliminary reaction with methanol and trifluoroacetic acid (TFA) was carried out, but did not seem to generate much product and has the disadvantage that TFA is soluble in methanol and therefore the reaction could not be stopped at a specific point. Instead, Dowex50^{-}.H^{+} was used as it is an insoluble resin. First of all, varying amounts of acid catalyst were tested (Figure 3.2.7) and then varying concentrations of water and methanol were tested (Figure 3.2.8), all for different amounts of time as the competing reactions have different reaction rates. Solutions were run on TLC to visualise the reaction products.

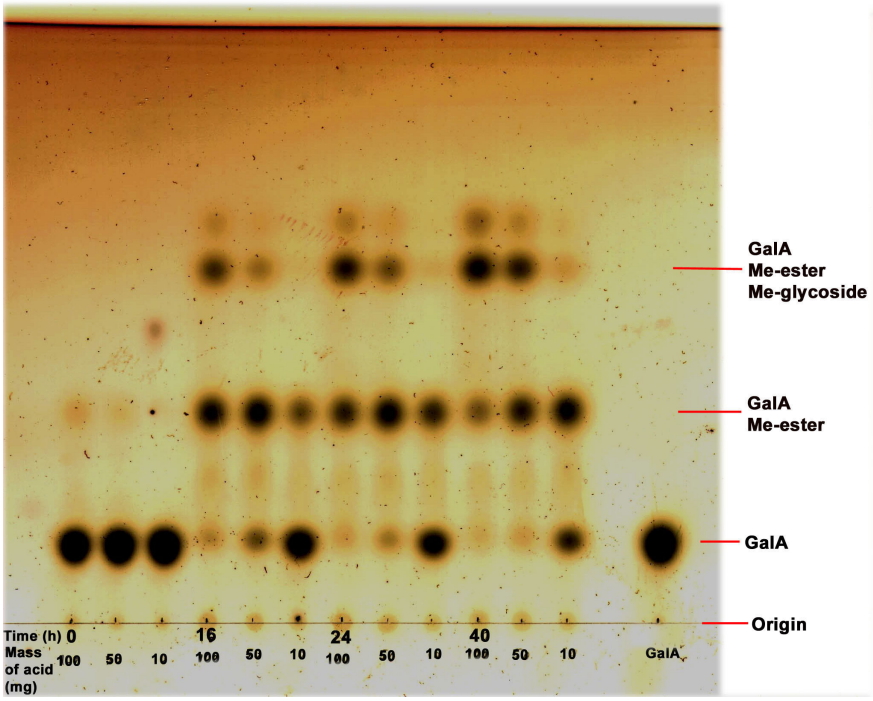

Figure 3.2.7 TLC showing the effect of different amounts of acid catalyst and time on the production of galacturonate methyl ester and methyl glycoside.
TLC was developed in BAW (3:1:1) over 8 h and stained with thymol. Volume of sample loaded onto TLC was 20 µl.

The product which ran furthest from the origin is the least polar compound possible and is therefore galacturonic acid with a methyl ester group at the uronic acid position as well as a methyl group at the anomeric position. The slowest running product is unreacted galacturonic acid, as confirmed by the external marker. The product which ran in between those two is therefore galacturonate methyl ester (GalAMe).

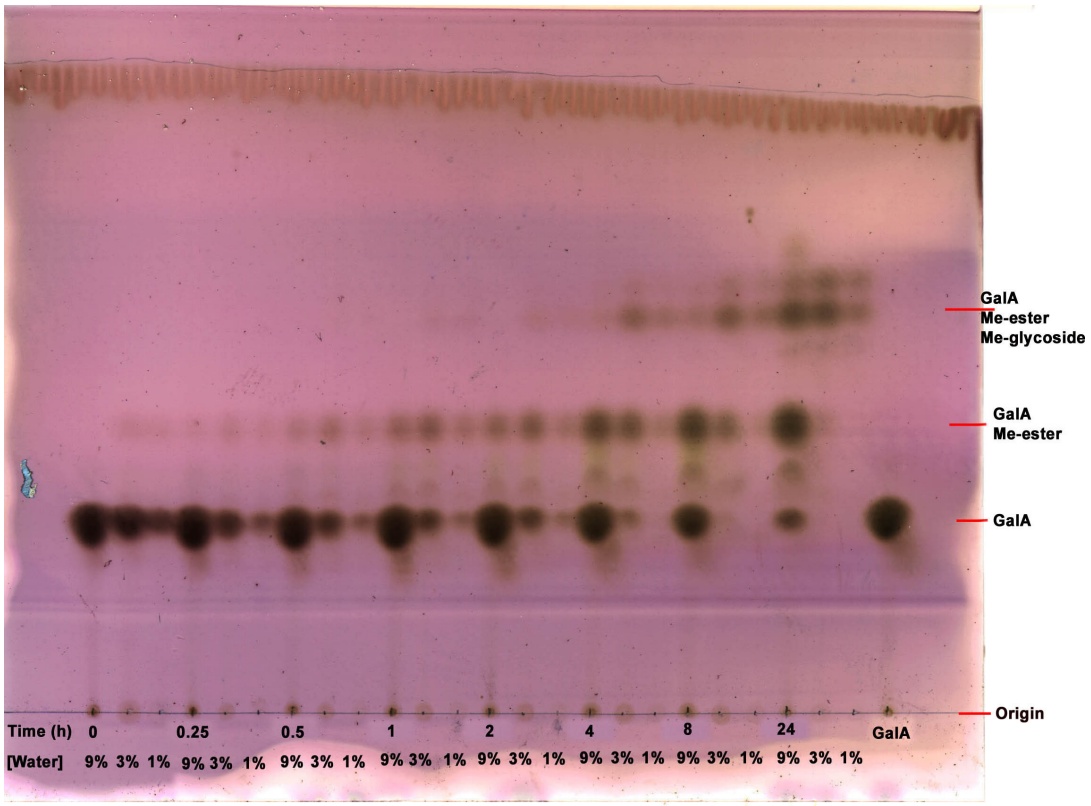

Figure 3.2.8 TLC showing the effect of different water concentrations on the production of galacturonate methyl ester and methyl glycoside.
TLC was developed in BAW (3:1:1) over 8 h and stained with thymol. Volume of sample loaded onto TLC was 20 µl.

From Figures 3.2.7 and 3.2.8, it was determined that the best system to get maximum amounts of galacturonate methyl ester with little amounts of methylation at the anomeric position and unreacted galacturonic acid was to use a 5:1 ratio by

mass of acid to starting material, with a final concentration of 9% water and to leave the reaction for 24 hours.

Another way to confirm that the correct product has been synthesised is to use ^{1}H-NMR spectroscopy. Figures 3.2.9 and 3.2.10 show ^{1}H-NMR spectra of pure GalA and the crude mixture of GalA and its methyl esters respectively. The large peaks around 3.26 ppm are typical of methyl ester groups. The presence of more than one methyl ester peak suggests several types of electronic environments experienced by methyl esters and confirms that there are several products as seen on the TLC.

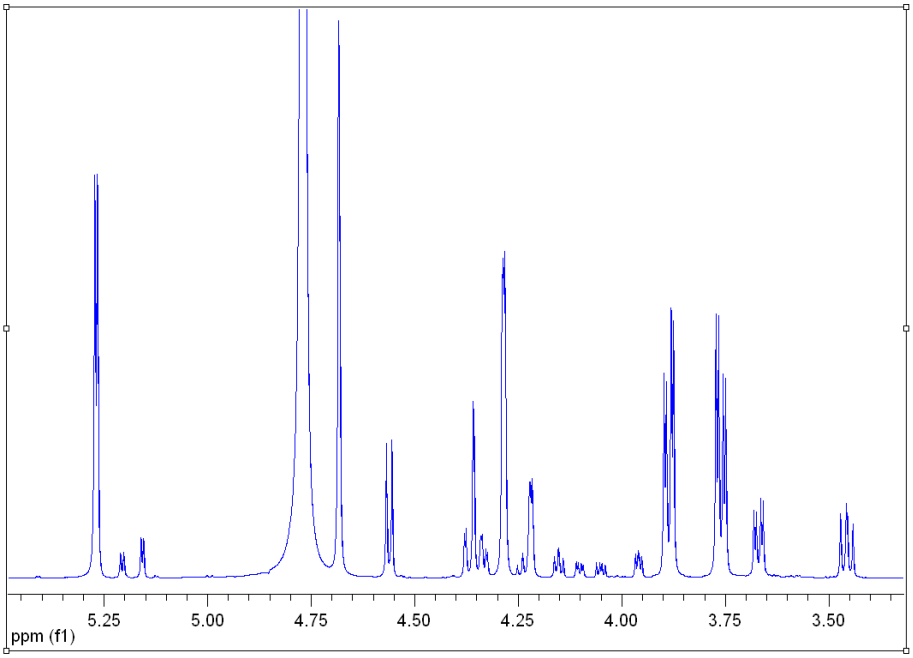

Figure 3.2.9 ^{1}H-NMR of galacturonic acid.
The ^{1}H-NMR spectrum was measured at 25 ℃ at 250 MHz using a Bruker ARX250 spectrometer, referenced to methyl signals in trimethylsilyltetradeuteriopropionate Na^{+} salt (TSP) as zero ppm.

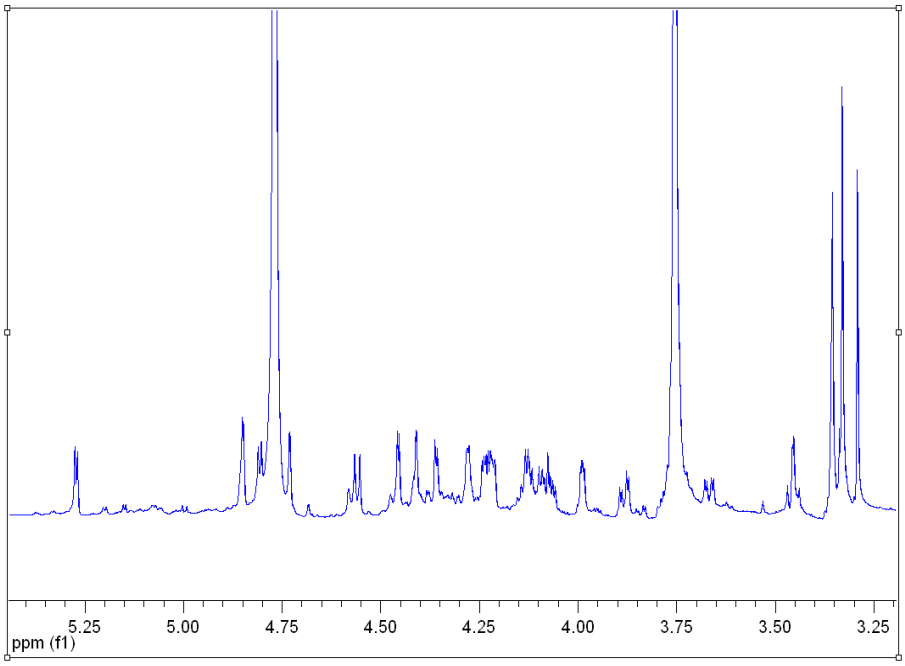

Figure 3.2.10 ^{1}H-NMR of galacturonic acid and its methyl ester crude mixture. Spectrum was recorded as per Figure 3.2.9.

Attempts were made to synthesise GalAMe with 1,2;3,4-Di-*O*-Isopropylidene galacturonic acid (Iso-GalA) as a starting product instead of GalA with the intention that the isopropylidene groups will protect from methylation at the anomeric position and allow methylation at the uronic position only. Despite slowing the reaction rate considerably, after 96 h the formation of GalAMe occurred at the same time as the synthesis of GalAMe methyl glycosides (seen running between GalAMe and Iso-GalA in Figure 3.2.11). This starting compound is therefore not suitable for the synthesis of GalAMe.

A new method was developed using dicyclohexylcarbodiimide (DCC) as an intermediary to activate the carboxylic acid. The synthesis of GalAMe was more successful than with the previous methods, however some impurities remained (Figure 3.2.12).

No further attempts to synthesise or purify GalAMe were made.

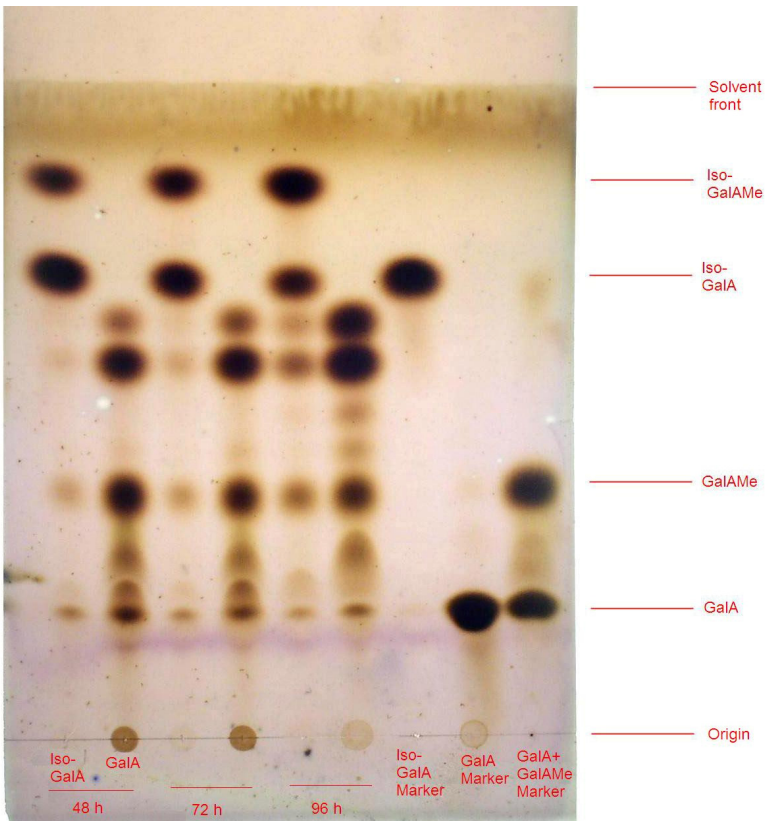

Figure 3.2.11 TLC showing the effect of using Iso-GalA instead of GalA for the synthesis of GalAMe.

TLC was developed in BAW (3:1:1) over 8 h and stained with thymol. Volume of sample loaded onto TLC was 20 µl.

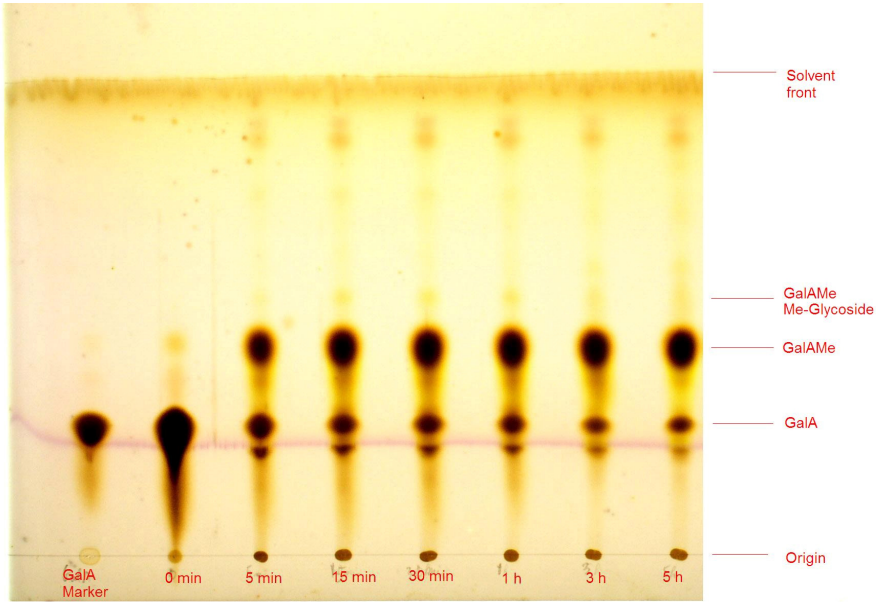

Figure 3.2.12 TLC showing the effect of using DCC as an intermediary for the synthesis of GalAMe.

TLC was developed in BAW (3:1:1) over 8 h and stained with thymol. Volume of sample loaded onto TLC was 20 µl.

3.2.2 ROS as part of a mechanism for methane production from pectin

3.2.2.1 Addition of ROS scavengers and generators to pectin sheets

A range of ROS scavengers were added to pectin solutions prior to drying on glass fibre sheets, subsequently irradiated with UV and methane emissions recorded (Figure 3.2.13). 1,4-diazabicyclo[2.2.2]octane (DABCO), reported to scavenge $^1O_2$ (Heiser *et al*., 2003), efficiently blocks UV-induced CH_4 emission from pectin. However, DABCO itself absorbs in the 280–350-nm UV range (Figure 3.2.14) and could thus potentially work as a simple UV-blocking filter.

The addition of KI, a known scavenger of H_2O_2 but also having a high rate-constant for reaction with $^{\bullet}OH$ of 1×10^{10} l mol^{-1} s^{-1} (Buxton *et al*., 1988) and acting as a quencher of singlet oxygen (Rosenthal & Frimer, 1976), to sheets of pectin reduced the UV-induced CH_4 emissions to trace levels. Unlike DABCO, KI does not absorb in the UV range (Figure 3.2.14) and is therefore not acting as a UV-blocking filter.

The addition of 2 mmol and 20 mmol mannitol, a $^{\bullet}OH$-specific scavenger, reduced methane emissions by 64% and 75% respectively. Like KI, mannitol does not absorb in the UV range (Figure 3.2.14) and it is therefore the $^{\bullet}OH$ scavenging which is the cause of the reduced methane emissions.

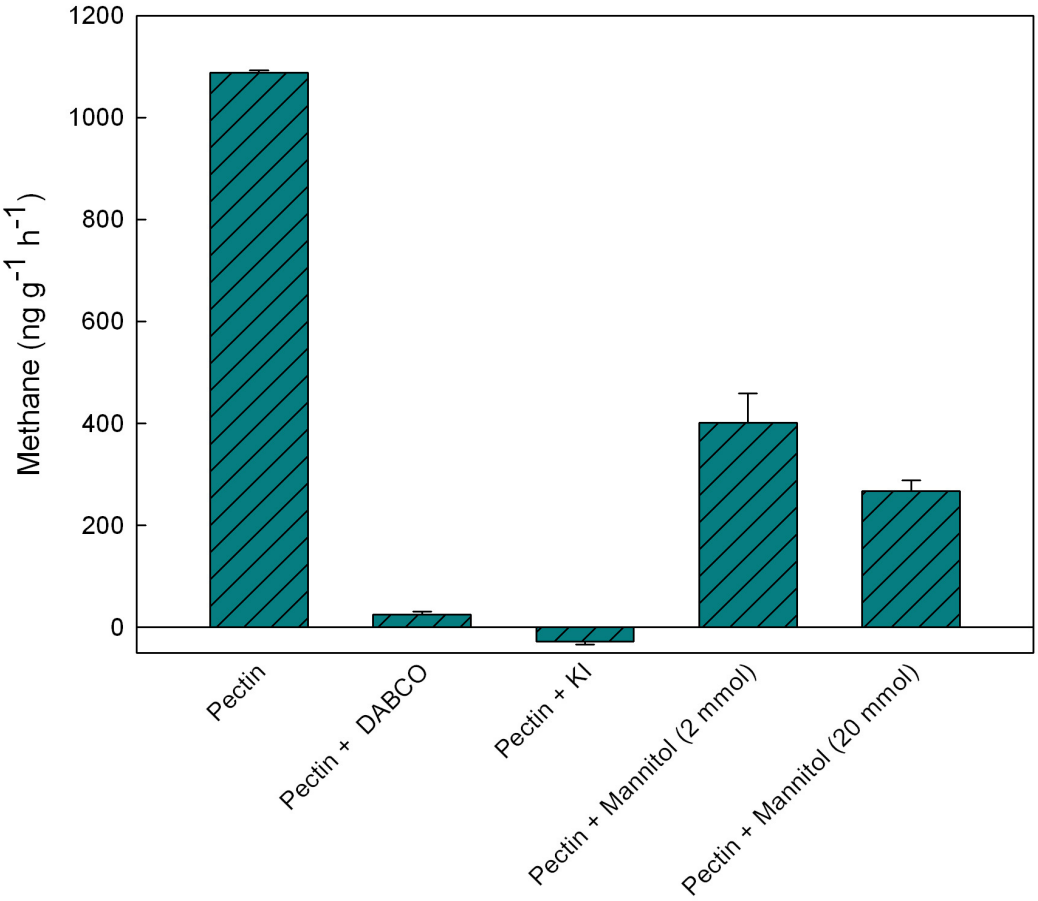

Figure 3.2.13 Methane emissions upon UV irradiation from pectin and the effect of the addition of ROS scavengers.
Data were recorded as per Figure 3.2.5. Values are means of three replicates with standard error.

Tryptophan, a $^1O_2$ generator when submitted to UV irradiation (Knox & Dodge, 1985), was added to glass fibre sheets of HG and HGMe which were irradiated with UV and methane emissions recorded (Figure 3.2.15). Large amounts of methane were evolved in the case of HGMe, with smaller amounts in the case of HG.

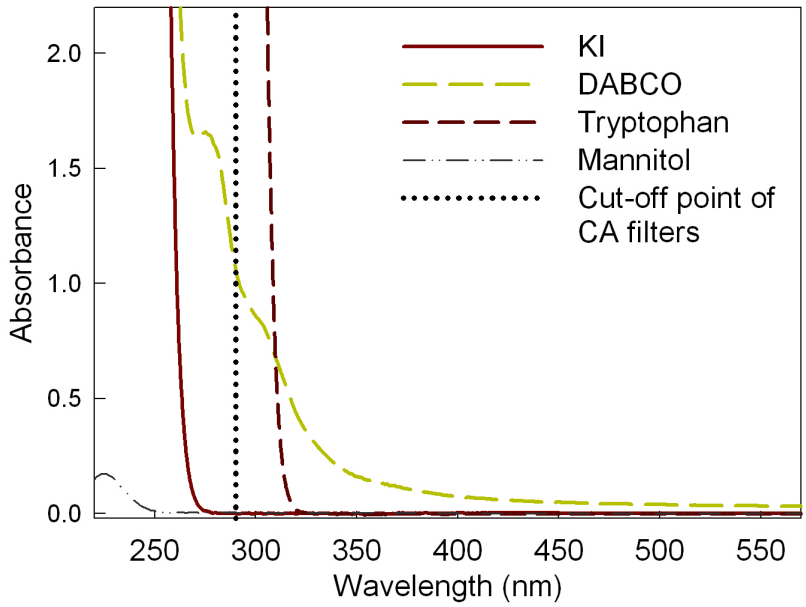

Figure 3.2.14 Absorption spectra of ROS scavengers and ROS generators.

All solutions were at 0.5% w/v. Data were recorded on a spectrophotometer (CECIL, series 8000).

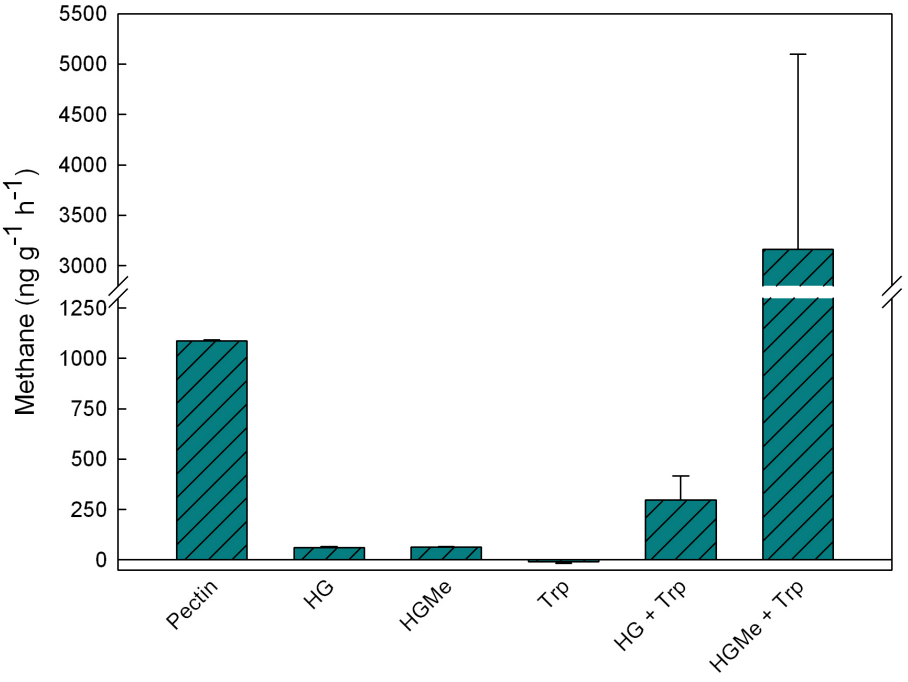

Figure 3.2.15 Methane emissions upon UV irradiation from HG, HGMe and the effect of the addition of a ROS generator.

Data were recorded as per Figure 3.2.5. Values are means of three replicates with standard error.

3.2.2.2 Addition of ROS to solutions of polysaccharides

H_2O_2, KO_2 and Fenton reagents (ascorbic acid, $CuSO_4$ and H_2O_2, a mixture known to generate hydroxyl radicals), were added to solutions of a range of polysaccharides and methane emissions were recorded at 0 h, 1 h, 3 h and 5 h (Figure 3.2.16).

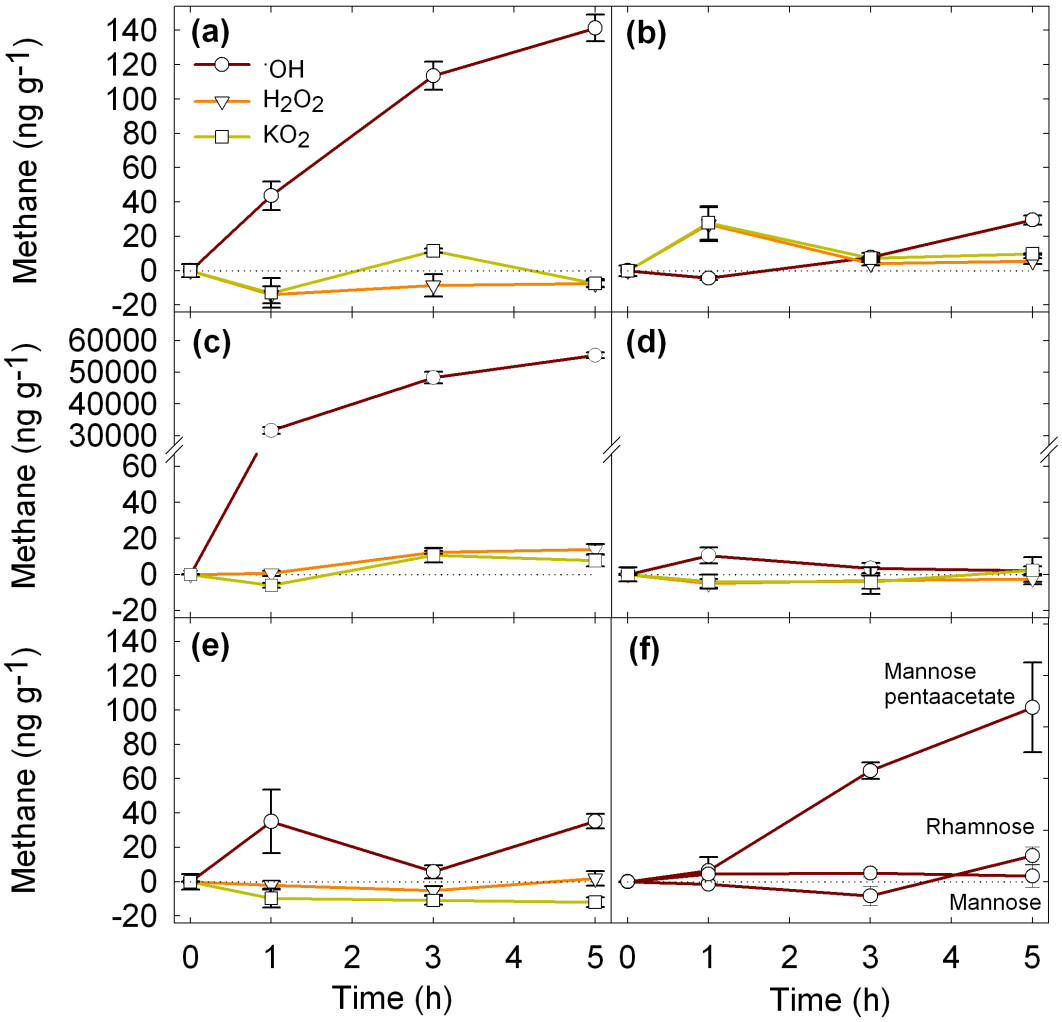

Figure 3.2.16 Methane emissions in the dark from solutions of pectin and other carbohydrates upon addition of ROS.

Sources of ROS were: $^{\bullet}OH$ = 5 mM ascorbic acid, 5 µM $CuSO_4$ and 5 mM hydrogen peroxide (○), H_2O_2 = 5 mM hydrogen peroxide (▽), KO_2 = 5 mM potassium superoxide (□). The carbohydrates treated were: (a) 1% w/v pectin, (b) 1% w/v pectate, (c) 1% w/v HGMe, (d) 1% w/v HG, (e) 1% w/v pectin with 0.5 M mannitol, (f) 1% w/v mannose pentaacetate, 1% w/v rhamnose and 1% w/v mannose. Data were recorded as per Figure 3.2.1, except for the use of an autosampler which was replaced by manual injection. Values are means of three replicates with standard error.

Very little methane emissions were observed from the addition of H_2O_2 and superoxide to any of the polysaccharide solutions. However, the addition of $^{\bullet}OH$ to pectin produced methane at rates up to 44 ng g^{-1} h^{-1}. The emissions were not observed in the case of pectate and HG, and were severely reduced when 0.5 M mannitol was present in solution. Very large methane emission upon the addition of $^{\bullet}OH$ to HGMe solutions were observed, ~500 times more than from pectin. Whilst this substantiates the observation that $^{\bullet}OH$ attack of pectin produced methane, the scale of the emissions from HGMe is difficult to explain. Although the compound was synthesised with care and lyophilised before use in further experiments, it is possible trace amounts of DMSO or CH_3I were present. The generation of $^{\bullet}OH$ in solutions of only CH_3I (1% v/v), DMSO (1% v/v) or HG-TBA (1% w/v) however did not produce significant methane emissions, therefore excluding them as the source of this large production of methane (data not shown). Another hypothesis for the emissions is the structural difference between pectin and HGMe. A mixture of pectin/HGMe (1:1 w/w, 1% (w/v) of each compound) was therefore submitted to $^{\bullet}OH$ attack and found to emit similar amounts of methane to a solution of HGMe only, thereby ruling out the possibility that pectin may contain a natural $^{\bullet}OH$ quencher, either in the form of a contaminant or in the ability of pectin to sequester $^{\bullet}OH$-generating transition metals in a Fenton-inactive form.

Small methane emissions from the addition of $^{\bullet}OH$ to mannose pentaacetate were observed, but no emissions from rhamnose or mannose were detected.

3.2.3 Methyl halide emissions from pectin

A possible mechanism for the formation of methane from methyl esters was suggested to involve radical formation (Sharpatyi, 2007). Indeed, the formation of ethylene and ethane at the same time as methane from UV-irradiated pectin sheets has also been reported and suggest a possible involvement of methyl radicals (McLeod *et al*., 2008). The presence of halide ions could therefore have the potential to form methyl halides from these methyl radicals.

The addition of 2 mmol KCl, KBr or KI to pectin sheets produced MeCl, MeBr and MeI respectively upon UV-irradiation (Figure 3.2.17). Pectin sheets produced small amounts of MeCl and MeBr (1429 ± 134 ng g^{-1} h^{-1} and 2863 ± 123 ng g^{-1} h^{-1} respectively), maybe due to the presence of contaminant Cl^- and Br^- ions. The addition of potassium halide salts to the sheets increased production by 95% and 211% respectively. Simultaneous methane production was decreased by 54% and 57% respectively. Pectin sheets did not produced any MeI, but upon addition of KI the emissions increased to 16175 ± 1001 ng g^{-1} h^{-1}. Methane production from these sheets was reduced to trace levels due to the ROS scavenging effect of KI.

In all cases several other compounds were evolved, possibly dimers or trimers of the methyl halides (compounds 1, 2, 3 and 4 in Figure 3.2.18). Efforts to identify these compounds by GC-MS were unsuccessful (data not shown).

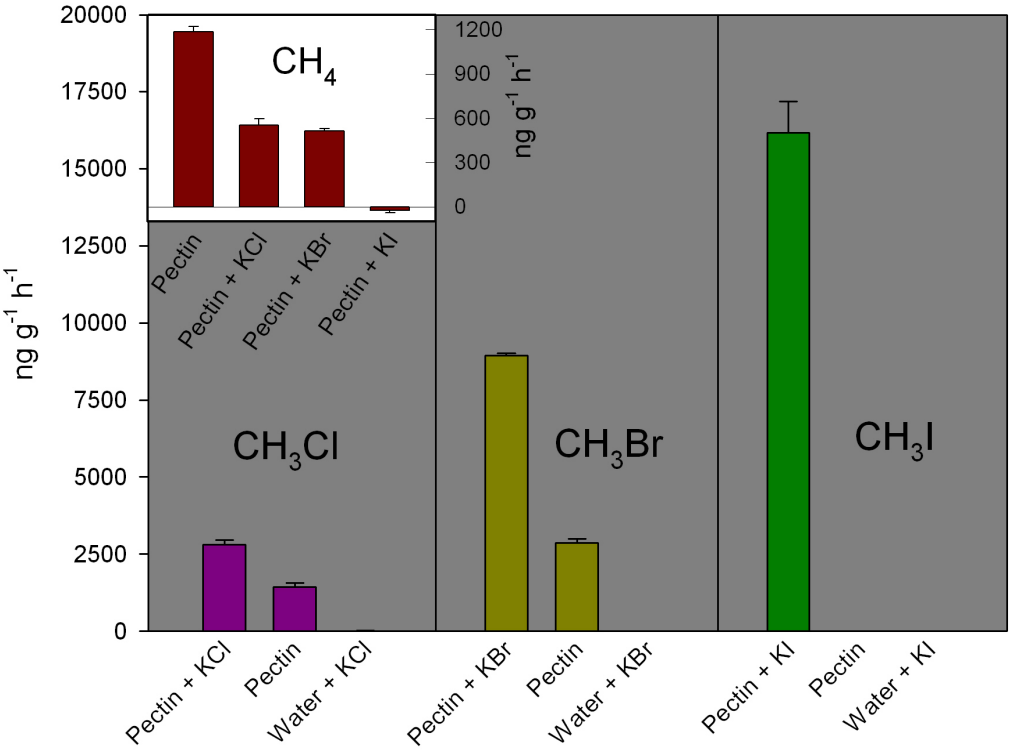

Figure 3.2.17 Methyl halide and methane emissions upon UV irradiation from pectin and pectin with added halide ions.

Data were recorded as per Figure 3.2.1, apart from the column temperature which was set at 120℃ in the case methyl halide analysis. Values are means of three replicates with standard error.

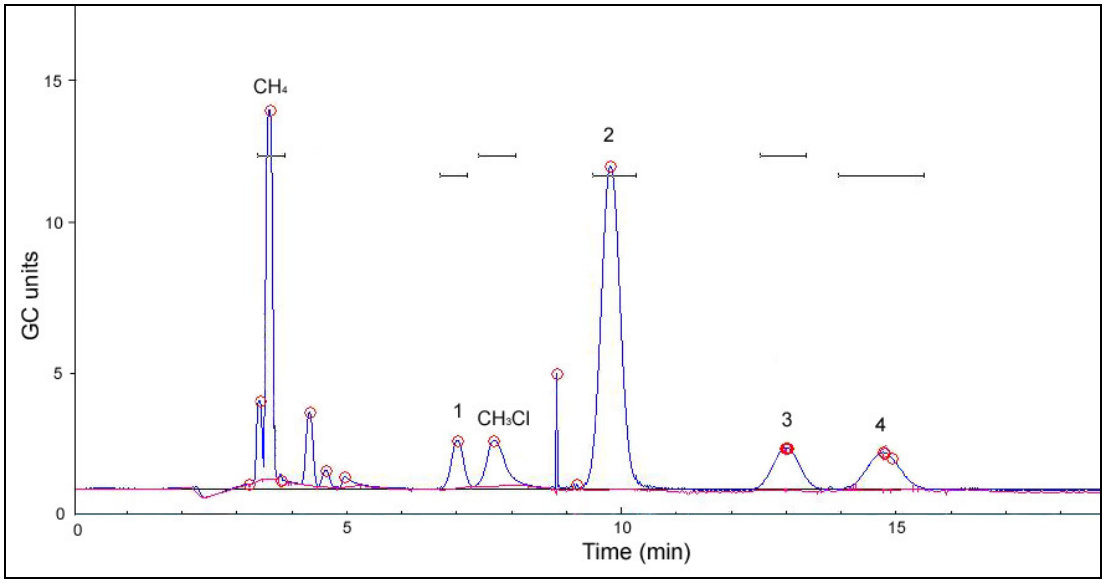

Figure 3.2.18 Gas Chromatography trace of methyl chloride and unknown compound emissions upon UV irradiation of a pectin sheet with 2 mmol KCl.

Data were recorded as per Figure 3.2.1, apart from the column temperature which was set at 120℃.

3.3 Generation of reactive oxygen species by UV and γ-irradiation

The methane experiments with pectin clearly show that ROS are produced upon UV irradiation if photo-sensitisers are present. In plants there are many UV screening compounds (Cockell & Knowland, 1999) and other photo-sensitisers which might absorb UV light to produce ROS *in vivo*. These could then attack methyl ester groups and evolve methane, or they might damage the cell wall and have unknown effects on the decomposition rate of leaves. In order to determine whether UV can have an effect on ROS production in the cell wall, a radio-labelling technique using NaB^3H_4 has been developed (Fry *et al*., 2001). If ROS attack cell wall polysaccharides, oxo groups are formed, which will then be reduced by NaB^3H_4 to —OH and —^{3}H groups. An assay for ^{3}H therefore allows quantification of the amount of oxo groups originally present, and therefore the level of ROS attack the polysaccharide experienced.

3.3.1 Experimenting with NaB^3H_4

The mechanism of NaB^3H_4-labelling of ROS-attacked monosaccharides and polysaccharides is shown in Figure 3.3.1.

Several samples of NaB^3H_4 were prepared (50 MBq, 6.3 MBq/μmol specific activity; 80 mM in 100 μl of 1 M NH_3 with 5 mM NaOH) from a higher specific activity stock (GE Healthcare, Chalfont St Giles, UK) and stored at -80°C until further use (carried out by Prof. S. Fry). An aliquot (40 μl) of one of these prepared samples was added to a xylose solution (6 mg in 160 μl of 1 M NH_3) to ensure the specific activity of the sample was correct. Xylose (in the straight-chain form)

contains an oxo group and should therefore be reduced to [^{3}H]xylitol in the presence of NaB^3H_4. This experiment was also carried out with a ten-fold dilution of the NaB^3H_4 sample. After radiolabelling, the solutions were run on a paper chromatogram which was then cut into 1-cm strips and assayed for radioactivity (Figure 3.3.2). Marker positions were obtained by running a 20-µl sample of a marker mix (0.5% w/v) and staining with silver nitrate.

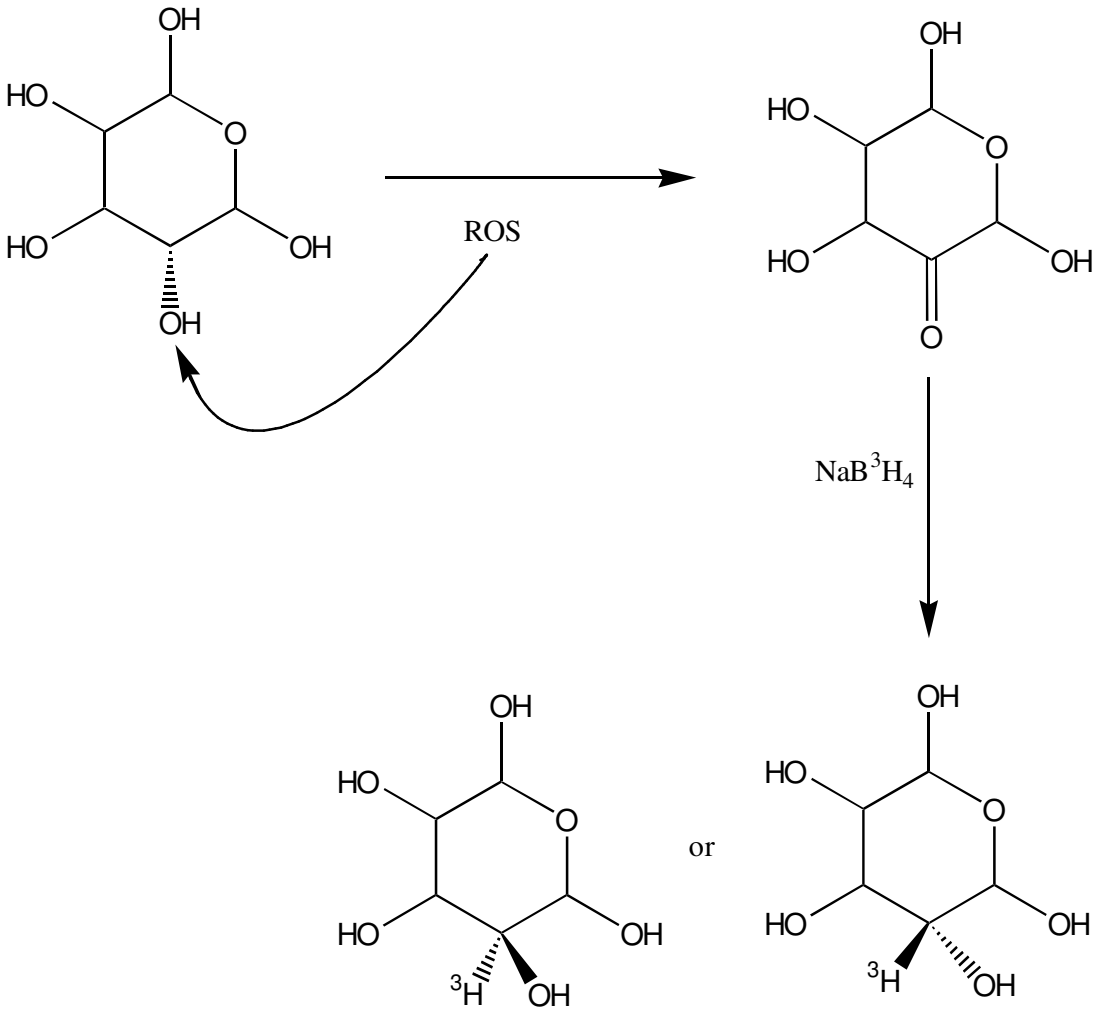

Figure 3.3.1 Simplified mechanism of NaB^3H_4-labelling of ROS-attacked sugars and polysaccharides.
For further details, see Fry *et al*. (2001).

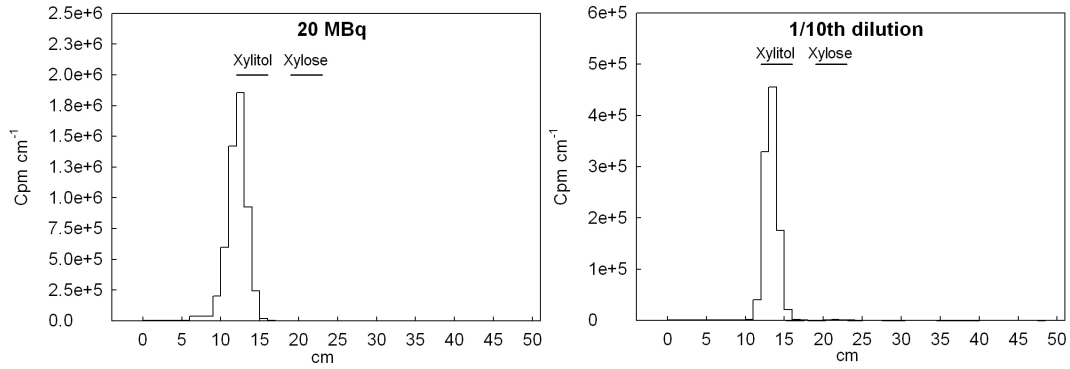

Figure 3.3.2 Testing the activity of stock NaB^3H_4 samples.
The samples (200 µl) were loaded onto Whatman 3MM paper and were run in EPW (8:2:1) for 16 h. Radioactivity was assayed a Beckman LS 6500 multi-purpose scintillation counter.

The conversion of xylose into [^{3}H]xylitol by NaB^3H_4 seems to have been successful. By adding up the entire radioactivity detected from each sample, and taking into account a 7% efficiency of ^{3}H counting by the scintillation counter, we can calculate that the activity of [^{3}H]xylitol from the full strength NaB^3H_4 sample was approximately 12.9 MBq, and that of the tenth-dilution sample was 2.5 MBq. While the full strength sample gave a lower value than the theoretical amount of radioactivity (20 MBq), the ten-fold dilution sample gave a reading much closer to the value expected (2 MBq). We therefore assumed that the specific activity of the stock NaB^3H_4 was still approximately 6.3 MBq/µmol.

3.3.2 Radio-labelling of ash leaves from field experiment

The UV filtration field experiment in Surrey allowed a direct comparison of plants grown under ambient UV conditions and several levels of reduced UV. A radio-labelling experiment was performed to evaluate any difference in ROS levels due to UV treatments.

3.3.2.1 Quantitative difference in radio-labelling from UV treatments

Eight leaves from four replicates of each UV treatment were collected, submitted to NaB^3H_4 labelling and assayed for radioactivity (Figure 3.3.3).

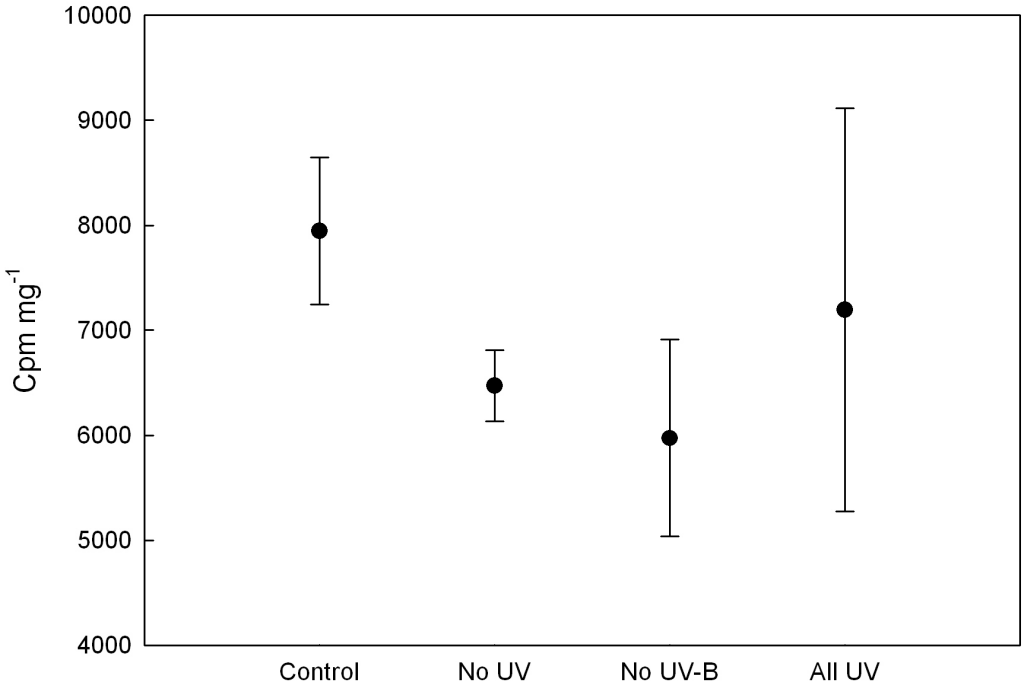

Figure 3.3.3 Assayed radioactivity from NaB^3H_4-labelled leaf AIR from each UV treatment.
AIR was suspended in dH_2O (100 µl) and 'Optiphase HiSafe' scintillation fluid (1 ml) was added. Radioactivity was assayed a Beckman LS 6500 multi-purpose scintillation counter. Data is expressed in counts per minute (cpm) per mg of AIR dry weight before labelling.

An analysis of this data (Table 3.3.1) showed no statistically significant difference between the any of the treatments.

Radioactivity (cpm mg^{-1})				ANOVA	
Control	No UV	No UV-B	All UV	*F* ratio	*P* value
6247 ± 519	5116 ± 356	4611 ± 749	5621 ± 1570	0.57	0.64

Table 3.3.1 Statistical analysis of the radio-labelling data from UV treatments. Data were analysed with a one-way ANOVA (N=4).

3.3.2.2 Qualitative difference in radio-labelling from UV treatments

The radio-labelled leaf solids were submitted to TFA hydrolysis, followed by Driselase digestion. An aliquot of the supernatant after hydrolysis and one from after digestion of two replicates of each UV treatment were run on paper chromatograms. These were then cut into 1-cm strips and assayed for radioactivity (Figure 3.3.4). Marker positions were obtained by running a 20-µl sample of a marker mix (0.5% w/v) and staining with silver nitrate.

Figure 3.3.4a shows that there are two main regions in the chromatogram with radio-labelled compounds from the TFA hydrolysis (18–21 cm and 28–31 cm), which co-eluted with the galactose and arabinose markers. These radio-labelled sugars were eluted from the paper separately and re-run on a paper chromatogram with phenol (80% w/w) as the eluting solvent, which has very different separating properties than BAW/EPW. This chromatogram was then cut into small strips and assayed for radioactivity (Figure 3.3.5). The position of the markers was obtained by silver nitrate staining. This allowed confirmation that one of the main radio-labelled sugars released from a TFA hydrolysis is [^{3}H]galactose, while the other sample of eluted sugars seems to contain at least three radio-labelled sugars, one of which is [^{3}H]arabinose. No difference in sugar labelling was observed between UV treatments.

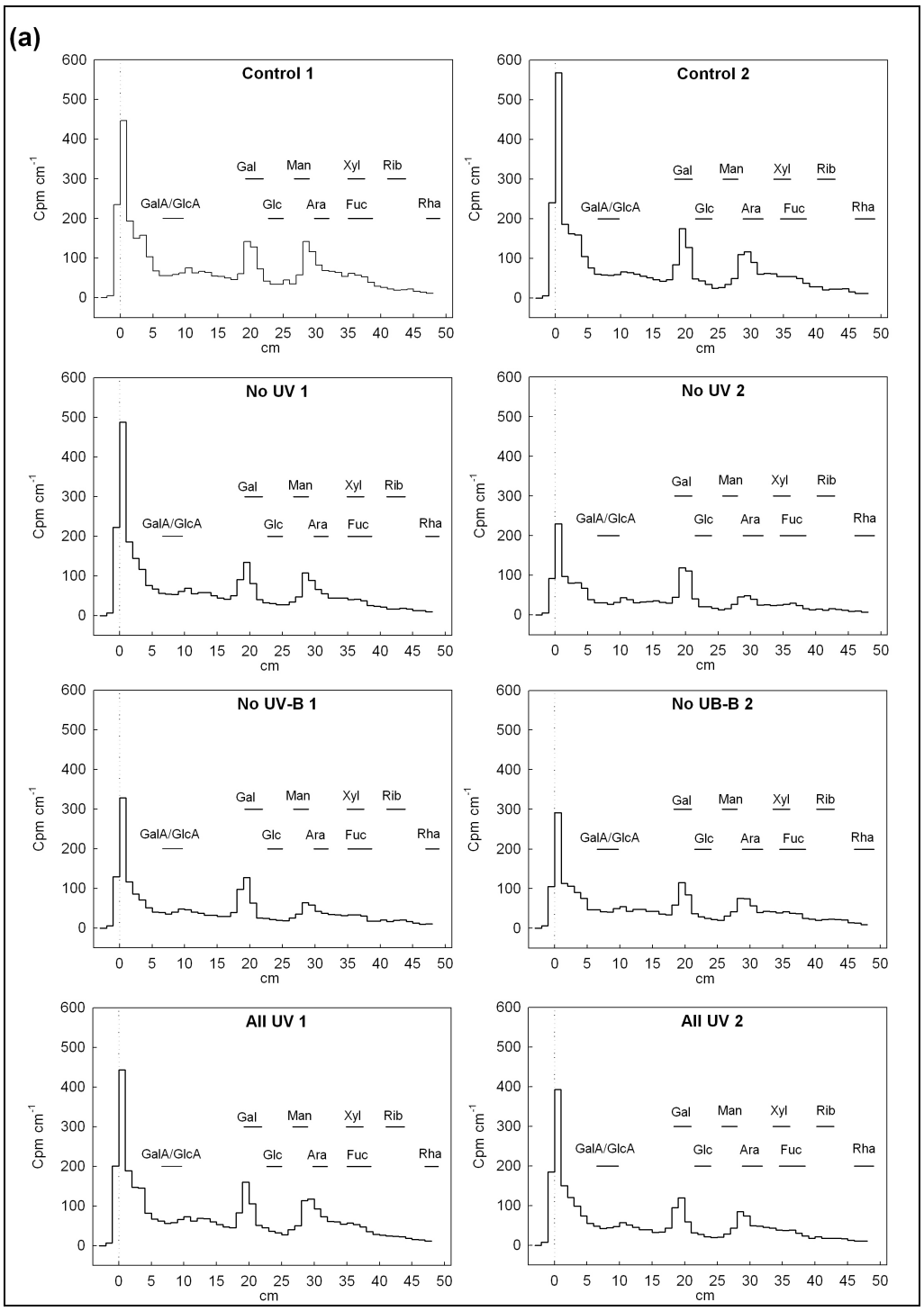

Figure 3.3.4 Profile of radioactivity of paper chromatograms.

(a) TFA hydrolysis and (b) Driselase digest. Samples (20 µl) were loaded on to S&S paper and were run in BAW (12:3:5) for 48 h followed by EPW (8:2:1) for 96 h. Radioactivity was assayed a Beckman LS 6500 multi-purpose scintillation counter. *(continued overleaf)*

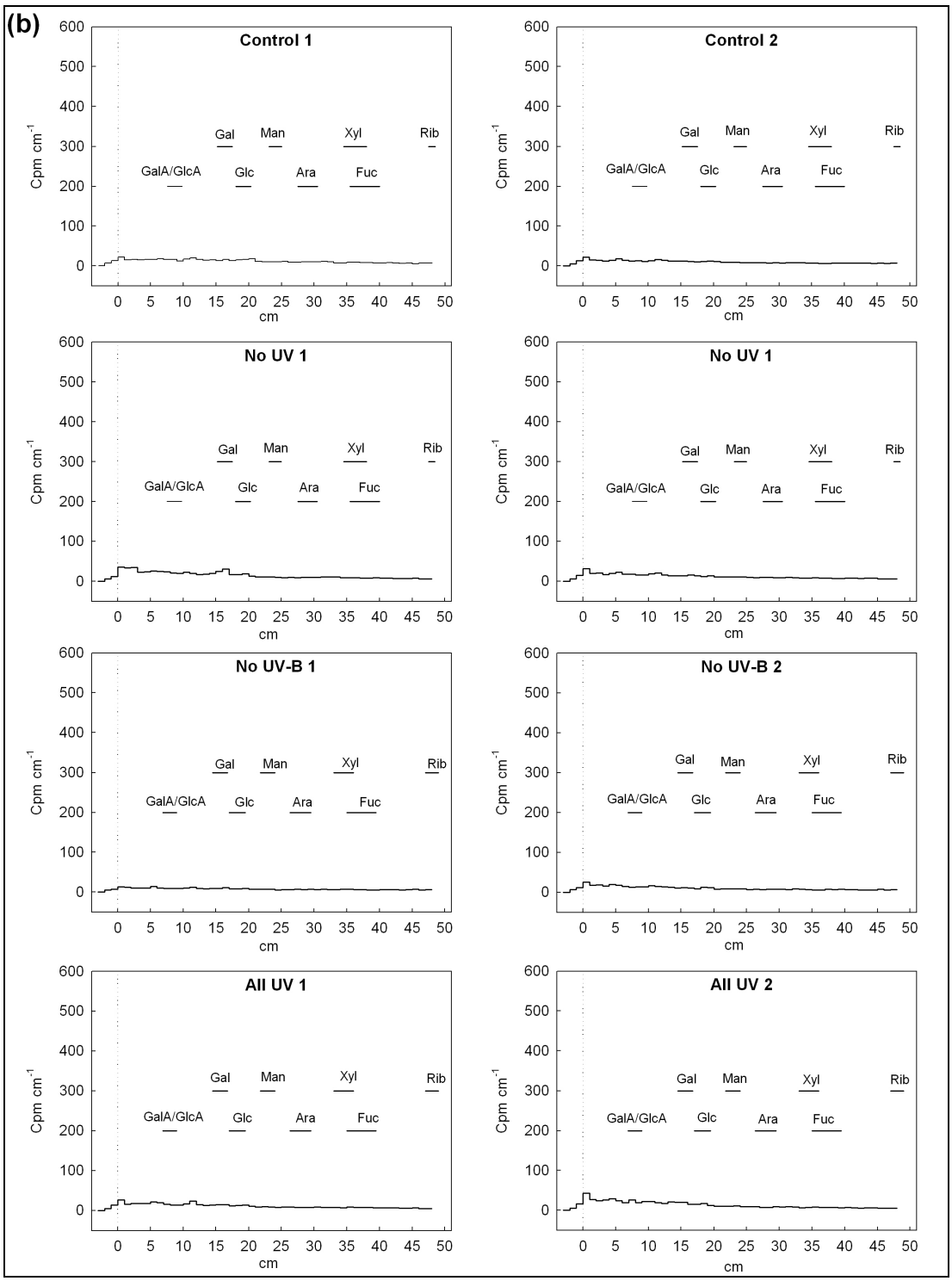

Figure 3.3.4 Profile of radioactivity of paper chromatograms. *(continued)*

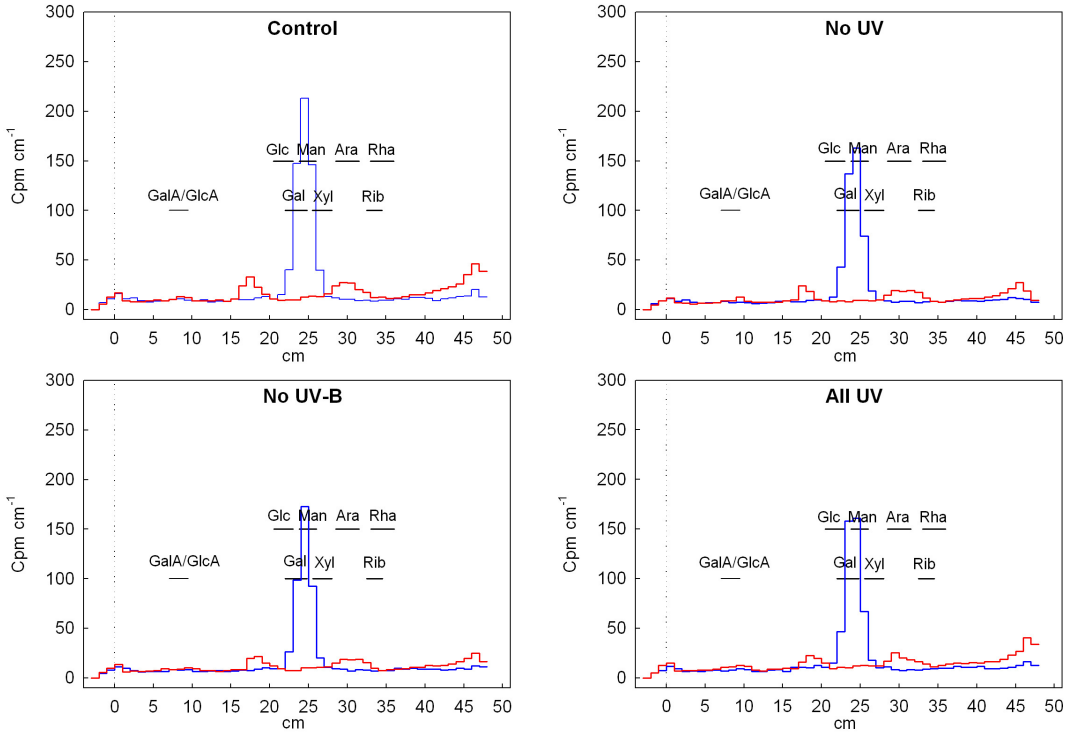

Figure 3.3.5 Radioactivity profile of the paper chromatogram run of the eluted radio-labelled sugars.

The samples (20 µl) were loaded onto Whatman 3MM paper and were run in phenol (80% w/w) for 19 h. Radioactivity was assayed a Beckman LS 6500 multi-purpose scintillation counter.

Figure 3.3.4b shows only background radioactivity on the paper chromatogram runs of samples from the Driselase digest. A silver nitrate staining of a reconstituted track from the paper chromatogram shows that as expected the cellulosic glucose was released by the Driselase digestion (Figure 3.3.6). Therefore, we must conclude that the cellulose was not labelled by the NaB^3H_4 and that the cellulose does not contain any oxo groups. This was the case in all four UV treatments.

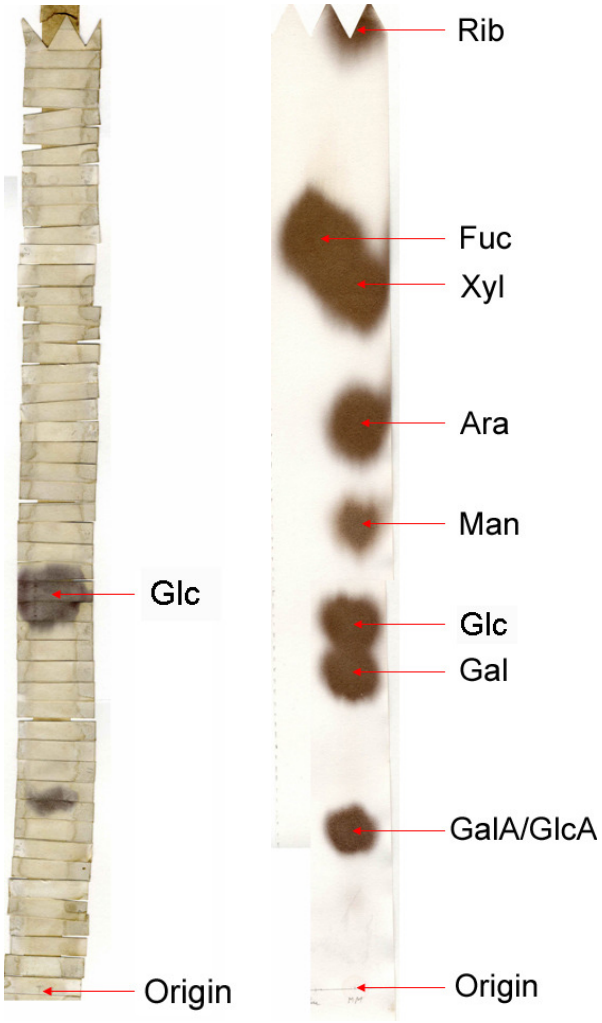

Figure 3.3.6 Markers and a reconstituted track of a paper chromatogram of the Driselase digest.

Chromatograms were run as per Figure 3.3.4. Strips of paper from one track of the paper chromatogram were stained with silver nitrate, as were the markers.

3.3.3 Irradiation of leaves

3.3.3.1 UV-irradiation of leaves

Kalanchoe and lettuce leaves were irradiated with UV light for 18 h and then submitted to radio-labelling with NaB^3H_4 and assayed for radioactivity (Figure 3.3.7).

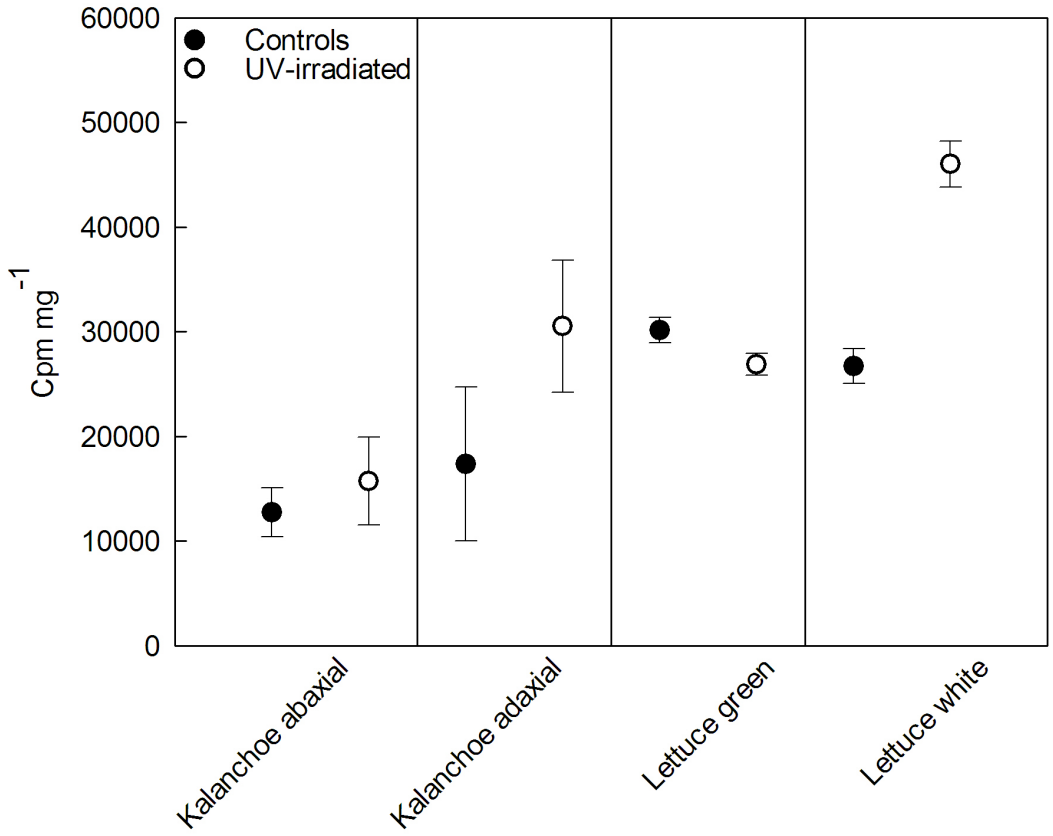

Figure 3.3.7 Results of radio-labelling of UV-irradiated *Kalanchoe* and lettuce leaves.
Leaves were irradiated with UV light for 18 h (UV313, The Q-Panel Company, Cleveland, USA; 8.71 W m^{-2}). Radioactivity data were obtained as per Figure 3.3.3.

A t-test of these data shows no significant effect of UV-irradiation on radio-labelling apart from in the case of the white part of the lettuce leaf where UV-irradiation caused a significant increase in radio-labelling (P<0.01).

The radio-labelled leaf materials were submitted to TFA hydrolysis and an aliquot of the water-soluble sugars was run on a paper chromatogram. This was then cut into 1-cm strips and assayed for radioactivity (Figure 3.3.8). Marker positions were obtained by running a 20-µl sample of a marker mix (0.5% w/v) and staining with silver nitrate.

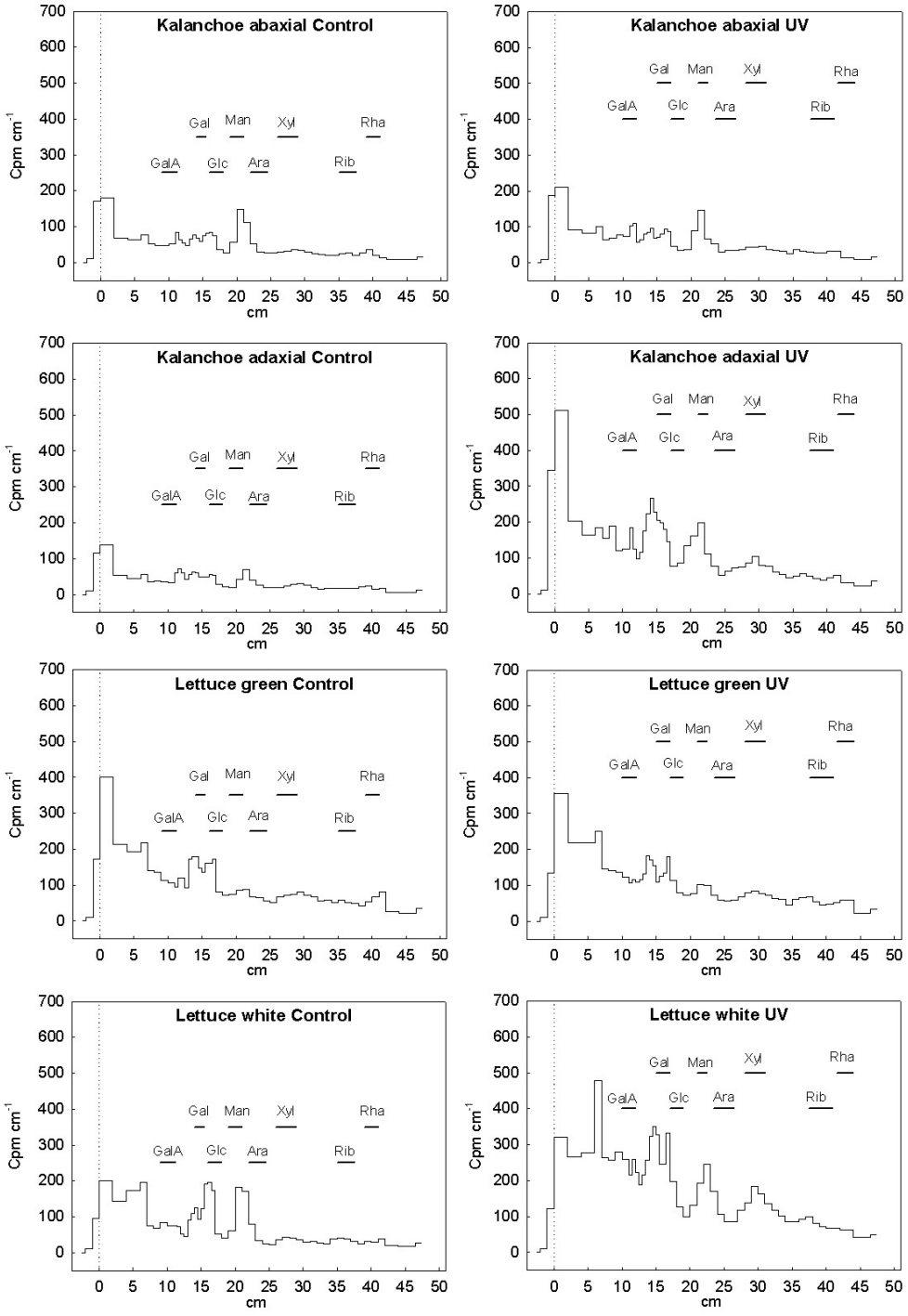

Figure 3.3.8 Profile of radioactivity of paper chromatogram of UV-irradiated leaves and controls.

Samples (20 µl) were loaded on to Whatmann 3MM paper and were run in BAW (12:3:5) for 16 h followed by EPW (8:2:1) for 16 h. Radioactivity was assayed a Beckman LS 6500 multi-purpose scintillation counter.

Very little difference can be observed between the UV treatment and the control in the case of the abaxial part of a *Kalanchoe* leaf or the green part of a

lettuce leaf. The amount of radioactivity found in the adaxial part of the *Kalanchoe* leaf which was UV-irradiated is higher than in the control, but as shown previously, this was not statistically significant if replicated. In the case of the white part of a lettuce leaf however, not only is the total amount of radioactivity higher, but the profile of radioactivity is different between treatments, with higher levels of radio-labelled compounds which co-migrated with uronic acids, galactose and xylose found in the UV-irradiated sample. The main other radio-labelled sugars found in both treatments co-migrated with glucose or ran in between the mannose and arabinose markers.

Since paper chromatography is not very effective at separating uronic acids, an aliquot of hydrolysed leaf material was run on paper electrophoresis, which was then submitted to fluorography (Figure 3.3.9). A small loading (30 µl) as well as a greater loading (80 µl) were applied since the radioactivities of the samples were very low. The 80-µl samples were clearly overloaded and ran slower than the smaller loadings and the markers, however the intensity of the bands on the film produced by fluorography (circled in blue in Figure 3.3.9) is greater and allows visual confirmation of the fainter bands produced by the smaller loading (circled in red in Figure 3.3.9).

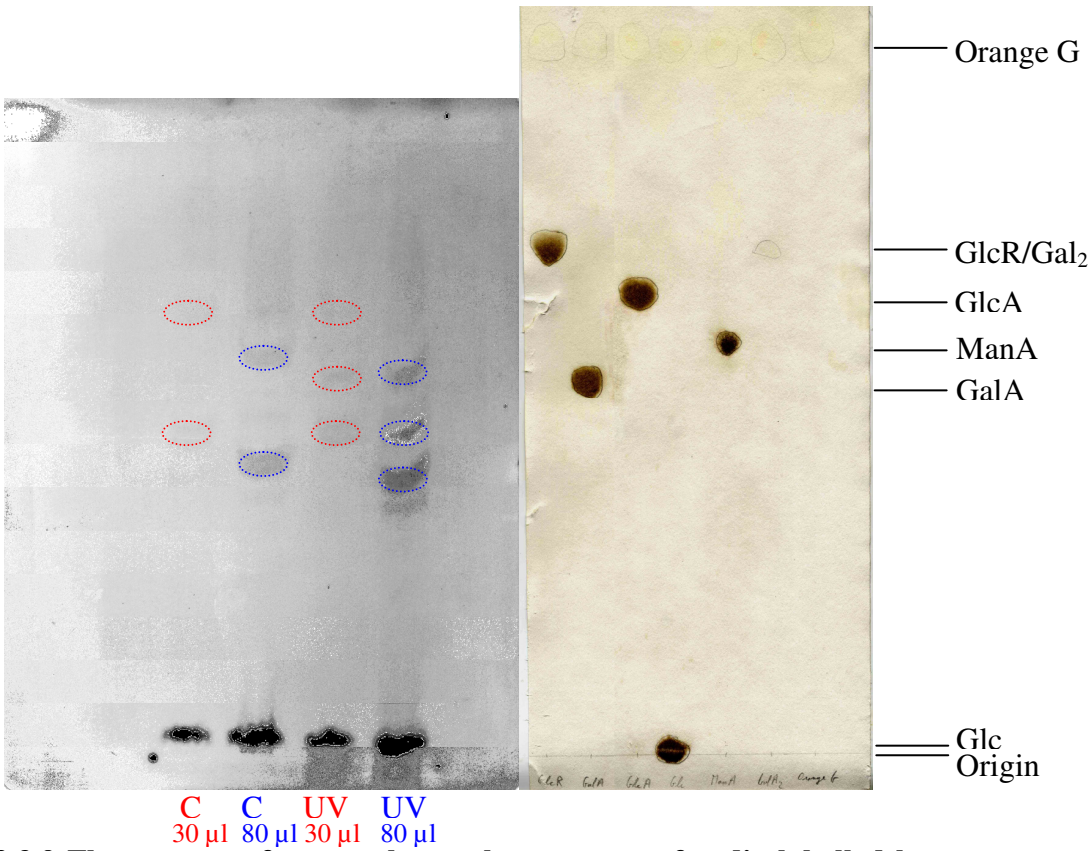

Figure 3.3.9 Fluorogram of paper electrophoretogram of radio-labelled lettuce white samples.

Samples (30 µl and 80 µl) of lettuce white control and UV-irradiated treatments were loaded on to Whatmann 3MM paper and were separated by electrophoresis (pH 3.5, 2.9 kV) for 1.5 h. The paper was then exposed to film (Kodak BioMax MR-1) for 4 weeks.

Apart from an intense band close to the origin in each sample (due to uncharged compounds), two bands due to radio-labelled charged compounds can be seen in the Control treatment, whereas three bands are found in the UV treatment. This extra band found in the UV treatment seemed to co-migrate close to the GalA and ManA markers. To enable further identification, the compound was eluted off the paper, submitted again to electrophoresis and the paper was cut into strips and assayed for radioactivity (Figure 3.3.10). The main peak of radioactivity co-migrated with the ManA marker.

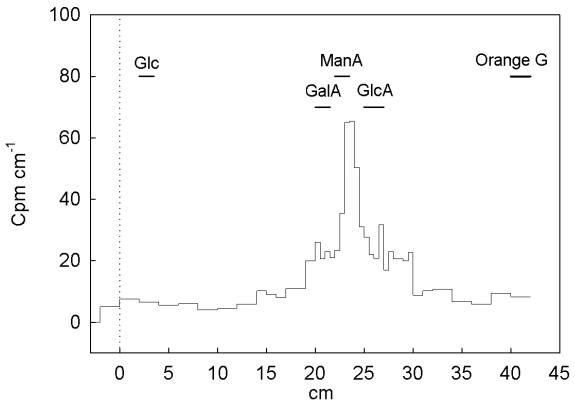

Figure 3.3.10 Profile of radioactivity of paper electrophoretogram of eluted radio-labelled compound.

Samples (20 µl) were loaded on to Whatmann 3MM paper and were separated by electrophoresis (pH 3.5, 2.9 kV) for 1.5 h. Radioactivity was assayed a Beckman LS 6500 multi-purpose scintillation counter.

3.3.3.2 γ-Irradiation of leaves

Ash and Birch leaves, irradiated with different levels of γ radiation (12 Gy h^{-1}), were submitted to radio-labelling with NaB^3H_4 and assayed for radioactivity (Figure 3.3.12). Table 3.3.2 shows that there is no statistically significant difference between treatments.

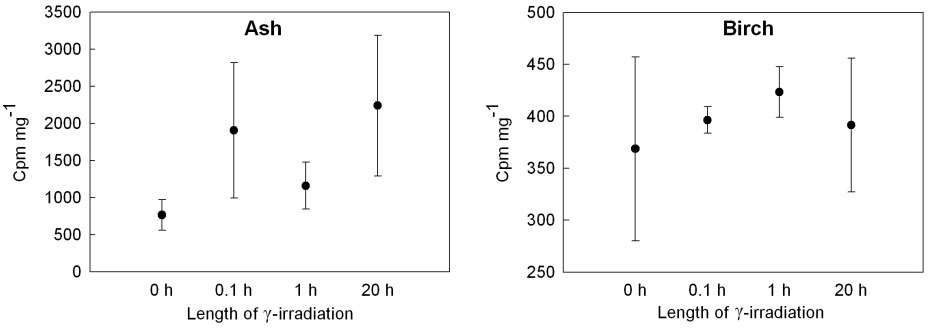

Figure 3.3.11 Results of radio-labelling of γ-irradiated Ash and Birch leaves.
Data were obtained as per Figure 3.3.3.

	Radioactivity (cpm mg^{-1})				ANOVA	
	0 h	0.1 h	1 h	20 h	*F* ratio	*P* value
Ash	764 ± 206	1906 ± 911	1160 ± 314	2238 ± 946	0.97	0.45
Birch	368 ± 88	396 ± 13	423 ± 24	391 ± 64	0.16	0.92

Table 3.3.2 Statistical analysis of data from radio-labelling of γ-irradiated Ash and Birch leaves.

Data were analysed with a one-way ANOVA (N=3).

4. DISCUSSION

4.1 Effects of UV filtration on Fraxinus excelsior seedlings

4.1.1 Environmental conditions

The aim of this field experiment was to create a difference in UV levels experienced by *F. excelsior* seedlings, and thus the monitoring of UV levels for each treatment had to be carried out carefully and in as many ways as possible. The transmission spectra of the three plastics (Figure 3.1.1), measured with an integrating sphere and a xenon arc lamp, showed them to be well suited in principle for the selective removal of UV-A and/or UV-B. Figure 3.1.2 shows that the design of the polytunnels successfully created an area of uniform light distribution in the centre of the enclosed area and, allowing for edge-effects, meant that only seedlings in a 1 × 1 m area in the centre of each plot were used for future analyses. However, the UV levels shown in Figure 3.1.2 were recorded with a UV broad-band sensor over a 1-minute period around solar noon and are therefore not representative of the UV levels experienced over a long period of time, particularly around sunrise and sunset. Therefore, UV-dosimeters were placed under one polytunnel of each treatment and used to record UV levels over a 7-day period (Table 3.1.1). This showed that all treatments received an appropriate dose of UV, apart from the 'All UV' treatment which only received approximately 57% of ambient erythemally-weighted UV. This is likely to be due to weathering effects on the plastics, as can be seen in Figure 3.1.3. While the transmittance of the UV absorbing plastic remained almost constant at all wavelengths throughout the experiment, the Mylar started to absorb more UV-A with

time, and the UV-transmitting plastic absorbed steadily more UV-A and UV-B through time. However, using these data and the record of UV levels for every day in near-by Chilton (Figure 3.1.4), an estimate of UV-A and UV-B dose received in each treatment (Table 3.1.2) showed that the difference between treatments, while smaller than originally desired, is still considerable, especially in the UV-B range.

As expected, the temperature under the plastics increased on average by 1.0 – 1.5°C, while the humidity decreased slightly when compared to ambient. Comparison of those three treatments with the ambient Control treatment (grown without plastic filters) should therefore be carried out carefully, as any effects found may not be due to a difference in UV levels but to a temperature or humidity effect. Comparison of the polytunnel 'No UV' treatment with the polytunnel 'All UV' treatment is therefore the most likely to reveal any real effects from UV.

4.1.2 Effects on ecological factors

The difference in average seedling height between treatments (Table 3.1.4) is likely to be due to a plant response to the increased temperature and protection from wind and rain found under the polytunnels. Again, this means that the most accurate comparison to make in future experiments is of the 'No UV' treatment with the 'All UV' treatment, and not with the 'Control' treatment.

The experimental set-up for the controlled decomposition of leaf litter from the field experiment (Figure 3.1.6) successfully remained until the last litter bag collection and no bags were lost. The leaf litter cover over the bags, despite being briefly disturbed during sample collection, stayed within the enclosure and did not leave any bags directly exposed to sunlight. The oven-dried leaf mass followed the

expected pattern of exponential decrease with time (Figure 3.1.7). While the difference in decomposition rate between treatments was not significant for the first six months, after one year, a significant difference between treatments with no UV-B and those exposed to ambient UV-B was found. Importantly, the 'All UV' and 'No UV' were significantly different, as were the 'All UV' and the 'No UV-B', showing that it was not a temperature effect which caused this change in decomposition rate, but the lack of UV-B. Additionally, the 'Control' treatment followed a similar decomposition rate to the 'All UV' treatment, suggesting that the change in temperature inside polytunnels and the presence of the plastic during leaf development actually had no effect on the decomposition rate. This increase in decomposition rate with decreased UV is surprising, since many of the more recent studies with increased UV also observed an increase in decomposition rate (Yue *et al*., 1998; Cybulski *et al*., 2000; Newsham *et al*., 2001a). However, this may show that plants have adapted to the ambient levels of UV, and increasing or decreasing these may have different effects, but which all lead to an increase in decomposition rate. To understand why the decomposition rate has changed, it is necessary to look at the biochemistry of the leaf, in particular of the cell wall.

4.1.3 Effects on leaf biochemistry

The analysis of the leaf cell walls showed some small differences between treatments. The hydrolysis of AIR with TFA gave an insight into the sugar composition of the cell wall, before and after one year of decomposition (Table 3.1.6). Several significant differences in rhamnose, galactose and glucose content were found before decomposition, as well as in total amount of monosaccharides

detected. However, no trend with UV was found. Indeed, while the 'No UV-B' treatment was often significantly different from the unenclosed 'Control', it was not significantly different from the 'No UV' or the 'All UV' treatments. In the case of glucose, those three treatments were all very different from the 'Control' but not from each other, suggesting that it was the presence of the polytunnel which caused this effect, possibly arising from an increase in starch production. After decomposition, several significant differences in rhamnose, arabinose and glucose content were found, but again no trend with UV treatments was observed. The change in decomposition rates between treatments can therefore not be explained by a change in the cell wall carbohydrate composition, and other structural changes in the cell wall must be considered.

Following a similar protocol to that carried out by McLeod *et al*. (2007), the extractability of carbohydrate from the AIR by a series of extractants of increasing severity was investigated (Table 3.1.5). Only in the case of the second weakest extractant, ammonium oxalate, was a significant difference between treatments found. However, it did not follow any trend with UV levels. Indeed, the three treatments with a plastic cover were not significantly different from each other, suggesting this may be an effect of the increased temperature and not a UV effect. Decreased UV-B did not seem to affect carbohydrate extractability from *F. excelsior* unlike increased UV-B in the study of McLeod *et al*. (2007), which found a 10% decrease in carbohydrate extractability with a phosphate buffer from *Quercus robur*. This extractability experiment involved a chemical process which was very different from the conditions the leaves experienced during decomposition in the field. An enzymic digestion with Driselase, which may mimic microbial decomposition

processes, was therefore carried out (Figure 3.1.9) and the amount of carbohydrate (Table 3.1.7) and monosaccharides (Table 3.1.8) were measured through time. The amount of carbohydrate extracted from the 'Control' samples was significantly lower than that extracted from some of the UV treatments during the first 24 h, but not afterwards. This effect is difficult to explain, and may be due to less available polysaccharides in the 'Control' samples for enzymic digestion. However, since it did not follow any trend with UV and was no longer significantly different after 24 h, it was not investigated any further. The quantification of individual monosaccharides at several time points by HPLC revealed the order of monosaccharide appearance in solution through time. It is interesting to note that no xylose or mannose were detected after 2 h, with small amounts appearing after 24 h, and finally much larger amounts being present after 672 h, more in fact than some other sugars which appeared earlier. This reveals that polysaccharides such as xylans and mannans were not available for enzymic digestion at the start, and once other polysaccharides had been digested they were released into solution. Several significant differences between treatments were observed, particularly in the cases of galactose and glucose, but no trend with UV levels was found. After 672 h, the amount of carbohydrate extracted was no longer increasing, even though fresh Driselase was added every 168 h in case denaturation of the enzymes had occurred. This suggests that only compounds such a lignin remained as the visible solid in suspension. Importantly, at no point was there a trend with UV-B levels, showing that Driselase digestion does not mimic the decomposition process found in the field. Also, the lack of difference in monosaccharide composition of the solutions with time may have simply been due to the fact that sugars are found in a variety of

different polysaccharides, and Driselase is a mixture of enzymes which will digest almost all of these polysaccharides. Therefore, any small difference in one polysaccharide content between treatments may be masked by the digestion of another with similar sugars. A more targeted digestion with selective enzymes in future experiments would reveal any smaller differences and may constitute a better approach towards the analysis of cell wall structure and content.

Several studies have reported on other properties which may explain differences in decomposition rate between UV treatments. Lignin and lignin:N ratios were found by Melillo *et al*. (1982) to be strongly correlated with mass loss rates. However, other studies did not find this effect (Moore, 1984; McClaugherty *et al*., 1985), while Taylor *et al*. (1989) have suggested that C:N ratios and %N content provide better indicators of decomposition rates. In this experiment, the lignin contents of each treatment was found not to be significantly different (Table 3.1.9). The %N and C:N ratios of air-dried leaves and AIR before decomposition were also measured and found to be significantly different between some treatments, but no trend with UV was found, while the %C between treatments was not significantly different. Importantly, the unenclosed 'Control' and polytunnel 'All UV' had significantly different %N but a similar decomposition rate. This trend was also found in AIR of leaf material after one year of decomposition, where %N was higher in the 'Control', and interestingly all samples had similar %C but almost double %N than before decomposition. These assays did not explain the difference in decomposition rate observed between treatments, suggesting that it may be due to other factors such as leaf toughness or cutin content (Gallardo & Merino, 1993) which were not measured in this study.

However, as similar experiments in the past have revealed (Newsham *et al*., 2005; Kotilainen *et al*., 2008), the change in UV levels had an effect on UV-absorbing compound content (Figure 3.1.10). The amount of four ethanol-extractable compounds was found to decrease with decreasing UV (Figure 3.1.11), suggesting that the plants did not synthesise these compounds, which may act as UV-screening agents, if they were not required. Unfortunately, the identity of these compounds remains unknown, despite their absorption spectra having been recorded (Figure 3.1.12). More leaf material would be necessary to obtain enough of the compounds to submit them to mass spectrometry and ^{1}H-NMR which would allow identification. Future studies in this area should therefore ensure that enough leaf material is collected to allow for this kind of investigation.

As an attempt at finding a link between UV levels and pectin methylesterification levels (as an explanation for methane emissions, see section 4.2), the total uronic acid content and methyl ester content of the AIR of samples from each UV treatment were measured. No significant difference in uronic acid content was found, but a significant difference in methyl ester content was found between the 'Control' samples and the other three treatments (Table 3.1.9). As there was no significant difference between the 'No UV' and the 'All UV' treatment, it suggests that this may have been a temperature effect. It is possible that the difference in UV levels was not great enough between treatments to see an effect in methyl ester content, or that the process of UV-filtration had no effect on demethylation. It would be interesting to carry out a similar experiment with UV-supplementation to see if the plants react differently.

4.2 Aerobic methane production from pectin

The controversy over the methane emissions observed by Keppler *et al*. (2006) largely resulted from the failed attempts to replicate his experiments (Beerling *et al*., 2007; Dueck *et al*., 2007), from the successful observations of methane emissions from other types of vegetation under aerobic conditions (Cao *et al*., 2008; Wang *et al*., 2008), from the debate over its potential significance in the global methane budget (Houweling *et al*., 2006; Kirschbaum *et al*., 2006; Miller *et al*., 2007) and from the lack of understanding about the mechanism of methane formation (Sharpatyi, 2007; Keppler *et al*., 2008). The contradicting results of the attempts to demonstrate similar results to the original experiments could arise from a difference in experimental set-up which may not have been identified at the time due to lack of understanding about the mechanism of methane formation. Indeed, Beerling *et al*. (2007) state in their conclusion that the gas-exchange chambers they used did not transmit all wavelengths of UV light. The debate over the significance of these emissions for the global methane budget was rendered difficult because each species observed by Keppler *et al*. (2006) emitted methane at different rates. Extrapolations to global biomass are flawed if some species (or organs of some species, such as roots) are not contributing or if some environmental conditions are unfavourable to aerobic methane production. Indeed, it is therefore the lack of understanding about the potential mechanism behind aerobic methane production which is the cause for most of these problems, and a clear understanding of the chemistry and environmental factors involved would allow the development of more realistic experiments to measure emissions from vegetation. These could then be used in conjunction with other data about factors which may influence this mechanism to

obtain global estimates and finally understand the significance of aerobic methane emissions in the global methane budget.

4.2.1 Effects of UV irradiation on pectin and other compounds

Keppler *et al*. (2006) suggested that pectin was a potential source of methane, based on the carbon isotope ratio of the methane emitted. Pectin has methyl ester groups on some of the galacturonic acid residues of its backbone (Figure 1.2.1a) which have a similar isotopic signature to that of the emitted methane measured by Keppler *et al*. (2006). In the experiments described in this thesis, UV-irradiation was chosen as a method of generating methane following the observation by Keppler *et al*. (2006) that methane emissions increased when sunlight was present. The irradiation of pectin sheets by a range of intensities of UV light by lamps of different spectral irradiances and by sunlight produced methane under aerobic conditions (Figure 3.2.1). The highest intensity of artificial UV irradiance from the lamps used (McLeod *et al*., 2008) was still well below the highest intensity of global erythemal UV irradiance (Liley & McKenzie, 2006), thus ensuring any emissions observed result from realistic UV levels. Whilst each type of UV-source had a linear response between unweighted irradiance and methane emissions, by applying a theoretical spectral weighting function which gave more importance to shorter wavelengths (in a similar way to the CIE erythemal action spectrum (McKinlay & Diffey, 1987) or the DNA damage action spectrum (Setlow, 1974)), a significant linear regression was obtained for the whole dataset (Figure 3.2.3; McLeod *et al*., 2008). However, the weighting function used was idealized and it is possible it simply gave a satisfactory fit and the actual action spectrum is different (Micheletti *et al*., 2003). The

construction of an action spectrum for the response of methane emissions from pectin due to UV irradiation is therefore necessary in the future.

While this type of data from an *in vitro* study of a purified polysaccharide may have limited value for extrapolation to methane emissions from vegetation, it does however prove that pectin can produce methane and that UV is part of a potential mechanism for such a process. The use of a total UV-filter (Courtgard) during one set of experiments resulted in pectin producing only trace amounts of methane and confirmed that it was the UV light causing the methane to be produced and not the small amounts of visible or infrared light emitted by the lamps. Indeed, while monosaccharides such as GalA did not absorb much in the UV range, commercial pectin absorbed considerably in the UV-A and UV-B (Figure 3.2.4). While pectin is known to contain some phenolic compounds (Fry 1982, 1983), it is possible the UV absorbance of commercial pectin was due to the presence of impurities present after the manufacturing process of this compound. It is possible that external UV-absorbing compounds were introduced, or that UV-absorbing compounds from within the citrus cells, such as flavonoids or terpenoids, became bound to the pectin (Jarvis, personal communication). Indeed, some of the UV-absorbance seemed to be due to small molecular weight chemical impurities, since washing with 75% (v/v) ethanol reduced the UV-absorbance of a pectin solution by 40% (Figure 3.2.4). Subsequent irradiation with UV produced methane emissions which were 36% lower than those from untreated pectin (Figure 3.2.5). These data suggest that chemically bound UV-absorbing groups, possibly phenolic groups, were present in the pectin and may be vital for a UV-driven methane generating mechanism. Even though it is difficult to be sure that the UV light was not being

absorbed by an impurity, this does not affect our understanding of the mechanism of methane generation from pectin *in vivo*.

The UV-irradiation of pectate, formed by saponification of pectin to remove ester groups, resulted in only trace amounts of methane being formed (Figure 3.2.5). While the UV-absorbance of pectate was lower than that of pectin, this was almost certainly due to the ethanol-precipitation stage of the preparation of pectate, as the absorption spectrum of pectate was very similar to that of washed pectin. However, instead of a ~36% reduction in methane emissions which would be expected due to washing in ethanol only, the emissions were reduced by over 99%. This strongly suggests that ester groups (probably methyl esters) were the source of the methane observed from UV-irradiation of pectin, and not a possible by-product of polysaccharide breakdown by high levels of UV energy.

Other types of methyl groups are, however, present in pectin, such as in '*C*-methyl-pentose' residues (e.g. rhamnose) which would be found abundantly in RG-I and RG-II regions of pectin, as well as *O*-acetyl esters. Importantly, while rhamnose would not have been affected by saponification, acetyl groups would have been removed in the previous experiment and the source of the methane can therefore not be solely ascribed to the methyl ester groups. Irradiation of rhamnose, mannose and mannose pentaacetate produced only trace amounts of methane in each case (Figure 3.2.6). However, this may simply have been due to their lack of absorbance in the UV-range (Figure 3.2.4). Further experiments (see section 4.2.2) were therefore necessary to determine the potential role of rhamnose and acetyl groups in the aerobic production of methane from pectin.

While the pectin molecule is made up of homogalacturonan (HG), xylogalacturonans, rhamnogalacturonan-I and rhamnogalacturonan-II (Willats *et al*., 2001), HG regions are the most common as well as the likely source of the methane since they contain the majority of the methyl ester groups. HG, a linear polysaccharide made up of GalA residues joined through (1→4)-bonding, can easily be purchased and therefore used as a simpler model for pectin in experiments. Adding methyl ester groups to HG can also be carried out, thereby forming HGMe. The HGMe synthesised in the laboratory contained approximately 43% of GalA residues with methyl esters. While this is lower than the degree of methyl esterification found in pectin (~70%), HGMe is still a useful model compound for the future study of pectin. The main difference between the homogalacturonan found in pectin and HGMe, apart from the degree of methyl esterification, is that the chemical addition of methyl ester groups results in a random distribution of esterified and non-esterified GalA residues, while in the pectin molecule methyl esterified GalA residues are generally found in a block-wise fashion because the methyl de-esterification is carried out enzymically (Limberg *et al*., 2000). This may have implications in future experiments (see section 4.2.2). UV-irradiation of HG and HGMe produced only trace amounts of methane, but as with rhamnose and mannose penta acetate, this may be due to their lack of absorbance in the UV-range (Figure 3.2.4).

If methyl esters are indeed the source of the methane, then an even simpler model to use in investigations would be GalA methyl ester (GalAMe). Indeed, the use of a monosaccharide would allow an evaluation of whether it is necessary for the compound to be found in a polysaccharide, or if this is irrelevant for the mechanism

of methane formation. The main problem encountered during the synthesis of GalAMe by methylation of GalA was the competing methylation reaction at the anomeric position. While this does not affect the methylation at the carboxylic acid position, the resulting product would contain methyl glycosides as well as methyl esters, which would be of no use in future methane experiments as it would be impossible to distinguish the origin of the methane. Experimenting with methanol and an acidic catalyst at different concentrations for different amounts of time resulted in the predominant synthesis of GalAMe, but always with a small amount of methyl glycoside present (Figures 3.2.7 and 3.2.8). Further attempts were made to synthesise GalAMe with different mechanisms (Figures 3.2.11 and 3.2.12) but were unsuccessful and the compound was not used in methane experiments. However, as the next section will show, the successful synthesis of HGMe was sufficient for the understanding of the mechanism of aerobic methane production.

4.2.2 ROS as part of a mechanism for methane production from pectin

The previous experiments indicated that methyl esters from the pectin backbone were the likely source of aerobic methane emissions and that the mechanism could be UV-driven, but they did not explain the chemistry behind the emissions. Indeed, the UV could not be turning methyl esters directly into methane since pure sugar residues and methyl esters do not absorb much in the UV-A or UV-B region (Bednarczyk & Marchlewski, 1938; Slein & Schnell, 1953; Hershenson, 1956). While the pectin molecule clearly contains UV-absorbing moieties (Figure 3.2.4), it was unclear how they could be transferring the energy from the UV light to the methyl esters to

generate methane. The only logical suggestion for this transfer would be the involvement of an intermediary.

Shortly after the first report of aerobic methane emissions by Keppler *et al.* (2006), Sharpatyi (2007) suggested, based on some previous work with photo- and ionising irradiation of polysaccharides, that the mechanism possibly involved free radical mechanisms. ROS, as highly unstable and oxidising molecules, would seem like a reasonable intermediary for this mechanism as they are known to cause polysaccharide breakdown and are readily found in plants, including their cell walls (Fry, 1998; Schopfer *et al.*, 2002). Experiments with ROS scavengers were therefore carried out. UV-irradiation of pectin sheets impregnated with ROS scavengers should not produce any methane if ROS are an intermediary; however, if they are not an intermediary, then methane emissions should be unaffected.

Figure 3.2.13 shows the observed effect of the presence of ROS scavengers on methane emissions from pectin sheets. While UV-irradiation of pectin produced over 1000 ng g^{-1} h^{-1} of methane, if DABCO was added to the pectin sheet then only trace amounts of methane evolved under identical conditions. Since DABCO is a $^1O_2$ scavenger (Heiser *et al.*, 2003), one might be led to think that the removal of $^1O_2$ prevented the formation of methane and therefore that $^1O_2$ was the intermediary. However, DABCO has a high absorbance in the relevant UV-range (Figure 3.2.14) and therefore might simply be absorbing the UV light before it reached the pectin molecule, acting as a UV-blocking agent rather than a ROS scavenger. Only ROS scavengers with a very small or no absorbance in the UV range would be of any use to evaluate this mechanism. Therefore, KI was added to pectin sheets since it is a

scavenger of H_2O_2, $^{\bullet}OH$ and $^1O_2$ and has almost no absorbance in the relevant UV-range (Figure 3.2.14). In this case, methane emissions from UV-irradiation were reduced to trace levels (Figure 3.2.13), suggesting that at least one of these three ROS was an intermediary in the mechanism of methane formation. The use of a more specific scavenger, mannitol, which has almost no absorbance in the UV range and scavenges $^{\bullet}OH$, reduced methane emissions by up to 70%. The fact that emissions were not completely stopped could suggest that another ROS such as $^1O_2$ is responsible for around 30% of observed emissions, or it could be that the concentration of mannitol was insufficient to achieve complete scavenging of $^{\bullet}OH$ and that $^{\bullet}OH$ may in fact have been solely responsible for methane production. This problem could not be solved at this stage and requires further investigation with ROS generators.

A suitable ROS generator was tryptophan, an amino acid found in all living organisms, which also has a high absorbance in the UV-range and, when irradiated with UV light, produces $^1O_2$ (Knox & Dodge, 1985). The addition of tryptophan to pectin sheets could have enhanced methane emissions, but it would not demonstrate that the generation of ROS was essential for the mechanism. Instead, HGMe and HG were used since neither emitted much methane when UV-irradiated and also both have a very low UV-absorbance. Upon UV-irradiation, HGMe produced almost three times more methane (over 3000 ng g^{-1} h^{-1}) than did pectin under similar conditions, while HG produced approximately 300 ng g^{-1} h^{-1} (Figure 3.2.15). Without the addition of tryptophan, both compounds produced under 100 ng g^{-1} h^{-1} (Figure 3.2.15). This experiment clearly demonstrated several points. Firstly, it was not necessary for the source compound to be absorbing the UV light in order to

produce methane, but a photosensitiser such as tryptophan could act as an intermediary. Secondly, the fact that methane emissions only occurred significantly when tryptophan was present showed that it was the generation of ROS, in this case $^1O_2$, which led to the production of methane. And finally, the fact that HGMe produced over 10 times more methane than did HG was another demonstration that methyl ester groups are the source of the methane and that polysaccharide breakdown by high levels of UV or ROS may have been responsible for only a very small amount of this methane. The reasons why HGMe produced so much more methane than pectin under identical conditions was not clear at this stage and further experiments with addition of ROS were therefore carried out.

If ROS are an intermediary in a mechanism of methane formation, then their generation by other means than UV light and a photosensitiser should lead to methane production, which would show that UV light is not essential for this process and that indeed any process which generates ROS could initiate the mechanism. The addition of H_2O_2, KO_2 and Fenton reagents, a known generator of $^{\bullet}OH$, to polysaccharide solutions was carried out and methane emissions were recorded (Figure 3.2.16). H_2O_2 and KO_2 addition produced no significant methane emissions in the case of pectin, pectate, HGMe and HG. This suggests that these two ROS were not those ROS responsible for methane emissions in the UV-irradiation experiments with pectin. The generation of $^{\bullet}OH$ with Fenton reagents, however, produced methane from pectin solutions at rates up to 44 ng g^{-1} h^{-1}. In the case of pectate, no significant methane emissions were observed, once again demonstrating that the lack of ester groups resulted in a lack of methane emissions. The data in Figure 3.2.16 corroborate the observation that mannitol reduced methane emissions

from pectin by over 70% upon UV-irradiation (Figure 3.2.13), suggesting that $^{\bullet}OH$ were involved in this mechanism. Also, addition of mannitol to the pectin solution considerably reduced $^{\bullet}OH$-induced methane emissions, confirming that it was the generation of $^{\bullet}OH$ which was producing the methane and not the action of one of the constituents of Fenton reagents. Addition of $^{\bullet}OH$ in a solution of HG produced no significant methane emissions, again suggesting that breakdown of the sugar residues was not a major source of methane. The addition of $^{\bullet}OH$ in the case of HGMe, however, caused very large methane emissions, over five hundred times more than in the case of pectin. Contaminant CH_3I or DMSO were determined not to be an explanation for this. Pectin contains RG-I and RG-II regions, which are also known as "hairy" regions since they branch out from the backbone of the molecule, and possibly effectively shield some of the methyl esters from $^{\bullet}OH$ attack by steric hindrance. Pectin also contains many other sugars than GalA, which could be preferentially scavenging $^{\bullet}OH$. Another major difference between pectin and HGMe is, as stated in section 4.2.1, the pattern of methyl esterification being random or in a block-wise fashion. This could result in a difference in the binding pattern of transition metals to the GalA residues which do not carry methyl ester groups, thereby causing a difference in the localisation of the generation of $^{\bullet}OH$. This is important because $^{\bullet}OH$ is very short-lived and is predicted to react with organic matter within ~1 nm of the site of radical production (Griffiths & Lunec, 1996). Indeed, $^{\bullet}OH$ generated in the case of HGMe may therefore be more likely to be close to a methyl ester group, and thus generate methane, than if it had been generated close to pectin, where the nearest methyl ester group may be not be close and would therefore not lead to the production of methane. Finally, it is also possible that

degradation of HG occurred during the synthesis of HGMe, resulting in methyl groups being inserted in forms other than methyl esters. Although unlikely to be a very fast reaction in the conditions the synthesis was carried out in (room temperature, in the dark for 24 h), it is possible that β-elimination of HG resulted in shorter HG molecules being formed with methyl groups at their extremities, as well as in methyl esters found attached to the GalA residues. This could result in methane originating from non-methyl esters being generated upon ROS-attack in large quantities if these new methyl groups have a high affinity for $^{\bullet}$OH. While testing these hypotheses would be interesting, it is not really necessary since HGMe is an artificial compound which was made to test a theory and therefore it is not directly relevant for the understanding of the mechanism of aerobic methane production from vegetation.

The addition of $^{\bullet}$OH to solutions of rhamnose and mannose produced no significant methane emissions (Figure 3.2.16). This showed that the absence of methane emissions after UV-irradiation of these compounds (Figure 3.2.6) was not due solely to their lack of absorbance in the UV range, but that even if ROS were generated, methane would not be produced from these compounds, and therefore '*C*-methyl-pentose' residues are not a potential source of methane. Addition of $^{\bullet}$OH to solutions of mannose pentaacetate, however, produced small but significant methane emissions, unlike following UV-irradiation. This suggests that UV radiation failed to produce methane because mannose pentaacetate did not absorb the UV and no ROS were generated. *O*-Acetyl esters, present in pectin but removed by saponification at the same time as methyl esters, are therefore a potential source of methane. This means that future experiments investigating the chemical origin of methane from

pectin (e.g. using ^{13}C-labelling as in Keppler *et al*. (2008)) need to take these acetate groups into consideration.

These results are summarised in McLeod *et al*. (2008), Messenger *et al*. (2009a) and Messenger *et al*. (2009b) (see Appendix).

4.2.3 Methyl halide emissions from pectin

These past experiments have shown that methane can evolve from pectin upon UV-irradiation, a process which involves a photosensitiser (required to absorb the UV light) generating ROS (predominantly $^{\bullet}OH$, but possibly also $^1O_2$) which then attack methyl esters groups (and acetate groups, though maybe to a lesser extent) to form methane. This last step in the mechanism, however, involves the formation of methyl radicals from methyl esters. These methyl radicals can then be converted into methane, but if a compound other than a hydrogen-donor and capable of reacting with these methyl radicals were present, then methane formation would be prevented and a different product would be formed. One such class of compounds is halides. Halide ions, namely Cl^-, Br^- and I^-, are present in vegetation and contribute to methyl halide emissions, a process which is poorly understood (Redeker *et al*., 2000; Hamilton *et al*., 2003). If methyl radicals were to react with a halide ion then methyl halides would be emitted, which signifies that instead of methane, UV-irradiation of pectin with halide ions would produce methyl halides.

The addition of halide ions to pectin sheets significantly increased emissions of methyl chloride and methyl bromide, as well as causing methyl iodide to be emitted (Figure 3.2.17). The fact that pectin was producing methyl chloride and methyl bromide even before any halide ions were added was possibly due to the

presence of a trace amount of these halides in commercial pectin. However, Figure 3.2.18 illustrates that many other compounds were emitted upon addition of halide ions, possibly di-halide compounds or halides of ethylene or ethane. Attempts to identify these by GC-MS were unsuccessful, meaning that calculations of conversion rates of halide ions to methyl halides are impossible, but the mechanism remains valid. It is possible that these compounds were generated due to the high concentration of methyl radicals and halide ions, which would not be found in vegetation, and therefore may not be generated *in vivo*. Importantly, the methane emissions measured at the same time as these methyl halide emissions were found to decrease when compared to the emissions of pectin alone. In the case of the addition of iodide, the emissions of methane were virtually absent, possibly because iodide is also a ROS scavenger and therefore it prevented the mechanism from taking place normally. MeI may have been formed from the small amount of methyl radicals formed by hydroxyl radicals which were not scavenged by the iodide ions. These data support the hypothesis that the conversion of methyl esters to methane involves the formation of methyl radicals and suggest that the mechanism of aerobic methane formation might also partly explain the mechanism of some methyl halide emissions from some vegetation. These emissions would likely be very dependent on the concentration of halide ions in the vegetation and may therefore be greater in plants growing in areas of high salt concentration. This mechanism may also explain the emissions of ethylene and ethane, possibly formed following the reaction of two methyl radicals, observed by McLeod *et al*. (2008). Ethylene is well-known to be emitted from certain plants in response to various stresses and as a signalling molecule in healthy tissues (Bleecker & Kende, 2000), but this would be a novel

non-enzymic mechanism for its formation and deserves further investigation. Additionally, isoprene is known to be emitted by some plants. Isoprene production from *Quercus* was found to increase upon increased UV irradiation, but this was not observed with *Mucuna* (Harley *et al*., 1996). However, this process is thought to be enzymic (Affek & Yakir, 2003). Interestingly, isoprene has recently been found to act as a ROS scavenger in leaves (Velikova *et al*., 2005) and it has been suggested that it may protect plants during abiotic stress (Velikova, 2008). Whether isoprene emissions have any effect on aerobic methane emissions from vegetation by scavenging ROS has not yet been studied and may explain the great difference in emission rates observed between some species by Keppler *et al*. (2006), which would have implications for the significance of aerobic methane emissions in the global methane budget. While it is difficult to obtain any estimates from these data regarding global emissions, the discovery of this mechanism will hopefully lead to further research into understanding how plants emit gases such as methyl halides or other hydrocarbons.

4.3 Generation of reactive oxygen species by UV and γ-irradiation

The research of the previous section clearly showed that UV was causing the generation of ROS *in vitro*. This process is known to occur *in vivo*, though possibly through different mechanisms (A.-H.-Mackerness, 2000; Langebartels *et al*., 2002). This means that the UV-driven methane production may have effects on plant physiology, especially in the cell wall where pectin is located, and may explain some

of the results observed in the field experiment on UV-filtration and decomposition of *F. excelsior* leaf litter.

4.3.1 NaB^3H_4-labelling of polysaccharides

Fry (1998) showed that hydroxyl radicals could be used for the oxidative scission of cell wall polysaccharides and suggested that they could act as site-specific oxidants and play a significant role in loosening of the cell wall during, for example, cell expansion or fruit ripening. Later, Fry *et al*. (2001) demonstrated that NaB^3H_4 could be used to reduce these ROS-attacked polysaccharides, which could then be treated to identify which sugars were labelled with ^3H. It was hypothesised that applying these methods to irradiated leaves might therefore demonstrate a link between irradiation and ROS-production, and thereby provide an insight into results discussed previously.

The field experiment with ash seedlings, despite having experimental artefacts such as anh increased temperature under the polytunnels or the change in UV-transmittance of the plastics with time, provided live material grown under several levels of UV-filtration. If ROS are indeed being generated *in vivo* by UV, then one would expect less ROS to have been generated in the plants grown under lower levels of UV light and for this to be detected by the NaB^3H_4-labelling method. An initial trial experiment with one leaf from each replicated treatment showed that the level of radio-labelling of the leaves was very variable (data not shown) and therefore a new experiment was carried out with eight samples from four replicates of each of the four treatments (Figure 3.3.3). The samples were ground in a cooled buffer and stored in the buffer at –80°C between preparation and labelling to

minimise loss of oxo groups. However, the NaB^3H_4-labelled AIR from the leaves of each treatment did not show a significant difference in radio-labelling (Table 3.3.1). Hydrolysis of the plant material with TFA showed that [^{3}H]galactose and [^{3}H]arabinose were the main labelled sugars present, with several unidentified sugars present as well (Figures 3.3.4a and 3.3.5). However, there was no visible qualitative difference in sugar-labelling between UV treatments. It was interesting to note that the cellulose of these leaves did not contain any [^{3}H]glucose (Figures 3.3.4b and 3.3.6), suggesting that cellulose microfibrils were less likely to be attacked by ROS than hemicelluloses and pectins. Fry *et al*. (2001) found that ROS-attack of pectins produced [^{3}H]galacturonate. While some radio-labelled sugars co-migrated with the galacturonate marker, there was no visible decrease in concentration of these compounds due to UV filtration, suggesting that ROS-attack of pectins was not affected by changes in UV irradiation. Also, it could be that the RG-I regions of pectin, which contain large side-chains made of arabinose and galactose, were shielding the homogalacturonan backbone of pectin from ROS-attack, thereby explaining the low levels of [^{3}H]galacturonate compared to [^{3}H]galactose or [^{3}H]arabinose. Clearly, only partial conclusions can be drawn from this experiment and further in-depth investigations are needed to identify which polysaccharides are being attacked by ROS.

These data suggest that the difference in UV levels had no significant effect on ROS levels in the seedlings of this field experiment. This may be because the difference in UV levels between treatments was actually lower than expected or the background production of ROS by other phenomenon was much higher than the level of ROS production due to UV and therefore any UV effect would be difficult to

detect. It could also be that the increased temperature under the polytunnels would have increased ROS production slightly, therefore minimising any decrease in ROS production due to lower UV levels. It would be interesting to repeat this type of field experiment with UV-supplementation instead of filtration to see if a plant response is detected.

4.3.2 UV- and γ-irradiation of leaves

While the UV-filtration in the field experiment did not produce any difference in ROS levels between UV treatments, a set of laboratory experiments were carried out with irradiation of freshly detached leaves to see if an increase in UV radiation produced the expected increase in ROS production. UV-irradiation of ash leaves was not possible because of a lack of plant material, so *Kalanchoe* and lettuce leaves, both readily available, were used instead. In both cases, only the epidermis was collected for NaB^3H_4-labelling since this is likely to be where the UV has maximum effect. Neither the abaxial or adaxial epidermis of the *Kalanchoe* leaf showed any significant increase in ROS levels with increased UV levels, nor did the green part of the Lettuce leaf (Figure 3.3.7). However, the epidermis from the white part of the lettuce leaf did show a significant increase in ROS-attacked polysaccharides with increased UV. This may be because the white part of the leaf is not adapted to receiving high levels of UV light, unlike the green part, and therefore contains less protective mechanisms such as UV screening agents or antioxidants. Thus, the lack of a detectable UV effect in the other plant tissues may simply be because the UV levels were not high enough to overcome the defence mechanisms in the leaf. This suggests that the NaB^3H_4 labelling method has the potential to detect differences in ROS-attacked polysaccharides created by increased or decreased UV levels, if such a

difference exists. A qualitative analysis (Figure 3.3.8) showed that an increase in UV levels caused an increase in radio-labelled galactose, glucose, arabinose, xylose and some uronic acids. Separation of radio-labelled compounds by paper electrophoresis (Figure 3.3.9) showed that the UV treatment resulted in the formation of three radio-labelled charged compounds, instead of two for the control. Further analysis suggested that this new compound was [^{3}H]ManA. However, it would be important to carry out further experiments with a wider range of plant species to ensure that the effect was not specific to lettuce leaves.

γ-Irradiation is known to produce hydroxyl radicals from water (LaVerne, 2000) and to increase ROS levels in plants (Kim *et al*., 2005). However, γ-irradiation (12 Gy h^{-1}) produced no increase in ROS-attacked polysaccharides in ash or birch leaves (Figure 3.3.11). This may be explained by the importance of dose and rate of γ-irradiation on the production of ROS. The rate of γ-irradiation was unfortunately fixed by the irradiator, and the dose was changed by modifying the time of irradiation, but it is possible that the leaves were not irradiated for long enough to see an increase in ROS levels. While of little physiological relevance to UV exposure, γ-irradiation was used as a way of confirming that the NaB^3H_4 labelling method was successful in detecting modified ROS levels *in vivo*. Unfortunately, it would seem that γ-irradiation under these circumstances was not an effective means of producing ROS *in vivo*, and while further experiments may find a way of increasing ROS levels, more relevant results would be obtained from further experiments with UV-irradiation.

4.4 Future work

This project aimed to develop an understanding of the relationship between UV-irradiation, methane emissions and ROS production in vegetation. Some of the links between these topics have been either established for the first time or the findings of other research groups have been confirmed. Nevertheless, several aspects of the project would benefit from further research. The field experiment yielded several interesting results, but would benefit from being repeated with either different types of UV-filtering plastics, or with the replacement of each plastic every 3 – 4 weeks to prevent changes in UV-transmission levels. The results obtained, such as the change in decomposition rates due to UV levels or the lack of changes in the cell wall components, could serve as the basis for future studies. It would also be interesting to replicate this type of study on other species such as oak, or even non-deciduous trees such as conifers, to investigate the importance of plant physiology, morphology or phytochemistry. Building on this work and that of Newsham *et al*. (2001a; 2001b) and McLeod *et al*. (2007) could lead to further insights into the effects of UV-irradiance on leaf decomposition rates and cell wall biochemistry.

Following on the work of Keppler *et al*. (2006), the UV-irradiation of pectin clearly demonstrated a potential mechanism for this process, and the subsequent studies with ROS scavengers and generators showed that ROS are an intermediary in this process. While the use of *in vitro* experiments such as these only allows for crude global estimates to be made, they should help other scientists who are currently carrying out experiments with live vegetation to understand which environmental factors need to be controlled or monitored, in ways which were not carried out in the studies of Dueck *et al*. (2007) or Beerling *et al*. (2007). Whether or not aerobic methane emissions from vegetation contribute significantly to the global methane

budget as estimated by Keppler *et al*. (2006), it is essential that further work in this field is carried out so that the significance of this process can be understood, and the validity of the global methane budget assured.

The generation of ROS due to UV-irradiation, or the lack thereof due to UV-filtration, is a difficult phenomenon to monitor. However, it is important to do so as it may explain many surprising results, whether in plant physiological processes such as growth or hormone production, or in microbial processes such decomposition. Indeed, the effects of ROS demethylesterification of pectin to produce methane in the plant cell wall may be very important during, for example, cell growth. It is vital that further research is carried out in this field to establish the importance of UV in ROS-generation processes *in vivo*.

Finally, the common factor to all parts of this project was plant cell walls. Several new facts about cell walls have emerged from this project, such as their lack of change in ash under field UV-filtration conditions, despite changes in decomposition levels, or their more surprising ability to generate methane under ROS-attack. Importantly, many of these findings were due to the diverse backgrounds of the researchers involved in this project, such as organic chemistry, plant science, UV photobiology and forest ecology. There is, however, a global trend in the scientific community towards studying what are seen as more modern and exciting fields such as genetic expression or systems biology, and neglecting the study of more fundamental processes such as plant cell wall biochemistry, which could not currently be predicted from studies of gene sequences or expression. Further, the increasing specialisation of scientists into very narrow fields of research

and their reticence to learn from scientists in other fields leads to misunderstandings, prevents lateral thinking and is counter-productive to the advancement of science. This project, however, was very much inter-disciplinary in nature, bringing together knowledge from several different backgrounds, studying fundamental biochemical processes, and it is the author's hope that more projects like this will be carried out in the future.

References

A.-H.-Mackerness S. (2000) Plant responses to ultraviolet-B (UV-B: 280–320 nm) stress: What are the key regulators? *Plant Growth Regulation* **32**, 27–39.

A.-H.-Mackerness S., John C.F., Jordan B., Thomas B. (2001) Early signaling components in ultraviolet-B responses: distinct roles for different reactive oxygen species and nitric oxide. *FEBS letters* **489**, 237–242.

Aber J.D., Melillo J.M., McClaugherty C.A. (1990) Predicting long-term patterns of mass loss, nitrogen dynamics, and Soil Organic Matter Formation from Initial Fine Litter Chemistry in Temperate Forest Ecosystems. *Canadian Journal of Botany* **68,** 2201–2208.

Affek H.P. & Yakir D. (2003) Natural abundance carbon isotope composition of isoprene reflects incomplete coupling between isoprene synthesis and photosynthetic carbon flow. *Plant Physiology* **131**, 1727–1736.

Apel K. & Hirt H. (2004) Reactive oxygen species: metabolism, oxidative stress, and signal transduction. *Annual Review of Plant Biology* **55**, 373–399.

Austin A.T. & Vivanco L. (2006) Plant litter decomposition in a semi-arid ecosystem controlled by photodegradation. *Nature* **442**, 555–558.

Batschauer A., Rocholl M., Kaiser T., Nagatani A., Furuya M., Schäfer E. (1996) Blue and UV-A light-regulated CHS expression in Arabidopsis independent of phytochrome A and phytochrome B. *Plant Journal* **9**, 63–69.

Baydoun E.A.-H. & Brett C.T. (1984) The effect of pH on the binding of calcium to pea epicotyl cell walls and its implications for the control of cell extension. *Journal of Experimental Botany* **35**, 1820–1831.

Bednarczyk W.I. & Marchlewski L. (1938) Information on sugar reduction V. *Biochemische Zeitschrift* **300**, 42–45.

Beerling D.J., Gardiner T., Leggett G., McLeod A., Quick W.P. (2007) Missing methane emissions from leaves of terrestrial plants. *Global Change Biology* **14**, 1–6.

Berry J. & Björkman O. (1980) Photosynthetic Response and Adaptation to Temperature in Higher Plants. *Annual Review of Plant Physiology* **31**, 491–543.

Björn L.O. (2002) *Photobiology*. Dordrecht: Kluwer Academic Publishers.

Bleecker A.B. & Kende H. (2000) Ethylene: A gaseous signal molecule in plants. *Annual Review of Cell and Developmental Biology* **16**, 1–18.

Blunier T., Chappellaz J., Schwander J., Stauffer B., Raynaud D. (1995) Vaiations in atmospheric methane concentration during the Holocen epoch. *Nature* **375**, 46–49.

Bousquet P., Ciais P., Miller J.B., Dlugokencky E.J., Hauglustaine D.A., Prigent C., Van der Werf G.R., Peylin P., Brunke E.G., Carouge C., Langenfelds R.L., Lathiere J., Papa F., Ramonet M., Schmidt M., Steele L.P., Tyler S.C., White J. (2006) Contribution of anthropogenic and natural sources of atmospheric methane variability. *Nature* **443**, 439–443.

Britt A.B. (1999) Molecular genetics of DNA repair in higher plants. *Trend in plant science* **4**, 20–25.

Buxton G.V., Greenstock C.L., Helman W.P., Ross A.B. (1988) Critical review of rate constants for reactions of hydrated electrons, hydrogen atoms and

hydroxyl radicals in aqueous solution. *Journal of Physical Chemistry Reference Data* **17**, 513–883.

Brosché M. & Strid Å. (2003) Molecular events following perception of ultraviolet-B radiation by plants. *Physiologia Plantarum* **117**, 1–10.

Caldwell M.M. (1971) Solar ultraviolet radiation and the growth and development of higher plants. In: *Photophysiology* (ed. Giese A.C.), pp. 131–177. New York Academic Press, New York, USA.

Caldwell M.M. & Flint S.D. (1994) Stratospheric ozone reduction, solar UV-B radiation and terrestrial ecosystems. *Climatic Change* **28**, 375–394.

Caldwell M.M. & Flint S.D. (1997) Uses of biological spectral weighting functions and the need to scaling for the ozone reduction problem. *Plant Ecololgy* **128**, 66–76.

Cao G., Xu X., Long R., Wang Q., Wang C., Du Y., Zhao X. (2008) Methane emissions by alpine plant communities in the Qinghai-Tibet Plateau. *Biology Letters*. doi: 10.1098/rsbl.2008.0373.

Chen Y-H. & Prinn R.G. (2006) Estimation of atmospheric methane emissions between 1996 and 2001 using a three-dimensional global chemical transport model. *Journal of Geophysical Research* **111**, D10307, doi:10.1029/2005JD006058.

Clarke L.J. & Robinson S.A. (2008) Cell wall-bound ultraviolet-screening compounds explain the high ultraviolet tolerance of the Antarctic moss, *Ceratodon purpureus*. *New Phytologist* **179**, 776–783.

Cockell C.S. & Knowland J. (1999) Ultraviolet radiation screening compounds. *Biological reviews* **74**, 311–345.

Conklin P.L., Williams E.H., Last R.L. (1996) Environmental stress sensitivity of an ascorbic acid-deficient Arabidopsis mutant. *Proceedings of the National Academy of Sciences* **93**, 9970–9974.

Crutzen P.J., Sanhueza E., Brenninkmeijer C.A.M. (2006) Methane production from mixed tropical savanna and forest vegetation in Venezuela. *Atmospheric Chemistry and Physics Discussion* **6**, 3093–3097.

Cybulski III W.J., Peterjohna W.T., Sullivan J.H. (2000) The influence of elevated ultraviolet-B radiation (UV-B) on tissue quality and decomposition of loblolly pine (*Pinus taeda* L.) needles. *Environmental and Experimental Botany* **44**, 231–241.

do Carmo J.B., Keller M., Dias J.D., de Camargo P.B., Crill P. (2006) A source of methane from upland forests in the Brazilian Amazon. *Geophyical Research Letters* **33**: article number L04809.

Day T.A. (2001) Multiple trophic levels in UV-B assessments – completing the ecosystem. *New Phytologist* **152**, 183−186.

Debevec E.M. & MacLean S.F. Jr (1993) Design of greenhouses for the manipulation of temperature in tundra plant communities. *Arctic and Alpine Research* **25**, 56–62.

Dlugokencky E.J., Houweling S., Bruhwiler L., Masarie K.A., Lang P.M., Miller J.B., Tans P.P. (2003) Atmospheric methane levels off: Temporary pause or a new steadystate? *Geophysical Research Letters* **30**, doi:10.1029/2003GL018126.

Doke N. (1985) NADPH-dependent O_2^- generation in membrane fractions isolated from wounded potato tubers inoculated with Phytophthora infestans. *Physiological plant pathology* **27**, 311–322.

Dueck T.A., de Visser R., Poorter H., Persijn S., Gorissen A., de Visser W., Schapendonk A., Verhagen J., Snel J., Harren F.J.M., Ngai A.K.Y., Verstappen F., Bouwmeester H., Voesenek L.A.C.J., van der Werf A.K. (2007) No evidence for substantial aerobic methane emission by terrestrial plants: a C-13-labelling approach. *New Phytologist* **175**, 29–35.

Dumville J.C. & Fry S.C. (2003) Solubilisation of tomato fruit pectins by ascorbate: a possible non-enzymic mechanism of fruit softening. *Planta* **217**, 951–961.

Eriksson K-E.L., Blanchette R.A., Ander P. (1990) Microbial and Enzymatic Degradation of Wood and Wood Components. pp 407. Springer-Verlag, Berlin, Germany.

Eshdat Y. & Mirelman D. (1972) An improved method for the recovery of compounds from paper chromatograms. *Journal of Chromatography* 65, 459–459.

Fahry G. & Schopfer P. (1998) Hydrogen peroxide production by roots and its stimulation by exogenous NADH. *Physiologia Plantarum* **103**, 395–404.

Fenton H.J.H. (1894) Oxidation of tartaric acid in presence of iron. *Journal of the Chemical Society Transactions* **65**, 899–911.

Ferretti D.F., Miller J.B., White J.W.C., Lassey K.R., Lowe D.C., Etheridge D.M. (2007) Stable isotopes provide revised global limits of aerobic methane emissions from plants. *Atmospheric Chemistry and Physics Discussions* **7**, 237–241.

Fiscus E.L. & Booker F.L. (2002) Growth of Arabidopsis flavonoid mutant is challenged by radiation longer than the UV-B band. *Environmental and Experimental Botany* **48**, 213–224.

Flint S.D. & Caldwell M.M. (2003) A biological spectral weighting function for ozone depletion research with higher plants. *Physiologia Plantarum* **117,** 137–144.

Foreman J., Demidchik V., Bothwell J.H.F., Mylona P., Miedema H., Angel Torresk M., Linstead P., Costa S., Brownlee C., Jonesk J.D.G., Davies J.M., Dolan L. (2003) Reactive oxygen species produced by NADPH oxidase regulate plant cell growth. *Nature* **422**, 442–446.

Fry S.C. (1982) Phenolic components of the primary cell wall. *Biochemical journal* **203**, 493–504.

Fry S.C. (1983) Feruloylated pectins from the primary cell wall: their structure and possible functions. *Planta* **157**, 111–123.

Fry S.C. (1986) Cross-linking of matrix polymers in the growing cell walls of angiosperms. *Annual Review of Plant Physiology* **37**, 165–186.

Fry S.C. (1989) The Structure and Functions of Xyloglucan. *Journal of Experimental Botany* **40**, 1–11.

Fry S.C. (1998) Oxidative scission of plant cell wall polysaccharides by ascorbate-induced hydroxyl radicals. *Biochemical Journal* **332**, 507–515.

Fry S.C., Dumville J.C., Miller J.G. (2001) Fingerprinting of polysaccharides attacked by hydroxyl radicals *in vitro* and in the cell walls of ripening pear fruit. *Biochemical Journal* **357**, 729–735.

Fry S.C., Miller J.G., Dumville J.C. (2002) A proposed role for copper ions in cell wall loosening. *Plant and Soil* **247**, 57–67.

Fry S.C., Smith R.C., Renwick K.F., Martin D.J., Hodge S.K., Matthews K.J. (1992) Xyloglucan endotransglycosylase, a new wall-loosening enzyme activity from plants. *Biochemical Journal* **282**, 821–828.

Gallardo A. & Merino J. (1993) Leaf Decomposition in Two Mediterranean Ecosystems of Southwest Spain: Influence of Substrate Quality. *Ecology* **74**, 152–161.

Gehrke C., Johanson U., Callaghan T.V., Chadwick D., Robinson C.H. (1995) The impact of enhanced ultraviolet-B radiation on litter quality and decomposition processes in *Vaccinium* leaves from the Subarctic. *Oikos* **72**, 213–222.

Grant J.J., Yun B.-W. & Loake G.J. (2000) Oxidative burst and cognate redox signalling reported by luciferase imaging: identification of a signal network that functions independently of ethylene, SA and Me-JA but is dependent on MAPKK activity. *The Plant Journal* **24**, 569–582.

Grantz D.A. (1990) Plant response to atmospheric humidity. *Plant, Cell & Environment* **13**, 667–679.

Green A.E.S, Sawada T., Shettle E.P. (1974) The middle ultraviolet reaching the ground. *Photochemistry and Photobiology* **19**, 251–259.

Griffiths H.R. & Lunec J. (1996) Investigating the effects of oxygen free radicals on carbohydrates in biological systems. In: *Free Radicals: a Practical Approach* (eds. Punchard N.A. & Kelly F.J.), pp. 185–200. IRL Press, Oxford, UK.

Grimes H.D., Perkins K.K., Boss W.F. (1983) Ozone degrades into hydroxyl radicals under physiological conditions. *Plant Physiology* **72**, 1016–1020.

Halliwell B. & Gutteridge J.M.C. (1990) Role of free radicals and catalytic metal ions in human disease: An overview. *Methods in Enzymology* **186**, 1–85.

Hamilton J.T.G., McRoberts W.C, Keppler F., Kalin R.M., Harper D.B. (2003) Chloride Methylation by Plant Pectin: An Efficient Environmentally Significant Process. *Science* **301**, 206–209.

Harley P., Deem G., Flint S., Caldwell M. (1996) Effects of growth under elevated UV-B on photosynthesis and isoprene emission in *Quercus gambelii* and *Mucuna pruriens*. *Global Change Biology* **2**, 149–154.

Hasegawa P.M., Bressan R.A., Zhu J-K., Bohnert H.J. (2000) Plant cellular and molecular responses to high salinity. *Annual Review of Plant Physiology and Plant Molecular Biology* **51**, 463–499.

Hatcher P.E. & Paul N.D. (1994) The effect of elevated UV-B radiation on herbivory of pea by *Autographa gamma*. *Entomological Experimental Applications* **71**, 227–233.

Hayashi T., Marsden M.P.F., Delmer D.P. (1987) Pea Xyloglucan and Cellulose: VI. Xyloglucan-Cellulose Interactions *in Vitro* and *in Vivo*. *Plant Physiology* **83**, 384–389.

Hein R., Crutzen P.J., Heimann M. (1997) An inverse modelling approach to investigate the global atmospheric methane cycle. *Global Biogeochemical Cycles* **11**, 43–76.

Heiser I., Sachs E., Liebermann B. (2003) Photodynamic oxygen activation by rubellin D, a phytotoxin produced by *Ramularia collo-cygni* (Sutton et Waller). *Physiological and Molecular Plant Pathology* **62**, 29–36.

Hershenson H.M. (1956) Ultraviolet and Visible Absorption Spectra: Index for 1930–1954. New York: Academic Press.

Houweling S., Dentener F., Lelieveld J. (2000) Simulation of preindustrial methane to constrain the global source strength of natural wetlands. *Journal of Geophysical Research* **105**, 17243–17255.

Houweling S., Röckmann T., Aben I., Keppler F., Krol M., Meirink J.F., Dlugokencky E.J., Frankenberg C. (2006) Atmospheric constraints on global emissions of methane from plants. *Geophysical Research Letters* **33**: article number L15821.

Iba K. (2002) Acclimative response to temperature sress in higher plants: Approaches of Gene Engineering for Temperature Tolerance. *Annual Review of Plant Biology* **53**, 225–245.

Ishii T. (1997) *O*-Acetylated oligosaccharides from pectins of potato tuber cell walls. *Plant Physiology* **113**, 1265–1272.

Ishii T. & Matsunaga T. (2001) Pectic polysaccharide rhamnogalacturonan II is covalently linked to homogalacturonan. *Phytochemistry* **57**, 969–974.

Jarvis M.C. (1982) The proportion of calcium-bound pectin in plant cell walls. *Planta* **154**, 344–346.

Jarvis M.C., Forsyth W., Duncan H.J. (1988) A Survey of the Pectic Content of Nonlignified Monocot Cell Walls. *Plant Physiology* **88**, 309–314.

Jiang C.-Z., Yen C.-N., Cronin K., Mitchell D., Britt A.B. (1997) UV- and Gamma-Radiation Sensitive Mutants of *Arabidopsis thaliana*. *Genetics* **147**, 1401–1409.

Johnston H.S. (1984) Human effects on the global atmosphere. *Annual Review of Physical Chemistry* **35**, 481–505.

Joo J.H., Bae Y.S., Lee J.S. (2001) Role of auxin-induced reactive oxygen species in root gravitropism. *Plant Physiology* **126**, 1055–1060.

Jordan B.R. (2002) Molecular response of plant cells to UV-B stress. *Functional Plant Biology* **29**, 909–916.

Kagawa T., Sakai T., Suetsugu N., Oikawa K., Ishiguro S., Kato T., Tabata S., Okada K., Wada M. (2001) Arabidopsis NPL1: a phototropin homolog controlling the chloroplast high-light avoidance response. *Science* **291**, 2138–2141.

Karl D.M., Beversdorf L., Björkman K.M., Church M.J., Martinez A., Delong E.F. (2008) Aerobic production of methane in the sea. *Nature Geoscience* **1**, 473–478.

Keppler F., Hamilton J.T.G., Brass M., Röckmann T. (2006) Methane emissions from terrestrial plants under aerobic conditions. *Nature* **439**, 187–191.

Keppler F., Hamilton J.T.G., McRoberts C.W., Vigano I., Brass M., Röckmann T. (2008) Methoxyl groups of plant pectin as a precursor of atmospheric methane: evidence from deuterium labelling studies. *New Phytologist* **178**, 808–814.

Kim J.H., Chung B.Y., Kim J.S., Wi S.G. (2005) Effects of *in planta* gamma-irradiation on growth, photosynthesis, and antioxidative capacity of red pepper (*Capsicum annuum* L.) plants. *Journal of Plant Biology* **48**, 47–56.

Kirschbaum M.U.F., Bruhn D., Etheridge D.M., Evans J.R., Farquhar G.D., Gifford R.M., Paul K.I., Winters A.J. (2006) A comment on the quantitative significance of aerobic methane release by plants. *Functional Plant Biology* **33**, 521–530.

Knight M.R. (2007) New ideas on root hair growth appear from the flanks. *Proceedings of the National Academy of Science USA* **104**, 20649–20650.

Knox J.P. & Dodge A.D. (1985) Singlet oxygen and plants. *Phytochemistry* **24**, 889–896.

Kotilainen T., Tegelberg R., Julkunen-Tiitto R., Lindfors A., Aphalo P.J. (2008) Metabolite specific effects of solar UV-A and UV-B on alder and birch leaf phenolics. *Global Change Biology* **14**, 1294–1304.

Kovacs E. & Keresztes A. (2002) Effect of gamma and UV-B/C radiation on plant cells. *Micron* **33**, 199–210.

Krizek D.T., Mirecki R.M., Britz S.J. (1997) Inhibitory effects of ambient levels of solar UV-A and UV-B radiation on growth of cucumber. *Physiologia Plantarum* **100**, 886–893.

Lacis A., Hansen J., Lee P., Mitchell T., Lebedeff S. (1981) Greenhouse effect of trace gases, 1970-1980. *Geophysical Research Letters* **8**, 1035–1038.

Laloi C., Apel K., Danon A. (2004) Reactive oxygen signalling: the latest news. *Current Opinion in Plant Biology* **7**, 323–328.

Lamb C. & Dixon R.A. (1997) The Oxidative burst in plant disease resistance. *Annual Review of Plant Physiology and Plant Molecular Biology* **48**, 251–275.

Langebartels C., Schraudner M., Heller W., Ernst D., Sandermann H. Jr. (2002) Oxidative stress and defense reactions in plants exposed to air pollutants and UV-B radiation. In: *Oxidative stress in plants*, (eds. Inzé D. & Van Montagu M.), pp. 105–136. Harwood Academic Publishers, Amsterdam, Netherlands.

LaVerne J.A. (2000) OH radicals and oxidizing products in the gamma radiolysis of water. *Radiation research* **153**, 196–200.

Leschine S.B. (1995) Cellulose Degradation in Anaerobic Environments. *Annual Reviews in Microbiology* **49**, 399–426.

Liley J.B. & McKenzie R.L. (2006) Where on earth has the highest uv? National Institute of Water and Atmospheric Research (NIWA) paper at http:/www.niwascience.co.nz/rc/atmos/uvconference/2006/Liley_2.pdf.

Limberg G., Körner R., Buchholt H.C., Christensen T.M.I.E., Roepstorff P., Mikkelsen J.D. (2000) Analysis of different de-esterification mechanisms for pectin by enzymatic fingerprinting using endopectin lyase and endopolygalacturonase II from *A. Niger*. *Carbohydrate Research* **327**, 293–307.

Lin C.C. & Kao C.H. (2002) Osmotic stress-induced changes in cell wall peroxidase activity and hydrogen peroxide level in roots of rice seedlings. *Plant Growth Regulation* **37**, 177–184.

Lindsay S.E. & Fry S.C. (2007) Redox and wall-restructuring. In: *The Expanding Cell* (eds. Verbelen J-P. & Vissenberg K.), pp. 159–190. Springer, Berlin, Germany.

Liskay A., Kenk B., Schopfer P. (2003) Evidence for the involvement of cell wall peroxidase in the generation of hydroxyl radicals mediating extension growth. *Planta* **217**, 658–667.

Low P.S. & Merida J.R. (1996) The oxidative burst in plant defense: function and signal transduction. *Physiologia Plantarum* **96**, 533–542.

Lyons T., Ollerenshaw J.H., Barnes J.D. (1999) Impacts of ozone on *Plantago major*: apoplastic and symplastic antioxidant status. *New Phytologist* **141**, 253–263.

Manning W.J. & Tiedemann A.V. (1995) Climate change: potential effects of increased atmospheric carbon dioxide (CO_2), ozone (O_3) and ultraviolet-B (UV-B) radiation on plant diseases. *Environmental Pollution* **88**, 219–245.

Maxie E.C., Eaks I.L., Sommer N.F., Rae H.L., El-Batal S. (1965) Effect of Gamma Radiation on Rate of Ethylene and Carbon Dioxide Evolution by Lemon Fruit. *Plant Physiology* **40**, 407–409.

McAinsh M.R., Clayton H., Mansfield T.A., Hetherington A.M. (1996) Changes in stomatal behaviour and guard cell cytosolic free calcium in response to oxidative stress. *Plant Physiology* **111**, 1031–1042.

McCann M.C., Wells B., Roberts K. (1990) Direct visualization of cross-links in the primary plant cell wall. *Journal of Cell Science* **96**, 323–330.

McClaugherty C.A., Pastor J., Aber J.D., Melillo J.M. (1985) Forest litter decomposition in relation to soil nitrogen dynamics and litter quality. *Ecology* **66**, 266–275.

McKinlay A.F. & Diffey B.L. (1987) A reference action spectrum for ultra-violet induced erythema in human skin. In: *Human exposure to ultra-violet radiation:*

Risks and regulations (eds. Passchier W.F., Bosnjakovic B.F.M.), pp. 83–87. Elsevier, Amsterdam, Netherlands.

McLeod A.R. (1997) Outdoor supplementation systems for studies of the effects of increased UV-B radiation. *Plant Ecology* **128**, 79–92.

McLeod A.R. & Newsham K.K. (1997) Impacts of elevated UV-B on forest ecosystems. In: *Plants and UV-B* (ed. Lumsden P.J.), pp. 247–281. Cambridge University Press, Cambridge, UK.

McLeod A.R., Newsham K.K., Fry S.C. (2007) Elevated UV-B radiation modifies the extractability of carbohydrate from leaf litter of *Quercus robur*. *Soil Biology and Biochemistry* **39**, 116–126.

McLeod A.R., Fry S.C., Loake G.J., Messenger D.J., Reay D.S., Smith K.A., Yun B. (2008) Ultraviolet radiation drives methane emissions from terrestrial plant pectins. *New Phytologist* **180**, 124–132.

McNeil M., Darvill A.G., Fry S.C., Albersheim P. (1984) Structure and function of the primary cell wall of plants. *Annual Review of Biochemistry* **53**, 625–663.

Melillo J.M., Aber J.D., Muratore J.F. (1982) Nitrogen and lignin control of hardwood leaf litter decomposition dynamics. *Ecology* **63**, 621–626.

Messenger D.J., McLeod A.R., Fry S.C. (2009a) The role of UV radiation, photosensitisers, reactive oxygen species, and ester groups in mechanisms of methane formation from pectin. *Plant, Cell & Environment* **32**, 1–9.

Messenger D.J., McLeod A.R., Fry S.C. (2009b) Reactive oxygen species in aerobic methane formation from vegetation. *Plant signaling and behavior* (*in press*).

Micheletti M.I., Piacentini R.D., Madronich S. (2003) Sensitivity of biologically active UV radiation to stratospheric ozone changes: Effects of action spectrum shape and wavelength range. *Photochemistry and Photobiology* **78**, 456–461.

Mikaloff Fletcher S.E., Tans P.P., Bruhwiler L.M., Miller J.B., Heimann M. (2004) CH_4 sources estimated from atmospheric observations of CH_4 and its $^{13}C/^{12}C$ isotopic ratios: Inverse modeling of source processes. *Global Biogeochemical Cycles* **18**, GB4004, doi:10.1029/2004GB002223.

Miller J.G. & Fry S.C. (2001) Characteristics of xyloglucan after attack by hydroxyl radicals. *Carbohydrate Research* **332**, 389–403.

Miller J.G. & Fry S.C. (2004) *N*-[^{3}H]Benzoylglycylglycylglycine as a probe for hydroxyl radicals. *Analytical Biochemistry* **335**, 126–134.

Miller J.B., Gatti L.V., d'Amelio M.T.S., Crotwell A.M., Dlugokencky E.J., Bakwin P., Artaxo P., Tans P.P. (2007) Airborne measurements indicate large methane emissions from the eastern Amazon basin. *Geophysical Research Letters* **34**: article number L10809.

Mittler R., Vanderauwera S., Gollery M., Van Breusegem F. (2004) Reactive oxygen gene network of plants. *Trends in Plant Science* **9**, 490–498.

Moody S.A., Newsham K.K., Ayres P.G., Paul N.D. (1999) Variation in the responses of litter and phylloplane fungi to UV-B radiation (290–315 nm). *Mycological Research* **103**, 1469–1477.

Moody S.A., Paul N.D., Björn L.O., Callaghan T.V., Lee J.A., Manetas Y., Rozema J., Gwynn-Jones D., Johanson U., Kyparissis A., Oudejans A.M.C. (2001) The direct effects of UV-B radiation on *Betula pubescens* litter decomposing at four European field sites. *Plant Ecology* **154**, 29–36.

Moore T.R. (1984) Litter decomposition in a subarctic spruce-lichen woodland, eastern Canada. *Ecology* **65,** 299–308.

Mori I.C. & Schroeder J.I. (2004) Reactive oxygen species activation of plant Ca^{2+} channels. A signalling mechanism in polar growth, hormone transduction, stress signaling, and hypothetically mechanotransduction. *Plant Physiology* **135**, 702–708.

Nagy F. & Schäfer E. (2000) Nuclear and cytosolic events of lightinduced, phytochrome-regulated signaling in higher plants. *The EMBO Journal* **19**, 157–163.

Nagy F. & Schäfer E. (2002) Phytochromes control photomorphogenesis by differentially regulated, interacting signalling pathways in higher plants. *Annual Review Plant Biology* **53**, 329–55.

Newsham K.K., McLeod A.R., Greenslade P.D., Emmett B.A. (1996) Appropriate controls in outdoor UV-B supplementation experiments. *Global change Biology* **2**, 319–324.

Newsham K.K., Geissler P.A., Nicolson M.J., Peat H.J., Lewis-Smith R.I. (2005) Sequential reduction of UV-B radiation in the field alters the pigmentation of an Antarctic leafy liverwort. *Environmental and Experimental Botany* **54,** 22–32.

Newsham K.K., Anderson J.M., Sparks T.H., Splatt P., Woods C., McLeod A.R. (2001a) UV-B effect on *Quercus robur* leaf litter decomposition persists over four years. *Global Change Biology* **7**, 479–483.

Newsham K.K., Splatt P., Coward P.A., Greenslade P.D., McLeod A.R., Anderson J.M. (2001b) Negligible influence of elevated UV-B radiation on leaf litter quality of *Quercus robur*. *Soil Biology & Biochemistry* **33**, 659–665.

Olivier J.G.J., Van Aardenne J.A., Dentener F., Ganzeveld L., Peters J.A.H.W. (2005) Recent trends in global greenhouse gas emissions: regional trends and spatial distribution of key sources. In: *Non-CO_2 Greenhouse Gases (NCGG-4)* (ed. van Amstel A.), pp. 325–330. Millpress, Rotterdam, The Netherlands.

Olson J.S. (1963) Energy storage and the balance of producers and decomposers in ecological systems. *Ecology* **44**, 322–331.

O'Neill M.A. & York W.S. (2003) The composition and structure of plant primary cell walls. In: *The Plant Cell Wall* (ed. Rose J.K.C.), pp. 1–54. Blackwell, Oxford, UK.

Pennell R.I. & Lamb C. (1997) Programmed Cell Death in Plants. *The Plant Cell* **9**, 1157–1168.

Perrone P., Hewage C.M., Thomson A.R., Bailey K., Sadler I.H., Fry S.C. (2002) Patterns of methyl and *O*-acetyl esterification in spinach pectins: new complexity. *Phytochemistry* **60**, 67–77.

Pollock W., Heidt L.E., Lueb R., Ehhalt D. (1980) Measurement of stratospheric water vapor by cryogenic collection. *Journal of Geophysical Research* **85**, 5555–5568.

Popper Z.A. & Fry S.C. (2003) Primary cell wall composition of bryophytes and charophytes. *Annals of Botany* **91**, 1–12.

Popper Z.A. & Fry S.C. (2004) Primary cell wall composition of pteridophytes and spermatophytes. *New Phytologist* **164**, 165–174.

Popper Z.A. & Fry S.C. (2005) Widespread occurrence of a covalent linkage between xyloglucan and acidic polysaccharides in suspension-cultured angiosperm cells. *Annals of Botany* **96**, 91–99.

Quaite F.E., Sutherland B.M., Sutherland J.C. (1992) Action spectrum for DNA damage in alfalfa lowers predicted impact of ozone depletion. *Nature* **358**, 576–578.

Ramanathan V. (1988) The greenhouse theory of climate change: a test by an inadvertent global experiment. *Science* **240**, 293–299.

Redeker K.R., Wang N.-Y., Low J.C., McMillan A., Tyler S.C., Cicerone R.J. (2000) Emissions of Methyl Halides and Methane from Rice Paddies. *Science* **290**, 966–969.

Richmond P.A. (1991) Occurrence and functions of native cellulose. In: *Biosynthesis and Biodegradation of cellulose* (eds. Haigler C.H., Weimer P.J.), pp. 5–23. Dekker, New York, USA.

Rosenthal I. & Frimer A. (1976) The quenching effect of iodide on singlet oxygen. *Photochemistry and Photobiology* **23**, 209–211.

Rozema J., Tosserams M., Nelissen H.J.M., van Heerwaarden L., Broekman R.A., Flierman N. (1997) Stratospheric ozone reduction and ecosystem processes: enhanced UV-B radiation affects chemical quality and decomposition of leaves of the dune grassland species *Calamagrostis epigeios*. *Plant Ecology* **128**, 285–294.

Ruhland C.T. & Day T.A. (2000) Effects of ultraviolet-B radiation on leaf elongation, production and phenylpropanoid concentrations of *Deschampsia*

antarctica and *Colobanthus quitensis* in Antarctica. *Physiologia Plantarum* **109**, 244–251.

Ruhland C.T., Xiong F.S., Clark W.D., Day T.A. (2005) The Influence of Ultraviolet-B Radiation on Growth, Hydroxycinnamic Acids and Flavonoids of *Deschampsia antarctica* during Springtime Ozone Depletion in Antarctica. *Photochemistry and Photobiology* **81**, 1086–1093.

Sanhueza E. & Donoso L. (2006) Methane emission from tropical savanna *Trachypogon sp*. grasses. *Atmospheric Chemistry and Physics* **6**, 5315–5319.

Sawidis T. (1988) Uptake of radionuclides by plants after the Chernobyl accident. *Environmental Pollution* **50**, 317–324.

Scheehle E.A., Irving W.N., Kruger D. (2002) Global anthropogenic methane emissions. In: *Non-CO_2 Greenhouse Gases: Scientific Understanding, Control Options and Policy Aspects*, (ed. van Ham *et al.*), pp. 257–262. Millpress, Rotterdam, The Netherlands.

Schellera H.V., Jensena J.K., Sørensena S.O., Harholta J., Geshi N. (2007) Biosynthesis of pectin. *Physiologia Plantarum* **129**, 283–295.

Schiermeier Q. (2006) The methane mystery. *Nature* **442**, 730–731.

Schopfer P. (2001) Hydroxyl radical-induced cell-wall loosening *in vitro* and *in vivo*: implications for the control of elongation growth. *Plant Journal* **28**, 679–688.

Schopfer P., Liszkay A., Bechtold M., Frahry G., Wagner A. (2002) Evidence that hydroxyl radicals mediate auxin-induced extension growth. *Planta* **214**, 821–828.

Searles P.S., Flint S.D., Caldwell M.M. (2001) A meta-analysis of plant field studies simulating stratospheric ozone depletion. *Oecologia* **127**, 1–10.

Semerdjieva S.I., Sheffield E., Phoenix G.K., Gwynn-Jones D., Callaghan T.V., Johnson G.N. (2003) Contrasting strategies for UV-B screening in sub-Arctic dwarf shrubs. *Plant, Cell & Environment* **26**, 957–964.

Setlow R.B. (1974) The wavelengths in sunlight effective in producing skin cancer: A theoretical analysis. *Proceedings of the National Academy of Science USA* **71**, 3363–3366.

Seymour G.B. & Knox J.P. (2002) *Pectins and their Manipulation.* Blackwell, Oxford, UK.

Sharpatyi V.A. (2007) On the mechanism of methane emission by terrestrial plants. *Oxidation Communications* **30**, 48–50.

Shin R. & Schachtman D.P. (2004) Hydrogen peroxide mediates plant root cell response to nutrient deprivation. *Proceedings of the National Academy of Sciences USA* **101**, 8827–8832.

Slein M.W. & Schnell G.W. (1953) The polysaccharide of Shigella flexneri, type 3. *Journal of Biological Chemistry* **203**, 837–848.

Solomon S. (1990) Progress towards a quantitative understanding of Antarctic ozone depletion. *Nature* **347**, 347–354.

Somerville C., Bauer S., Brininstool G., Facette M., Hamann T., Milne J., Osborne E., Paredez A., Persson S., Raab T., Vorwerk S., Youngs H. (2004) Toward a Systems Approach to Understanding Plant Cell Walls. *Science* **306**, 2206–2211.

Sticklen M.B. (2008) Plant genetic engineering for biofuel production: towards affordable cellulosic ethanol. *Nature Reviews Genetics* **9**, 433–443.

Sullivan J.H., Howells B.W., Ruhland C.T., Day T.A. (1996) Changes in leaf expansion and epidermal screening effectiveness in *Liquidambar styraciflua* and *Pinus taeda* in response to UV-B radiation. *Physiologia Plantarum* **98**, 349–357.

Sweet M.S. & Winandy J.E. (1999) Influence of Degree of Polymerization of Cellulose and Hemicellulose on Strength Loss in Fire-Retardant-Treated Southern Pine. *Holzforschung* **53**, 311–317.

Taylor B.R., Parkinson D., Parsons W.F.J. (1989) Nitrogen and lignin content as predictors of litter decay rates: a microcosm test. *Ecology* **70**, 97–104.

Tevini M., Mark U., Saile M. (1990) Plant experiments in growth chambers illuminated with natural sunlight. In: *Environmental Research with Plants in Closed Chambers* (eds. Payer H.D., Pfirrmann T., Mathy P.), pp. 240–251. Air pollution Res. Rep. 26, Commission of the European Communities, Brussels, Belgium.

Ueda J., Takeshita K., Matsumoto S., Yazaki K., Kawaguchi M., Ozawa T. (2003) Singlet oxygen-mediated hydroxyl radical production in the presence of phenols: whether DMPO–˙OH formation really indicates production of ˙OH? *Photochemistry and Photobiology* **77**, 165–170.

Uhrig J.F. & Hülskamp M. (2006) Plant GTPases: Regulation of Morphogenesis by ROPs and ROS. *Current Biology* **16**, 211–213.

Velikova V. (2008) Isoprene as a tool for plant protection against abiotic stresses. *Journal of Plant Interactions* **3**, 1–15.

Velikova V., Pinelli P., Pasqualini S., Reale L., Ferranti F., Loreto F. (2005) Isoprene decreases the concentration of nitric oxide in leaves exposed to elevated ozone. *New Phytologist* **166**, 419–426.

Vigano I., Holzinger R., van Weelden H., Keppler F., Röckmann T. (2008) Effect of uv radiation and temperature on the emission of methane from plant biomass and structural components. *Biogeosciences Discussions* **5**, 243–270.

Vreeburg R.A.M. & Fry S.C. (2005) Reactive oxygen species in cell walls. In: *Antioxidants and Reactive Oxygen Species in Plants*, (ed. Smirnoff N.), pp. 215–249. Blackwell, Oxford, UK.

Wade H.K., Bibikova T.N., Valentine W.J., Jenkins G.I. (2001) Interactions within a network of phytochrome, cryptochrome and UVB phototransduction pathways regulate chalcone synthase gene expression in Arabidopsis leaf tissue. *Plant Journal* **25**, 675–685.

Wahlen M. (1993) The global methane cycle. *Annual Review Earth Planetary Science* **21**, 407–426.

Wang J.S., Logan J.A., McElroy M.B. (2004) A 3-D model analysis of the slowdown and interannual variability in the methane growth rate from 1988 to 1997. *Global Biogeochemical Cycles* **18**, GB3011, doi:10.1029/2003GB002180.

Wang Y.B., Feng H.Y., Qu Y., Cheng J.Q., Zhao Z.G., Zhang M.X., Wang X.L., An L.Z. (2006) The relationship between reactive oxygen species and nitric oxide in ultraviolet-b-induced ethylene production in leaves of maize seedlings. *Environmental and Experimental Botany* **57**, 51–61.

Wang Z.P., Han X.G., Wang G.G., Song Y., Gulledge J. (2007) Aerobic methane emission from plants in the inner mongolia steppe. *Environmental Science and Technology* **42**, 62–68.

Wi S.G., Chung B.Y., Kim J.S., Kim J.H., Baek M.H., Lee J.W., Mm Y.S. (2007) Effects of gamma irradiation on morphological changes and biological responses in plants. *Micron* **38**, 553–564.

Willats W.G.T., McCartney L., Mackie W., Knox J.P. (2001) Pectin: cell biology and prospects for functional analysis. *Plant Molecular Biology* **47**, 9–27.

Wojtaszek P. (1997) Oxidative burst: an early plant response to pathogen infection. *Biochemical Journal* **322**, 681–692.

Wuebbles D.J. & Hayhoe K. (2002) Atmospheric methane and global change. *Earth-Science Reviews* **57**, 177–210.

Xiong L., Schumaker K.S., Zhu J-K. (2002) Cell Signaling during Cold, Drought, and Salt Stress. *Plant Cell* (suppl), S165–S183.

Yazawa M., Shimizu T., Hirao T (1992) Feeding response of the silkworm, *Bombyx mori*, to UV irradiation of mulberry leaves. *Journal of Chemical Ecology* **18**, 1573–1561.

Yue M., Li Y., Wang X. (1998) Effects of enhanced ultraviolet-B radiation on plant nutrients and decomposition of spring wheat under field conditions. *Environmental and Experimental Botany* **40**, 187–196.

Zarra I., Sanchez M., Queijeiro E., Pena M.J., Revilla G. (1999) The cell wall stiffening mechanism in *Pinus pinaster* Aiton: regulation by apoplastic levels of ascorbate and hydrogen peroxide. *Journal of the science of food and agriculture* **79**, 416–420.

Zengler K., Richnow H.H., Rosselló-Mora R., Michaelis W., Widdel F. (1999)

Methane formation from long-chain alkanes by anaerobic microorganisms. *Nature* **401**, 266–269.

Appendix

Research

New Phytologist

Ultraviolet radiation drives methane emissions from terrestrial plant pectins

Andy R. McLeod[1], Stephen C. Fry[2], Gary J. Loake[2], David J. Messenger[1,2], David S. Reay[1], Keith A. Smith[1] and Byung-Wook Yun[2]

[1]Institute of Atmospheric and Environmental Sciences, School of GeoSciences, The University of Edinburgh, Crew Building, West Mains Road, Edinburgh EH9 3JN, UK; [2]Institute of Molecular Plant Sciences, School of Biological Sciences, The University of Edinburgh, Daniel Rutherford Building, Mayfield Road, Edinburgh EH9 3JH, UK

Author for correspondence:
Andy McLeod
Tel: +44 131 650 5434
Fax: +44 131 650 0478
Email: andy.mcleod@ed.ac.uk

Received: *29 April 2008*
Accepted: *29 May 2008*

Summary

• Recent studies demonstrating an *in situ* formation of methane (CH_4) within foliage and separate observations that soil-derived CH_4 can be released from the stems of trees have continued the debate about the role of vegetation in CH_4 emissions to the atmosphere. Here, a study of the role of ultraviolet (UV) radiation in the formation of CH_4 and other trace gases from plant pectins *in vitro* and from leaves of tobacco (*Nicotiana tabacum*) *in planta* is reported.

• Plant pectins were investigated for CH_4 production under UV irradiation before and after de-methylesterification and with and without the singlet oxygen scavenger 1,4-diazabicyclo[2.2.2]octane (DABCO). Leaves of tobacco were also investigated under UV irradiation and following leaf infiltration with the singlet oxygen generator rose bengal or the bacterial pathogen *Pseudomonas syringae*.

• Results demonstrated production of CH_4, ethane and ethylene from pectins and from tobacco leaves following all treatments, that methyl-ester groups of pectin are a source of CH_4, and that reactive oxygen species (ROS) arising from environmental stresses have a potential role in mechanisms of CH_4 formation.

• Rates of CH_4 production were lower than those previously reported for intact plants in sunlight but the results clearly show that foliage can emit CH_4 under aerobic conditions.

Key words: DABCO (1,4-diazabicyclo[2.2.2]octane), methane, pectin, reactive oxygen species, *Nicotiana tabacum* (tobacco), ultraviolet radiation, vegetation.

New Phytologist (2008) **180**: 124–132

doi: 10.1111/j.1469-8137.2008.02571.x

Introduction

There remains considerable discussion among plant physiologists about recent observations of the production of CH_4 by vegetation foliage under aerobic conditions (Dueck & van der Werf, 2008). Observations by Keppler *et al.* (2006) first demonstrated that dry and live leaf material could produce CH_4, with rates influenced by sunlight and temperature, and this was suggested as a possible explanation for unexpectedly high atmospheric concentrations of CH_4 detected over tropical rainforests (Bergamaschi *et al.*, 2007). Biospheric CH_4 emissions to the atmosphere are thought to originate mostly from anaerobic microbial processes but experimental observations (Keppler *et al.*, 2006; Sanhueza & Donoso, 2006; Wang *et al.*, 2008), atmospheric measurements (Crutzen *et al.*, 2006; do Carmo *et al.*, 2006; Miller *et al.*, 2007) and subsequent analyses (Bousquet *et al.*, 2006; Houweling *et al.*, 2006; Ferretti *et al.*, 2007) do suggest the possibility of a modest CH_4 flux from terrestrial vegetation. Two subsequent investigations were unable to demonstrate CH_4 emissions (Dueck *et al.*, 2007; Beerling *et al.*, 2008) but a recent study, using measurements in the dark, has suggested that some woody plants, but not grasses, may emit small amounts of CH_4 (Wang *et al.*, 2008). The CH_4 was hypothesized to originate from methoxyl groups (Keppler

et al., 2006), and recently Keppler *et al.* (2008) have used isotope analysis to demonstrate an influence of temperature and UV radiation on CH_4 emissions from pectin and polygalacturonic acid *in vitro*. The roles of UV radiation and temperature in CH_4 emission from leaves have also been demonstrated by Vigano *et al.* (2008), while observations that CH_4 emissions from vegetation may arise from dissolution of soil CH_4 and its transport above ground in the transpiration stream (Rusch & Rennenberg, 1998; Terazawa *et al.*, 2007) have widened the debate about possible CH_4 sources in vegetation. At present, the mechanisms by which terrestrial vegetation may emit CH_4 from foliage under aerobic conditions remain to be identified (Schiermeier, 2006, 2007; Dueck & van der Werf, 2008).

The role of temperature and sunlight in the observations of Keppler *et al.* (2006) and the well-known role of UV radiation in photodegradation of plant material (Austin & Vivanco, 2006) led us to investigate the role of UV radiation in CH_4 production from foliage. In earlier experiments, we found that leaf litter from oak (*Quercus robur* L.) grown under elevated UV radiation had an accelerated decomposition rate and reduced extractability of carbohydrates which implied changes to cell wall components (McLeod *et al.*, 2007). Over half of plant primary cell wall dry mass may be comprised of pectins, which are cell wall polysaccharides rich in α-D-galacturonate residues with variable proportions of methylesterification (Seymour & Knox, 2002). We therefore investigated the release of CH_4 and other gases from pectin-impregnated glass fibre sheets, dried and exposed to UV radiation (from experimental lamps and from sunlight) inside gas-tight UV-transmitting bags filled with ambient air at 30°C. Care was taken in the experimental design to eliminate possible confounding effects from any contamination of the glass fibre or the release of low-molecular-weight hydrocarbons from the gas bag material. We also examined trace gas production from UV-irradiated leaves of the C3 subtropical herb *Nicotiana tabacum* (tobacco) that were detached in order to limit transpiration as a possible CH_4 source. Sharpatyi (2007) recently suggested that a free-radical process would produce CH_4 from plant polysaccharides under the influence of UV radiation, which is well known to produce reactive oxygen species (ROS) in plant tissue (Björn, 2002). We therefore investigated CH_4 production from glass fibre impregnated with pectin and the ROS-scavenger 1,4-diazabicyclo[2.2.2]octane (DABCO) (Wang *et al.*, 2006) and also from de-methylesterified pectin. ROS are generated in foliage by a range of environmental stresses, including drought, nutrient deficiency, attempted pathogen infection, high temperature, acidic precipitation and ozone exposure (Apel & Hirt, 2004; Wang *et al.*, 2006). We therefore also compared the effects of UV irradiation on CH_4 production from tobacco leaves with effects on CH_4 production from leaves infiltrated with water, the singlet oxygen generator rose bengal (Filkowski *et al.*, 2004) or the bacterial pathogen *Pseudomonas syringae* in order to demonstrate the potential role of ROS in CH_4 formation.

Materials and Methods

Pectin sheets

Pectin or pectate-impregnated sheets (20.3 × 25.4 cm) were prepared from glass microfibre filters (Whatman GF/A) and commercial pectin derived from citrus fruits (Sigma-Aldrich Chemical Co., Poole, UK). Before use, glass fibre sheets were baked overnight in a furnace at 300°C in order to remove any organic contaminants. Citrus pectin (10 g; Sigma P9135; galacturonic acid content 84%; methoxy content 9.4%; loss on drying 4.1%) was wetted with 20 ml of ethanol to form a slurry, which was dispersed in *c.* 950 ml of deionized water with vigorous shaking. After several hours of stirring until the slurry dissolved to form a slightly hazy solution, the volume was adjusted to 1 l with water. Pectate (de-methylesterified pectin) was prepared by addition of 400 ml of 1% pectin solution to 40 ml of 1.0 M NaOH, and incubation at 20°C for 30 min. Then, with vigorous shaking, sufficient 1 M H_3PO_4 was added to bring the pH to 7.4–7.6. To each 20.3 × 25.4-cm sheet of Whatman GF/A glass microfibre filter, 25 ml of the pectin or pectate solution was then applied and allowed to dry in air. With pectin, this resulted in 240 mg of polysaccharide (210 mg of galacturonic acid residues) per sheet (equivalent to 23.5 mg (= 760 μmol) methyl-ester groups per sheet, giving a theoretical maximum yield of 12.1 mg CH_4 (*c.* 17 ml at STP)). With pectate, there was 175 mg of galacturonic acid residue per sheet. Control sheets of glass fibre were prepared in the same way with 25 ml of 2% ethanol. Pectin sheets containing DABCO (Sigma-Aldrich Chemical Co.) were prepared as above except that the pectin solution contained 8 mM DABCO. The absorbance spectrum of a 2.5 g l^{-1} solution of pectin in distilled water was measured in a scanning spectrometer (Lambda 900 UV/VIS/NIR; Perkin Elmer Inc., Waltham, MA, USA) for evaluation of the UV absorbance of pectin.

Plant growth and leaf infiltration

Tobacco plants (*Nicotiana tabacum* L. cv. Xanthi) were grown from seed in a temperature-regulated glasshouse in 7.5-l pots containing a mixture of 75% peat and 25% sand with 750 g of ground limestone, 1200 g of 'Osmocote Exact High K' slow-release fertilizer (N:P:K 10 : 11 : 18 + 2 MgO + trace elements; The Scotts (UK) Company, Ipswich, UK) and 6 g of 'Intercept 60WP' insecticide (a.i. imidacloprid; Bayer CropScience, Cambridge, UK) per 250 l of soil mixture. The day:night temperature was 21 : 18°C, the light intensity was *c.*150 μmol m^{-2} s^{-1} and daylength was extended to 18 h with supplemental sodium lighting. After 8–10 wk, the youngest fully expanded leaves were infiltrated on the abaxial surface, using a 1-ml syringe, with 2 ml of distilled water, 2 ml of 10 μM rose bengal in water (Sigma-Aldrich Chemical Co.) or 2 ml of a water suspension (optical density (OD_{600}) 0.2) of *Pseudomonas*

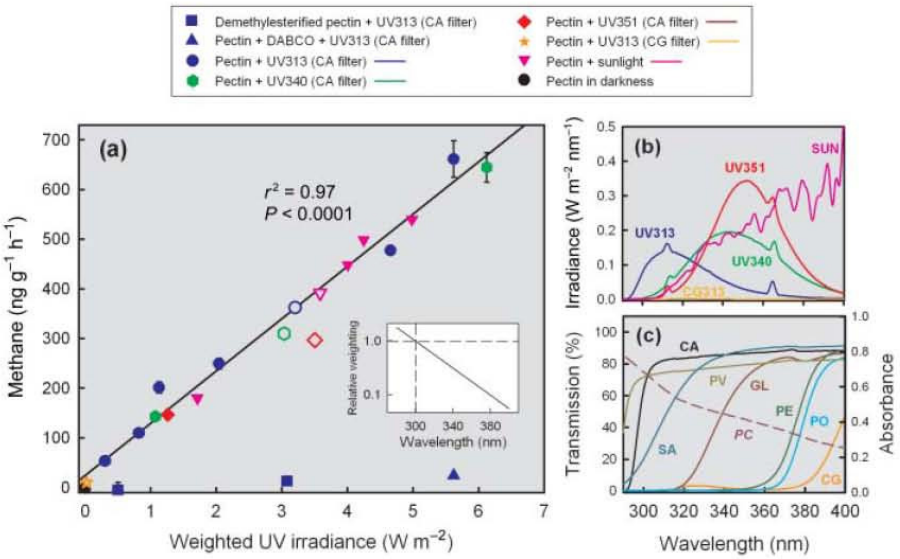

Fig. 1 Methane production from citrus pectin. (a) Linear regression of CH_4 production with ultraviolet irradiance weighted with the inset spectral weighting function, using cellulose diacetate (CA)-filtered UV313, UV340 and UV351 lamps, UV-opaque 'Courtgard' (CG) polyester-filtered UV313 lamps and sunlight. Open symbols correspond to spectra in (b). For lamp sources, values are means of three replicates and standard errors are less than symbol size except where visible. For sunlight, values are individual measurements. Other symbols (close to the horizontal axis) show CH_4 production from pectin plus the reactive oxygen species (ROS)-scavenger 1,4-diazabicyclo[2.2.2]octane (DABCO) and from de-methylesterified pectin. The temperature was 30°C. (b) Spectra of sunlight (SUN) and CA-filtered lamps (UV313, UV340 and UV351) and CG-filtered UV313 lamps (CG313) used in experiments. (c) Transmission spectra (solid lines) of filters used in experiments (CA, cellulose diacetate; CG, 'Courtgard' UV-opaque polyester), of materials commonly used to construct experimental plant chambers (GL, 4-mm window glass; PE, 3.8-mm 'Perspex'; PO, 2.7-mm polycarbonate; SA, 4-mm 'Sanalux' glass) and the absorbance spectrum (right-hand axis) of 2.5 g l^{-1} pectin (*PC*) in water (hatched line).

syringae pv. *tomato* DC3000 (*Pst*DC3000) carrying the avirulence gene *avrB*. The bacterium was grown in King's broth (KB) liquid medium (King *et al.*, 1954) supplemented with 50 mg l^{-1} rifampicin and 50 mg l^{-1} kanamycin at 30°C overnight. Bacterial cells were harvested by centrifugation and re-suspended to 0.2 at OD_{600} (the equivalent of 10^8 colony-forming units (cfu) ml^{-1}) in 10 mM $MgCl_2$.

Ultraviolet radiation sources

UV radiation was provided by three types of lamp (UV313, UV340 and UB351; The Q-Panel Company, Cleveland, OH, USA) filtered with closely wrapped 125-μm cellulose diacetate, which had a shortwave cut-off at *c.* 290 nm (cellulose diacetate (CA) lamp filter; Fig. 1b) and so removed UV-C wavelengths (< 280 nm). We also used a filter of 0.036-mm UV-opaque polyester ('Courtgard' (CG) lamp filter; CPFilms Inc., Martinsville, VA, USA) to remove UV-B and most UV-A wavelengths (< 380 nm). Examples of the spectral irradiance of lamp/filter combinations, including the gas sampling bag, are shown in Fig. 1(b). Lamp irradiation was adjusted using a phase-angle dimming system. Experiments performed in natural sunlight took place in the horticultural gardens of the University of Edinburgh at UK National Grid Reference NT 270705 (55°55′N, 3°10′W), between 6 and 21 September 2006.

Ultraviolet radiation measurements

UV spectral irradiance was measured with a double monochromator spectroradiometer (SR991-PC; Macam Photometrics, Livingston, UK) which was calibrated against tungsten and deuterium lamps traceable to National Physical Laboratory Standards (SR903; Macam Photometrics). During outdoor experiments the solar spectrum was scanned at *c.* 15-min intervals and monitored continuously with a broad-band UV sensor (Model PMA2102; Solar Light Inc., Glenside, PA, USA) that was used to calculate changes in spectral irradiance between scans.

Preparation of sample bags

New 5-l gas sampling bags of 25-μm UV-transparent polyvinylfluoride film (SKC Inc., Eighty Four, PA, USA) were cut open on one side to allow insertion of glass fibre sheets

and re-sealed using 40-μm aluminium (Al) adhesive tape. Bags were flushed five times before filling with 250 ml of stock external ambient air. Each pair of sample bags was used for three replicate experiments (which were determined not to have modified UV transmission of the bag material). Experiments using rose bengal, *P. syringae* and UV with tobacco were performed with 200 ml of air and a 20 cm × 20 cm window of 4-mm 'Sanalux' glass (Deutsche Spezialglas AG, Delligsen, Germany) attached with Al tape and the remainder of the bag shaded with Al foil. The spectral transmissions of polyvinylfluoride film, Sanalux glass and a range of typical chamber and cuvette construction materials were measured using a scanning spectrometer (Perkin Elmer Lambda 900 UV/VIS/NIR) and are shown in Fig. 1(c).

Experimental exposures of pectin and leaves

Experiments on pectin with UV lamps used one sample bag containing one pectin-impregnated glass fibre sheet and another sample bag containing a control glass fibre sheet. Bags were supported on a black butyl rubber sheet (pond liner) on the surface of a thermostatically controlled water bath at 30°C. After 2 h, the CH_4 production was determined and then the pectin-impregnated and control sheets were reversed between bags for a further 2-h exposure. This allowed any difference in CH_4 production from the sample bags themselves to be eliminated from the estimate of CH_4 production from pectins. The CH_4 production inside control bags containing control glass fibre sheets was up to 6.6 ng CH_4 h^{-1} in sunlight and a maximum of 24.6 ng CH_4 h^{-1} in lamp experiments at the highest irradiance of UV313 lamps. Outdoor experiments were performed with bags clipped to a temperature-controlled brass plate also covered with a black butyl rubber sheet. Temperature was measured inside a sample bag with thermocouples connected to a PC-based control system that adjusted the temperature of water from a re-circulating water bath. As outdoor UV levels were variable, experiments were conducted for one period of 2 h without reversing the treatment and control bags. However, the bags were reversed before the next experiment.

Experiments with leaves of *N. tabacum* used one leaf per gas sample bag and were performed inside a growth room at 25–30°C with 18 $W m^{-2}$ photosynthetically active radiation (PAR: 400–700 nm) provided by fluorescent lamps (Philips Master TLD 36W/830, Philips Lighting, Guildford, UK) and 3.1 $W m^{-2}$ unweighted total UV provided by CA-filtered UV313 lamps (described in 'Ultraviolet radiation sources' above). Experiments with PAR and with PAR plus UV radiation were also performed using empty bags as a control and the control gas production was subtracted from treatment values.

Gas concentration measurement

Methane, ethane and ethylene concentrations were determined with a gas chromatograph (Hewlett Packard Series II 5890; Hewlett Packard, Altrincham, UK) equipped with a flame ionization detector and a column packed with HayeSep Q (80–100 mesh) at 70°C, with N_2 as the carrier gas. Peak integration and autosampling were controlled using a chromatography data system (PeakSimple Model 202, SRI Instruments, Torrance, CA, USA). CO_2 was measured with a gas chromatograph (Perkin Elmer 8310) equipped with a thermal conductivity detector, using manual injection. Before and after sample analysis, the gas chromatographs were calibrated using standards of known mixing ratios that spanned the sample values.

Statistical analysis

Rates of CH_4 production from pectin are reported as the mean of three replicates ± SE and were analysed by linear regression against UV irradiance values. Trace gas concentrations produced by UV, *P. syringae* and rose bengal treatments of tobacco are also means of three replicates ± SE and were analysed by individual treatment comparison with the water control using ANOVA with replicate gas bags nested within treatment to achieve a repeated measures analysis (Neter *et al.*, 1996). All statistical tests were performed with the MiniTab statistical package (version 14.1, Minitab Ltd, Coventry, UK).

Results and Discussion

The experiments on pectin used fluorescent lamps (filtered to exclude wavelengths < 290 nm) in order to provide both UV-B (280–315 nm) and UV-A (315–400 nm) radiation (Fig. 1b) up to the highest intensity of global erythemal UV irradiance (Liley & McKenzie, 2006) (Table 1) and experiments were also conducted in the field with sunlight (Fig. 1b). The absorbance of a 2.5 $g l^{-1}$ solution of pectin (Fig 1c) demonstrated the presence of UV-absorbing components. Methane production from pectin (Table 1) had an approximately linear relationship to total UV irradiance for each lamp type alone or for sunlight, but considerable scatter when all sources were plotted together. We therefore calculated UV irradiance using a range of idealized (Micheletti *et al.*, 2003) and common spectral weighting functions (Table 1). Straight-line logarithmic weighting functions (e.g. Micheletti *et al.*, 2003) provided significant linear relationships with CH_4 emissions. The best fit was achieved by an idealized function that decayed one decade in 80-nm wavelength (Fig. 1a, inset) giving a significant linear regression between weighted-UV and CH_4 production (Fig. 1a).

These rates of CH_4 production exceed values previously reported for pectin with CH_4-free air inside glass vials (Keppler *et al.*, 2006). Methane production in the dark was undetectable and was reduced to low rates by a UV-opaque filter (Table 1). De-methylesterification of the pectin also reduced CH_4 production to low rates (Fig. 1a).

As free-radical mechanisms could also produce carboxylate radicals and potential dimerization of methyl radicals, we also

Table 1 Ultraviolet irradiance and methane (CH_4) production from citrus pectin

	Ultraviolet irradiance (W m^{-2})										Methane (ng g^{-1} h^{-1})	
Lamp source/ location	Total UV (280–400 nm)	UV-A (315–400 nm)	UV-B (280–315 nm)	ERY[a]	PAS[b]	PGR[c]	QUT[d]	DNA[e]	STN[f]	MET[g]	Mean	SE
UV313-CA[h]	0.55	0.36	0.19	< 0.01	0.09	0.08	0.12	0.07	0.23	0.30	53.1	4.0
	1.51	1.00	0.51	0.13	0.23	0.22	0.32	0.19	0.64	0.82	109.3	0.6
	2.07	1.37	0.70	0.18	0.32	0.31	0.44	0.26	0.87	1.13	201.2	11.4
	3.69	2.39	1.30	0.34	0.59	0.57	0.82	0.48	1.59	2.04	249.0	11.3
	5.70	3.61	2.09	0.55	0.95	0.92	1.31	0.79	2.52	3.20	361.9	8.2
	8.62	5.74	2.88	0.73	1.27	1.24	1.79	1.01	3.60	4.66	446.6	29.8
	9.48	5.55	3.93	1.10	1.90	1.82	2.53	1.66	4.52	5.62	660.8	36.7
UV340-CA[h]	3.70	3.56	0.14	0.02	0.03	0.10	0.10	0.02	0.60	1.07	143.0	3.8
	10.46	10.08	0.38	0.06	0.08	0.28	0.29	0.04	1.70	3.03	310.0	11.6
	20.35	19.49	0.86	0.13	0.19	0.58	0.64	0.10	3.51	6.13	644.6	29.8
UV351-CA[h]	5.27	5.21	0.06	0.01	< 0.01	0.12	0.05	< 0.01	0.61	1.26	146.3	6.6
	14.56	14.39	0.17	0.03	0.03	0.33	0.16	0.02	1.72	3.50	296.8	10.2
UV313-CG[i]	0.05	0.05	< 0.01	< 0.01	< 0.01	< 0.01	< 0.01	< 0.01	0.01	0.02	10.2	1.4
Dark	0.00	0.00	0.00	0.00	0.00	0.00	0.00	0.00	0.00	0.00	–1.1	1.1
Sunlight	26.51	26.27	0.24	0.04	0.03	0.54	0.25	0.01	2.33	4.98	539.5	–
	7.98	7.88	0.10	0.02	0.01	0.17	0.11	< 0.01	0.85	1.71	180.1	–
	22.60	22.40	0.20	0.03	0.03	0.46	0.21	0.01	1.98	4.25	498.3	–
	21.31	21.12	0.19	0.03	0.03	0.43	0.20	< 0.01	1.87	4.01	448.5	–
	19.07	18.91	0.16	0.03	0.02	0.39	0.17	< 0.01	1.67	3.58	391.4	–
Cuzco, Peru[j]	–	–	–	0.63	–	–	–	–	–	–	–	–

Values of CH_4 production are the mean of three replicate measurements for lamp sources and individual measurements in sunlight (see Materials and Methods).
[a]ERY: UV (280–400 nm) weighted with the Commission Internationale de l'Eclairage (CIE) erythemal action spectrum (McKinlay & Diffey, 1987).
[b]PAS: UV (280–400 nm) weighted with a mathematical formulation (Green *et al.*, 1974) of the general plant action spectrum (Caldwell, 1971).
[c]PGR: UV (280–400 nm) weighted with a new plant growth function (Flint & Caldwell, 2003).
[d]QUT: UV (280–400 nm) weighted with the pyridine dimer action spectrum (Quaite *et al.*, 1992).
[e]DNA: UV (280–400 nm) weighted with the DNA damage action spectrum (Setlow, 1974).
[f]STN: UV (280–400 nm) weighted with the plant growth inhibition function (Steinmuller, 1986).
[g]MET: Idealized spectral weighting function for CH_4 production that decays one decade in 80 nm.
[h]Lamps filtered with 125-μm cellulose diacetate which filters UV wavelengths < 290 nm (see Fig. 1b).
[i]UV313 lamps filtered with 'Courtgard' polyester which filters UV wavelengths < 380 nm (see Fig. 1b).
[j]Highest estimated global erythemal irradiation at Cuzco, Peru calculated from the UV index (Liley & McKenzie, 2006).

examined the production of ethane, ethylene and CO_2, as well as CH_4, resulting from UV irradiation of pectin and found production of all four gases with a molecular ratio of CH_4:C_2H_4:C_2H_6:CO_2 of 1.0 : 0.1 : 0.2 : 240 at a total unweighted UV irradiance of 9.48 W m^{-2} (Table 2). UV-induced production of ROS (Björn, 2002) is also a potential free-radical mechanism leading to CH_4 production from the methyl groups of pectins. We therefore examined CH_4 production from pectin-impregnated glass fibre containing the ROS-scavenger DABCO (Wang *et al.*, 2006) and found CH_4 production reduced to low rates (Fig. 1a), thus demonstrating a role of ROS in CH_4 generation from pectins. ROS include hydrogen peroxide (H_2O_2), the superoxide ion ($O_2^{\bullet-}$) and its nonionized equivalent the hydroperoxyl radical ($HO_2^{\bullet}$), the hydroxyl radical ($^{\bullet}OH$), and singlet oxygen ($^1O_2$). Of these five, only $^{\bullet}OH$ has been reported to cause extensive oxidative scission of plant polysaccharides (Fry, 1998; Fry *et al.*, 2001). However, DABCO is usually reported as a singlet oxygen scavenger (Wang *et al.*, 2006), thus implicating singlet oxygen in CH_4 generation. More detailed studies using a range of ROS scavengers are needed to evaluate the precise molecular mechanisms of the UV-induced CH_4 formation found in this study and those of Keppler *et al.* (2008) and Vigano *et al.* (2008), which reported some CH_4 production from nonmethylesterified organic material.

UV-photosensitizing compounds (e.g. furocoumarins) are abundant in some plants; therefore ROS formation may be much greater in the foliage of certain plant species than in extracted pectins, although cuticular reflectance of UV and UV-screening compounds (McLeod & Newsham, 1997) will reduce the effective exposure of underlying structures. ROS are generated in foliage by a range of environmental stresses and we therefore also investigated the production of CH_4 from leaves of the C3 subtropical herb *N. tabacum*. Infiltration of leaves of *N. tabacum* cv. Xanthi with the singlet oxygen generator rose bengal (Filkowski *et al.*, 2004) produced leaf necrosis

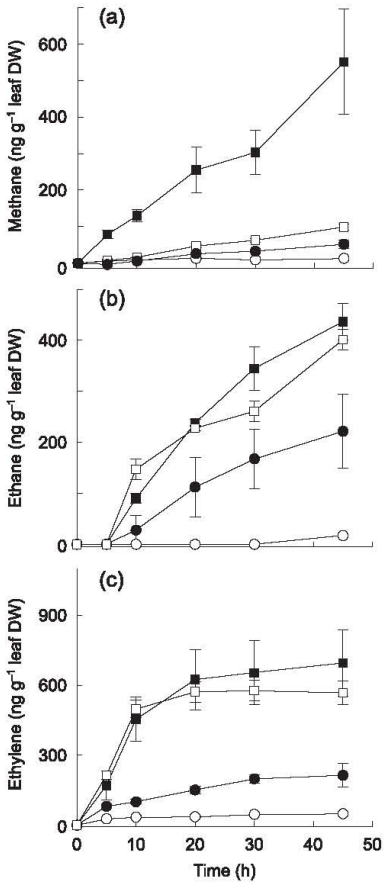

Fig. 2 Trace gas production from tobacco (*Nicotiana tabacum* cv. Xanthi). (a) Methane, (b) ethane, and (c) ethylene. Leaves were infiltrated with 2 ml of water (open circles), 2 ml of a suspension of *Pseudomonas syringae* pv. *tomato* DC3000 carrying the avirulence gene *avrB* (open squares), 2 ml of a 10 μM rose bengal solution (closed circles) or 2 ml of water plus UV irradiation (closed squares). All treatments were under 18 W m^{-2} (87 μmol m^{-2} s^{-1}) photosynthetically active radiation (PAR; 400–700 nm). The UV irradiation treatment was 3.14 W m^{-2} (280–399 nm) (equivalent to 1.47 W m^{-2} UV_{CH_4}; see Fig. 1a) and temperature was 25–30°C. Values are means of three replicates and standard errors are smaller than the symbol except where visible. DW, dry weight.

while infiltration with the bacterial pathogen *Pst*DC3000 carrying the avirulence gene *avrB* (Whalen *et al.*, 1991) resulted in a hypersensitive response (a genetically programmed cell death mechanism; Apel & Hirt, 2004). All treatments resulted in some CH_4 formation but even greater amounts of ethylene and ethane over the subsequent 45 h (Fig. 2). Ethane production was only detected after 5 h in all treatments. The amount of

Table 2 Production of trace gases from ultraviolet irradiation of citrus pectin

Methane (ng g^{-1} h^{-1})		Ethane (ng g^{-1} h^{-1})		Ethylene (ng g^{-1} h^{-1})		CO_2 (μg g^{-1} h^{-1})	
Mean	SE	Mean	SE	Mean	SE	Mean	SE
660.8	36.7	125.2	14.1	271.0	9.5	433.4	3.6

Values are the mean of three replicate experiments. Total UV irradiance was 9.48 W m^{-2} (280–400 nm) with corresponding weighted irradiance values using a range of common spectral weighting functions shown in Table 1.

CH_4 production was significantly different from that of the water control for each of the three treatments (repeated measures ANOVA (UV: $F_{1,4} = 18.51$, $P = 0.013$; *P. syringae*: $F_{1,4} = 68.48$, $P = 0.001$; rose bengal: $F_{1,4} = 11.20$, $P = 0.029$) but the mean rate caused by UV irradiation was much greater than that of other treatments. Methane production caused by the UV treatment, which appeared linear with time over 45 h, was 12.3 ± 3.2 ng g^{-1} leaf dry weight h^{-1}, which is similar to rates previously reported for detached leaves from a range of species (Keppler *et al.*, 2006) but much lower than their reported rates for intact plants.

There is a potential for much higher UV-driven emissions at lower latitudes, where all sites between 50°S and 40°N experience peak erythemally weighted (McKinlay & Diffey, 1987) UV irradiances that exceed 0.25 W m^{-2} (Liley & McKenzie, 2006). Sunlight-driven CH_4 emissions from vegetation were suggested by Keppler *et al.* (2006) as a possible explanation for unexpectedly high atmospheric concentrations of CH_4 detected over tropical regions by satellite remote sensing (Bergamaschi *et al.*, 2007; Schneising *et al.*, 2008). More recent studies have shown that the CH_4 data retrieval was positively biased in tropical regions as a result of spectroscopic interference by water vapour, but source inversions based upon an updated data retrieval method still point to substantial tropical CH_4 emissions (Frankenberg *et al.*, 2008). Conversion of low-latitude erythemal irradiances > 0.25 W m^{-2} using typical spectra derived from a spectral radiation transfer model (Gueymard, 1995, 2001) and use of the weighting function for CH_4 production (Fig. 1a, inset) suggest equivalent values > 11 W m^{-2} on the CH_4-weighted irradiance scale of Fig. 1(a) and > 30 W m^{-2} CH_4-weighted UV for the highest global irradiance measured at Cuzco, Peru (Liley & McKenzie, 2006). However, the relationship between appropriately weighted UV radiation and CH_4 production from plants *in vivo* (and also from dead plant material) should be determined over the full range of global irradiance values before up-scaling to estimates of global emissions as the relationship may not be linear at higher irradiances and may not persist through time as the substrate becomes modified. The steep response of the process to shorter wavelengths (Fig. 1a, inset) makes it essential to filter experimental lamps to remove wavelengths

< 290 nm (McLeod, 1997) in order to ensure realistic exposures in experimental studies.

The use of detached tobacco leaves limited any potential contribution of CH_4 dissolved in the transpiration stream, but raised a question about the effect of leaf detachment on observed gas production. The leaves infiltrated with water served as a control and indicated a negligible effect of leaf detachment on gas production, including stress ethylene, during the 45-h experiment. Ethylene is a well-known signal molecule produced by environmental stress in plants (Apel & Hirt, 2004; Wang *et al.*, 2006) and the effect of UV-B irradiation on ethylene production from aminocyclopropane-1-carboxylic acid in tobacco and consequent leaf damage has been reported by Nara & Takeuchi (2002). However, ethylene production directly resulting from UV irradiation of pectins (Table 2) suggests a novel mechanism distinct from the classical ethylene biosynthesis pathways (Wang *et al.*, 2006), which may have implications for ethylene signalling.

These observations in which environmental stresses, particularly from UV irradiation, result in CH_4 emissions from foliage under aerobic conditions may contribute to resolving the mystery of CH_4 sources from terrestrial vegetation in daylight. However, the night-time observations of CH_4 (Crutzen *et al.*, 2006) and experimental detection in darkness (Wang *et al.*, 2008) suggest that potential CH_4 sources from the transpiration stream (Terazawa *et al.*, 2007) should also be evaluated further. The rates of CH_4 production induced by rose bengal and *P. syringae* were much lower than those induced by UV irradiation, even though the general oxidative stress caused by these chemical and biological treatments were widespread in the leaf and caused cell death. The trace gas emissions caused by these treatments may originate from different processes (such as lipid oxidation) from those caused by UV irradiation. Nevertheless, the potential effects of ROS generated by other environmental stresses should be considered. Experimental studies are generally undertaken using plants that have not been subjected to environmental stress or disease and without UV irradiation (e.g. Dueck *et al.*, 2007; Beerling *et al.*, 2008). Another likely reason why studies have failed to report a role of UV radiation in CH_4 production is that materials used in the construction of experimental leaf chambers and cuvettes, such as glass, polymethyl methacrylate (PMMA, 'Perspex' or 'Plexiglas') and polycarbonate do not transmit all UV wavelengths (Fig. 1c), and plastic polymers may themselves release hydrocarbons under UV irradiation (Lonneman *et al.*, 1981). The suggestion (Schiermeier, 2006) that some plant species emit up to 4000 times more CH_4 than others may reflect the variability of leaf structures, UV-screening pigments (McLeod & Newsham, 1997), UV-photosensitizers (Björn, 2002) and ROS-scavenging mechanisms (Apel & Hirt, 2004) found in plants. Previous measurements of CH_4 production from vegetation inside glass and 'Plexiglas' chambers (Keppler *et al.*, 2006; Dueck *et al.*, 2007) would have excluded some of the more energetic shorter wavelength UV in solar radiation so that rates of CH_4 emission in the field may be larger than suggested from past experiments. However, reported experimental CH_4 emissions (Keppler *et al.*, 2006; Sanhueza & Donoso, 2006) may also reflect a combination of experimental stress factors that could include heat and desiccation (and UV irradiance) as well as possible artefacts suggested by Kirschbaum *et al.* (2007). Sharpatyi (2007) also implied that gamma radiation is a driver of free radical mechanisms that may lead to CH_4 production, and consequently the effect of gamma sterilization of vegetation samples to eliminate microbial effects (e.g. Keppler *et al.*, 2006) should also be tested carefully to ensure that it does not cause biochemical changes that influence subsequent experimental results.

Conclusions

These results provide further evidence that plant pectins can act as a source of CH_4 under aerobic conditions when exposed to UV radiation within the ambient range (280–400 nm) from experimental lamps and sunlight. They also provide a first step in understanding the potential mechanisms by demonstrating a role of ROS in CH_4 production and the additional production of ethane, ethylene and CO_2.

The rate of CH_4 production (*c.* 13 ng g^{-1} h^{-1}) from tobacco leaves was similar to values reported for detached leaves by Keppler *et al.* (2006), but much lower than their values obtained using intact plants. Nevertheless, vegetation stress factors, especially UV radiation, may have wider implications for biosphere–atmosphere interactions, as any ROS-forming mechanism may have the potential to produce not only CH_4 but also other atmospheric trace gases such as C_2 hydrocarbons and the methyl halides from terrestrial plant sources. A deeper understanding of the biochemical mechanisms for CH_4 production may provide the potential to minimize CH_4 generation from large-scale planting of crops and trees by selection for effective ROS-scavenging and/or UV-screening properties. Consequently, the potential of high UV irradiance in the tropics and a range of environmental stress factors to cause ROS formation and trace gas emissions requires examination in a range of species, using realistic spectral irradiance and experimental treatments, in order to fully understand the role of these processes in global emissions.

Acknowledgements

We thank Julia Drewer, Caroline Nichol, Frank Keppler, Ann Webb, Nigel Paul, Ruth Doherty, Geoff Holmes, Robert Vreeburg, Éva Hedig, Paul Palmer and Lesley Yellowlees for helpful discussions and Colin Kaye, Robert Howard, Alex Hart, Bill Adams, Sophie Haupt and Chris McLellan for assistance. This work was supported by research awards from the Natural Environment Research Council (to ARM), the Moray Endowment Fund (to ARM), the Biotechnology and Biological Sciences Research Council (to SCF, GJL and B-WY), a

NERC Fellowship (to DSR), the University of Edinburgh Development Trust (to DJM) and the University of Edinburgh Donald Mackenzie Scholarship (to DJM).

References

Apel K, Hirt H. 2004. Reactive oxygen species: metabolism, oxidative stress, and signal transduction. *Annual Review of Plant Biology* 55: 373–399.

Austin AT, Vivanco L. 2006. Plant litter decomposition in a semi-arid ecosystem controlled by photodegradation. *Nature* 442: 555–558.

Beerling DJ, Gardiner T, Leggett G, McLeod A, Quick WP. 2008. Missing methane emissions from leaves of terrestrial plants. *Global Change Biology* 14: 1–6.

Bergamaschi P, Frankenberg C, Meirink JF, Krol M, Dentener F, Wagner T, Platt U, Kaplan JO, Korner S, Heimann M *et al.* 2007. Satellite chartography of atmospheric methane from SCIAMACHY on board ENVISAT: 2. Evaluation based on inverse model simulations. *Journal of Geophysical Research-Atmospheres* 112: article number D02304.

Björn LO, ed. 2002. *Photobiology*. Dordrecht, the Netherlands: Kluwer Academic Publishers.

Bousquet P, Ciais P, Miller JB, Dlugokencky EJ, Hauglustaine DA, Prigent C, Van der Werf GR, Peylin P, Brunke E-G, Carouge C *et al.* 2006. Contribution of anthropogenic and natural sources of atmospheric methane variability. *Nature* 443: 439–443.

Caldwell MM. 1971. Solar ultraviolet radiation and the growth and development of higher plants. In: Giese AC, ed. *Photophysiology*. New York, NY, USA: Academic Press, 131–177.

do Carmo JB, Keller M, Dias JD, de Camargo PB, Crill P. 2006. A source of methane from upland forests in the Brazilian Amazon. *Geophysical Research Letters* 33: article number L04809.

Crutzen PJ, Sanhueza E, Brenninkmeijer CAM. 2006. Methane production from mixed tropical savanna and forest vegetation in Venezuela. *Atmospheric Chemistry and Physics Discussions* 6: 3093–3097.

Dueck TA, de Visser R, Poorter H, Persijn S, Gorissen A, de Visser W, Schapendonk A, Verhagen J, Snel J, Harren FJM *et al.* 2007. No evidence for substantial aerobic methane emission by terrestrial plants: a ^{13}C-labelling approach. *New Phytologist* 175: 29–35.

Dueck TA, van der Werf A. 2008. Are plants precursors for methane? *New Phytologist* 178: 693–695.

Ferretti DF, Miller JB, White JWC, Lassey KR, Lowe DC, Etheridge DM. 2007. Stable isotopes provide revised global limits of aerobic methane emissions from plants. *Atmospheric Chemistry and Physics Discussions* 7: 237–241.

Filkowski J, Kovalchuk O, Kovalchuk I. 2004. Genome stability of vtc1, tt4, and tt5 *Arabidopsis thaliana* mutants impaired in protection against oxidative stress. *Plant Journal* 38: 60–69.

Flint SD, Caldwell MM. 2003. A biological spectral weighting function for ozone depletion research with higher plants. *Physiologia Plantarum* 117: 137–144.

Frankenberg F, Bergamaschi P, Butz A, Houweling S, Meirink JF, Notholt J, Petersen AK, Schrijver H, Warneke T, Aben I. 2008. Tropical methane emissions: a revised view from SCIAMACHY onboard ENVISAT. *Geophysical Research Letters*, doi: 10.1029/2008GL034300

Fry SC. 1998. Oxidative scission of plant cell wall polysaccharides by ascorbate-induced hydroxyl radicals. *Biochemical Journal* 332: 507–515.

Fry SC, Dumville JC, Miller JG. 2001. Fingerprinting of polysaccharides attacked by hydroxyl radicals in vitro and in the cell walls of ripening pear fruit. *Biochemical Journal* 357: 729–737.

Green AES, Sawada T, Shettle EP. 1974. The middle ultraviolet reaching the ground. *Photochemistry and Photobiology* 19: 251–259.

Gueymard C. 1995. *SMARTS, a simple model of the atmospheric radiative transfer of sunshine: algorithms and performance assessment*. Professional Paper FSEC-PF-270-95. Cocoa, FL, USA: Florida Solar Energy Center.

Gueymard C. 2001. Parameterized transmittance model for direct beam and circumsolar spectral irradiance. *Solar Energy* 71: 325–346.

Houweling S, Röckmann T, Aben I, Keppler F, Krol M, Meirink JF, Dlugokencky EJ, Frankenberg C. 2006. Atmospheric constraints on global emissions of methane from plants. *Geophysical Research Letters* 33: article number L15821.

Keppler F, Hamilton JTG, Brass M, Röckmann T. 2006. Methane emissions from terrestrial plants under aerobic conditions. *Nature* 439: 187–191.

Keppler F, Hamilton JTG, McRoberts WC, Vigano I, Brass M, Röckmann T. 2008. Methoxyl groups of plant pectin as a precursor of atmospheric methane: evidence from deuterium labelling studies. *New Phytologist* 178: 808–814.

King EO, Ward MK, Raney DE. 1954. Two simple media for the demonstration of pyocyanin and fluorescin. *Journal of Laboratory and Clinical Medicine* 44: 301–307.

Kirschbaum MUF, Niinemets U, Bruhn D, Winters AJ. 2007. How important is aerobic methane release by plants? *Functional Plant Science and Technology* 1: 138–145.

Liley JB, McKenzie RL. 2006. *Where on earth has the highest UV?* Lauder, New Zealand: National Institute of Water and Atmospheric Research (NIWA). http://www.niwa.cri.nz/rc/atmos/uvconference/2006/papers

Lonneman WA, Bufalini JJ, Kuntz RL, Meeks SA. 1981. Contamination from fluorcarbon films. *Environmental Science and Technology* 15: 99–103.

McKinlay AF, Diffey BL. 1987. A reference action spectrum for ultra-violet induced erythema in human skin. In: Passchier WF, Bosnjakovic BFM, eds. *Human exposure to ultra-violet radiation: risks and regulations*. Amsterdam, the Netherlands: Elsevier, 83–87.

McLeod AR. 1997. Outdoor supplementation systems for studies of the effects of increased UV-B radiation. *Plant Ecology* 128: 78–92.

McLeod AR, Newsham KK. 1997. Impacts of elevated UV-B on forest ecosystems. In: Lumsden PJ, ed. *Plants and UV-B*. Cambridge, UK: Cambridge University Press, 247–281.

McLeod AR, Newsham KK, Fry SC. 2007. Elevated UV-B radiation modifies the extractability of carbohydrate from leaflitter of *Quercus robur*. *Soil Biology and Biochemistry* 39: 116–126.

Micheletti MI, Piacentini RD, Madronich S. 2003. Sensitivity of biologically active UV radiation to stratospheric ozone changes: effects of action spectrum shape and wavelength range. *Photochemistry and Photobiology* 78: 456–461.

Miller JB, Gatti LV, d'Amelio MTS, Crotwell AM, Dlugokencky EJ, Bakwin P, Artaxo P, Tans PP. 2007. Airborne measurements indicate large methane emissions from the eastern Amazon basin. *Geophysical Research Letters* 34: article number L10809.

Nara A, Takeuchi Y. 2002. Ethylene evolution from tobacco leaves irradiated with UV-B. *Journal of Plant Research* 115: 247–253.

Neter J, Kutner MH, Nachtsheim CJ, Wasserman W. 1996. *Applied linear statistical models*. Boston, MA, USA: WCB/McGraw-Hill.

Quaite FE, Sutherland BM, Sutherland JC. 1992. Action spectrum for DNA damage in alfalfa lowers predicted impact of ozone depletion. *Nature* 358: 576–578.

Rusch H, Rennenberg H. 1998. Black alder (*Alnus glutinosa* (L.) Gaertn.) trees mediate methane and nitrous oxide emission from the soil to the atmosphere. *Plant and Soil* 201: 1–7.

Sanhueza E, Donoso L. 2006. Methane emission from tropical savanna *Trachypogon sp.* grasses. *Atmospheric Chemistry and Physics* 6: 5315–5319.

Schiermeier Q. 2006. The methane mystery. *Nature* 442: 730–731.

Schiermeier Q. 2007. Methane mystery continues. *Nature News*, doi:10.1038/news.2007.307.

Schneising O, Buchwitz M, Burrows JP, Bovensmann H, Bergamaschi P, Peters W. 2008. Three years of greenhouse gas column-averaged dry air mole fractions retrieved from satellite – Part 2: methane. *Atmospheric Chemistry and Physics Discussions* **8**: 8273–8326.

Setlow RB. 1974. The wavelengths in sunlight effective in producing skin cancer: a theoretical analysis. *Proceedings of the National Academy of Sciences, USA* **71**: 3363–3366.

Seymour GB, Knox JP, eds. 2002. *Pectins and their manipulation.* Oxford, UK/Boca Raton, FL, USA: Blackwell Publishing Limited/CRC Press LLC.

Sharpatyi VA. 2007. On the mechanism of methane emission by terrestrial plants. *Oxidation Communications* **30**: 48–50.

Steinmuller D. 1986. Zur Wirkung ultravioletter Strahlung (UV-B) auf die Struktur von Blättoberflachen und zu Wirkungsmechanismen bei der Akkumulation und Biosynthese der Kutikularlipide einiger Nutzpflanzen. *Karlsruher Beiträge zur Entwicklungs- und Ökophysiologie der Pflanzen* **6**: 1–174.

Terazawa K, Ishizuka S, Sakatac T, Yamada K, Takahashi M. 2007. Methane emissions from stems of *Fraxinus mandshurica* var. *japonica* trees in a floodplain forest. *Soil Biology & Biochemistry* **39**: 2689–2692.

Vigano I, van Weelden H, Holzinger R, Keppler F, McLeod A, Röckmann T. 2008. Effect of UV radiation and temperature on the emission of methane from plant biomass and structural components. *Biogeosciences* **5**: 937–947.

Wang YB, Feng HY, Qu Y, Cheng JQ, Zhao ZG, Zhang MX, Wang XL, An LZ. 2006. The relationship between reactive oxygen species and nitric oxide in ultraviolet-B-induced ethylene production in leaves of maize seedlings. *Environmental and Experimental Botany* **57**: 51–61.

Wang ZP, Han XG, Wang GG, Song Y, Gulledge J. 2008. Aerobic methane emission from plants in the Inner Mongolia Steppe. *Environmental Science and Technology* **42**: 62–68.

Whalen MC, Innes RW, Bent AF, Staskawicz BJ. 1991. Identification of *Pseudomonas syringae* pathogens of *Arabidopsis* and a bacterial locus determining avirulence on both *Arabidopsis* and soybean. *Plant Cell* **3**: 49–59.

Plant, Cell and Environment (2009) **32**, 1–9 doi: 10.1111/j.1365-3040.2008.01892.x

The role of ultraviolet radiation, photosensitizers, reactive oxygen species and ester groups in mechanisms of methane formation from pectin

DAVID J. MESSENGER[1,2], ANDY R. MCLEOD[2] & STEPHEN C. FRY[1]

[1]*Institute of Molecular Plant Sciences, School of Biological Sciences and* [2]*Institute of Atmospheric and Environmental Sciences, School of GeoSciences, The University of Edinburgh, Edinburgh, UK*

ABSTRACT

Ultraviolet (UV) radiation has recently been demonstrated to drive an aerobic production of methane (CH_4) from plant tissues and pectins, as do agents that generate reactive oxygen species (ROS) *in vivo* independently of UV. As the major building-blocks of pectin do not absorb solar UV found at the earth's surface (i.e. >280 nm), we explored the hypothesis that UV radiation affects pectin indirectly via generation of ROS which themselves release CH_4 from pectin. Decreasing the UV absorbance of commercial pectin by ethanol washing diminished UV-dependent CH_4 production, and this was restored by the addition of the UV photosensitizer tryptophan. Certain ROS scavengers [mannitol, a hydroxyl radical ('OH) scavenger; 1,4-diazabicyclo[2.2.2] octane; and iodide] strongly inhibited UV-induced CH_4 production from dry pectin. Furthermore, pectin solutions emitted CH_4 in darkness upon the addition of 'OH, but not superoxide or H_2O_2. Model carbohydrates reacted similarly if they possessed —CH_3 groups [e.g. methyl esters or (more weakly) acetyl esters but not rhamnose]. We conclude that UV evokes CH_4 production from pectic methyl groups by interacting with UV photosensitizers to generate 'OH. We suggest that diverse processes generating 'OH could contribute to CH_4 emissions independently of UV irradiation, and that environmental stresses and constitutive physiological processes generating ROS require careful evaluation in studies of CH_4 formation from foliage.

Key-words: acetyl esters; CH_4; homogalacturonan methyl ester; hydroxyl radical; pectic polysaccharides; plant cell walls; ROS; singlet oxygen; UV.

Abbreviations: DABCO, 1,4-diazabicyclo[2.2.2]octane; GalA, α-D-galacturonic acid; HG, homogalacturonan; HGMe, homogalacturonan methyl ester; ROS, reactive oxygen species; TBA, tetrabutyl ammonium hydroxide; UV, ultraviolet.

Correspondence: S. C. Fry. Fax: +44 (0) 131 650 5392; e-mail: S.Fry@ed.ac.uk

INTRODUCTION

The first observations of methane (CH_4) emission from plant foliage under aerobic conditions and initial estimates of the global total from vegetation sources (Keppler *et al.* 2006) caused much controversy and debate (Bousquet *et al.* 2006; Houweling *et al.* 2006; Kirschbaum *et al.* 2006; Miller *et al.* 2007). In some subsequent studies, no CH_4 emissions were observed from several plant species (Beerling *et al.* 2007; Dueck *et al.* 2007); nevertheless, in recent studies Wang *et al.* (2008), using measurements in the dark, reported CH_4 emissions from several woody species but not from grasses, whereas Cao *et al.* (2008), using chambers covered with white cloth, reported CH_4 emissions from grasses but not from a shrub community. A novel mechanism for aerobic CH_4 production in the marine environment has also been reported (Karl *et al.* 2008).

Uptake of dissolved CH_4 from the soil and subsequent release from transpiring leaves had been suggested as a possible CH_4 source from vegetation by Rusch & Rennenberg (1998) and Terazawa *et al.* (2007). Most recently, however, three studies have reported that UV radiation (280–400 nm) causes CH_4 production not only from terrestrial plant foliage, but also from plant structural components such as pectic polysaccharides in which transpiration cannot have been occurring (Keppler *et al.* 2008; McLeod *et al.* 2008; Vigano *et al.* 2008). This range of studies suggests that different plant species have different CH_4 emission rates, and that different mechanisms may be operating.

Measurements of $\delta^{13}C$ of the emitted CH_4 led Keppler *et al.* (2006) to suggest that CH_4 originated from the plant's C_1 metabolite pool, for example from the methyl ester groups of pectic polysaccharides. These polymers are major components of the primary cell walls of dicots and most other non-poalean plants (Popper & Fry 2003, 2004) and they are major components of the middle lamella. Pectic polysaccharides are rich in α-D-galacturonic acid (GalA) residues and consist of several different, covalently linked, polymeric domains: acidic homogalacturonan [HG; in which (1→4)-linked α-D-GalA are the sole sugar residues], methyl-esterified homogalacturonan (HGMe), rhamnogalacturonan-I (RG-I; 'hairy regions', comprising mainly GalA, rhamnose, arabinose and galactose residues) and smaller amounts of RG-II and xylogalacturonan (Seymour

& Knox 2002; O'Neill & York 2003). Some of the HG (and/or HGMe) and RG-I domains also possess *O*-acetyl ester groups (Ishii 1997; Perrone *et al.* 2002) and, in certain plants, phenolic groups such as ferulic acid (Fry 1983). Pectins thus have various types of —CH_3 groups: the methyl esters, carbon-2 of acetyl esters, carbon-6 of rhamnose (= 6-deoxymannose) and in some taxa the methyl ether of ferulate. Commercial citrus 'pectin' includes HG, HGMe and RG-I domains, although the RG-I domains are likely to have lower than normal proportions of arabinose owing to the acidic treatments used during extraction (Seymour & Knox 2002). Pectin that has been demethylesterified is called pectate.

The CH_4 emissions reported by Keppler *et al.* (2006) increased with both temperature and sunlight, an observation which led us to initiate studies of UV irradiation of leaves and of pectin as the potential source of the observed CH_4. Using both artificial UV sources and sunlight, we demonstrated a linear relationship between CH_4 emission from pectin and a spectrally weighted UV irradiance (McLeod *et al.* 2008). UV irradiation of pectate (made by de-esterification of commercial pectin) produced only traces of CH_4 compared with commercial pectin (McLeod *et al.* 2008), supporting a key role for ester groups although not distinguishing between methyl and acetyl esters. Similar emission rates caused by UV irradiation of pectin, and several other plant structural components (cellulose, lignin and palmitic acid) have also been reported by Vigano *et al.* (2008).

McLeod *et al.* (2008) observed for the first time that not only CH_4 but also ethylene, ethane and CO_2 were produced upon UV irradiation of pectin. It is possible that the effects of UV on leaves and on pectin are attributable to the production of ROS. The formation of ROS in living tobacco leaves (*Nicotiana tabacum*) induced by leaf infiltration with the singlet oxygen generator rose bengal or the bacterial pathogen *Pseudomonas syringae* pv. tomato DC3000 carrying the avirulence gene *avrB* [*Pst*DC3000 (*avrB*)] also led to the production of CH_4, ethylene and ethane in varying rates and quantities (McLeod *et al.* 2008). Similarly, CH_4, ethylene and ethane were evolved from tobacco leaves under UV irradiation. These data from both *in-vivo* and *in-vitro* studies suggested a mechanism involving production of methyl radicals (generating CH_4) followed by some dimerization (generating C_2H_6 and C_2H_4), and also the production of carboxylate radicals (generating CO_2), similar to the type of mechanism proposed by Sharpatyi (2007).

In addition to occurring by UV- and/or ROS-dependent mechanisms, the emission of certain hydrocarbons by living plant tissues is possible by several other mechanisms in healthy, unstressed plants. Ethylene is a well-known, constitutive plant hydrocarbon, produced by aminocyclopropane-1-carboxylic acid oxidase in response to various stresses and as a signalling molecule in healthy tissues (Bleecker & Kende 2000). In addition, isoprene is commonly evolved by plants. Harley *et al.* (1996) showed that constitutive isoprene production is unaffected by UV in *Mucuna*, although it is enhanced by UV in *Quercus*. Isoprene is produced only in living plants, by the action of the enzyme isoprene synthase on dimethylallyl pyrophosphate. Isoprene production is affected by sunlight because this: (1) up-regulates the gene for isoprene synthase; and (2) affects photosynthesis and associated metabolism, including the synthesis of dimethylallyl pyrophosphate (Affek & Yakir 2003). Thus, even in *Quercus*, where sunlight enhances isoprene generation, this hydrocarbon emission is thought to be enzymic and not an abiotic UV-driven photochemical process.

In contrast, plants have no known CH_4-generating enzymes, and it is thought that aerobic CH_4 production from vegetation (living and dead) must be non-enzymic (Schiermeier 2006), which recent observations suggest can be driven by UV radiation and/or ROS (McLeod *et al.* 2008). Nevertheless, the production of ROS may itself be enzymic: healthy plant tissues naturally produce certain ROS, probably including apoplastic (wall-localized) hydroxyl radicals ($^{\bullet}OH$) by the action of ascorbate/Cu^{2+}-dependent Fenton reactions (Fry 1998; Vreeburg & Fry 2005; Lindsay & Fry 2007) or superoxide/peroxidase-dependent Haber–Weiss reactions (Chen & Schopfer 1999; Liszkay, Kenk & Schopfer 2003). In addition, diseased plant tissues often produce ROS as part of an oxidative burst (Wojtaszek 1997; Grant, Yun & Loake 2000; Vreeburg & Fry 2005). The $^{\bullet}OH$ radical is exceedingly short-lived: in a biological milieu, it is predicted to react with organic matter within ≈1 nm of the site of radical production (Griffiths & Lunec 1996); and in the cell wall, this organic matter may include pectic polysaccharides, potentially generating CH_4. In this sense, some CH_4 generation may be 'indirectly enzymic' since the accumulation of apoplastic ascorbate or superoxide (two of the proposed generators of $^{\bullet}OH$) is enzyme-dependent.

Concerning UV-dependent CH_4 production, it is interesting that the major components of pectic polysaccharides (sugar residues, methyl esters and *O*-acetyl groups) do not appreciably absorb UV radiation in the 280–380 nm range (Bednarczyk & Marchlewski 1938; Slein & Schnell 1953; Hershenson 1956). It is thus not immediately obvious how UV interacts with these polysaccharides to generate ROS and/or CH_4.

The main aims of the present work on UV-induced CH_4 production from pectin were: (1) to strengthen the evidence for a role of ROS, especially by use of scavengers; (2) to evaluate the relative roles of different ROS, especially $^{\bullet}OH$; (3) to investigate the ability of UV photosensitizers to render pectin susceptible to UV radiation; and (4) to determine which of the three types of methyl group present in pectin is/are the source of CH_4.

MATERIALS AND METHODS

All chemicals were obtained from the Sigma-Aldrich Chemical Company, Poole, UK.

Preparation of washed pectin and pectate

To investigate the contribution of UV-absorbing low-M_r contaminants, we dissolved commercial citrus fruit pectin

(Sigma P9135; galacturonic acid content 84%; methoxy content 9.4%; loss on drying 4.1%) at 1% (w/v) in water, then precipitated it in ethanol (75% v/v, final concentration), filtered and then lyophilized the residue. The residue was dissolved at 1% w/v in water and the process was repeated with ethanol : formic acid (15:1 v/v), providing a purified pectin sample. The protocol for the preparation of pectate was as described by McLeod *et al.* (2008).

Synthesis of partially methyl-esterified homogalacturonan (HGMe)

A 5% w/v HG ('polygalacturonic acid'; Na^+ salt) solution (pH 7.0 adjusted with TBA) was lyophilized and redissolved in a minimum volume of dimethylsulphoxide (dried with molecular sieves, type 4A) in a sealed flask. CH_3I was added (1.1 mol mol^{-1} GalA residues) and stirred in darkness for 24 h. The solution was dialysed once against 0.2 M NaCl and twice against water, and lyophilized.

Determination of methyl ester content

To release methyl esters as methanol, we added 200 μL of 200 mM KOH to a 0.75 mL sample of HGMe (0.2% w/v), which was incubated at room temperature for 1 h, followed by the addition of 66 μL of 1 M KH_2PO_4. As an unhydrolysed control, another 0.75 mL sample of HGMe was treated with the same dose of pre-mixed KOH/KH_2PO_4. A 50 μL aliquot of 20 mM 4-aminoantipyrine and 120 mM phenol was added to 500 μL of each sample, followed by 50 μL of a horseradish peroxidase solution (200 U mL^{-1}) and 40 μL of alcohol oxidase (400 U mL^{-1}), and incubated at room temperature for 10 min. Absorbance at 546 nm of the first sample solution was taken, and the absorbance of the second sample solution was deducted from it. A calibration curve was made with standard solutions containing 50–500 nmol of methanol.

Measurement of UV absorbance

The absorbance spectrum of a 0.5% (w/v) solution in deionized water of the carbohydrates (pectin, pectate, washed pectin, HG, HGMe, mannose pentaacetate); the ROS scavengers (KI, DABCO, mannitol) and the ROS generator (L-tryptophan; Trp) was measured in a scanning spectrometer (CECIL 8000 series, Cecil Instruments Ltd., Cambridge, UK).

Preparation of impregnated glass fibre sheets

Glass microfibre filters (Whatman GF/A, Maidstone, Kent, UK; 20.3 × 25.4 cm) were baked overnight in a furnace at 300 °C to remove organic contaminants. Citrus pectin, pectate, HG or HGMe (250 mg in 25 mL of deionized water) was applied to each sheet and allowed to dry overnight. Where indicated, ROS scavengers [DABCO (2 mmol), KI (2 mmol) or mannitol (2 or 20 mmol)] or a potential UV photosensitizer (Trp, 2 mmol) were pre-mixed with the polysaccharide before application to the sheets. Control sheets received water only with the respective ROS scavenger or generator.

UV radiation sources and measurement

UV radiation was provided by four UV313 lamps (The Q-Panel Company, Cleveland, OH, USA) filtered with a 125 μm cellulose diacetate sheet, which removed wavelengths below 290 nm including UV-C radiation. UV spectral irradiance was measured with a double monochromator spectroradiometer (SR991-PC; Macam Photometrics, Livingstone, UK) which was calibrated against tungsten and deuterium lamps traceable to National Physical Laboratory Standards (SR903, Macam Photometrics). Spectral characteristics of the lamps and filters are given by McLeod *et al.* (2008). All experiments were carried out at an irradiation level of 8.71 W m^{-2} (unweighted UV: 280–400 nm), equivalent to 5.14 W m^{-2} using the spectral weighting function for CH_4 production from pectin described in McLeod *et al.* (2008).

UV irradiation of impregnated glass fibre sheets

UV irradiation of impregnated glass fibre sheets was performed inside new 5-l gas sampling bags of 25 μm UV-transparent polyvinylfluoride film (SKC, Inc., Eighty Four, PA, USA). These were cut open on one side for insertion of glass fibre sheets and re-sealed with 40 μm Al adhesive tape. Bags were flushed five times before filling with 250 mL of stock external ambient air. Experiments used one sample bag containing an impregnated glass fibre sheet and another sample bag containing a control glass fibre sheet. Bags were supported on a black butyl rubber sheet (pond liner) on the surface of a thermostatically controlled water bath at 30 °C. After 2 h, the CH_4 concentration was determined and the net CH_4 production was calculated. Each experiment was replicated three times, and the mean and standard error were calculated. The transmission spectrum of polyvinylfluoride film is given by McLeod *et al.* (2008).

ROS effects on polysaccharide solutions in the dark

To evaluate ROS effects on the carbohydrates (pectin, pectate, HGMe, HG, pectin with 0.5 M mannitol, mannose pentaacetate, rhamnose and mannose), we placed 15 mL of a 1% w/v solution of each substance in deionized water in a 20 mL glass vial with a seal and crimp-cap. Effects of superoxide ($O_2^{\bullet-}$), and/or its non-ionized equivalent the hydroperoxyl radical ($HO_2^{\bullet}$), were determined by addition of KO_2 crystals to a final concentration of 5 mM. Effects of H_2O_2 were determined by addition of a suitable volume of a 33% solution to obtain a final concentration of 5 mM H_2O_2.

Effects of 'OH were determined by addition of Fenton reagent to achieve a final concentration of 5 mM ascorbic acid, 5 μM $CuSO_4$ and 5 mM H_2O_2. Effects of 'OH scavenging were determined by addition of mannitol to a final concentration of 0.5 M. For exclusion of sunlight, all vials were wrapped in Al foil.

In all experiments, three replicate vials were maintained at room temperature, and CH_4 concentration in the head space was assayed at 1, 3 and 5 h, and the mean and standard error were calculated.

Gas concentration measurement

CH_4 concentration was determined with a gas chromatograph (Hewlett Packard Series II 5890, Altrincham, UK) equipped with a flame ionization detector and a column packed with Haysep 80–100 mesh 'Porapak Q' at 70 °C with N_2 as carrier gas. All experiments on glass fibre sheets used an automatic sampler to which gas sample bags were directly attached. For studies on polysaccharide solutions, 2 mL of the vial head space air was injected directly into the carrier gas. Vials were fitted with syringes containing 6 mL ambient air to compensate for volume reduction and keep air pressure constant. Peak integration and autosampling were controlled by a chromatography data system (PeakSimple model 203, SRI Instruments, Torrance, CA, USA).

RESULTS AND DISCUSSION

Role of UV-absorbing components in methane generation

Our previous experiments with DABCO (McLeod *et al.* 2008) led us to suggest that ROS are involved in mechanisms of UV-induced CH_4 formation, and that methyl ester groups of pectic polysaccharides are a major source of the CH_4; however, the precise nature and role of the ROS were unclear, and the possible contribution of methyl groups other than methyl esters had not been evaluated. In the present work, we verified that dried citrus pectin yields appreciable amounts of CH_4 when UV irradiated (Fig. 1). Glass fibre sheets with no added polysaccharide yielded no CH_4 (data not shown). The yield (≈300 ng kg^{-1} s^{-1}) corresponds to an hourly conversion to CH_4 of ≈0.0023% of the pectic methyl ester groups, if these are the major source. Estimates of the potential global CH_4 source from pectin would require a detailed evaluation of leaf pectin content and this pectin's exposure to UV; the rates and persistence of CH_4 production *in vivo*; the spectral response of CH_4 production to UV; the extent of ROS formation by constitutive processes occurring in unstressed plants and in response to diverse environmental stresses; and how these factors vary between plant types owing to differences in leaf structure, UV-screening pigments and ROS-scavenging mechanisms. Such an assessment is beyond the scope of this study.

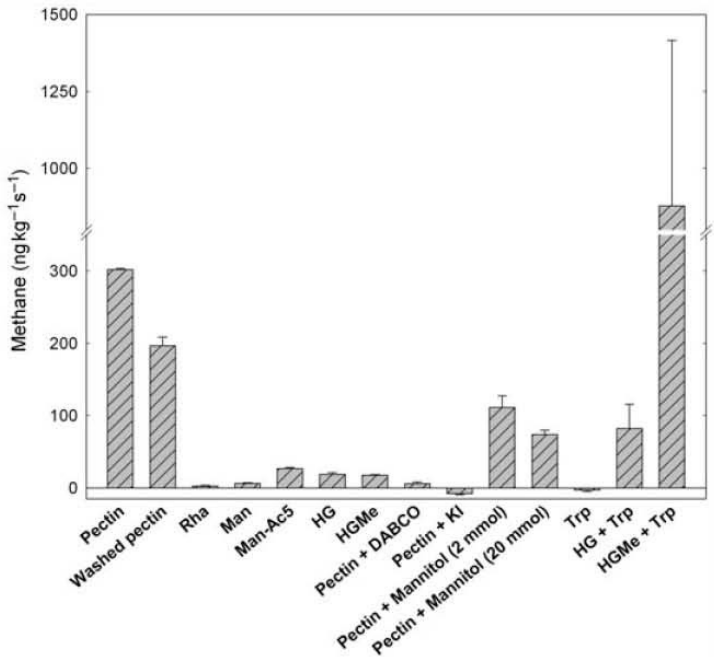

Figure 1. UV-induced methane emissions from glass fibre sheets impregnated with various carbohydrates, and the effect of ROS scavengers and ROS generators. Glass fibre sheets contained 250 mg of source compound with the ROS scavenger or generator in the indicated amounts. The unweighted UV-irradiation treatment was 8.71 W m^{-2} (equivalent to 5.14 W m^{-2} weighted for CH_4 production; see text). Temperature was 30 °C. CH_4 production was recorded after 2 h of irradiation and is reported as ng CH_4 (kg source compound)$^{-1}$ s^{-1}. In the case of Trp alone, the Trp was regarded as the potential 'source compound'. Values are means of three replicates with standard error bars. Abbreviations used: Ac_5, pentaacetate; DABCO, 1,4-diazabicyclo[2.2.2]octane; HG, homogalacturonan; HGMe, partially methylesterified homogalacturonan; Man, mannose; Rha, rhamnose; Trp, tryptophan.

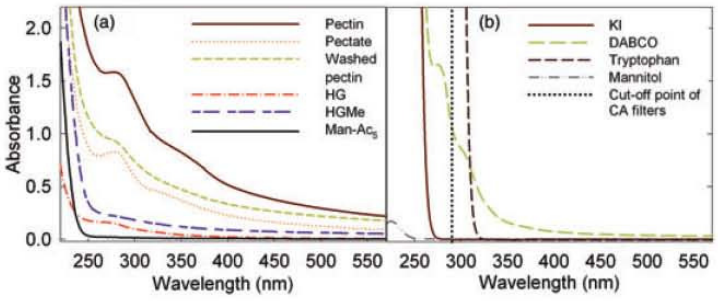

Figure 2. Absorption spectra of carbohydrates, ROS scavengers and ROS generators. Each substance was tested as an aqueous solution at 0.5% (w/v). (a) Potential sources of CH_4; (b) ROS scavengers and ROS generators. Absorbance was measured in a 10 mm path-length cuvette.

It is surprising that pectin is affected by UV-A or UV-B because pure sugar residues (including GalA and its unsaturated derivative produced by lyase action, and the 6-deoxysugar rhamnose), methyl esters and acetyl esters do not appreciably absorb in this region of the spectrum (Bednarczyk & Marchlewski 1938; Slein & Schnell 1953; Hershenson 1956). However, solutions of commercial citrus pectin do absorb UV in the 280–380 nm range (Fig. 2a). This observation suggested that unidentified UV-absorbing components, probably aromatic, present in the citrus pectin were responsible for UV-induced CH_4 emission. To determine whether these UV-absorbing components were covalently attached to the pectic polysaccharide chains, we washed the pectin with ethanol and acidified ethanol, in which polysaccharides are insoluble. About 40% of the UV-absorbing material was removed by such washing, suggesting that 60% of it was covalently linked to polysaccharides (Fig. 2a). Little additional UV-absorbing material was removed by NaOH treatment (Fig. 2a; 'pectate'), indicating that most of it was not ester linked to the polysaccharides (e.g. feruloyl esters); instead, it may have been ether linked. Ethanol-washed pectin generated ≈36% less CH_4 than unwashed pectin, supporting a role for the UV-absorbing components in the mechanism of UV-induced CH_4 emission.

Inability of UV non-absorbing compounds to support UV-induced methane generation

Pectin contains methyl groups of three kinds: methyl esters, '*C*-methyl-pentose' residues (e.g. rhamnose) and the —CH_3 group of *O*-acetyl esters. We explored the ability of any of these to sustain UV-induced CH_4 production in the absence of direct UV absorption.

Firstly, HGMe was synthesized with a degree of methyl esterification of around 43% (on a GalA residue basis). This substance showed little absorbance in the 280–380 nm range (Fig. 2b). On UV irradiation, it gave only a low rate of CH_4 emission, ≈6% of that obtained with pectin and similar to that obtained with non-esterified HG (Fig. 1). Our results accord with those of Keppler *et al.* (2008), who saw emission rates of up to 10 ng kg^{-1} s^{-1} upon UV irradiation of HGMe. These low rates indicate that, in the absence of UV-absorbing groups, GalA methyl esters support little UV-induced CH_4 production.

Secondly, the ability of rhamnose (= 6-deoxymannose) to exhibit UV-induced CH_4 production was extremely low, and similar to that of mannose itself, included as a control. Neither of these compounds has any appreciable absorbance in the 280–380 nm range (data not shown). Thus, the methyl groups of pectic rhamnose residues have no innate ability to contribute to UV-induced aerobic CH_4 emission.

Thirdly, we investigated the —CH_3 groups of acetyl esters by testing the model compound, mannose pentaacetate. This substance showed extremely low UV absorbance (Fig. 2a), and exhibited only traces of UV-induced CH_4 emission (Fig. 1).

In conclusion, none of the three types of methyl groups present in pectin exhibited substantial UV-induced CH_4 production in the absence of UV-absorbing groups.

UV photosensitizing action of tryptophan

We next attempted to restore or enhance UV-induced CH_4 production by deliberately adding UV-absorbing aromatic substances. Some of the substances tested (e.g. *o*-coumaric acid) blocked the innate ability of commercial citrus pectin to yield CH_4 (data not shown), probably by acting as a UV-blocking filter. However, one UV-absorbing substance, tryptophan, very effectively conferred on HGMe the ability to emit CH_4 upon UV irradiation (Fig. 1). The CH_4 yield achieved from HGMe + Trp was about three times greater than from commercial citrus pectin. The methyl ester groups of the HGMe were the main source of the CH_4 in the presence of Trp because non-esterified HG was less than one-tenth as effective as HGMe (Fig. 1). Trp itself gave no CH_4 on UV irradiation.

Trp is a known generator of singlet oxygen ($^1O_2$) when irradiated with UV light (Knox & Dodge 1985). Furthermore, $^1O_2$ can be converted to the much more reactive $^{\bullet}OH$ in the presence of biological reductants such as phenols (Ueda *et al.* 2003). Our data therefore suggest that $^1O_2$ and/or downstream-generated related ROS were responsible for the conversion of pectic methyl ester groups to CH_4. An alternative possibility, at this point in the argument, however, is that Trp binds to pectic polysaccharides, funnelling the energy of the UV radiation to the polysaccharide. On either interpretation, we conclude that

photosensitizers, exemplified experimentally by Trp, can enable UV radiation to release CH_4 from pectin. It is likely that in the cell walls of sunlit leaves, other photosensitizers than Trp are more relevant to CH_4 production.

ROS scavengers block UV-induced methane generation

To explore the role of specific ROS in UV-induced CH_4 release from pectin, we UV irradiated commercial citrus pectin pre-mixed with each of three ROS scavengers. DABCO is reported to scavenge $^1O_2$, and, as reported before (McLeod *et al.* 2008), efficiently blocks UV-induced CH_4 emission from pectin (Fig. 1). This observation is compatible with a role for $^1O_2$ in CH_4 production. However, DABCO itself absorbs in the 280–350 nm UV range (Fig. 2b) and could thus potentially work as a simple UV-blocking filter, like *o*-coumaric acid.

The addition of KI, a known scavenger of H_2O_2 but also having a high rate constant for reaction with $^{\bullet}OH$ of 1×10^{10} L mol^{-1} s^{-1} (Buxton *et al.* 1988) and acting as a quencher of singlet oxygen (Rosenthal & Frimer 1976), to sheets of pectin reduced the UV-induced CH_4 emissions to trace levels (Fig. 1). This shows that one or more of these ROS are likely to be intermediates in this mechanism. KI starts absorbing only below 270 nm (Fig. 2b), well below the ambient and our experimental UV-B range, and therefore demonstrates that a ROS-scavenging effect is involved and not an effect of UV absorption.

The addition of mannitol, an $^{\bullet}OH$ scavenger with a rate constant of 1.7×10^9 L mol^{-1} s^{-1} (Buxton *et al.* 1988), to the pectin sheets substantially reduced UV-induced CH_4 emissions compared with pectin alone (Fig. 1); mannitol does not absorb at all in the 280–380 nm UV range (Fig. 2b). The inhibition caused by 2 and 20 mmol mannitol (per sheet of pectin) was 64 and 75%, respectively. This suggests that $^{\bullet}OH$ may be responsible for at least 75% of the observed CH_4 emissions. The other 25% could be attributable to the inability of dried mannitol to scavenge all $^{\bullet}OH$ radicals including those generated on pectin molecules themselves.

Our results, especially with the UV non-absorbing KI and mannitol, strongly imply that ROS production mediates the effect of UV on CH_4 release from pectic methyl esters. Comparable ROS mechanisms probably also explain the data of Keppler *et al.* (2008), who saw emission rates of up to 10 ng kg^{-1} s^{-1} from UV-irradiated HGMe.

The inability of scavengers to completely block the $^{\bullet}OH$-induced scission of biopolymers such as DNA (Burkitt 1994) and cell wall polysaccharides (Fry 1998; Fry, Miller & Dumville 2002) has been reported before. A plausible explanation for this is that transition metal ions such as Cu^{2+}, involved in ROS generation, are ligated to the biopolymers, thus targeting the exceedingly reactive and short-lived $^{\bullet}OH$ radicals precisely at vulnerable sites in the polymer so that (relatively dilute) scavengers in free solution are unable to interfere.

Hydroxyl radicals generate methane from pectic methyl ester groups in the dark

To investigate the CH_4-generating potential of different ROS, we added superoxide, H_2O_2 and a source of $^{\bullet}OH$ in identical concentrations to solutions of pectin and other polysaccharides. Addition of superoxide and H_2O_2 produced no appreciable CH_4 from pectin over 5 h (Fig. 3a), and these two ROS are therefore unlikely to be intermediates in the mechanism. The same conclusion can be drawn in the case of solutions of pectate, HGMe and HG (Fig. 3b–d). However, when Fenton reagent was present in the pectin solution to produce $^{\bullet}OH$, a net production of CH_4 from pectin was observed at rates of up to 12 ng kg^{-1} s^{-1}. In the case of pectate and HG, $^{\bullet}OH$ attack produced only trace levels of CH_4 (Fig. 3b,d), supporting the idea that the dominant CH_4 source in pectin was the methyl esters.

Addition of 0.5 M mannitol largely blocked the ability of $^{\bullet}OH$ to generate CH_4 from pectin (Fig. 3e), reducing emissions to levels similar to those obtained from pectate. As mannitol scavenges $^{\bullet}OH$ but not the other ROS, this observation indicates that $^{\bullet}OH$ was responsible for the CH_4 generation.

Generation of $^{\bullet}OH$ in HGMe solutions produced very large amounts of CH_4, almost 500 times more than from similar amounts of pectin (Fig. 3c). The yield ($\approx$50 μg g^{-1}) corresponds to a conversion to CH_4 of $\approx$0.13% of the methyl ester groups of HGMe. This large difference in production between HGMe and pectin (0.00025% of the methyl ester groups converted to CH_4) is interesting. We eliminated several potential artefacts such as: (1) neither dimethylsulphoxide, HG–TBA nor CH_3I (traces of which might potentially remain from the preparation of HGMe despite the dialysis and freeze-drying steps) released appreciable amounts of CH_4 in the presence of $^{\bullet}OH$ (data not shown); and (2) $^{\bullet}OH$ induced similar CH_4 emissions from a pectin/HGMe mixture (each 1% w/v) as from HGMe alone, indicating that the difference in CH_4 emissions was not due either to an ROS quencher found in pectin only or to a strong ability of pectin to sequester $^{\bullet}OH$-generating transition metals in a Fenton-inactive form (data not shown). The main differences between HGMe and pectin (Seymour & Knox 2002) that might account for their difference in $^{\bullet}OH$-induced CH_4 production are: (1) the presence of other sugar residues than GalA (rhamnose, arabinose and galactose of the 'hairy regions') in pectin but not HGMe; (2) the distribution of methyl ester groups being random in HGMe, but blockwise in pectin; and (3) the pectin being of higher molecular weight than HGMe. It is possible that the neutral sugar residues of pectin effectively shield the GalA methyl ester groups by preferentially scavenging $^{\bullet}OH$. Alternatively, it is possible that there are specific sequences of methylesterified and non-esterified GalA residues that occur, randomly, in HGMe but not in natural pectin, and that such sequences are particularly liable to generate CH_4 in the presence of $^{\bullet}OH$. Distinguishing these possibilities will be an interesting subject for future chemical experiments.

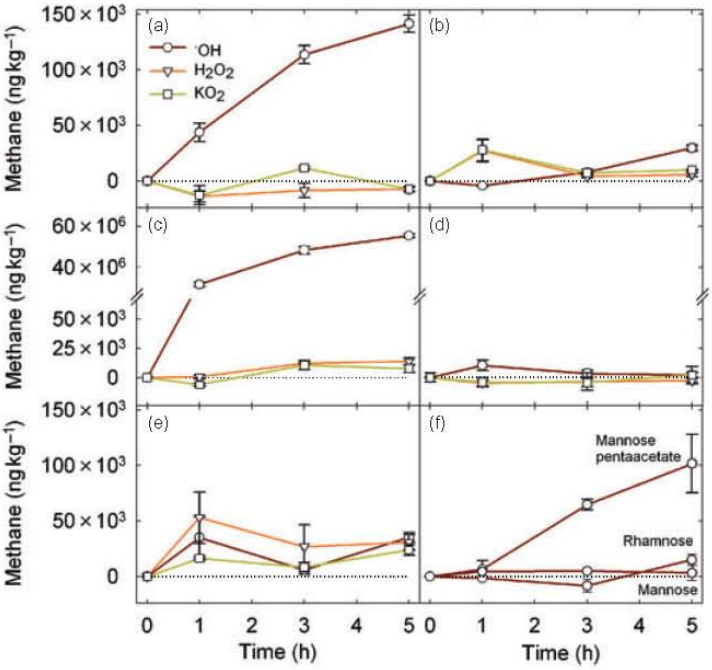

Figure 3. Methane emissions in the dark from solutions of pectin and other carbohydrates upon addition of ROS. Sources of ROS were: ·OH = 5 mM ascorbic acid, 5 μM $CuSO_4$ and 5 mM hydrogen peroxide (○); H_2O_2 = 5 mM hydrogen peroxide (▽); KO_2 = 5 mM potassium superoxide (□). The carbohydrates treated were: (a) 1% w/v pectin, (b) 1% w/v pectate, (c) 1% w/v partially methylesterified homogalacturonan, (d) 1% w/v homogalacturonan, (e) 1% w/v pectin with 0.5 M mannitol, (f) 1% w/v mannose pentaacetate, 1% w/v rhamnose and 1% w/v mannose. Values are means of three replicates with standard error bars.

Hydroxyl radicals generate methane from acetyl groups but not rhamnose

Concerning the potential of pectic methyl groups other than methyl esters to yield CH_4, we found that addition of Fenton reagent to solutions of rhamnose (which can be regarded as a 'methyl pentose') produced no detectable CH_4; as expected, the same result was obtained with mannose, which lacks a methyl group (Fig. 3f). Thus, methyl groups carbon-bonded to a sugar ring, as in rhamnose, are not a potential CH_4 source.

In contrast, solutions of mannose pentaacetate produced significant CH_4 emissions (at rates up to 7 ng kg^{-1} s^{-1}) (Fig. 3f). These data support the conclusion of Fig. 1 that *O*-acetyl groups are a potential minor CH_4 source and may account for discrepancies in previous labelling experiments (Keppler *et al.* 2008). This involvement of acetyl esters was unexpected because acetate has a low rate constant for reaction with ·OH (Buxton *et al.* 1988).

CONCLUSION

Our data strongly indicate that UV-induced CH_4 emission originates mainly from pectic methyl ester groups, thus supporting earlier suggestions by Keppler *et al.* (2008) and McLeod *et al.* (2008). While methyl ester groups account for the majority of CH_4 emissions, acetate groups are also a potential source.

The data also show that UV radiation does not act directly on methyl ester groups, but that a 'photosensitizer' is required, whose role is to generate ROS rather than simply to absorb energy from the UV radiation and 'funnel' it to methyl ester groups. Our work with scavengers and with added ROS suggests that ·OH, in some cases possibly formed *in vivo* from $^1O_2$, is the main ROS serving to generate CH_4 from pectin. The action of endogenous ROS on pectic polysaccharides could account for an ability of plants to evolve CH_4 in the absence of UV (Cao *et al.* 2008; Wang *et al.* 2008) in addition to any dissolution of soil-derived CH_4 carried above-ground in the transpiration stream. In this connection, it is interesting that grasses, reported to produce little CH_4 in the dark (Wang *et al.* 2008), are particularly poor in pectins compared with other land plants (O'Neill & York 2003; Popper & Fry 2004).

UV radiation is one well-known source of ·OH and singlet oxygen, and thus potentially of natural CH_4 emission from vegetation. If ambient UV light reaches pectin-linked photosensitizers in plant cell walls, despite the presence of UV-screening compounds and cuticular reflectance of UV (McLeod & Newsham 1997), and if the photosensitizers produce ROS that attack neighbouring pectic polysaccharides, then this mechanism of CH_4 formation is likely to occur *in vivo*.

Other environmental stresses such as drought; high temperature; nutrient deficiency; pathogen infection; and exposure to herbicides, heavy metals or ozone can also lead to ROS generation *in vivo* (Apel & Hirt 2004), and studies into

their effects on CH_4 production are required in order for their potential contribution to the global CH_4 budget to be estimated. For example, the ability of ozone to generate $^{\bullet}OH$ in the presence of water (Grimes, Perkins & Boss 1983) (e.g. in the apoplast) (Lyons, Ollerenshaw & Barnes 1999), may also lead to the generation of CH_4 from the mesophyll cell wall – a process that may now be increasing owing to the rising concentrations of tropospheric ozone (Crutzen 1988).

In addition, wall-localized $^{\bullet}OH$ production in healthy, non-stressed, uninfected plant tissues is proposed to be a normal feature of plant growth and development, contributing to the mechanism of wall loosening during cell expansion (Fry 1998; Schopfer 2001; Schopfer *et al.* 2002) and/or fruit softening (Fry, Dumville & Miller 2001; Dumville & Fry 2003). Such UV-independent $^{\bullet}OH$ production would enable pectic polysaccharides to generate CH_4 in tissues other than leaves (e.g. roots and fruits). Studies of various tissues during specific phases of plant growth and development may therefore also reveal CH_4 production.

ACKNOWLEDGMENTS

We thank Robert Howard, David Reay and Keith Smith for valuable advice and assistance with the GC analyses. The method for the synthesis of HGMe was kindly recommended by Dr M-C. Ralet from INRA, Nantes, France. This work was supported by research awards from the Natural Environment Research Council (to A.R.M.), the University of Edinburgh Development Trust and the University of Edinburgh Donald Mackenzie Scholarship (to D.J.M.) and the Biotechnology and Biological Sciences Research Council (to S.C.F.).

REFERENCES

Affek H.P. & Yakir D. (2003) Natural abundance carbon isotope composition of isoprene reflects incomplete coupling between isoprene synthesis and photosynthetic carbon flow. *Plant Physiology* **131,** 1727–1736.

Apel K. & Hirt H. (2004) Reactive oxygen species: metabolism, oxidative stress, and signal transduction. *Annual Review of Plant Biology* **55,** 373–399.

Bednarczyk W.I. & Marchlewski L. (1938) Information on sugar reduction V. *Biochemische Zeitschrift* **300,** 42–45.

Beerling D.J., Gardiner T., Leggett G., McLeod A. & Quick W.P. (2007) Missing methane emissions from leaves of terrestrial plants. *Global Change Biology* **14,** 1–6.

Bleecker A.B. & Kende H. (2000) Ethylene: a gaseous signal molecule in plants. *Annual Review of Cell and Developmental Biology* **16,** 1–18.

Bousquet P., Ciais P., Miller J.B., *et al.* (2006) Contribution of anthropogenic and natural sources of atmospheric methane variability. *Nature* **443,** 439–443.

Burkitt M.J. (1994) Copper – DNA adducts. *Methods in Enzymology* **234,** 66–79.

Buxton G.V., Greenstock C.L., Helman W.P. & Ross A.B. (1988) Critical review of rate constants for reactions of hydrated electrons, hydrogen atoms and hydroxyl radicals ($^{\bullet}OH/^{\bullet}O^{-}$) in aqueous solution. *Journal of Physical Chemical Reference Data* **17,** 513–886.

Cao G., Xu X., Long R., Wang Q., Wang C., Du Y. & Zhao X. (2008) Methane emissions by alpine plant communities in the Qinghai-Tibet Plateau. *Biology Letters*. doi: 10.1098/rsbl.2008.0373.

Chen S.X. & Schopfer P. (1999) Hydroxyl-radical production in physiological reactions. A novel function of peroxidase. *European Journal of Biochemistry* **260,** 726–735.

Crutzen P.J. (1988) Tropospheric ozone: an overview. In *Tropospheric Ozone: Regional and Global Scale Interactions* (ed. I.S.A. Isaksen), pp. 3–32. Kluwer Academic Publishers, Dordrecht, the Netherlands.

Dueck T.A., de Visser R., Poorter H., *et al.* (2007) No evidence for substantial aerobic methane emission by terrestrial plants: a ^{13}C-labelling approach. *New Phytologist* **175,** 29–35.

Dumville J.C. & Fry S.C. (2003) Solubilisation of tomato fruit pectins by ascorbate: a possible non-enzymic mechanism of fruit softening. *Planta* **217,** 951–961.

Fry S.C. (1983) Feruloylated pectins from the primary cell wall: their structure and possible functions. *Planta* **157,** 111–123.

Fry S.C. (1998) Oxidative scission of plant cell wall polysaccharides by ascorbate-induced hydroxyl radicals. *Biochemical Journal* **332,** 507–515.

Fry S.C., Dumville J.C. & Miller J.G. (2001) Fingerprinting of polysaccharides attacked by hydroxyl radicals *in vitro* and in the cell walls of ripening pear fruit. *Biochemical Journal* **357,** 729–735.

Fry S.C., Miller J.G. & Dumville J.C. (2002) A proposed role for copper ions in cell wall loosening. *Plant and Soil* **247,** 57–67.

Grant J.J., Yun B.-W. & Loake G.J. (2000) Oxidative burst and cognate redox signalling reported by luciferase imaging: identification of a signal network that functions independently of ethylene, SA and Me-JA but is dependent on MAPKK activity. *The Plant Journal* **24,** 569–582.

Griffiths H.R. & Lunec J. (1996) Investigating the effects of oxygen free radicals on carbohydrates in biological systems. In *Free Radicals: A Practical Approach* (eds N.A. Punchard & F.J. Kelly), pp. 185–200. IRL Press, Oxford, UK.

Grimes H.D., Perkins K.K. & Boss W.F. (1983) Ozone degrades into hydroxyl radicals under physiological conditions. *Plant Physiology* **72,** 1016–1020.

Harley P., Deem G., Flint S. & Caldwell M. (1996) Effects of growth under elevated UV-B on photosynthesis and isoprene emission in *Quercus gambelii* and *Mucuna pruriens*. *Global Change Biology* **2,** 149–154.

Hershenson H.M. (1956) *Ultraviolet and Visible Absorption Spectra: Index for 1930–1954*. Academic Press, New York, NY, USA.

Houweling S., Röckmann T., Aben I., Keppler F., Krol M., Meirink J.F., Dlugokencky E.J. & Frankenberg C. (2006) Atmospheric constraints on global emissions of methane from plants. *Geophysical Research Letters* **33,** article number L15821.

Ishii T. (1997) *O*-Acetylated oligosaccharides from pectins of potato tuber cell walls. *Plant Physiology* **113,** 1265–1272.

Karl D.M., Beversdorf L., Björkman K.M., Church M.J., Martinez A. & DeLong E.F. (2008) Aerobic production of methane in the sea. *Nature Geoscience* **1,** 473–478.

Keppler F., Hamilton J.T.G., Brass M. & Röckmann T. (2006) Methane emissions from terrestrial plants under aerobic conditions. *Nature* **439,** 187–191.

Keppler F., Hamilton J.T.G., McRoberts C.W., Vigano I., Brass M. & Röckmann T. (2008) Methoxyl groups of plant pectin as a precursor of atmospheric methane: evidence from deuterium labelling studies. *New Phytologist* **178,** 808–814.

Kirschbaum M.U.F., Bruhn D., Etheridge D.M., Evans J.R., Farquhar G.D., Gifford R.M., Paul K.I. & Winters A.J. (2006) A comment on the quantitative significance of aerobic methane release by plants. *Functional Plant Biology* **33,** 521–530.

Knox J.P. & Dodge A.D. (1985) Singlet oxygen and plants. *Phytochemistry* **24,** 889–896.
Lindsay S.E. & Fry S.C. (2007) Redox and wall-restructuring. In *The Expanding Cell* (eds J.-P. Verbelen & K. Vissenberg), pp. 159–190. Springer, Berlin, Germany.
Liszkay A., Kenk B. & Schopfer P. (2003) Evidence for the involvement of cell wall peroxidase in the generation of hydroxyl radicals mediating extension growth. *Planta* **217,** 658–667.
Lyons T., Ollerenshaw J.H. & Barnes J.D. (1999) Impacts of ozone on *Plantago major*: apoplastic and symplastic antioxidant status. *New Phytologist* **141,** 253–263.
McLeod A.R. & Newsham K.K. (1997) Impacts of elevated UV-B on forest ecosystems. In *Plants and UV-B* (ed. P.J. Lumsden), pp. 247–281. Cambridge University Press, Cambridge, UK.
McLeod A.R., Fry S.C., Loake G.J., Messenger D.J., Reay D.S., Smith K.A. & Yun B.-W. (2008) Ultraviolet radiation drives methane emissions from terrestrial plant pectins. *New Phytologist* **180,** 124–132.
Miller J.B., Gatti L.V., d'Amelio M.T.S., Crotwell A.M., Dlugokencky E.J., Bakwin P., Artaxo P. & Tans P.P. (2007) Airborne measurements indicate large methane emissions from the eastern Amazon basin. *Geophysical Research Letters* **34,** article number L10809.
O'Neill M.A. & York W.S. (2003) The composition and structure of plant primary cell walls. In *The Plant Cell Wall* (ed. J.K.C. Rose), pp. 1–54. Blackwell, Oxford, UK.
Perrone P., Hewage C.M., Thomson A.R., Bailey K., Sadler I.H. & Fry S.C. (2002) Patterns of methyl and *O*-acetyl esterification in spinach pectins: new complexity. *Phytochemistry* **60,** 67–77.
Popper Z.A. & Fry S.C. (2003) Primary cell wall composition of bryophytes and charophytes. *Annals of Botany* **91,** 1–12.
Popper Z.A. & Fry S.C. (2004) Primary cell wall composition of pteridophytes and spermatophytes. *New Phytologist* **164,** 165–174.
Rosenthal I. & Frimer A. (1976) The quenching effect of iodide on singlet oxygen. *Photochemistry and Photobiology* **23,** 209–211.
Rusch H. & Rennenberg H. (1998) Black alder [*Alnus glutinosa* (L.) Gaertn.] trees mediate methane and nitrous oxide emission from the soil to the atmosphere. *Plant and Soil* **201,** 1–7.
Schiermeier Q. (2006) The methane mystery. *Nature* **442,** 730–731.
Schopfer P. (2001) Hydroxyl radical-induced cell-wall loosening *in vitro* and *in vivo*: implications for the control of elongation growth. *The Plant Journal* **28,** 679–688.
Schopfer P., Liszkay A., Bechtold M., Frahry G. & Wagner A. (2002) Evidence that hydroxyl radicals mediate auxin-induced extension growth. *Planta* **214,** 821–828.
Seymour G.B. & Knox J.P. (eds.) (2002) *Pectins and Their Manipulation*. Blackwell, Oxford, UK.
Sharpatyi V.A. (2007) On the mechanism of methane emission by terrestrial plants. *Oxidation Communications* **30,** 48–50.
Slein M.W. & Schnell G.W. (1953) The polysaccharide of *Shigella flexneri*, type 3. *Journal of Biological Chemistry* **203,** 837–848.
Terazawa K., Ishizuka S., Sakata T., Yamada K. & Takahashi M. (2007) Methane emissions from stems of *Fraxinus mandshurica* var. *japonica* trees in a floodplain forest. *Soil Biology & Biochemistry* **39,** 2689–2692.
Ueda J., Takeshita K., Matsumoto S., Yazaki K., Kawaguchi M. & Ozawa T. (2003) Singlet oxygen-mediated hydroxyl radical production in the presence of phenols: whether DMPO–$^{\bullet}$OH formation really indicates production of $^{\bullet}$OH? *Photochemistry and Photobiology* **77,** 165–170.
Vigano I., van Weelden H., Holzinger R., Keppler F., McLeod A. & Röckmann T. (2008) Effect of UV radiation and temperature on the emission of methane from plant biomass and structural components. *Biogeosciences* **5,** 937–947.
Vreeburg R.A.M. & Fry S.C. (2005) Reactive oxygen species in cell walls. In *Antioxidants and Reactive Oxygen Species in Plants* (ed. N. Smirnoff), pp. 215–249. Blackwell, Oxford, UK.
Wang Z.P., Han X.G., Wang G.G., Song Y. & Gulledge J. (2008) Aerobic methane emission from plants in the Inner Mongolia steppe. *Environmental Science & Technology* **42,** 62–68.
Wojtaszek P. (1997) Oxidative burst: an early plant response to pathogen infection. *Biochemical Journal* **322,** 681–692.

Received 3 July 2008; received in revised form 4 September 2008; accepted for publication 7 September 2008

[Plant Signaling & Behavior 4:7, 1-2; July 2009]; ©2009 Landes Bioscience

Article Addendum

Reactive oxygen species in aerobic methane formation from vegetation

David J. Messenger,[1,2] Andy R. McLeod[2] and Stephen C. Fry[1,*]

[1]The Edinburgh Cell Wall Group; Institute of Molecular Plant Sciences; School of Biological Sciences; and [2]School of GeoSciences; The University of Edinburgh; Edinburgh, UK

Abbreviations: •OH, hydroxyl radical; ROS, reactive oxygen species; UV, ultraviolet

Key words: methane, hydroxyl radicals, reactive oxygen species, UV, methyl esters, pectin

The first report of aerobic methane emissions from vegetation by an unknown mechanism[1] suggested that this potential new source may make a significant contribution to global methane emissions. We recently investigated possible mechanisms and reported[2,3] experiments in which UV-irradiation caused methane emissions from pectin, a major plant cell wall polysaccharide. Our findings also suggest that UV-generated reactive oxygen species (ROS) release methane from pectin. This has implications for all other, UV-independent processes which may generate ROS in or close to the plant cell wall and suggests a need to evaluate additional systems for ROS-generated methane emissions in leaves.

Until recently, the global methane budget was thought to be well understood, the only natural process for methane generation being an anaerobic microbial mechanism.[4] However, observations by Keppler et al.[1] of aerobic methane emissions from vegetation caused controversy and called for a re-assessment of the natural sources of methane. While no mechanism was originally suggested, a putative source, the methyl ester groups of pectin, was proposed based on carbon isotope analyses.[1] We tested this hypothesis directly and reported that UV light could drive methane emissions from pectin in vitro under aerobic conditions.[2] While UV light was necessary for generation of methane from pectin, it is not tenable that UV was directly attacking pectic methyl ester groups since these do not absorb UV of the wavelengths used (280–400 nm). Instead, we proposed that the energy from the UV light was being absorbed by compounds such as phenolics, and that a reactive intermediary would be formed in the process. Importantly, our process had to be non-enzymic since no enzymes were present in either experimental system.[1,2] Following this hypothesis, we tested the effect of reactive oxygen species (ROS) on pectin in vitro and discovered that certain ROS cause production of methane: hydroxyl radicals (•OH) and singlet oxygen were effective, but hydrogen peroxide and superoxide were not.[3] Also, the addition of ROS-specific scavengers to pectin sheets stopped or severely reduced UV-induced methane emissions from pectin, suggesting that ROS are the intermediary in the mechanism of aerobic methane formation from pectin (Fig. 1). De-esterified pectin was produced by saponification and emitted only trace amounts of methane upon UV-irradiation, clearly establishing ester groups as the source of methane[2,3] and confirming findings of other research groups.[5,6] However, we also found that acetyl ester groups may contribute to methane emissions from pectin and should therefore be considered in future experiments attempting to identify methane sources. Interestingly, we also observed, for the first time, ethylene, ethane and CO_2 emissions from pectin upon UV-irradiation,[2] which corroborates the ROS hypothesis since ROS attack of methyl esters is likely to form methyl radicals, which can then either form methane or dimerise to form ethylene or ethane.

ROS are produced and destroyed constantly throughout the lifetime of plants. The generation of ROS in vivo can generally be linked to two sources: (i) a response to an external stimulus which may be perceived as a threat or (ii) a signalling process in the cell which may happen during growth, hormone action or programmed cell death.[7] Our experiments showed that ROS could lead to methane formation from methyl ester groups; however, the origin of the ROS may not be important, only their nature. Indeed, hydrogen peroxide and superoxide, widely reported to be formed during an oxidative burst following a biotic stress,[8] did not generate methane from pectin in vitro, and are therefore unlikely to do so in vivo. Only the hydroxyl radical (•OH) and singlet oxygen generation led to methane formation, and therefore any process which generates them could also trigger UV-independent methane production. Abiotic stresses, such as drought, heat or salinity, which have been shown to lead to the production of •OH in vegetation,[9] could therefore be processes leading to aerobic methane formation, as could exposure to elevated ozone concentrations.[10] Indeed,

*Correspondence to: Stephen C. Fry; The Edinburgh Cell Wall Group; Institute of Molecular Plant Sciences; School of Biological Sciences; The University of Edinburgh; The King's Buildings; Mayfield Road; Edinburgh EH9 3JH UK; Fax: +44.131.650.5392; Email: S.Fry@Ed.Ac.UK

Submitted: 05/06/09; Accepted: 05/07/09

Previously published online as a *Plant Signaling & Behavior* E-publication: http://www.landesbioscience.com/journals/psb/article/8968

Addendum to: Messenger DJ, McLeod AR, Fry SC. The role of UV radiation, photosensitisers, reactive oxygen species and ester groups in mechanisms of methane formation from pectin. Plant Cell Environm 2009; 32:1–9; PMID: 18811731; DOI: 10.1111/j.1365-3040.2008.01892.x

physical injury (by cutting) of plant material has recently been demonstrated to cause methane emissions.[11]

The origin of the ROS may not be important, as long as their generation is in or close to the pectin of the plant cell wall, since •OH cannot travel far within a cell. Indeed, it is estimated that •OH typically reacts with organic matter within ~1 nm of the site of radical production.[12] Processes such as growth[13,14] and calcium signalling,[15] which both involve ROS production as an intermediary in the mechanism but are not necessarily due to external stress, may therefore have the potential to generate methane aerobically. Any process involved in the complicated pathways of ROS-regulation, for which 152 genes are responsible in *Arabidopsis thaliana*,[16] could be involved in methane emission if the ROS generation is localised close to pectin or other potential substrates.

In addition, hydrogen peroxide, which is generated in the cell walls of healthy plants,[17] can be converted in the cell wall into •OH by processes such as the Fenton reaction,[18,19] especially in the presence of apoplastic ascorbate.[20,21] A complete analysis of the potential for •OH and singlet oxygen to be present in the plant cell wall is therefore necessary for a proper understanding of the different mechanisms that may drive aerobic methane generation. Further experiments into the effects of abiotic stresses other than UV on aerobic methane production from different types of vegetation are necessary in order that future in-vitro studies under simulated natural conditions can be carried out correctly. This type of study, in conjunction with direct in-vivo field studies and satellite observations, are essential to allow global estimates to be made accurately in the future and help us understand the significance of ROS-driven methane emission.

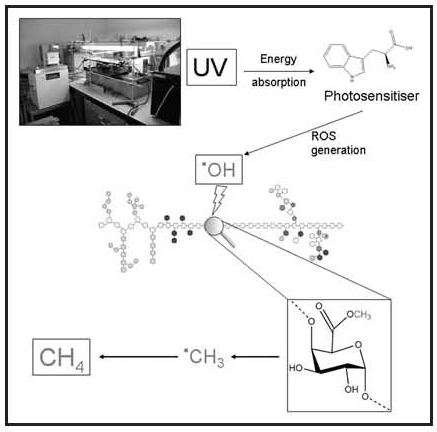

Figure 1. Proposed pathway for •OH-driven methane generation from pectin upon UV irradiation. The compound illustrated here, L-tryptophan, is merely an example of a possible photosensitiser. Hydroxyl radicals (•OH) are shown to attack a methyl galacturonate residue of the homogalacturonan component of the pectin molecule since this is likely to be the most abundant source of methane, but the methyl esters found in xylogalacturonan domains and the acetyl esters found in homogalacturonan and rhamnogalacturonan domains are also possible methane sources. Note that only ~70% of all galacturonic acid residues of the pectin backbone are methyl-esterified. *Inset photograph* shows experimental set-up during UV-irradiation of pectin.

Acknowledgements

This work was supported by research awards from the Natural Environment Research Council (to A.R.M.), the University of Edinburgh Development Trust and the University of Edinburgh Donald Mackenzie Scholarship (to D.J.M.) and the Biotechnology and Biological Sciences Research Council (to S.C.F.).

References

1. Keppler F, Hamilton JTG, Brass M, Röckmann T. Methane emissions from terrestrial plants under aerobic conditions. Nature 2006; 439:187-91.
2. McLeod AR, Fry SC, Loake GJ, Messenger DJ, Reay DS, Smith KA, Yun B. Ultraviolet radiation drives methane emissions from terrestrial plant pectins. New Phytol 2008; 180:124-32.
3. Messenger DJ, McLeod AR, Fry SC. The role of UV radiation, photosensitisers, reactive oxygen species and ester groups in mechanisms of methane formation from pectin. Plant Cell Environm 2009; 32:1-9.
4. Zengler K, Richnow HH, Rosselló-Mora R, Michaelis W, Widdel F. Methane formation from long-chain alkanes by anaerobic microorganisms. Nature 1999; 401:266-9.
5. Keppler F, Hamilton JTG, McRoberts CW, Vigano I, Brass M, Röckmann T. Methoxyl groups of plant pectin as a precursor of atmospheric methane: evidence from deuterium labelling studies. New Phytol 2008; 178:808-14.
6. Vigano I, Holzinger R, van Weelden H, Keppler F, Röckmann T. Effect of UV radiation and temperature on the emission of methane from plant biomass and structural components. Biogeosciences 2008; 5:937-47.
7. Apel K, Hirt H. Reactive oxygen species: metabolism, oxidative stress and signal transduction. Ann Rev Plant Biol 2004; 55:373-99.
8. Doke N. NADPH-dependent O_2^- generation in membrane fractions isolated from wounded potato tubers inoculated with Phytophthora infestans. Physiol Plant Pathol 1985; 27:311-22.
9. Xiong L, Schumaker KS, Zhu J-K. Cell Signaling during Cold, Drought and Salt Stress. Plant Cell 2002; 165-83.
10. Grimes HD, Perkins KK, Boss WF. Ozone degrades into hydroxyl radicals under physiological conditions. Plant Physiol 1983; 72:1016-20.
11. Wang Z-P, Gulledge J, Zheng J-Q, Liu W, Li L-H, Han X-G. Physical injury stimulates aerobic methane emissions from terrestrial plants. Biogeosciences 2009; 6:615-21.
12. Griffiths HR, Lunec J. Investigating the effects of oxygen free radicals on carbohydrates in biological systems. In: *Free Radicals: a Practical Approach* (Punchard NA, Kelly FJ, eds.), IRL Press, Oxford UK 1996; 185-200.
13. Foreman J, Demidchik V, Bothwell JHF, Mylona P, Miedema H, Angel Torresk M, et al. Reactive oxygen species produced by NADPH oxidase regulate plant cell growth. Nature 2003; 422:442-6.
14. Schopfer P, Liszkay A, Bechthold M, Fahry G, Wagner A. Hydroxyl radicals mediate cell-wall loosening and extension growth in plants. Planta 2002; 214:821-8.
15. Mori IC, Schroeder JI. Reactive oxygen species activation of plant Ca^{2+} channels. A signalling mechanism in polar growth, hormone transduction, stress signaling and hypothetically mechanotransduction. Plant Physiol 2004; 135:702-8.
16. Mittler R, Vanderauwera S, Gollery M, Van Breusegem F. Reactive oxygen gene network of plants. Trends Plant Sci 2004; 9:490-8.
17. Schopfer P, Plachy C, Frahry G. Release of reactive oxygen intermediates (superoxide radicals, hydrogen peroxide and hydroxyl radicals) and peroxidase in germinating radish seeds controlled by light, gibberellin and abscisic acid. Plant Physiol 2001; 125:1591-602.
18. Fry SC, Dumville JC, Miller JG. Fingerprinting of polysaccharides attacked by hydroxyl radicals in vitro and in the cell walls of ripening pear fruit. Biochem J 2001; 357:729-35.
19. Fry SC, Miller JG, Dumville JC. A proposed role for copper ions in cell wall loosening. Plant Soil 2002; 247:57-67.
20. Fry SC. Oxidative scission of plant cell wall polysaccharides by ascorbate-induced hydroxyl radicals. Biochem J 1998; 332:507-15.
21. Green MA, Fry SC. Vitamin C degradation in plant cells via enzymatic hydrolysis of 4-*O*-oxalyl-L-threonate. Nature 2005; 433:83-7.